PREFACE

A proton precession magnetometer for recording the intensity of the earth's total magnetic field has been in operation at Ahmedabad since November 1962. In the first part of the thesis, the experimental set-up is described and the observed magnetic field at Ahmedabad is compared with the data obtained from the nearest standard magnetic observatory at Alibag.

In the second part of the thesis, a study is made of the sudden changes (SC,SI,Sfe) in the geomagnetic field at the equatorial stations which were operating during IGY/IGC. The sudden changes in the strength of the equatorial electrojet current in all respects viz. local time, latitude and longitude.

The third part of the thesis deals with lunar tidal variations in the geomagnetic field at the ground at various stations near the magnetic equator viz. Trivandrum, Addis Ababa, Koror, Jarvis, Huancayo and Kodaikanal. The lunar daily variations and lunar monthly variations are evaluated from a large volume of data. The methods of fixed lunar age and fixed solar time are employed for the computations. The conclusions presented from these analysis have a bearing on the dynamo theories which are used to explain solar and luni-solar daily variations. It is clearly seen that the lunar tidal oscillations in geomagnetic field at the equatorial stations are intimately connected with the electrojet currents and hence of variations in ion density and/or motions of the layer or layers of charged particles responsible for the varia-tions. The situation is complicated as the controlling factors are many. They include, besides the graviational action of both sun and moon, the action of the earth's magnetic field on the ions and electrons, and indirectly on neutral particles which collide with them.

Author

Nalin. B. Trivedi

RG Rastogi
23/11/68

Countersigned.

K R Ramanathan
23/11/68

ACKNOWLEDGEMENTS

I wish to express my gratitude to Professor K.R. RAMANATHAN who introduced me to the subject and gave valuable guidance throughout the course of the work. I am grateful to Prof. R.G. RASTOGI without whose unstinting help and guidance, this work would not have been possible. I have pleasure in acknowledging with many thanks the help and guidance of Dr. J.S. Shirke and Dr. T.S.G. Sastry during the experimental work. I would like to thank the staff of the Computing Centre, in particular Messers C.G. Rathod, I.V. Vayeda and P.S. Shah for their generous help in data processing on IBM Computer. I thank Mrs. Lila Deshpande for supplying the programme for computing lunar tides and Mr. Amar Gargesh for computational help. I thank Mr. M.E. Latif for maintaining the proton precession magnetometer unit. I thank Mr. Unnikrishnan for the excellent typing work he has done.

Nalin. B. Trivedi

NALIN.B. TRIVEDI

CONTENTS

PART - 1

1.1 Experimental set up of Proton Precession Magnetometer at Ahmedabad.

1.2 Comparison of geomagnetic field as recorded by the Proton Precession Magnetometer at Ahmedabad with the field recorded at magnetic observatory at Alibag.

1.1 Experimental set up of Proton Precession Magnetometer at Ahmedabad

INTRODUCTION

The phenomenon of nuclear magnetic induction is the basis of the development of nuclear precession magnetometers. Bloch (1946) observed that the direct observation of nuclear magnetic induction should be possible. Purcell (1952) remarked in his Nobel lecture about his looking on snow with new eyes "There the snow lay around my door-step - great heaps of protons quietly precessing in the earth's magnetic field". However it was left to Packard and Varian (1954) to translate Purcell's remark into an instrument for the measurement of geomagnetic field intensity. Waters (1955, 1958) constructed a Magnetometer based on the phenomenon of precession of protons in the earth's magnetic field.

Principle of operation

About 500 c.c. of water is subjected to a polarizing magnetic field of about 100 oersted for a few seconds. The polarizing field is approximately perpendicular to the geomagnetic field. When the polarizing field is suddenly switched off the protons in the water precess about the earth's magnetic field vector with a frequency proportional to the ambient magnetic field intensity.

$$\therefore \quad 2\pi f = \gamma F \qquad \text{.........(1)}$$

where f is the precession frequency of protons.

γ is the gyromagnetic ratio of protons.

F is the ambient magnetic field.

The value of the gyromagnetic ratio (γ) for the proton has been measured by Driscoll and Bender (1958) to be

$$\gamma_p = 2.67513 \pm 0.00002 \times 10^{-4} \text{ gauss}^{-1} \text{ sec.}^{-1}$$

The expression (1) reduces to

$$\frac{F}{f} = \frac{2\pi}{\gamma} = 23.4874 \qquad \text{.........(2)}$$

An accurate measurement of f the frequency of precession leads to a precise determination of F the ambient magnetic field. The frequency of precession is 4257.60 $\pm$ 0.03 cps per gauss.

Theory

The quantum mechanical description postulates the emission of quanta of energy as the protons flip from one quantized state to another. Zeeman splitting of the proton energy state in a uniform magnetic field leads to parallel and antiparallel states of magnetization amongst the proton population. The transition between these two states occurs at the resonance radiation $h\nu_0 = \frac{\mu F}{I}$ where μ is the proton magnetic moment associated with its angular momentum. Ih due to the single spin state $I = \frac{1}{2}$. The angular frequency of the resonance radiation is linearly related to the field by the expression

$$\omega_0 = 2\pi\nu_0 = \gamma F.$$

The above expression is the same as expression (1). Between the two energy states the probability of a transition to a lower energy state from a higher energy state is by far larger compared to the reverse action. The number of protons excess in the lower energy state is proportional to the magnetic field intensity. If the proton population is abruptly transferred to a smaller ambient field from a much higher magnetic field then a redistribution of proton population between the two energy states will take place. The transition frequency and the previously mentioned frequency of the proton precession are identical. A rigorous quantum mechanical treatment of this principle can be found in the works on nuclear resonance. viz. Andrew (1956), Pake (1958).

Hall (1962) has derived the following expression for the induced proton precession signal on the basis of the quantum theory.

$$V = K_1 \vartheta M_o^1 \sin^2\theta \sin\omega_o t \quad \exp(-t/\tau_2) \,..(3)$$

Expression (3) shows that the induced signal of magnitude V at a Larmor angular frequency ω_o is proportional the coil constant K_1 the volume of fluid ϑ, the net magnetization M_o^1 attained during the time t for which the external magnetic field was operating and to the term $\sin^2\theta$ where θ is the angle between the axis of the coil and the ambient magnetic field F. The induced signal decays exponentially and the rate of decay depends on the relaxation time T2 of the protons in the sample fluid. The relaxation time determines the duration of the nuclear precession signal and is known to be different for different proton sources.

Description of the equipment

The proton precession magnetometer constructed at the Physical Research Laboratory, Ahmedabad is described in the following. Shirke (1964) has given the details of construction for this equipment. The block diagram of the set up is given in Fig. 1 and some of the operational details are given below. Each block has been described later in further detail. The magnetometer unit

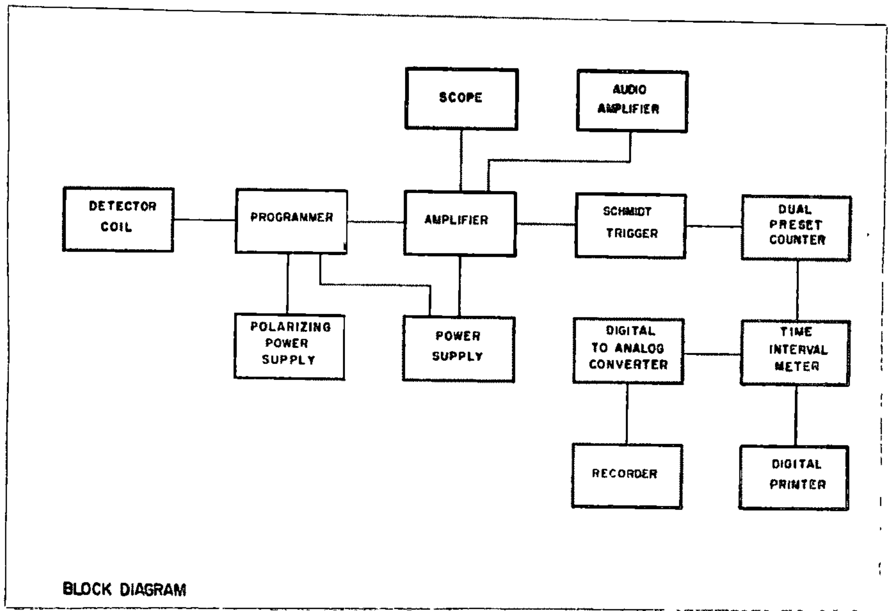

Fig - 1

consists mainly of the following units, a programmer, a detection assembly, a frequency measuring unit and a recording system.

The sensing coil is suspended in a vessel filled with kerosene. The coil is kept fully immersed in kerosene with its axis in the eastward direction. The coil assembly is located about forty to fifty feet away from the building where in the electronic units are housed. Besides separating the coil from the RCC structures it is lifted above the ground level by about one metre using a wooden stool. Firstly current of about five amperes is passed through the coil for about five seconds, a time sufficient to polarize a large number of the protons in the sample. The current is then suddenly switched off and the coil connected to the amplifier. The gradually decaying precession signal induced in the coil is usually of the order of a few microvolts and has to be brought to a convenient magnitude of a few volts for a successful measurement of the frequency of precession. The remaining circuitary is therefore for the precise measurement of the frequency of the precession signal. The error of one cycle in the measurement of the precession frequency corresponds to an error of about 23 γ in that of the magnetic field which is sufficient to obliterate the daily variation in the total geomagnetic field intensity. An elaborate frequency measuring system is therefore employed leading to an accuracy of $\pm 1 \gamma$ in the measurement of the geomagnetic field intensity.

Detector assembly

The detector assembly consists of a coil and a sample fluid rich in proton content. Water is the most suitable sample for ground based magnetometers. It has got a convenient relaxation time with a facility to alter the same by the addition of certain paramagnetic salts. Moreover the gyromagnetic ratio of protons for water is known with a high degree of accuracy. The duration of the precession signal can be lengthened by removal of dissolved oxygen from the water. At the Physical Research Laboratory kerosene is used as the proton source. Kerosene is preferred to water in this system because kerosene does not give electrolytic action even when the coil is immersed in the same. The gyromagnetic ratio for kerosene is believed to be close to that for distilled water. Other than water and kerosene there are fluids which could be used as a source of protons. The values of the relaxation time T_2 are listed for a few known fluids.

Water	- two to three seconds
Kerosene	- about two seconds
n-heptane	- five to six seconds
Benzene	- eighteen seconds.

The coil wound from enammeled copper wire is used for polarizing the protons in the sample fluid as well as for detecting the precession signal. Two forms of the coil design are normally observed.

(1) A simple solenoidal form

(2) Toroidal form in which the wire is wound on a hollow acrylyc ring.

Toroidal winding is normally more difficult however it picks up less noise generated in the vicinity of the coil. Some of the major requirements for the construction of a good coil are stated below.

(1) The coil should have a large number of turns to obtain a large signal.

(2) It should have a high **Q** so as to avoid excessive noise.

(3) It should have a large volume within so as to accommodate large sample.

(4) It should be capable of producing a uniform polarizing field.

In the instrument designed at the Physical Research Laboratory detecting element consists of a pair of copper coils connected in series bucking. This arrangement is found to reduce pick up from noise sources situated outside the coil assembly. Each coil is wound with a twin wire with S.W.G. 18 gauge. Each coil has 500 turns of double wire. The winding length of each coil is five inches and the inner diameter of the coil is also of the same dimension. The series bucking combination of the two coils with a total of 2000 turns offers a resistance of 2.6 ohms and gives an inductance of 40 mH. The coil assembly is rather big in size but generates a polarizing field of a few hundred gauss by passing a current of four to five amperes giving a signal well above the noise level. Initially each of the coils were wound on a former and the former removed carefully thereafter. The coil was indirectly warmed to remove any absorbed water vapour. Before the coil could reabsorb water vapour it was given a thick coating of araldite.

<u>Amplifier and Schmidt trigger</u>

The voltage induced in the coil due to the precession motion of protons is of the order of a few microvolts. This signal voltage suffers some attenuation in the forty to fifty feet long cable connecting the coil to the amplifier. To bring the microvolt signal to a workable level of a few volts a high gain low noise amplifier is necessary. Such an amplifier should be protected against microphonics and should have a stabilized gain.

The circuit diagram of the amplifier used is given in Fig. 2. The circuit is the same as designed by Tepley (1961). It is a three stage RC coupled amplifier, the fourth stage is a cathode follower output. The input circuit of the amplifier consisting of the sensing coil is tuned by means of a condenser to resonant frequency of 1885 cps which is close to the precession frequency normally observed at Ahmedabad. Another tuned circuit is introduced at the input end of the third stage. The band width of the amplifier is considerably reduced by

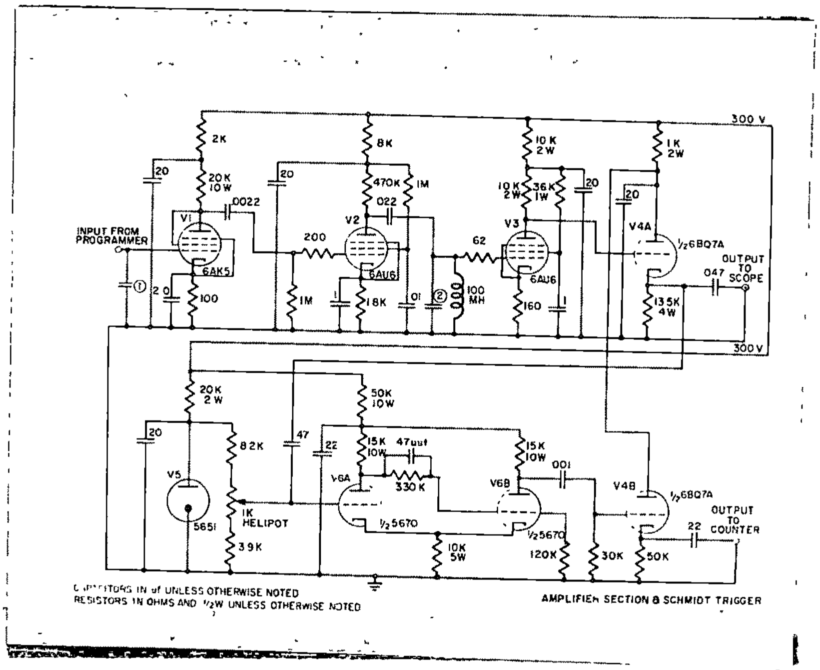

Fig -2

means of the two tuned stages. The first stage tube of the amplifier is mounted on a rubber grommet. This helps reduction in microphonic noise to a great extent. Proper negative feed back incorporated in the amplifier stabilizes the amplifier gain. The overall gain of the amplifier is of the order of 120 db. The output voltage falls exponentially and mixes with the noise in a second or two. The signal to noise ratio of the amplifier is fairly high.

Following this a Schmidt trigger circuit is used so as to give pulses with sharp rise time. One such pulse corresponds to each of the sinusoidal wave from the precession signal. The circuit is shown in Fig. 2. The circuit consists of a cathode coupled multivibrator giving a square pulse corresponding to each sine wave fed to it. It could be adjusted to give its leading edge when the sine wave is passing through its mean value. For this setting the effect of a given noise amplitude is minimum in determining the time interval between a fixed number of wavelength of the precession signal. Hence the Schmidt trigger circuit determines the accuracy of the field measurements. Extreme care has to be taken for the stable operation of this circuit.

Dual Preset Counter

The dual preset counter is constructed similar to the design given by Messers Phillips using decatron E1T tubes. It is a fully automatic four decade counter device which will count any predetermined number upto 10000. After the desired cycle of counts has been completed the counter is automatically reset to its starting position and a pulse is produced which operates a relay by means of an additional output stage. The relay breaks the circuit and the preset counter does not receive input pulses. The minimum duration of a complete cycle of counts is 1/3000 cycles. During this operation it issues two pulses first at the beginning of the predetermined count and second at its end.

The output from the Schmidt trigger is fed to the dual preset counter. The counter is adjusted to give two pulses at an interval of 1000 cycles of the (input) precession signal. Further the counter is adjusted to issue the first pulse after rejecting first couple of hundred cycles in the precession signal which might be mixed with spurious pulses due to electrical noise generated by the relays.

Gate generator and gate amplifier

In this circuit a unishot multivibrator is employed to generate a gate pulse. The two pulses provided by the dual preset counter are fed in to the unishot multivibrator. Each pulse will drive the multivibrator from one stable condition to another. This ultimately gives out a square pulse with a duration equal to the total period of 1000 cycles of the precession signal.

The above gate pulse then controls a gated r.f. amplifier. A pentode valve is kept in a cut-off state and gives no output. It gives output only when the gate pulse is fed to the screen grid of the pentode. At the control grid of the pentode a sinusoidal input of 1 Mc/s is fed from a crystal controlled oscillator. The 1 Mc/s signal is now available at the plate electrode of the amplifier only for the duration of the gate pulse which in the present case corresponds to 1000 cycles of the precession signal.

The 1 Mc/s sinusoid output of the gated amplifier is converted into sharp pulses of equal frequency with very small rise time employing another Schmidt trigger circuit.

Frequency Counter

The frequency counter unit consists of six decade counters in succession. Each decade counter consists of four binary stages with a feedback system, simulating sixteen counts for only ten counts at the input of the decade unit. The first counter is specially designed so as to respond to 1 Mc/s input signal. The following decade counters all identical to each other and have an upper limit of counting speed of 120 KC/S. There is a provision in each decade unit to give a stair case output when the circuit is operating. The stair case output is ladder like having ten steps corresponding to counts 0 through 9. The resetting of a decade is done by disconnecting momentarily the grid leak resistance of the right hand sections of the binaries from the earth point. For visual read out ten neon bulbs are appropriately incorporated in the circuit.

Recording Unit

A triplex Evershed Recording Milliammeter is used to record simultaneously the outputs of the three decade units which show the most significant figures in the diurnal variation of geomagnetic field. The stair case output voltages from the decades are fed to the recording meters through proper impedance matching.

A change of one count on a decade representing units in a Mc/s frequency counting system corresponds to a change of 0.08 gamma in the total magnetic field. A change of one count on a decade representation ten, hundred and thousand in a Mc/s frequency counting system correspond to a change of 0.8, 8 and 80 gamma respectively. The channels representing change in a unit step of 0.8, 8 and 80 gamma are recorded on the chart. A sample record chart is reproduced in Fig. 3. The chart speed is 1" per hour.

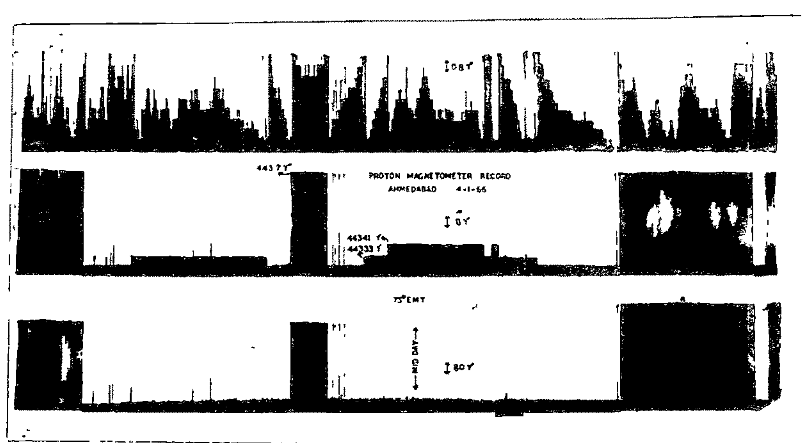

Fig-3

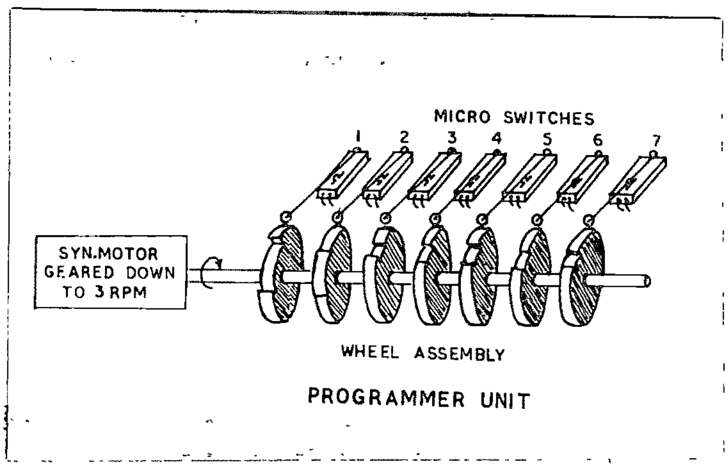

Fig -4

Programmer

The sequence of operation of the various units is achieved through a programmer unit. It consists of a synchronous motor geared down to a speed of one revolution in 20 seconds. This rotates an assembly of Geneva wheels which are given suitable cuts on the periphery so that each wheel makes and breaks a circuit through a micro-switch at appropriate instances in each revolution. The various operations managed by the programmer unit are shown in Fig. 4. The switch No. 2 a relay which keeps the detector coil connected to the polarizer just prior to each sensing for about four to five seconds. As the cam rotates, the polarizer is disconnected from the coil and through another relay operated by switch 1, the amplifier gets connected to the sensing coil. This operates the dual preset counter giving the appropriate gate for passing on the microsecond pulses, derived from the crystal oscillator, to the Mc/s counter. During the period the counting is on switches No. 3, 4, 5 keep three recording meters shorted. Just prior to each sensing switch No. 6 presets the decade counters. Once the counting is over switches 3, 4 and 5 are released and the output of the final three decade counters is recorded on the meters.

1.2 Comparison of Geomagnetic Field as recorded by the Proton Precession Magnetometer at Ahmedabad with the field recorded at magnetic observatory at Alibag

A proton precession magnetometer installed at Ahmedabad has been recording earth's total magnetic field intensity since November 1962. The coordinates of Ahmedabad are given below:

Geographic latitude = 23°01'N

Geographic longitude = 72°36'E

Geomagnetic latitude = 14°01'N

Magnetic dip = 34°N

The total geomagnetic field is recorded at the interval of twenty five seconds. Accuracy of ± 1 γ is claimed in the measurement made by the proton precession magnetometer.

A typical magnetogram record is presented in Fig. 3. of Chapter 1. The record clearly indicates diurnal variation in the total field. The average range of diurnal variation in the total geomagnetic field at Ahmedabad is about 20 γ to 25 γ . During night-time total field intensity practically remain constant, by sunrise it starts increasing, reaches maximum at about midday and later starts falling, reaches night-time value by sunset. In Fig. 1 are shown average Sq variation for

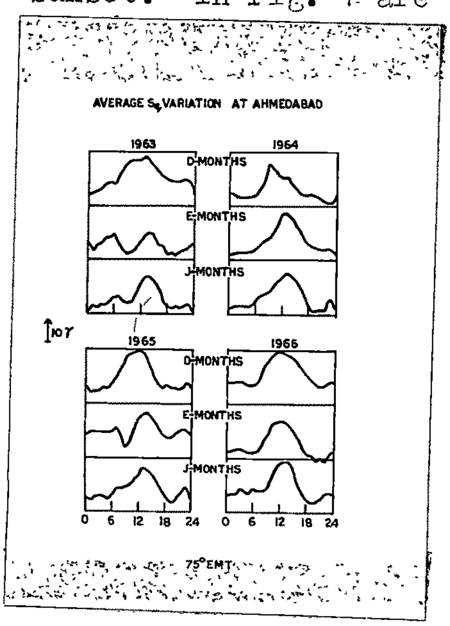

Fig-1

each season for the years 1963, 1964, 1965 and 1966.

The total magnetic field variation observed at Ahmedabad are compared with similar observations made at a standard magnetic observatory of Alibag (18.6°N, 76°E, (Geographic), 24.6° dip). The data used for the comparison are of the year 1964. The magnetic data published for Alibag presents variations in H, D and Z components of the geomagnetic field. For exact comparison with total field observations of Ahmedabad, total field is calculated for Alibag using the relation $F^2 = H^2 + V^2$. For the comparison of the magnetic field variation at the two stations monthly mean Sq variations derived from the five quiet days of each month is considered. In Fig. 2 are shown

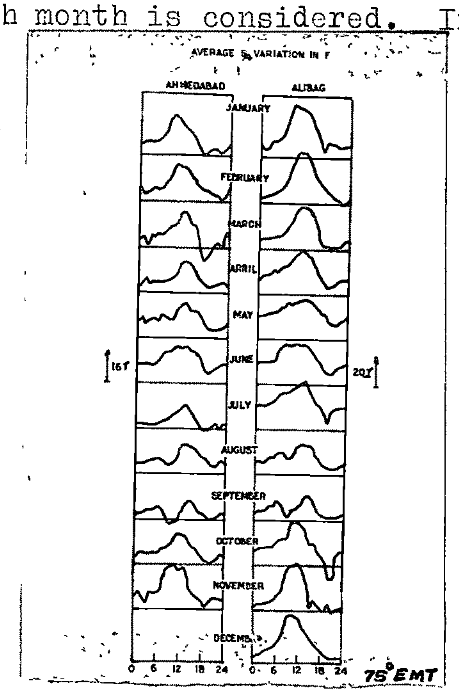

Figure.2.

the Sq variation for each month of the year 1964. At Ahmedabad the data for the December month is lost due to failure of the equipment. It is seen from the diagram that total magnetic field variations at Ahmedabad are similar to Alibag total field variations. The range of daily variation at Alibag is slightly more compared to the range at Ahmedabad. In general the range of diurnal variation in total field is less compared to range in H variation. However the H variation at Alibag and F variation at Ahmedabad are similar in shape. The daily variation curves for a few days with different C_p index are illustrated for both the stations. Refer Fig. 3 and Fig. 4.

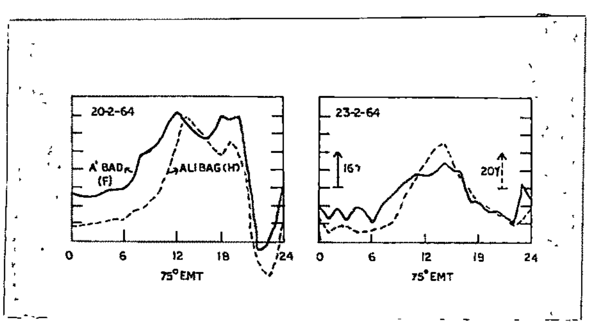

Figure.3.

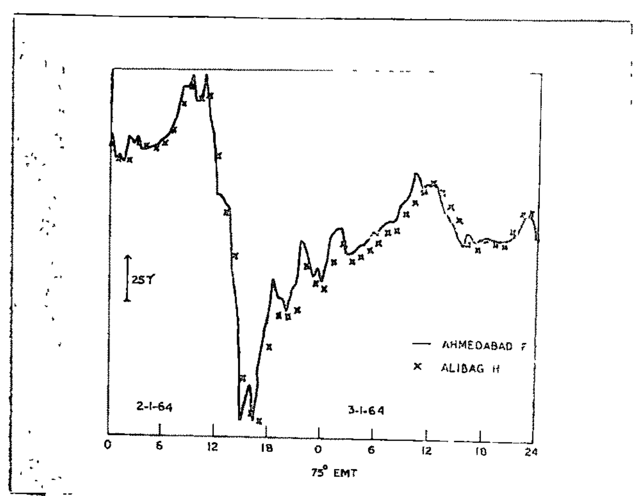

Figure.4.

Besides comparing Sq variation at Alibag and Ahmedabad comparison is necessary for the daily variation on the days having various degrees of disturbances. It is seen above that Ahmedabad F and Alibag H variations possess same character. Here Ahmedabad F and Alibag H data for the year 1964 are grouped according to the following index ranges.

1. C_p value between 0.0 to 0.4
2. C_p value between 0.5 to 0.9
3. C_p value between 1.0 to 1.4
4. C_p value between 1.5 and more.

Magnetic character figures C_p are prepared by the university of Gottingen and published in Journal of Geophysical Research by J. Virginia Lincoln. Average

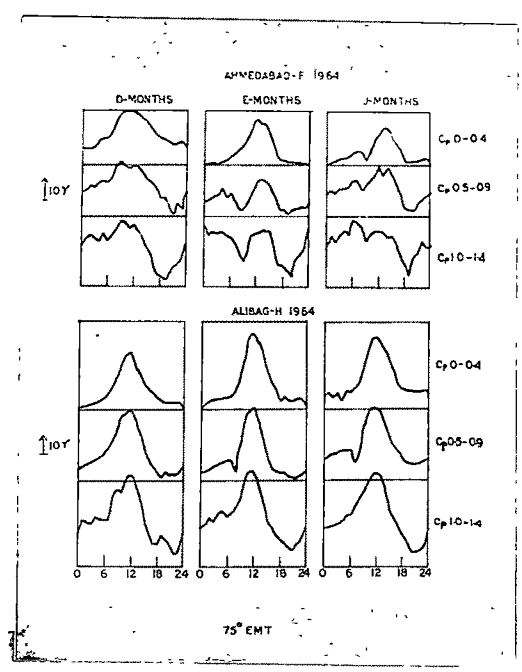

Figure.5.

daily magnetic variation for each group was computed and plotted as shown in the diagram. In the Fig. 5 left hand side it is seen that Ahmedabad F closely follows Alibag H in character and nature.

Several magnetic storms have been recorded at Ahmedabad. In our records sudden commencement does not stand out clearly. The increase in total field is found to be gradual. The storm following SC is determined from the published data of other magnetic observatories. If there is some relationship between the occurrence of magnetic storm and the period of the suns rotation some disturbance will be followed by about 27 days after the initial storm. It is tried to group all magnetic storm with many series of storms following at an interval of about 27 days. We find storms have a tendency to recur at an interval of 27 days. Two disturbances during 1963 were found to persist for seven rotations of the Sun. On most of the other occassions recurrence for three cycles was observed. H.W. Newton (1949, 1950) has pointed out the recurrence feature of the storm of 24-26 January 1949 and also observed a marked resemblance of the repeating storm to the first storm in the same sequence. In certain cases such similarity is observed from Ahmedabad records.

REFERENCES

Andrew, E.R. Cambridge University Press. 1956

Bloch, F. Phy.Rev.Vol.70, 474, 1946.

Driscoll R.L. and Bender P.L., Phy.Rev.Lett.1, 413,1958.

Hall S.H., Geophy.J.R. Astro.Soc. 7,131,1962.

Newton, H.W. Observatory 69,75,1949.

Packard, M.E. and Varian R.H.; Phy.Rev. 93 , 941 , 1954.

Pake G.E., Scientific American Aug., 1958.

Purcell, E.M., Nobel Lecture 1952.

Shirke J.S., Ind.J.Pure & App.Phy.2,23,1964.

Tepley L.R., Rep.Lockheed Missiles and Space Division, Sunnyvale Calif. (1961).

Waters, G.S., Nature (London) 176,691 (1955)

Waters G.S., J.Sc.Instru. 351,98,1958.

PART - 2

2.1 Brief review of the geomagnetic field in the neighbourhood of the magnetic equator.

2.2 Sudden changes in the geomagnetic field near the magnetic equator.

2.3 Collection of publications in support of the results described in 2.2.

2.1 Brief review of the geomagnetic field in the neighbourhood of the magnetic equator

It has been observed long ago that compass needle executes a regular oscillation during the course of a day. Balfour Stewart (1882) connected these magnetic variations with region which we know as the ionosphere. He postulated existence of electric currents in the upper atmosphere to account for the daily variation in the earth's magnetic field. The presence of ionosphere was implied by Marconi's transatlantic radio wave transmission in 1901 and confirmed in 1925 by Appleton, and Breit and Tuve. Schuster in (1908) made remarkable guesses about the conductivity of the upper atmosphere and gave detailed theory of dynamo action proposed by B. Stewart. Chapman (1913, 1919) developed a dynamo theory suitable to both solar and lunar variations in the geomagnetic field. He proposed ten times higher conductivity than that estimated by Schuster. His qualitative explanation: tidal movements of the neutral atmosphere coupled with the earth's main magnetic field generate a sufficient emf (dynamo action) to derive currents and produce additional electrostatic fields (polarization field) capable of moving the plasma in the ionosphere. The concentration of current flow takes place in the region where conductivity is maximum i.e. the height at which electro-neutral collision frequency equals the gyromagnetic frequency. Two current loops (one in each hemisphere), fixed in relation to the sun are proposed. The daily magnetic variations at ground observatories result as the stations pass beneath the current systems (Chapman and Bartels, 1940). Currents in the northern loop flow counter clockwise and those in the southern loop clockwise leading to a West to East current flow near the equator.

The ionospheric studies revealed that observed conductivity was far less than the value proposed by Chapman. Later investigation on the atmospheric oscillations by Taylor (1936), Pekeris (1937) and Wilkes (1949) showed that tidal velocities could be expected to increase with the inverse square root of air density. Since Chapman's calculation of the conductivity considered that at all heights tidal motions are comparable with the tidal motions at ground level, the value of conductivity was high. Thus the theoretical conductivity was brought into a more reasonable agreement with existing observations. Matsushita (1949, 1950) showed compatibility of low wind speed and high conductivity in the dynamo region.

As early as 1922 when the Department of Terrestrial Magnetism of Carnegie Institution established a magnetic observatory at Huancayo (12°S, 75°.3W - Geographic) situated very close to the magnetic equator, abnormally large daily variation in horizontal magnetic intensity was noticed. McNish (1923) attributed this anomally to locally concentrated currents flowing eastwards; the enhancement in eastward currents was ascribed by him to the non-coincidence of the earth's geographic and magnetic axes. Egedal (1948) was one of the earliest to recognise enhancement of Sq(H) range near the equator as a global phenomenon rather than localised affair as shown by McNish. Subsequent measurements made by Walter in Uganda (Chapman, 1948), Pontier (1950) in Togo, Giesecke (1951) in Peru, Madwar (1953) in Sudan, Gulatee (1950), Pramanik and Yegnanarayanan (1952) and Pramanik and Hariharan (1953) in India showed that enhancement of $S_q(H)$ is found near the dip equator all along the globe.

Martyn (1948, 1949) attributed enhancement of Sq(H) at the magnetic equator to an increase of conductivity of the ionosphere. Further he suggested that the conductivity of the ionosphere may be enhanced if vertical (Hall) currents are prevented from flowing by polarization, along lines investigated first by Cowling (1933) for the solar atmosphere. Cowling and Borger (1948) showed that although Martyn's suggestion could not be accepted in toto but it was certainly valid in a narrow region near the magnetic equator.

Although the mechanism of the growth of the electrojet is not understood completely but its plausible explanation in terms of local enhancement of ionospheric conductivity has been given by Hirono (1952), Baker and Martyn (1953). Chapman (1956) has reviewed the ionospheric conductivity, depending on the magnetic field direction, collision frequencies and electron density together with global pattern of tidal winds which determine the resulting current density. The various componenets of the conductivity tensor have maxima in the ionosphere at the heights between 100 km and 150 km.

At the magnetic dip equator the earth's magnetic field is horizontal and northward. The electric field is horizontal and in the eastward direction (perpendicular to the magnetic field). The Hall effect will produce vertical current flow. This can result in a space charge that effectively cancels the Hall voltage. The conductivity then approaches the direct conductivity along the magnetic field vector and the current is enhanced in a narrow region. The enhancement of the current about the magnetic dip equator is known as equatorial electrojet after Chapman (1951).

In the past several years after the theoretical explanation of the electrojet phenomenon extensive investigations were made towards its distribution, location and intensity. Most of the discussions on the properties of electrojet currents have resulted from the geomagnetic observations made in the equatorial regions at the ground level viz. Forbush and Casaverde (1961) in Peru; Onwumechilli (1959), Ogbuchi and Onwumechilli (1961) in Nigeria; Godivier and Crenn (1965) in Chad; Pisharoty and Shreenivasan (1962), Yacob and Khanna (1966), Chapman and Raja Rao (1965), Rao, Rao and Rao (1966) in India. A major number of rockets have been launched into the electrojet and the Sq current system (Cahill, 1959; Maynard, Cahill and Sastry, 1965; Davis et al, 1967; Maynard, 1967). R. Hutton (1967) has done an excellent job of tabulating all the published results and deduc-tions. Recently Onwumechilli (1967) has reviewed the present knowledge regarding the equatorial electrojet currents. Table showing electrojet characteristics from ground-based magnetometer is reproduced from the review article of Onwumechilli.

Longitudinal variation in the equatorial electrojet

Rastogi (1962) studied the enhancement of the diurnal range of the horizontal component (H) of the earth's magnetic field over the magnetic equator in different longitude zones.

viz. (a) American zone with Huancayo as reference observatory.

Summary of Information on Electrojet from Ground-based Magnetometers; Row 2 is Not Separated into External and Internal

	Epoch	No. of days	Longitude range	Latitude range	Total width (KM)	East jet (amp)	East wide S_q (amp)	Total east S_q (amp)	Reference
	1	2	3	4	5	6	7	8	9
1 A	November '56– January '57.	57	3.4°E–8.5°E	6.6°N–13.0°N	460	87,900	25,600	113,600	Onwumechilli (1959a,b)
1 B	November '56– January '57.	57	3.4°E–8.5°E	6.6°N–13.0°N	530	56,100	84,400	140,500	Onwumechilli
2	September '58– April '59.	61	3.4°E–7.6°E	6.6°N–13.0°N	600	114,100	–	–	Rivers (1964)
3 A	May '62– July '62.	53	3.4°E–7.6°E	6.6°N–13.7°N	440	35,500	23,800	59,300	Ogbuehi (1964)
3 B	May '62– July '62.	53	3.4°E–7.6°E	6.6°N–13.7°N	920	46,100	74,200	120,300	Onwumechilli
4 A	August '62– October '62.	47	3.4°E–7.6°E	6.6°N–13.7°N	380	37,000	19,000	56,000	Ogbuehi (1964)
4 B	August '62– October '62.	47	3.4°E–7.6°E	6.6°N–13.7°N	790	46,700	59,500	106,200	Onwumechilli
5 A	March '57– May '57.	65	70.0°W–81.3°W	0°N–22.0°S	660	93,700	72,600	166,300	Forbush and Casaverde (1961)
5 B	March '57– May '57.	65	70.0°W–81.3°W	0°N–22.0°S	920	114,000	155,300	269,300	Onwumechilli
6	November '62– January '63.	56	3.9°E–7.6°E	7.4°N–11.1°N	314	27,000	14,000	41,000	Ogbuehi and Onwumechilli (1964)
7	February '63– April '63.	51	3.9°E–7.6°E	7.4°N–11.1°N	344	31,000	15,000	46,000	Ogbuehi and Onwumechilli (1964)
8	May '63– July '63.	49	3.9°E–7.6°E	7.4°N–11.1°N	420	28,000	13,000	41,000	Ogbuehi and Onwumechilli (1964)
9	April '58– August '58 and '59.	?	72.9°E–77.0°E	8.5°N–18.6°N	580	50,500	35,400	85,800	Yacob and Khanna (1963)

(b) African zone with Ibadan as reference observatory.

(c) Indian zone with Kodaikanal as reference observatory.

For each zone he plotted ratio of H range at temporary station to reference station against dip magnetic latitude, and made a comparative study of enhancement of the range over magnetic equator. He found enhancement of the range (Refer Fig.1.)

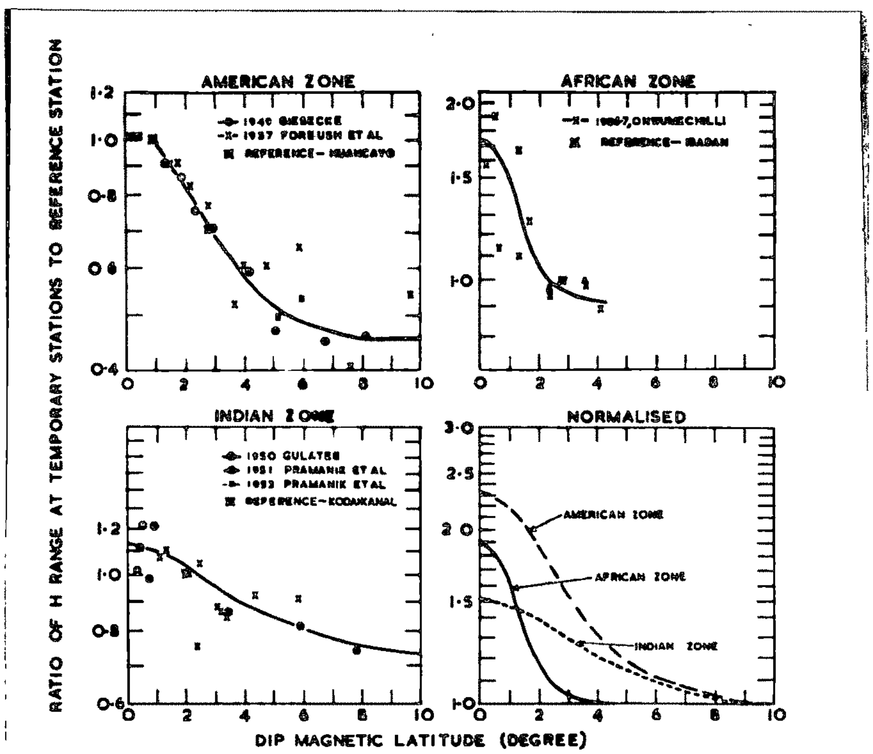

Fig. 1. The variation with latitude of the ratio of the diurnal range in *H* at survey to a permanent observatory for the American, African and Indian zone.

Figure.1.

over the magnetic equator most pronounced in America, less so in Africa and least in India. Price (1964) studied the quiet day magnetic variation during the IGY which showed the great enhancement of Sq(H) in the immediate vicinity of the dip equator. His results are tabulated below.

Ranges of Sq(X) gamma for stations near the dip equator:

Station	Dip latitude	J-months	E-months	D-months
Muntinlupa	7.2°	88	94	79
Chidambaram	2.7°	111	137	91
Jarvis	1.1°	116	164	170
Huancayo	1.0°	164	214	177
Koror	0.0°	161	198	160
Trivandrum	-0.3°	145	188	120
Addis Ababa	-0.5°	136	177	128
Bangui	-7.0°	81	95	77

The table indicates that the jet intensity is greater in South America than elsewhere in agreement with conclusion reached by Rastogi (1962). The above table indicates another longitudinal effect, at Huancayo and Jarvis island the range of Sq(X) is greater for the D-months than for the J-months. At Koror the ranges are about equal and at Trivandrum and Addis Ababa the range for D-months is less than for the J-months.

Studying the SC(H) occurring during the period 1951-61, Rastogi (1963) showed that the day-time enhancement of SC(H) is much weaker at the ... n station, Kodaikanal, than ... o, ... of electro- ... resenting

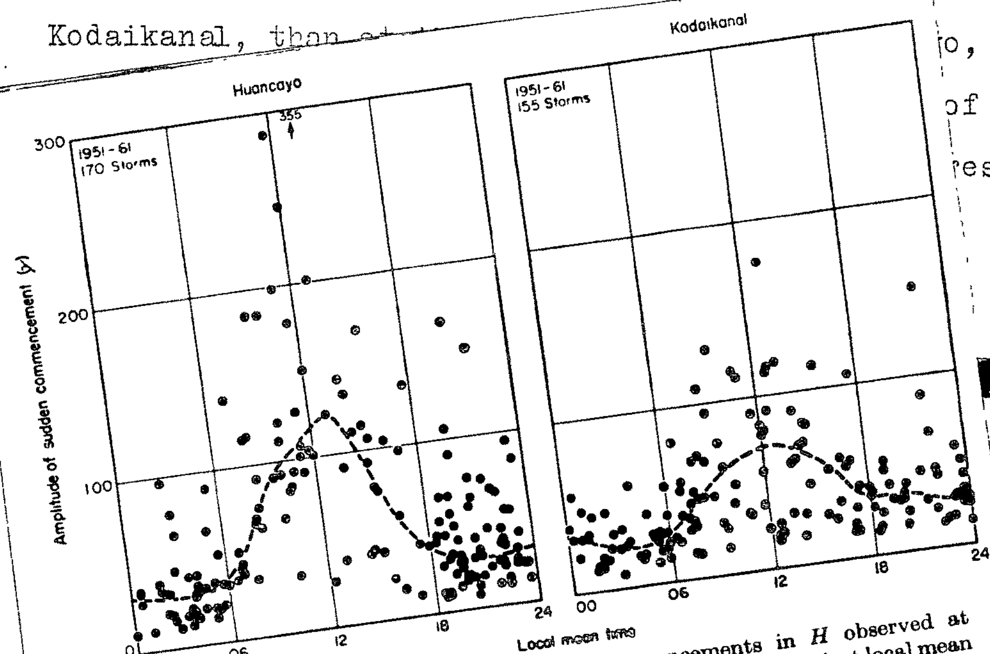

Fig. 2. Amplitudes of individual sudden commencements in *H* observed at Huancayo and Kodaikanal during the period 1951–1961 plotted against local mean time.

[redacted]

Figure.2.

Sugiura and Cain (1966) determined cross-sectional conductivity profiles for various longitudes along the dip equator using a set of 48 gauss coefficients for the earth's magnetic field. They found electrojet profile varying appreciably with longitude and stated the reason could be due to the asymmetry of the magnetic field. The maximum current density for 280°E longitude (Peru) was found to be much more than that for the longitude 80°E (India). Their theoretical estimations were in agreement with the observations.

2.2 Sudden changes in the geomagnetic field near the dip equator

Many investigators have shown a close association of electrojet current system with the normal Sq current system. The day-time electrojet is essentially due to the westward flow of electrons. The magnetograms give no indication of night-time electrojet current. Theoretically westward flow of electrojet current should be present. However experimental verification of night-time current flow is not available except recent report by Balsley (1966). It could be due primarily to the decreased night-time electron density or the electrojet phenomenon might be manifestation of an anomalous decrease in ionospheric conductivity during night hours which disappear around midday.

These possibilities could be tested by the study of short time changes such as sudden commencements, sudden impulses, solar flare effects or short time fluctuations in the geomagnetic field.

Sugiura (1953) was the first to suggest enhancements of amplitude of sudden commencements of magnetic storms at Huancayo during the daylight hours. Forbush and Vestine (1955) suggested that the current system causing the day-time enhancement of the size of SC at Huancayo is closely associated with the electrojet effect responsible for large diurnal variation in H at Huancayo. Forbush and Casaverde (1961) showed for the first time that the amplitude of sudden commencements in H at midday hours at the equatorial stations in Peru varied with latitude in a manner similar to variations at the places of all solar daily range in H. Rastogi (1963) showed that the average night-time values of SCs were not significantly different at Huancayo and Kodaikanal, but the average day-time value was 120 γ at Huancayo and only about 70 γ at Kodaikanal.

Thus these properties of sudden commencements of amplitudes seemed very analogous to that of normal solar diurnal variation itself and prompted to study the variation of sudden commencements of amplitudes with the time of the day, latitude and longitude in greater detail. During the IGY period a chain of magnetic observatories was established in the equatorial electrojet region in South America. In the Indian zone in the neighbourhood of the magnetic equator standard magnetic observatories were in operation from quite few years time. This gave an ideal opportunity to study sudden changes in the geomagnetic field simultaneously in two zones approximately 180 degrees apart. The stations considered in the study are listed below:-

Station	Dip
Huancayo	1.9°N
Yauca	4.4°S
Chimbote	6.4°N
Chiclayo	9.8°N
Talara	12.6°N
Paramaribo	33°N
San Juan	52°N
Trivandrum	0.7°S
Kodaikanal	3.6°N
Annamalainagar	5.3°N
Alibag	24.6°N

Besides storm sudden commencements, sudden impulses, solar flare effects and short period fluctuations are also included in the study to ensure the reliability of the results.

The results from the above mentioned study are described below. The results are based on the papers attached at the end. The papers are assigned numbers according to the chronological order. In the description of the results the papers are referred by the numbers assigned to them.

(1) The average character of the decrease of sudden commencement amplitude with latitude is very similar to decrease of diurnal range of H and thus it is concluded that the latitudinal variation of the amplitude of sudden commencements and the electrojet strengths are similar. (Refer paper I).

(2) The enhancement of SC amplitude at the equator with respect to that at the mid-latitude is much stronger for the American zone than for the Indian zone which is similar to the longitudinal variation of electrojet strength. (Refer paper II).

(3) The latitudinal variation of solar flare effects in H is very similar to that of Sq-H range suggesting electrojet effects. This effect is again more enhanced in the American zone than in the Indian zone. (Refer paper II).

(4) For any particular zone, the enhancement of the solar flare effects are stronger than that of sudden

commencements and it has been suggested that the current systems for solar flare effects are located at lower heights than that for the sudden commencements. (Refer paper II).

(5) In the Indian zone there has been no systematic latitudinal variation of sudden commencements which occurred during the night-time hours indicating the absence of any concentrated electric currents at the equator in the Indian zone during the night hours. (Refer paper III).

(6) In the American zone, the sudden commencements amplitude during the nighttime have an equatorial enhancement though much weaker than the same for the day-time indicating that there is some remnant electric currents flowing even during the night hours in the American zone. Electrojet currents during night-time are stronger in the American zone compared to the Indian zone. (Refer paper III).

(7) The ratio of fluctuations at any station with respect to station of the magnetic equator showed the decrease with latitude similar to that of electrojet currents indicating that besides sudden changes, even fluctuations, of the order of 5 to 30 mts. period are also affected by electrojet currents. (Refer paper IV).

(8) The ratio of these fluctuations at equatorial and non-equatorial stations shows pronounced longitudinal variation similar to that of electrojet currents. (Refer paper IV).

(9) This ratio is maximum at the noon hours and minimum during the night hours. The mean ratio for the night hours in the Indian zone is almost equal to unity suggesting the absence of equatorial enhancements while in the American zone the ratio is statistically greater than 1.0 suggesting the existence of weak electric currents even during the night hours. (Refer paper IV).

(10) The changes in H due to solar effects is maximum very close to the magnetic equator and changes in Z alter its sign very close to the equator suggesting that the current systems are very approximately to that suggested by Chapman method due to sheet of thin currents at the height of about 110 km. (Refer paper IV).

(11) The latitudinal variations of H and Z at the equatorial stations during the daytime closely resemble the curve expected from the idealised current system approximating the thin sheet model.

(12) The sudden commencements occurring at the night-time in the American zone produce changes in Z component altering its sign at a latitude significantly away from the magnetic equator and the variations of H and Z during the night-time SCs cannot be explained by simple current system. (Refer paper V).

(13) The sudden commencements occurring at the night-time in the Indian zone produce changes in Z compo-

nent altering its sign at a latitude significantly away from the magnetic equator and the variations of H and Z during the night-time SCs cannot be explained by simple current system. In the Indian zone even during the daytime the change of SC(Z) sign does not take place at the magnetic equator. The change-over point is slightly north to the magnetic equator. (Refer paper VI).

(14) The latitudinal enhancement of SCs or SIs at the equatorial stations in the American zone and the Indian zone for either the daytime or for the nighttime hours were found to be identical suggesting that the mechanism for the occurrence of sudden commencements or sudden impulses are probably the same. (Refer paper V).

(15) The daily variation of enhancement ratio at low latitude stations in the American zone showed slight differences between SC and SI. The curves for SC are almost symmetrical about the local noon whereas those for SI are having the maximum, hours before the noon. (Refer paper V).

The above mentioned results are discussed in greater detail in the papers published. The list of publications is given below:-

I. "Some relations between the sudden commencement in H and the equatorial electrojet", Journal of Atmospheric and Terrestrial Physics, 1964, Vol. 26, pp. 771-776.

II. "Solar flare crochet and sudden commencement in H within the equatorial electrojet region", Journal of Atmospheric & Terrestrial Physics, 1965, Vol. 27, pp. 663-668.

III. "Night-time sudden commencements in H within the equatorial electrojet region", Journal of Atmospheric & Terrestrial Physics, 1966, Vol. 28, pp. 131-136.

IV. "Night-time disturbance fluctuations in geomagnetic field at equatorial stations", Journal of Atmospheric & Terrestrial Physics, 1966, Vol. 28, pp. 303-310.

V. "Studies of the sudden changes in H at equatorial stations in the American zone", To be published in Annales de Geophysique in September 1968 issue.

VI. "Studies of the sudden changes in H and Z at equatorial stations in the Indian zone", To be published in Annales de Geophysique in fourth issue of 1968.

2·3 I

Reprinted from

Journal of
ATMOSPHERIC AND TERRESTRIAL PHYSICS

PERGAMON PRESS

OXFORD · LONDON · NEW YORK · PARIS

Journal of Atmospheric and Terrestrial Physics, 1964, Vol. 26, pp. 771 to 776. Pergamon Press Ltd. Printed in Northern Ireland

Some relations between the sudden commencement in H and the equatorial electrojet

(*Received* 14 *April* 1964)

THE similarity in the solar diurnal variation of the average size of sudden commencement (SC) in H and of H itself in the equatorial region was shown by FERRARO and UNTHANK (1951). Comparing the sizes of SC in H at Huancayo and Cheltenham, stations on the same meridian but at different latitudes, SUGIURA (1953) noted a considerable enhancement in the size of daytime SC near the geomagnetic equator. FERRARO (1954) found that apart from Huancayo, other stations e.g. Cheltenham, Tucson, San Juan, Honolulu and Watheroo did not show any exceptional daytime enhancement of SC. Later the enhancement of SC was found at other equatorial stations (SRINIVASAMURTHY, 1960; MATSUSHITA, 1960 and MAEDA and YAMAMOTO, 1960).

FORBUSH and VESTINE (1955) suggested that the current system causing the daytime enhancement of the size of SC at Huancayo is closely associated with the electrojet effect responsible for large diurnal variation in H at Huancayo. FORBUSH and CASAVERDE (1961) showed that the amplitude of SC at the equatorial stations in Peru varied with latitude exactly in a similar way as the solar diurnal range of H at these stations.

RASTOGI (1962) has shown pronounced longitudinal inequalities in the strength of the electrojet, being strongest in the American zone and weakest in the Indian zone. Comparing the sizes of SC observed at Huancayo and Kodaikanal during the period 1951–1961, RASTOGI (1963) showed that the average night-time values of SC were not significantly different at the two stations, but the average daytime value was 120 γ at Huancayo and only about 70 γ at Kodaikanal. This indicated a longitudinal effect in SC amplitude along the magnetic equator similar to that of the strength of equatorial electrojet.

To elucidate further the relations between the SC size and the electrojet, it was felt useful to compare the equatorial enhancement of the amplitude of SC during the daylight hours at stations in the American and in the Indian zones.

In the American zone, a chain of five magnetic observatories in Peru, between the magnetic latitudes of $-2°$ to $+6°$, were operative during I.G.Y. and I.G.C. Similarly, since October 1957, there have been three equatorial magnetic observatories in India having the magnetic latitudes of $-0{\cdot}3°$ to $+2{\cdot}7°$N.

The amplitudes of the SC at all the Peruvian stations occurring between 1000–1400 hours L.M.T. were read from the microfilm copies of the magnetograms obtained through the courtesy of W.D.C. (A) for the Ionosphere and airglow at Boulder. The variations of H at the various stations during the period following the S.C. were found to be very similar to each other. Every movement or impulse in one of the magnetograms was easily identified with similar movement in others. Care was taken to measure the amplitudes of SC between the identical points in the magnetogram of all the stations. The amplitudes of SC in H at the American stations are given in Table 1.

The amplitudes of SC at the equatorial stations in India which are maintained by the India Meteorological Department were read from microfilm copies of the magnetograms supplied by W.D.C.(A) for Geomagnetism in Washington D.C. There are some differences between the values measured by the authors and those published by the observatories in the I.G.Y. Bulletins. Such differences were specially noted during the S.C's having a small negative impulse followed by the main positive impulse or in SC's having series of impulses closely following the first one, and seem to be due to different points being taken to constitute the amplitude of SC

Table 1. List of sudden commencement in H at American stations during 1000–1400 hours L.M.T. in I.G.Y. and I.G.C. years

Serial Number	Date	Time 75° W.M.T.	Huancayo γ	Yauca γ	Chimbote γ	Chiclayo γ	Talara γ
1	6 November 1957	1321	255	(213)	178	131	104
2	31 May 1958	1153	245	172	140	104	(88)
3	21 July 1958	1136	188	159	127	95	80
4	27 October 1958	1023	83	60	50	39	28
5	17 December 1958	1046	93	(70)	50	37	34
6	9 January 1959	0959	92	(71)	53	44	31
7	9 April 1959	1330	143	126	89	74	55
8	11 July 1959	1125	130	102	76	61	40
9	17 July 1959	1138	287	230	200	168	106
10	13 January 1960	1359	142	105	80	62	58
	Mean amplitude (γ)		166	131	104	82	62
	Ratio		1·00	0·79	0·63	0·49	0·38
	Magnetic latitude		1·0°N	2·2°S	3·2°N	4·9°N	6·3°N

Table 2.(Revised) List of sudden commencements in H at Indian stations during 1000–1400 hours L.M.T. in I.G.Y. and I.C.C. years

Serial Number	Date	Time 75° E.M.T.	Trivandrum γ	Kodaikanal γ	Annamalainagar γ	Alibag γ
1	19 December 1957	1436	37	(36)	35	19
2	5 March 1958	1039	38	33	39	17
3	17 March 1958	1251	37	33	29	9
4	2 April 1958	1000	61	51	51	12
5	28 June 1958	1215	92	72	79	26
6	8 July 1958	1251	146	146	140	95
7	17 August 1958	1118	96	90	81	52
8	3 September 1958	1338	72	61	59	33
9	24 October 1958	1228	111	108	98	33
10	28 October 1958	1149	69	62	56	25
11	11 February 1959	1256	65	59	62	26
12	26 March 1959	1342	95	89	87	39
13	29 June 1959	1230	125	116	108	37
14	15 July 1959	1302	189	118	131	79
15	5 December 1959	1157	88	80	85	46
Mean amplitude	All SC		88γ	77γ	76γ	37γ
Ratio	All SC		1·00	0·89	0·86	0·42
Mean amplitude	All SC except on 15 July 1959		81γ	74γ	72γ	34γ
Ratio	All SC except on 15 July 1959		1·00	0·91	0·89	0·42
Magnetic latitude			0·3°S	1·7°N	2·7°N	13·9°N

by different observatories. For the present study neglecting the preliminary negative impulse if any, the amplitude of SC was taken as the first positive impulse only. It was found that for Indian stations also, the rapid variations in H at Trivandrum, Kodaikanal and Annamalainagar were very similar to each other except for the SC at 1302 hours 75° E.M.T. on 15 July 1959 when the H variation at Trivandrum was not similar and abnormally large compared to those at Kodaikanal and Annamalainagar.

Figure 1 shows the tracings of the SC on 9 April 1959 observed at Huancayo, Yauca and Chimbote as well as another SC on 29 June 1959 at Trivandrum, Kodaikanal and Annamalainagar.

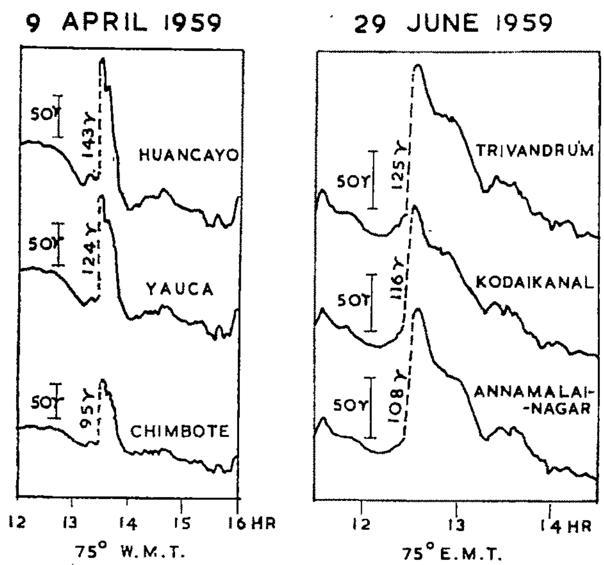

Fig. 1. Tracings of H magnetograms during the sudden commencement at the equatorial stations in the American and the Indian Zones.

Similarities in the movements of the H-traces at all the three stations in the same longitude zone is clearly seen in the diagrams.

Further the amplitude of SC is largest at Huancayo in the American zone and at Trivandrum in the Indian zone indicating the enhancement of the amplitude over the magnetic equator.

The SC is listed in Tables 1 and 2 are shown in Fig. 2 as amplitude versus magnetic latitude. The points for the same SC are joined by a line bearing a number corresponding to the serial number of the SC in the corresponding Table.

Considering the SC at American stations it is seen that each of the ten SC's observed near midday hours of I.G.Y. and I.G.C. has the largest amplitude at Huancayo, less at Yauca, and still less at Chimbote. The mean amplitude was 166 γ at Huancayo, 131 γ at Yauca and 104 γ at Chimbote. The decrease of the amplitude with latitude even within 3° from the magnetic equator is distinct and definite, indicating a pronounced enhancement of the SC amplitude over the magnetic equator.

Considering the SC at Indian stations the above features are present but to a lesser degree. The SC amplitude at Trivandrum is only slightly larger than that at Kodaikanal. The SC amplitude at Annamalainagar is always less than that at Trivandrum, but in a few cases it is comparable or slightly higher than that at Kodaikanal. Excluding the SC at 1302 hours 75° E.M.T. on 15 July 1959, the mean amplitude of SC was 81 γ at Trivandrum, 74 γ at Kodaikanal and 72 γ at Annamalainagar. The average amplitude of SC having 166 γ at Huancayo and only 81 γ at Trivandrum for the same period confirms an earlier suggestion (RASTOGI, 1963) about this longitudinal inequality in SC amplitude over the magnetic equator. Further the change of SC

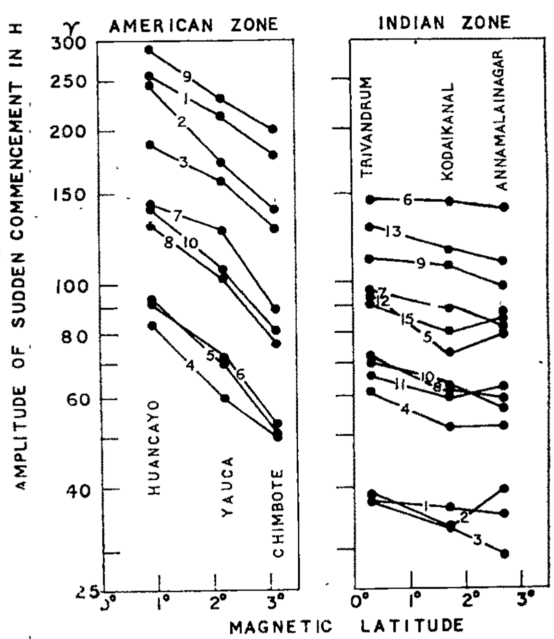

Fig. 2. The variations with magnetic latitude of the SC in H between 1000–1400 hours L.M.T. during I.G.Y. and I.G.C. at American and Indian stations. The numbers on the lines joining the points refer to the serial numbers of the SC in Tables 1 and 2.

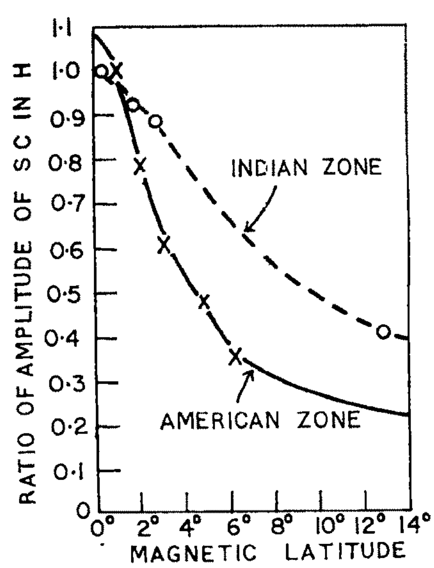

Fig. 3. The variations with magnetic latitude of the average amplitude of SC in H during midday hours at American and Indian stations during I.G.Y. and I.G.C.

amplitude within 3° from the magnetic equator is only about 10 γ in the Indian zone as compared to about 60 γ within the same latitude range in the American zone.

To compare the relative enhancements of the SC amplitude over the magnetic equator ratios were found of the average amplitudes at any station with respect to the station closest to the magnetic equator viz. Huancayo for the American zone and Trivandrum for the Indian zone. The latitudinal variations of these ratios are plotted in Fig. 3. The analysis of other stations e.g. Chiclayo and Talara in American zone and Alibag in Indian zone are also included in Fig. 3 to compare the latitude variations over the whole equatorial electrojet region. The curve for the American zone is much sharper than the same for the Indian zone. These curves are analogous to the curves given for the enhancement of the solar diurnal range of H in the two zones (RASTOGI, 1962).

Thus there is a more pronounced enhancement of the amplitude of SC in H at the American stations, analogous to the strongest enhancement of the solar diurnal range of H in the same zone. It is concluded that the equatorial enhancement of the amplitude of SC in H in a particular longitude zone is associated with the strength of the equatorial electrojet in the same zone and there exists definite longitudinal differences in the amplitude of the sudden commencement, being on the average largest in the American zone and weakest in the Indian zone.

Acknowledgement—Grateful thanks are due to the Directors of the Instituto Geofisico del Peru, the Colaba and Alibag Observatories and the Astrophysical Observatory Kodaikanal for permission to use the data collected by their staff and to the World Data Centres in Boulder and Washington for supplying the microfilm copies of the magnetograms. Thanks are also due to Mr. B. N. BHARGAVA and Mr. K. N. RAO for giving useful additional information and to Prof. K. R. RAMANATHAN for stimulating discussions and suggestions during the course of the study.

Physical Research Laboratory
Ahmedabad-9
India

R. G. RASTOGI
N. B. TRIVEDI
N. D. KAUSHIKA

REFERENCES

FERRARO V. C. A. and UNTHANK H. W. 1951 *Geophys. pur. appl.* **20**, 3.
FERRARO V. C. A 1954 *J. Geophys. Res.* **59**, 309.
FORBUSH S. E. and VESTINE E. H. 1955 *J. Geophys. Res.* **60**, 299.
FORBUSH S. E. and CASAVERDE M. 1961 *Equatorial Electrojet in Peru.* C.I.W. Publ. No. 620.
MAEDA H. and YAMAMOTO M. 1960 *J. Geophys. Res.* **65**, 2538.
MATSUSHITA S. 1960 *J. Geophys. Res.* **65**, 1423.
RASTOGI R. G. 1962 *J. Atmosph. Terr. Phys.* **24**, 1031.
RASTOGI R. G. 1963 *J. Atmosph. Terres. Phys.* **25**, 393.
SRINIVASAMURTHY B. 1960 *Ind. J. Met. Geophys.* **11**, 64.
SUGIURA M. 1953 *J. Geophys. Res.* **58**, 588.

2·3 II

Reprinted from

Journal of

ATMOSPHERIC AND TERRESTRIAL PHYSICS

PERGAMON PRESS

OXFORD · LONDON · NEW YORK · PARIS

Journal of Atmospheric and Terrestrial Physics, 1965, Vol. 27, pp. 663 to 668. Pergamon Press Ltd. Printed in Northern Ireland

Solar flare crochet and sudden commencement in H within the equatorial electrojet region

(*Received* 11 *August* 1964)

AN ENHANCEMENT of the amplitude of sudden commencement (SC) of magnetic storms in the horizontal component, H, of the earth's magnetic field, during daylight hours has been found at equatorial stations (SUGIURA, 1953; FERRARO, 1954; SRINIVASAMURTHY, 1960; MAEDA and YAMAMOTO, 1960). FORBUSH and CASAVERDE (1961) showed that the amplitude of SC in H during mid-day hours at the equatorial stations in Peru varied with latitude in a manner very similar to the variation at these places of the solar daily range of H. RASTOGI *et al.* (1964) showed that the equatorial enhancement of SC in H is stronger in the American zone than in the Indian zone which is similar to the longitudinal variation of the electrojet. FORBUSH and VESTINE (1955) suggested that e.m.f.'s generated in the polar regions during SC impel the dynamo current to flow over a large part of the earth, some of which is concentrated along the narrow electrojet belt of high electrical conductivity at a height of 100–120 km over the magnetic equator.

One of the effects of a solar flare is to cause a short-lived increase in H in the sun-lit hemisphere. The amplitude of these magnetic "crochets" in H at Huancayo has been found by NAGATA (1952) to be abnormal compared to those at other low latitude stations. FORBUSH and CASAVERDE (1961) showed that the amplitude of magnetic crochets in H at Peruvian stations varied with latitude in a manner similar to the diurnal range in H and that a band current with the same geometry as that presumed to be responsible for the equatorial electrojet could also account for the crochets. ELLISON (1955) suggested that the currents causing the crochets at the time of solar flares may be located at a lower height, about 60–70 km, than the current system responsible for the diurnal variation. VOLLAND and TAUBENHEIM (1958) found a systematic phase difference between the S_q and crochet current system and estimated that both E-layer and D-layer contribute equally to the geomagentic s.f.e.

In this article, we have studied the amplitudes of solar flare crochets and SC's in H occurring during daylight hours (0700–1800 hours L.M.T.) at the Peruvian and the Indian stations operating during I.G.Y. and I.G.C. These amplitudes were read from microfilm copies of magnetograms of these observatories obtained through the courtesy of World Data Centres for Ionosphere and Airglow at Boulder U.S.A. and for Geomagnetism at Washington D.C. The occurrences of crochets or SC's were checked against lists published in IAGA Bulletin Nos. 12e, $12m_2$ and $12n_2$.

In Fig. 1 are shown the amplitudes and the local time of occurrence of individual crochet in H observed during I.G.Y–I.G.C. at Huancayo and Trivandrum. It is seen that at either of the two stations the larger amplitudes are found in the morning than in the afternoon hours. As the two stations are about 150° apart in longitude, the above effect cannot be attributed to any Universal Time Effect of the occurrence of stronger crochets. The diurnal curve of the mean amplitude is asymmetric with a peak occurring earlier than the local noon. There is no significant difference in the probability of occurrence of crochet at different times of the daylight hours.

In Fig. 2 are shown the amplitudes of the crochets observed near noon hours simultaneously at the three stations near the magnetic equator viz. at Huancayo, Yauca and Chimbote for the American zone and at Trivandrum, Kodaikanal and Annamalainagar in the Indian zone. These crochets are listed in Table 1. The numbers in Fig. 2 on the line joining the points for the same crochet observed at three stations are the serial number of the crochets listed in Table 1

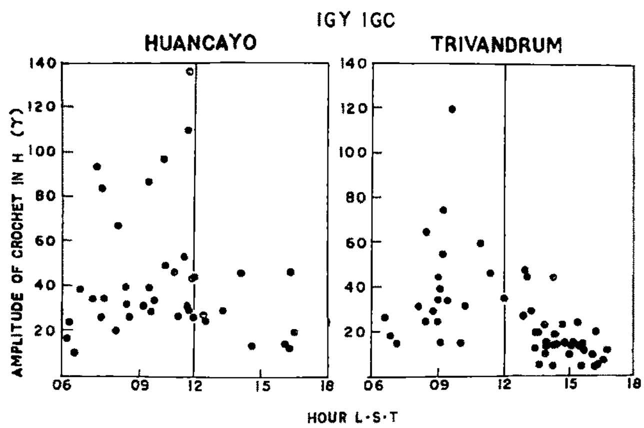

Fig. 1. Mass plot of the amplitude of solar flare crochet in H at Huancayo and Trivandrum during I.G.Y.–I.G.C.

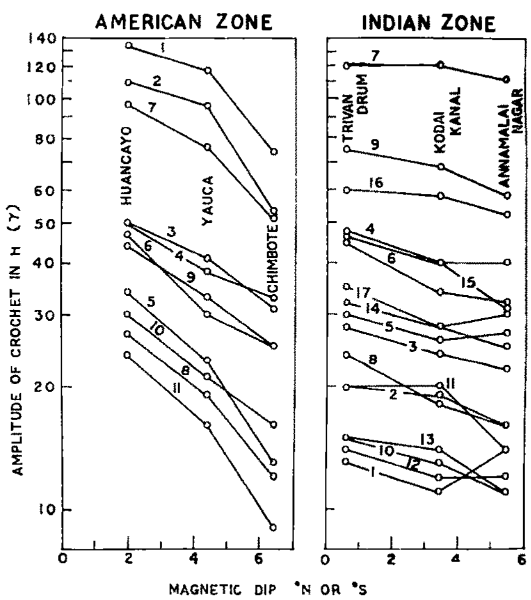

Fig. 2. Latitudinal variation of the amplitude of solar flare crochets around local mid-day hours.

Table 1. Amplitudes of solar flare crochet in H between about 1000–1400 hours L.S.T. in American and Indian zones

Indian zone						American zone					
S. No.	Date	Time (75° E.M.T.)	Trivand-rum γ	Kokaik-anal γ	Annama-lainager γ	S. No.	Date	Time (75° W.M.T.)	Huan-cayo γ	Yau-ca γ	Chim-bote γ
1	Oct. 18, 1957	1323	13	11	14	1	Oct. 20, 1957	1144	136	118	74
2	Nov. 6, 1957	1336	20	19	16	2	Jan. 15, 1958	1140	110	96	53
3	Nov. 23, 1957	1256	28	24	22	3	Mar. 9, 1958	1041	50	41	31
4	Dec. 19, 1957	1300	48	40	40	4	Mar. 24, 1958	1048	50	38	33
5	May 30, 1958	1316	30	26	27	5	June 3, 1958	1010	34	23	13
6	Aug. 10, 1958	1306	−45	−34	−32	6	July 19, 1958	1406	47	30	25
7	Aug. 16, 1958	0934	120	120	112	7	Sept. 8, 1958	1038	97	76	51
8	Sept. 14, 1958	1351	24	18	16	8	Sept. 15, 1958	1200	27	19	12
9	Feb. 1, 1959	0920	75	68	58	9	Jan. 21, 1959	1202	44	33	25
10	Feb. 18, 1959	1003	15	13	11	10	Apr. 9, 1959	1147	30	21	16
11	Apr. 15, 1959	1333	20	20	14	11	Aug. 28, 1959	1200	−24	−16	9
12	Apr. 27, 1959	1355	14	12	12						
13	Apr. 28, 1959	1359	15	14	11						
14	May 13, 1959	1012	32	28	25						
15	June 16, 1959	1123	47	40	31						
16	Aug. 3, 1959	1054	60	58	52						
17	Sept. 12, 1959	1207	35	28	30						

Table 2. Amplitude of solar flare crochets and sudden commencement in H during I.G.Y. and I.G.C. at equatorial stations in American and Indian zones

Station	Magnetic dip	Crochet in H Mean amplitude γ	Crochet in H mean ratio	Sudden commencement in H Mean amplitude γ	Sudden commencement in H Mean ratio
Huancayo	2·0° N	43	1·00 ± 0·00	154	1·00 ± 0·00
Yauca	4·4° S	32	0·75 ± 0·05	121	0·80 ± 0·05
Chimbote	6·4° N	21	0 52 ± 0·07	86	0·62 ± 0·03
Chiclayo	9·8° N	13	0·31 ± 0·07	71	0·49 ± 0·05
Talara	12·6° N	10	0·25 ± 0·06	58	0·39 ± 0·06
Trivandrum	0·6° S	26	1·00 ± 0·00	75	1·00 ± 0·00
Kodaikanal	3·4° N	24	0·86 ± 0·07	70	0·93 ± 0·08
Annamalainagar	5·4° N	21	0·82 ± 0·11	68	0·90 ± 0·07
Alibag	24·5° N	9	0·39 ± 0·12	35	0·47 ± 0·15

for the corresponding zone. It is seen that the amplitude of crochet in H decreases in all cases as one proceeds from Huancayo, Yauca to Chimbote within about 2–3° in magnetic latitude. Similarly for most of the cases the amplitude decreases progressively from Trivandrum, Kodaikanal to Annamalainagar. However the decrease seems to be larger in the American than in the Indian zone for the same change in latitude. To elucidate this point more clearly for a particular event a ratio was found between the amplitude at any station to that at the station nearest to the magnetic equator viz. at Huancayo for the American zone and Trivandrum for the Indian zone. In Table 2 are listed the mean magnitude as well as the mean ratio together with its standard deviation of the amplitude of solar flare crochet and sudden commencements in American and Indian zone for the period I.G.Y.–I.G.C. The mean ratios for the amplitude of solar flare crochet normalized to the value of 1·0 at the magnetic equator are plotted against

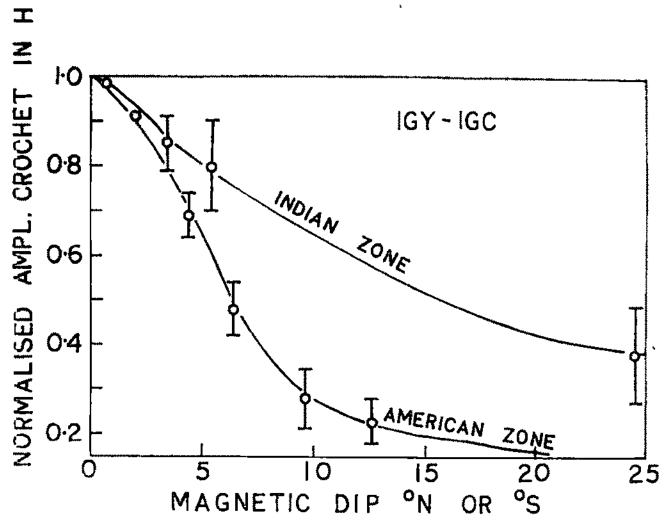

Fig. 3. Variation with magnetic dip of the amplitude of solar flare crochet in H within the equatorial electrojet region of the American and Indian zones.

the magnetic dip angle in Fig. 3. It is clearly seen that the decrease of the amplitude of crochet with increasing dip from the equator is much faster for the American than the Indian zone or in other words the equatorial enhancement of the amplitude is more pronounced in the American zone. RASTOGI (1962) has shown that the daily range of H at equatorial stations decreases with increasing dip angle at a faster rate in the American than in the Indian zone. Thus the longitudinal differences in the latitudinal variation of the amplitude of crochet in H and the strength of electrojet currents are in good correspondence.

In Fig. 4 are compared the latitudinal variation of the ratios of crochets and SC's for the two zones separately. It is seen that the ratio at any station is less for crochet than for SC. This difference is statistically significant for the American zone but for the Indian zone the difference in the ratios of crochet and SC is smaller than their standard deviations and so should be considered with some caution. However, it is quite evident that the equatorial enhancement of the amplitude is stronger for crochets than for SC's

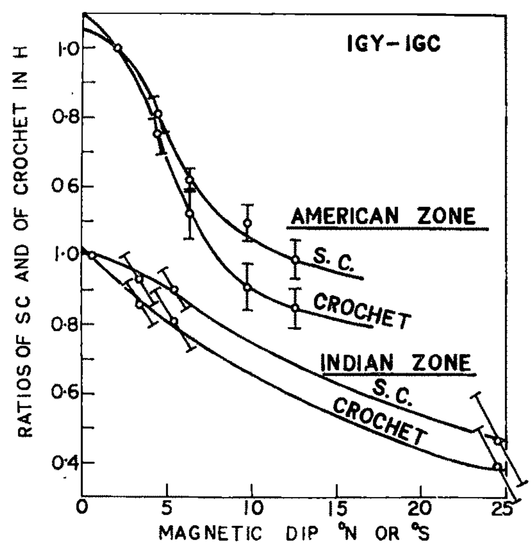

Fig. 4. Variations with magnetic dip of the sudden commencement and solar flare crochet in H within equatorial electrojet region of the American and Indian zones.

Thus the comparative study of the amplitudes of solar flare crochets and SC's at low latitude stations suggests that the current system for these two phenomena may not be identical. The stronger equatorial enhancement of the crochets than of SC's indicate that the solar flare current system is situated at lower height than the SC current system.

CONCLUSIONS

The mean daily variation of the amplitude of solar flare crochet in H is asymmetric about noon, the maximum being in the forenoon hours.

The equatorial enhancement of the amplitude of solar flare crochet in H is more pronounced in the American than in the Indian zone, corresponding to similar variation of the electrojet current strength.

For a particular zone the equatorial enhancement of the amplitude of solar flare crochet in H is more pronounced than that of sudden commencement of magnetic storms.

The current system for solar flare crochets and SC's seem to be qualitatively similar but located at different altitudes, the one for crochets being lower.

Acknowledgements—Thanks are due to World Data Centres (for the Ionosphere and Airglow at Boulder and for Geomagnetism at Washington, D.C.) for supplying the microfilms of the magnetograms of these observatories. Thanks are due to the Directors of Instituto Geofisico del Peru, Astrophysical Observatory Kodaikanal and of Colaba and Alibag Observatory for permission to use the data. It is a pleasure to acknowledge thanks to Prof. K. R. RAMANATHAN for his interest and stimulating discussions during the course of work.

Physical Research Laboratory
Ahmedabad-9, India

R. G. RASTOGI
N. D. KAUSHIKA
N. B. TRIVEDI

REFERENCES

ELLISON M. A.	1955	*Observatory* **75**, 61.
FERRARO V. C. A.	1954	*J. Geophys. Res.* **59**, 309.
FORBUSH S. E. and CASAVERDE M.	1961	*Equatorial Electrojet in Peru*, C.I.W. Publ. No. 620.
FORBUSH S. E. and VESTINE E. H.	1955	*J. Geophys. Res.* **60**, 299.
MAEDA H. and YAMAMOTO M.	1960	*J. Geophys. Res.* **65**, 2538.
NAGATA T.	1952	*J. Geophys. Res.* **57**, 1.
RASTOGI R. G., TRIVEDI N. and KAUSHIKA N. D.	1964	*J. Atmosph. Terr. Phys.* **26**, 771.
RASTOGI R. G.	1962	*J. Atmosph. Terr. Phys.* **24**, 1031.
SRIVINIVASAMURTHY B.	1960	*Indian J. Met. Geophys.* **11**, 64.
SUGIURA M.	1953	*J. Geophys. Res.* **58**, 558.
VOLLAND H. and TAUBENHEIM J.	1958	*J. Atmosph. Terr. Phys.* **12**, 258.

2·3 III

Reprinted from

Journal of
ATMOSPHERIC AND TERRESTRIAL PHYSICS

PERGAMON PRESS

OXFORD · LONDON · NEW YORK · PARIS

Journal of Atmospheric and Terrestrial Physics, 1966, Vol. 28, pp. 131 to 136. Pergamon Press Ltd. Printed in Northern Ireland

SHORT PAPER

Night-time sudden commencements in H within the equatorial electrojet region

R. G. RASTOGI, N. B. TRIVEDI and N. D. KAUSHIKA
Physical Research Laboratory, Ahmedabad-9, India

(*Received* 9 *January* 1965)

Abstract—It is shown that during the night the change of H accompanying a SC is greater at small magnetic dips than at large magnetic dips in the American zone but that this difference is not so clearly marked in the Indian zone.

AN ENHANCEMENT of the amplitude of sudden commencement (SC) of magnetic storms in the horizontal component, H, of the earth's magnetic field, during daylight hours has been found at equatorial stations (SUGIURA, 1953; FERRARO, 1954; SRINIVASAMURTHY, 1960; MAEDA and YAMAMOTO, 1960). FORBUSH and CASAVERDE (1961) showed that the amplitude of daytime SC in H is enhanced over the magnetic equator in the same way as the daily range in H itself. RASTOGI *et al.* (1964) showed that the enhancement of SC amplitude in H occurring around noon is more pronounced in the American than in the Indian zone. It was concluded that the equatorial enhancement of noon time amplitude in H is very closely associated with the strength of the electrojet in that particular zone. It was felt necessary to study the latitudinal variation of SC amplitude during night-time when the ionospheric E-region conductivities would be extremely low and hence the electrojet currents would be very weak. The amplitude of SC in H occurring between 2100 and 0300 hours L.S.T. at the magnetic observatories in the American and Indian zone operating during I.G.Y. and I.G.C. were read from the microfilm copies of the magnetograms as described in (RASTOGI *et al.*, 1964).

In Fig. 1 are shown retraced portions of the magnetograms of the SCs during the night-time on 17 August 1958 and 19 August 1959 at the American stations. It is clearly seen that the fluctuations at all the stations are very similar but the amplitude of SC progressively decreases from Huancayo to San Juan indicating an enhancement of the amplitude over the magnetic equator.

In Fig. 2 are shown the retraced portions of magnetograms of the SCs during the night-time on 17 July 1959, 21 July 1958 and 31 May 1958 at the Indian stations. The fluctuations at these stations are also very similar to each other but the amplitudes of SCs do not show any systematic variation with latitude.

For any particular SC a ratio of the amplitude at each station was found with respect to the same at the station closest to the magnetic equator in that longitude zone. The reference stations being Huancayo for American zone and Trivandrum for the Indian zone. A mean ratio together with its standard deviation was found separately for the SCs occurring between 1000 and 1400 hours and between 2100 and 0300 hours L.S.T. for each station of the American and Indian zones.

Tables 1 and 2 give the night-time SC amplitudes in gammas and the amplitude ratio with respect to the corresponding reference observatory for the American and Indian zone, respectively. The values of amplitude ratio of the daytime SC, are also given for comparison. These amplitude ratios are plotted in Fig. 3.

Within the American zone, the ratio of SC amplitudes shows a distinct maximum over the magnetic equator during the midday as well as midnight hours, the former being more pronounced. The amplitude of night-time SC in H at Talara (magnetic dip 12·6°N) decreases to a value of 0·69 times the same at Huancayo (dip 1·9°N), consequent of the decrease of magnetic latitude by about 5·0°. Thus the enhancement of night-time SC (H) amplitude over the magnetic equator in the American zone is very significant and is of the same order as the enhancement of daytime SC (H) amplitude over the magnetic equator in the Indian zone.

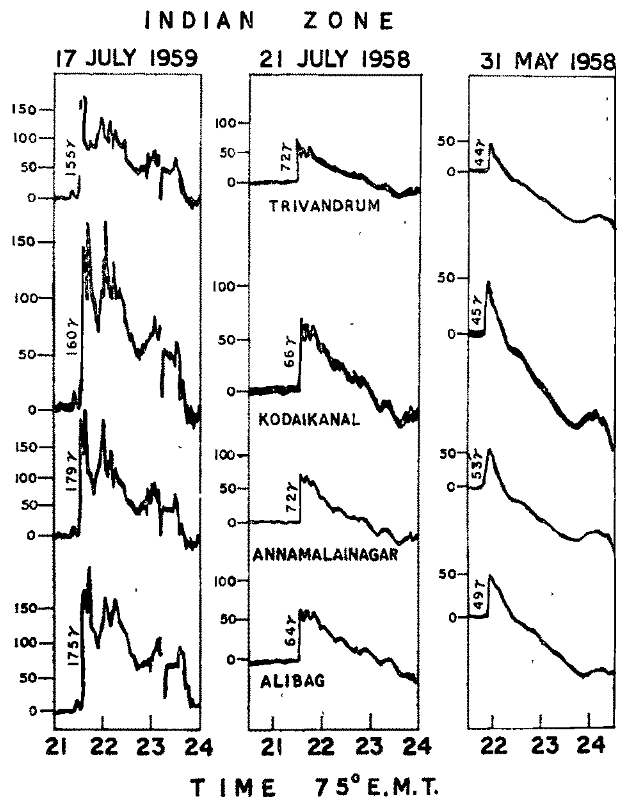

Fig. 1. Tracings of H magnetogram during the night-time sudden commencements in H at American Stations.

Within the Indian zone, there is distinct enhancement of the SC (H) amplitude during the daytime hours, the largest amplitude occurring at Trivandrum (dip 0·6°S). During the night time hours the amplitudes of SC (H) at Trivandrum and Kodaikanal are not significantly different from each other, the ratio ranges between 0·91 and 1·09, the mean ratio being 1·00 ± 0·06. However the SCs at Annamalainagar are in general larger than those at Trivandrum or Kodaikanal, the mean ratio being 1·21 ± 0·09. The amplitudes of SC at Alibag are of the same order as at other Indian stations, the ratio being 0·99 ± 0·13. Thus it is definite that unlike American zone, the enhancement of night-time SC amplitude over the magnetic equator is absent in the Indian zone. Rather there seems to be small decrease of amplitude over the magnetic equator or a small enhancement over the latitude of Annamalainagar (dip 5·4°N).

Forbush and Casaverde (1961) have studied four SCs occurring during the night-time in the American zone and did not find any latitudinal variation of the amplitude of SC in H. However, the deviation in vertical field changed its sign at 8°S which corresponds to the location of cosmic ray equator at the same longitude. They suggested that the current system responsible for SC on the dark side of the earth may also flow in the upper atmosphere. ONWUMECHILLI and OGBUEHI (1962) have studied the latitudinal variation of the amplitude of fluctuations in H in the American zone during the daytime and night-time hours. They found the presence of equatorial enhancement in the amplitude of fluctuation during the daytime as well as the night-time hours. However the values of amplitude ratios for different stations given by them indicate that the equatorial enhancement is more pronounced during the daytime than the night-time

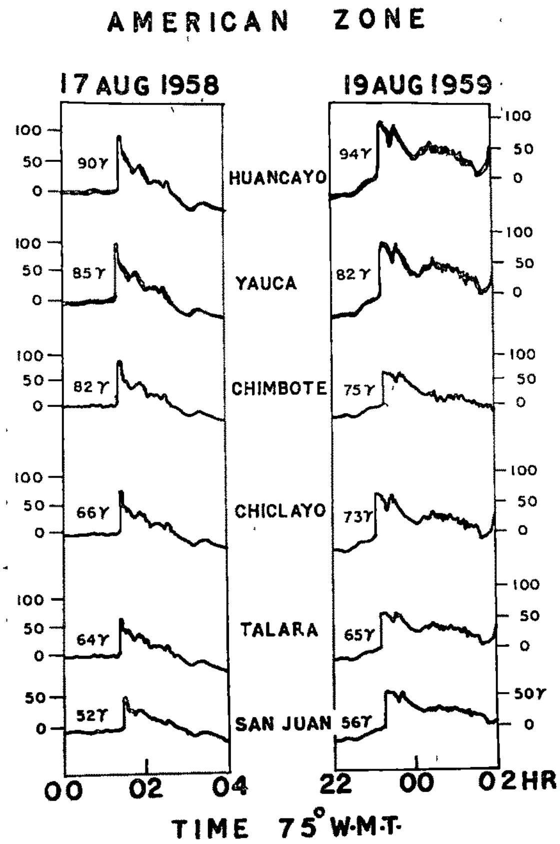

Fig. 2. Tracings of H magnetograms during the night-time sudden commencements in H at Indian stations.

hours. YACOB and KHANNA (1964) have shown that the equatorial enhancement of the amplitude of fluctuations in H in the Indian region is distinct during the daytime hours but is absent during the night-time hours.

The present analysis shows that the enhancement of the night-time SC is significantly pronounced in the American zone and rather doubtfully pronounced in the Indian zone. Actually the night-time enhancement of the amplitude of SC in H in the American zone is comparable to the daytime enhancement of SC in the Indian zone during the midday hours when the electrojet current is maximum in that longitude zone. If the amplitude of sudden commencement in H is assumed to be proportional to the instantaneous value of the electrojet current flowing in that longitude zone, then the electrojet currents during the night hours over the American longitudes should be almost as strong as the electrojet currents during the daytime hours in the Indian longitudes. Thus it may be concluded that the electrojet currents during the night-time hours are absent or very weak in the Indian zone but quite strong in the American zone.

Table 1. Amplitudes of sudden commencements in H during I.G.Y.–I.G.C. at American stations and their ratio with respect to the same at Huancayo

Sr. No.	Date	Time 75° W.M.T.	Huancayo amplitude (γ)	Yauca amplitude (γ)	Yauca ratio	Chimbote amplitude (γ)	Chimbote ratio	Chiclayo amplitude (γ)	Chiclayo ratio	Talara amplitude (γ)	Talara ratio	Sanjuan amplitude (γ)	Sanjuan ratio
NIGHT-TIME (2100 to 0300 hours)													
1	Sept. 1, 1957	2215	36	—	—	—		—	—	24	0·666	—	—
2	Sept. 22, 1957	2135	160	143	0·837	—	—	115	0·718	—	—	80	0·50
3	Dec. 4, 1957	2230	16	13	0·812	14	0·875	12	0·750	—	—	10	0·625
4	June 28, 1958	0212	21	18	0·850	17	0·810	15	0·720	14	0·660	12	0·571
5	Aug. 17, 1958	0122	90	85	0·954	82	0·911	66	0·733	64	0·710	52	0·577
6	Aug. 21, 1958	2127	74	70	0·954	60	0·810	52	0·702	45	0·608	36	0·486
7	Sept. 24, 1958	2307	32	32	1·000	28	0·875	26	0·810	25	0·800	20	0·625
8	Oct. 21, 1958	2215	44	42	0·954	42	0·954	30	0·681	28	0·630	23	0·522
9	Oct. 24, 1958	0230	32	31	0·968	31	0·968	26	0·812	24	0·750	24	0·750
10	Feb. 10, 1959	2217	23	25	1·060	19	0·826	—	—	16	0·700	9	0·391
11	May 24, 1959	0040	28	24	0·860	22	0·790	22	0·790	20	0·715	23	0·820
12	June 29, 1959	0228	19	15	0·789	—	—	16	0·842	16	0·842	18	0·947
13	July 15, 1959	0303	78	68	0·871	—	—	61	0·785	51	0·653	53	0·670
14	Aug. 15, 1059	2303	26	24	0·923	24	0·923	17	0·653	16	0·630	15	0·576
15	Aug. 19, 1959	2312	94	82	0·872	75	0·797	73	0·776	65	0·691	56	0·595
16	Dec. 5, 1959	0159	34	34	1·000	27	0·794	—	—	20	0·590	13	0·380
Mean of mid-night SCs					0·91 ± 0·08		0·86 ± 0·06		0 75 ± 0·05		0·69 ± 0·07		0·60 ± 0·14
Mean of midday SC (1000 to 1400 hours L.S.T.)					0·80 ± 0·05		0·62 ± 0·06		0·48 ± 0·05		0·37 ± 0·04		0·16 ± 0 07

Table 2. Amplitudes of sudden commencements in H during I.G.Y.–I.G.C. at Indian stations and their ratio with respect to the same at Trivandrum

Sr. No.	Date	Time 75° E.M.T.	Trivandrum amplitude (γ)	Kodaikanal amplitude (γ)	Kodaikanal ratio	Annamalaingar amplitude (γ)	Annamalaingar ratio	Alibag amplitude (γ)	Alibag ratio
NIGHT-TIME SC (2100 to 0300 hours)									
1	Nov. 6, 1957	2320	44	48	1·09	62	1·41	32	0·73
2	Feb. 16, 1958	2142	23	24	1·04	31	1·35	26	1·13
3	Mar. 25, 1958	2041	49	50	1·02	64	1·20	53	1·08
4	May 31, 1958	2152	44	45	1·02	53	1·30	49	1·11
5	June 8, 1958	2229	9	8	0·90	12	1·33	11	1·22
6	June 14, 1958	2328	22	24	1·09	28	1·27	26	1·19
7	July 21, 1958	2137	72	66	0·92	72	1·00	64	0·88
8	July 31, 1958	2030	22	24	1·09	28	1·27	21	0·95
9	Oct. 27, 1958	2023	13	13	1·00	15	1·23	13	1·00
10	Dec. 16, 1958	0122	15	14	0·93	17	1·13	14	0·93
11	Dec. 17, 1958	2318	41	39	0·95	45	1·09	37	0·90
12	Apr. 9, 1959	2328	35	38	1·08	37	1·06	36	1·03
13	May 5, 1959	0120	11	11	1·00	(12)	—	10	0·90
14	July 11, 1959	2125	105	96	0·91	110	1·04	80	0·76
15	July 17, 1959	2138	155	160	1·03	179	1·15	175	1·12
16	Sept. 4, 1959	0300	34	33	0·97	40	1·18	34	1·00
Mean of midnight SC					1·00 ± 0·06		1·21 ± 0·09		0·99 ± 0·13
Mean of midday SC (1000 to 1400 hours L.S.T.)					0 91 ± 0·06		0·89 ± 0·07		0·41 ± 0·11

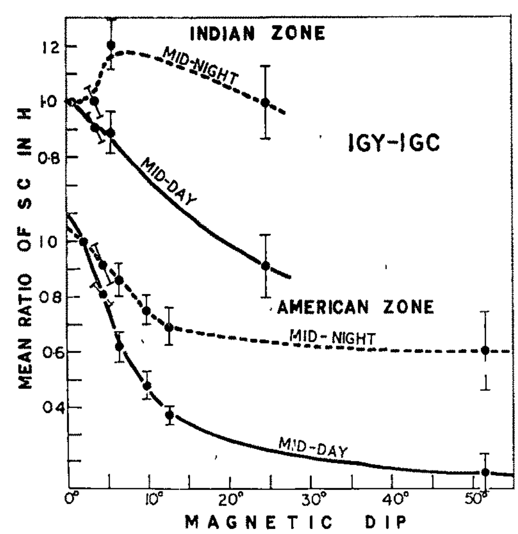

Fig. 3. The variation with magnetic dip of the mean ratio of amplitude of SC in H occurring during the midday and midnight hours at American and Indian zones during the I.G.Y., I.G.C.

This difference in electrojet during the night-time at the two longitude zones may be associated with similar differences in other geomagnetic and ionospheric variations during the night hours and require further investigations.

Acknowledgement—Thanks are due to the World Data Centres (for the ionosphere and airglow at Boulder and for geomagnetism at Washington D.C.) for supplying the microfilms of the magnetograms of these observatories. Thanks are also due to the Directors of Instituto Geofisico del Peru, Astrophysical Observatory Kodaikanal and of Colaba and Alibag Observatory for permission to use the data. It is a pleasure to acknowledge thanks to Professor K. R. RAMANATHAN for his interest and stimulating discussions during the course of work.

REFERENCES

FERRARO V. C. A. 1954 *J. Geophys. Res.* **59**, 309.

FORBUSH S. E. and CASAVERDE M. 1961 *Equatorial Electrojet in Peru*, C.I.W. Publ. No. 620.

MAEDA H. and YAMAMOTO M. 1960 *J. Geophys. Res.* **65**, 2538.

ONWUMECHILLI A. and OGBUEHI P. O. 1962 *J. Atmosph. Terr. Phys.* **24**, 173.

RASTOGI R. G., TRIVEDI N. B. and KAUSHIKA N. D. 1964 *J. Atmosph. Terr. Phys.* **26**, 771.

SRINIVASAMURTHY B. 1960 *Indian. J. Met. Geophys.* **11**, 64.

SUGIURA M. 1953 *J. Geophys. Res.* **58**, 588.

YACOB A. and KHANNA K. B. 1964 *Indian. J. Met. Geophys.* **15**, 83.

2·3 IV

Reprinted from

Journal of

ATMOSPHERIC AND TERRESTRIAL PHYSICS

PERGAMON PRESS

OXFORD • LONDON • NEW YORK • PARIS

Journal of Atmospheric and Terrestrial Physics, 1966, Vol. 28, pp. 303–310. Pergamon Press Ltd. Printed in Northern Ireland

Night-time disturbance fluctuations in geomagnetic field at equatorial stations

R. G. Rastogi, N. D. Kaushika and N. B. Trivedi
Physical Research Laboratory, Ahmedabad 9, India

(*Received* 8 *September* 1965)

Abstract—The fluctuations in horizontal geomagnetic field H, during the night-time magnetic storms at stations within the equatorial electrojet are studied. The mean ratio of the amplitudes of corresponding fluctuations in H at Huancayo (dip 2°N) to that at San Juan (dip 52°N) is about 8·0 for the midday hours and about 1·7 for the midnight hours. A close similarity in the night-time fluctuations of ΔH is noticed at all equatorial stations in Peru, the mean amplitude having a maximum over the magnetic equator; within a distance of 6° latitude from the magnetic equator the amplitude is reduced to 0·6 times its equatorial value. It is concluded that the fluctuations in ΔH during the night-time hours are significantly enhanced over the magnetic equator for the American zone where the daytime equatorial electrojet currents are strongest, and are due to the remnant equatorial current system flowing during the night-time hours.

Ferraro and Unthank (1951) and Sugiura (1953) showed that the amplitudes of sudden storm commencements are enhanced at Huancayo during the hours of sunlight. Later the enhancement of SC has been found at other longitudes (Srinivasamurthy, 1960; Matsushita, 1960; Maeda and Yamamoto, 1960). Forbush and Casaverde (1961) have shown that the latitudinal variation of the amplitude of SC in H and that of the range in H at equatorial stations in Peru are very similar to each other. Rastogi *et al.* (1964) have studied the latitudinal variations of the amplitude of SC in H at stations in American and Indian zones for the IGY–IGC period and have shown that the enhancement of the amplitude over the magnetic equator is more pronounced in American than in the Indian zone.

Forbush and Casaverde (1961) have found that the deviation in the vertical field (ΔZ) at Peruvian stations due to the SC in the night-time changed its sign at about 8°S geographic latitude and suggested that the equatorial current system on the dark side of the Earth may also flow in the upper atmosphere. Rastogi *et al.* (1966) have studied the SC in H occurring during the night-time at equatorial stations in the American and the Indian zone during IGY–IGC, and found that the enhancement of night-time SC in H is significantly pronounced in the American zone and rather doubtfully pronounced in the Indian zone. The ratio of amplitude of SC in H at San Juan to the same at Huancayo was found to be $0{\cdot}16 \pm 0{\cdot}07$ for the daytime hours and $0{\cdot}60 \pm 0{\cdot}14$ for the night-time hours. However, the ratio ΔH at Alibag/ΔH at Trivandrum was found to be $0{\cdot}41 \pm 0{\cdot}11$ for the midday and $0{\cdot}99 \pm 0{\cdot}13$ for the midnight hours. They suggested the existence of remnant current system over the magnetic equator in the American zone even in the night-time hours.

Forbush and Vestine (1955) have shown that the deviations of H during the initial phase of the magnetic storm are also enhanced over the magnetic equator. Onwumechilli and Ogbuehi (1962) have shown that the fluctuations in H in African zone are enhanced over the magnetic equator during the daytime as well as during the night-time. Comparing the ratio of irregular storm variations at an equatorial and non-equatorial observatories both in the same longitude zone, CHAPMAN and RAJA RAO (1965) have shown the daytime enhancement of the irregular storm fluctuations and indicated that the enhancement does not continue throughout the night. They found that the daytime enhancement was greatest for the Pacific pair of stations and least for the Indian pair, but have not shown the same for the American zone. Having found that the SC in H during the night-time is significantly enhanced over the magnetic equator along the American zone even during the night-time hours, it was felt necessary to study the irregular fluctuations in H following the magnetic storms at stations along the American zone.

Huancayo (12·1°S, 75·3°W, dip 1·9°N) and San Juan (18·4°N, 66·1°W; dip 52°N) were chosen as the equatorial and non-equatorial observatories respectively within the American zone. There is a difference of only 37 min between the local mean times at the two places and so no corrections are made in the observed individual fluctuations at the two places. Significant fluctuations in H at Huancayo and San Juan having close correspondence were noted and peak to peak deviations ΔH(HU) and ΔH(SJ) were measured. Figures 1 and 2 are the tracings of H magnetograms at Huancayo and San Juan showing significant fluctuations during the night-time and the daytime hours respectively. It was found that most of the night-time fluctuations have very close correspondence at the two stations as seen in Fig. 1. During the daytime hours, very large and frequent fluctuations were observed at Huancayo many of which were not reproduced in San Juan. Further very large daily variation in H at Huancayo causes large error in measuring the peak to peak value of the fluctuations caused by only the storm effect. So only sharp fluctuations of duration less than 30 min were read. Consequently comparatively fewer observations could be obtained for the daytime fluctuations having correspondence between the two places. The ratio $\Delta H(\mathrm{HU})/\Delta H(\mathrm{SJ})$ were computed for each fluctuations and 427 such ratios were obtained spread over all hours of the day and night. These ratios were grouped according to the local time of the peak at Huancayo. The mean value $\Delta H(\mathrm{HU})/\Delta H(\mathrm{SJ})$ was calculated for each hour and is shown in Fig. 3. The diagram also shows the standard deviation of each of the mean ratio.

It is interesting to note that only 17 out of 427 cases were found when the ratio $\Delta H(\mathrm{HU})/\Delta H(\mathrm{SJ})$ was equal to or less than unity. There is a distinct enhancement of the fluctuations during the daytime, the smooth curve passing through the points for the individual hour is asymmetric about noon. If the local time difference were taken into account the maximum of the ratio should be shifted at a time later than noon, while the observed maximum is earlier than noon. Similar curve given by CHAPMAN and RAJA RAO (1965) for Jarvis/Honolulu pair clearly indicates the peak at 11 hr. It may be noted from RASTOGI *et al.* (1965) that the mean daily variation of the amplitude of solar flare crochet in H at equatorial station is asymmetric about noon, the maximum being in the forenoon hours.

The individual values of the ratio for midday hours varied over a large range due to reasons mentioned earlier, giving rise to large standard deviation of the mean ratio. The mean value of the ratio for 9–13 hr is $8{\cdot}00 \pm 3{\cdot}4$ for Huancayo and San Juan pair. The mean value of the ratio over 9–13 hr derived from the curves

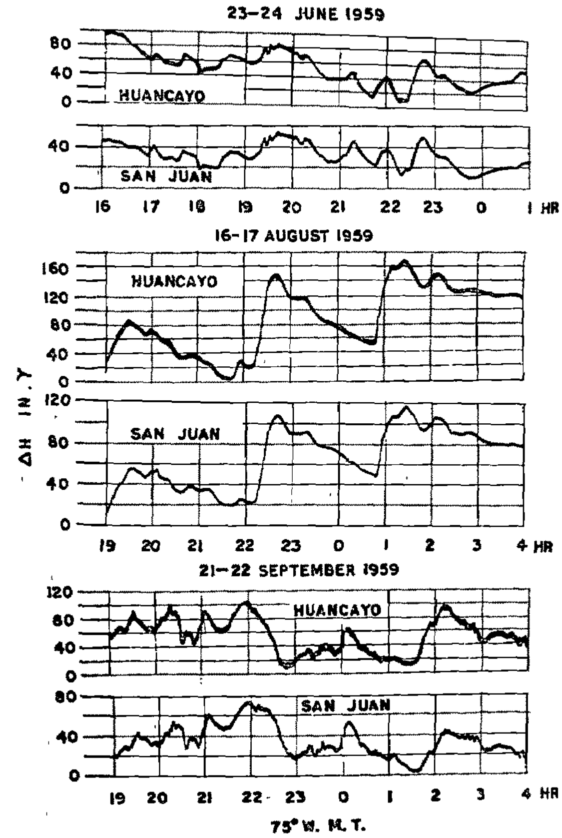

Fig. 1. Tracings of H magnetograms of Huancayo and San Juan during the night-time disturbances.

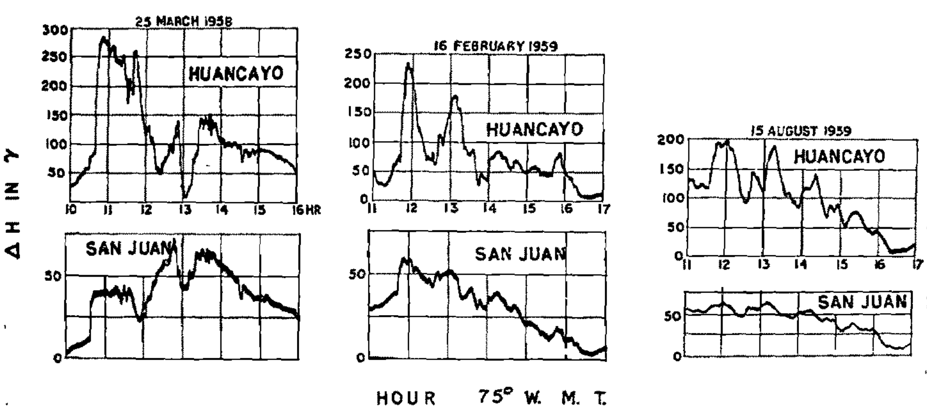

Fig. 2. Tracings of H magnetograms of Huancayo and San Juan during the day-time disturbances.

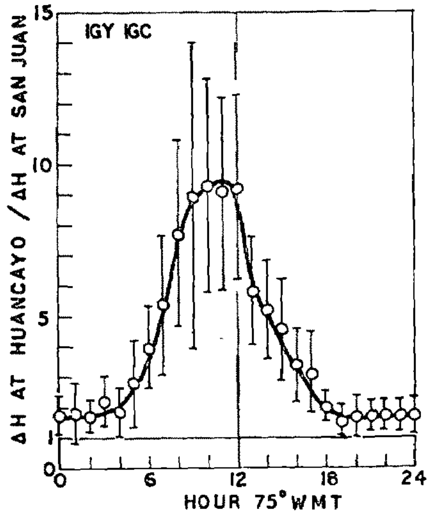

Fig. 3. Variation of the ratio of ΔH at Huancayo to the same at San Juan at different times of the day.

given by Chapman and Raja Rao is 4·3 for Jarvis/Honolulu pair; 2·7 for Koror/Muntinlupa pair and 2·3 for Trivandrum/Alibag pair. RASTOGI *et al.* (1966) have found the ratios of midday SC (H) amplitude to be 6·25 for Huancayo/San Juan pair and 2·44 for Trivandrum/Alibag pair. Thus the daytime enhancement of storm fluctuations in H is greatest along the American zone, and least along the Indian zone and intermediate along the pacific zone. This is very similar to the longitudinal variation of the daily range of H along the magnetic equator (RASTOGI 1962). Thus the daytime storm fluctuations in H are enhanced over the magnetic equator and are further related to the strength of the normal electrojet in the particular longitudes.

The mean ratio of $\Delta H(\mathrm{HU})/\Delta H(\mathrm{SJ})$ for storm fluctuations during the night-time hours vary between 1·50–2·20, the mean value over 2200–0200 hrs 75° W.M.T. is 1·73 ± 0·66 and hence is significantly greater than unity. The corresponding value derived from the curves given by CHAPMAN and RAJ RAO (1965) are 1·18 for Jarvis/Honolulu pair, 0·80 for Koror/Muntinlupa pair and 0·95 for Trivandrum/Alibag pair. RASTOGI *et al.* (1966) have found that ratio of midnight SC in H to be 1·67 for Huancayo/San Juan pair and 1·01 Trivandrum/Alibag pair. Thus it may be concluded that during the night-time the storm fluctuations are enhanced over the magnetic equator along the American zone, to lesser degree along the Pacific zone and the effect is not evident along the Indian zone. This behaviour is again analogous to the longitudinal variation of the electrojet strength.

To further check the electrojet effect in the storm time fluctuations series of magnetograms at closely spaced observatories in Peru viz. Huancayo (dip 1·9°N), Yauca (dip 4·4°S), Chimbote (dip 6·4°N), Chiclayo (9·8°N) and Talara (dip 12·6°N) during two post-storm fluctuations have been reproduced in Fig. 4 for the daytime hours and Fig. 5 for the night-time hours. Referring to Fig. 4 one sees that the fluctuations are very faithfully reproduced in all the five magnetic observatories.

A gradual and distinct decrease of the amplitude from Huancayo to Talara is clearly noticed. Further the enhancement of the amplitude at Huancayo in relation to the same at other observatories is more pronounced for the hours around noon than for the evening hours.

Referring to Fig. 5 one sees a remarkable similarity in the fluctuations at individual observatories. A close examination of the relative amplitudes indicate that the amplitude decreases steadily from Huancayo to Talara. The mean ratio of the

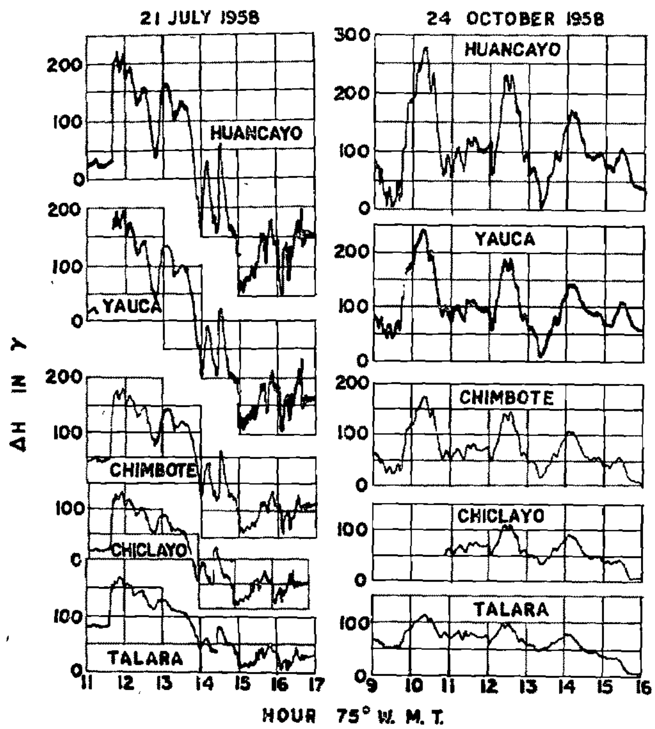

Fig. 4. Tracings of H magnetograms at equatorial observatories in Peru during the daytime disturbances.

peak to peak fluctuations at each station with respect to the same at Huancayo have been computed and are plotted against the magnetic dip in Fig. 6. There is a distinct maximum of the ratio over the magnetic equator. The ratio rapidly falls to about 0·6 at Talara which is about 6° away from the equator. Beyond Talara the ratio decreases very slowly, it decreases from a value of 0·65 at Talara to a value of 0·57 at San Juan (Geog. lat 18·4°N). Thus it is concluded that the night-time storm fluctuations in H are sharply enhanced over the magnetic equator similar to various other phenomena associated with the equatorial electrojet.

If the enhancement in the amplitude of storm-time fluctuations of the horizontal component, ΔH, over the magnetic equator during the night-time is due to the remnant night-time equatorial electrojet then one would expect the corresponding variations in the vertical magnetic field, ΔZ, also to be controlled by the equatorial

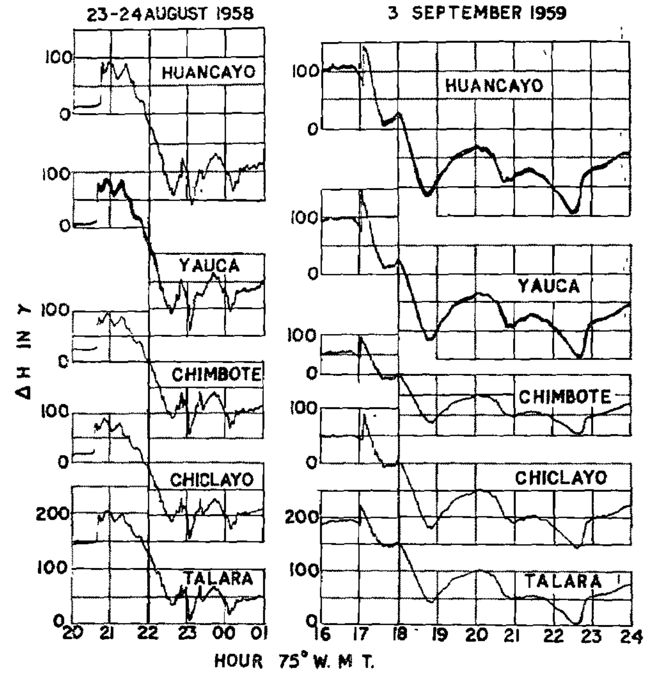

Fig. 5. Tracings of H magnetograms at equatorial observatories in Peru during the night-time disturbances.

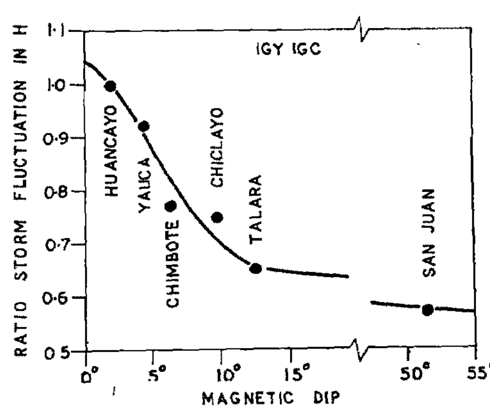

Fig. 6. The variation with magnetic dip of the storm-time fluctuations in H relative to that at Huancayo.

electrojet. Variations of ΔH with latitude during sudden commencements and solar flares have been described in earlier papers RASTOGI *et al.* (1965, 1966). The mean ratios of $\Delta H_n/\Delta H_0$ and $\Delta Z_n/\Delta H_0$; where H_0 is the change in H at Huancayo and ΔH_n and ΔZ_n are the corresponding changes in H and Z respectively at any other stations, are calculated for daytime sudden commencements, solar flare effects and night-time sudden commencements at all the Peruvian observatories. The latitudinal variation of $\Delta H_n/\Delta H_0$ and $\Delta Z_n/\Delta H_0$ for these three disturbances are shown in the Fig. 7.

It is seen from Fig. 7 that the maximum value of $\Delta H_n/\Delta H_0$ during S.F.E. or SC occurs close to Huancayo. The $\Delta Z_n/\Delta H_0$ also changes its sign at Huancayo which is about 1° north of the dip equator. In the case of night-time SC's the maximum value of $\Delta H_n/\Delta H_0$ occurs close to Huancayo but $\Delta Z_n/\Delta H_0$ change sign somewhere between Chimbote and Chiclayo.

Assuming the electrojet to be confined in a band of uniform current density and having a certain width flowing at a certain height above the surface of the plane earth one expects that there would be maximum H at the centre of the electrojet

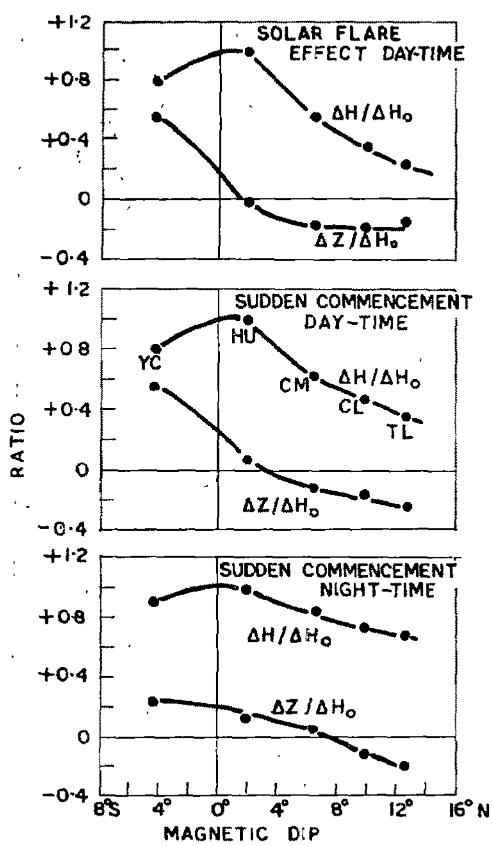

Fig. 7. Variation with magnetic dip of the ratios $\Delta H_n/\Delta H_0$, $\Delta Z_n/\Delta H_0$ of solar flare crochet day time SC and night-time SC at Peruvian stations.

where ΔZ would change its sign (Chapman, 1951; Onwumechilli, 1959). If the observed changes in H and Z are due to the super-imposition of the electrojet effect over the effect due to normal S_q current then the peak in ΔH and zero value of ΔZ would be shifted from the position of the dip equator by an amount depending upon the amplitude and phase interaction between the electrojet effect and the normal variation.

Along the Peruvian longitudes the dip and dipole equators are respectively at 13°S and 11°S geographic latitude. The centre of the electrojet, at Huancayo is midway between these equators. Still the existence of the peak ΔH at Huancayo and minimum $|\Delta Z|$ near Chimbote for the night-time SC's is not clearly understood.

Conclusions

The daytime storm fluctuations in H are enhanced over the magnetic equator and are related to the strength of the normal electrojet in the particular longitude zone.

The night-time storm fluctuations in H in American zone is enhanced over the magnetic equator similar to various other phenomena controlled by the equatorial electrojet, suggesting the existence of a remnant equatorial electrojet current during the night-time. No such enhancement is seen for the Indian zone.

Acknowledgements—Thanks are due to world data centres (for the Ionosphere and Airglow at Boulder and for Geomagnetism at Washington, D.C) for supplying the microfilm of the magnetograms of these observatories. It is a pleasure to acknowledge thanks to Professor K. R. Ramanathan for his interest and suggestions during the course of work.

References

Chapman S.	1951	*Arch. Met. Geophys. Bioklim.* **4A**, 368.
Chapman S. and Raja Rao K. S.	1965	*J. Atmosph. Terr. Phys.* **27**, 559.
Ferraro V. C. A. and Unthank H. W.	1951	*Geofis. Pura. Appl.* **20**, 3.
Forbush S. E. and Casaverde M.	1961	Equatorial Electrojet in Peru, *C.I.W. Publ. No.* 620.
Forbush S. E. and Vestine E. H.	1955	*J. Geophys. Res.* **60**, 299.
Meada H. and Yamamoto M.	1960	*J. Geophys. Res.* **65**, 2538.
Matsushita S.	1960	*J. Geophys. Res.* **65**, 1423.
Onwumechilli C. A.	1959	*J. Atmosph. Terr. Phys.* **13**, 235.
Onwumechilli C. A. and Ogbuehi P. O.	1962	*J. Atmosph. Terr. Phys.* **24**, 173.
Rastogi R. G.	1962	*J. Atmosph. Terr. Phys.* **24**, 1031.
Rastogi R. G., Trivedi N. B. and Kaushika N. D.	1964	*J. Atmosph. Terr. Phys.* **26**, 771.
Rastogi R. G., Kaushika N. D. and Trivedi N. B.	1965	*J. Atmosph. Terr. Phys.* **27**, 663.
Rastogi R. G., Trivedi N. B. and Kaushika N. D.	1966	*J. Atmosph. Terr. Phys.* **28**, 131.
Srinivasamurthy B.	1960	*Indian J. Met. Geophys.* **11**, 64.
Sugiura M.	1953	*J. Geophys. Res.* **58**, 588.

2.3 V Studies of the sudden changes in H at Equatorial stations in American zone

Summary

The storm sudden commencements (SC) and sudden impulses (SI) in H at equatorial stations in American zone during IGY/IGC are discussed. The occurrence of SI is most frequent around midday whereas distribution of SC frequency with local time is uncertain. The amplitude of both SC and SI at the equatorial stations are enhanced during daylight hours. At any particular hour the amplitudes are enhanced only over a narrow zone over the magnetic equator. The enhancement is identical for SC and SI. It is suggested that the mechanism for equatorial enhancement for SC and SI is same.

Introduction

A significant difference in the daily variation of the amplitude of sudden commencement (SC) of magnetic storm at the equatorial station Huancayo and at other stations was first pointed out by Ferraro and Unthank (19 1); the maximum amplitude at Huancayo occurred around noon while at other stations it had a tendency to occur around mid-night. The maximum amplitude at Huancayo was considerably larger than at other stations. Similar noon-time maximum of the SC and SI amplitude have been reported for equatorial stations by other authors (Sugiura, 1953, Srinivasa Murthy, 1960, Matsushita, 1960, Maeda and Yamamoto 1960a, 1960b). Comparing the amplitudes for the same SC's in H at equatorial stations within the same longitude zone, Rastogi et al (1964) showed an enhancement of the amplitude occurring around 10-14 hrs. L.M.T. over the magnetic equator very similar to the latitudinal variation of the daily range of H. Later Rastogi et al (1966a and b), pointed out that, during night-time at stations in the American zone, the amplitude of SC in H was slightly enhanced over the magnetic equator (although not comparable to the midday enhancement) and that the fluctuations in H were also slightly enhanced. Therefore it seemed worthwhile to study in detail all the sudden changes in H at equatorial stations. The present paper discusses the daily variation in amplitude of storm sudden commencements (SC) and sudden impulses (SI) in H at American stations during IGY/IGC.

The stations studied and their coordinates are given in Table 1. The amplitudes of sudden changes (SC or SI) were read from the microfilm copies of the magnetograms obtained through the courtesies of W.D.C. for Geomagnetism in Washington D.C., U.S.A. Occurrence of SC or SI were checked with the lists published in IAGA bulletins Nos.

Table-1.

The geographic coordinates and magnetic dip angle of the stations studied

Station	Dip	Geog. lat.	Geog. long.
Huancayo	1.9°N	12°03'S	75°20'W
Yauca	4.4°S	15°32'S	74°40'W
Chimbote	6.4°N	9°06'S	78°36'W
Chiclayo	9.8°N	6°48'S	79°48'W
Talara	12.6°N	4°38'S	81°18'W
Paramaribo	33°N	5°49'N	55°13'W
San Juan	52°N	18°01'N	66°09'W

121, 12m2 and 12n2 giving list of rapid variations for the years 1957 to 1959. The sudden changes in all the three components of the magnetic field occurring at the same time which were preceded by a quiet condition and followed by disturbed condition were designated as SC, while others were designated as sudden impulse SI. The amplitudes of SC or SI were read as those between the predisturbed level to the first major peak following the sudden change. Care was taken to measure the amplitude between identical points on the magnetograms of different stations, and only those events were utilised in the analyses which were identified at all the stations.

As described by earlier authors (Ferraro et al, 1951; Beagley, 1952) the SC or SI may have major positive deviation or major negative deviations, and at times these may have preliminary small deviations in a direction reverse to the main one. Following Akasofu and Chapman (1960) these are denoted as SC(+), SC(-), SC(+ -) or SC(- +) indicating the sign of the change (S) in H and also their order, when there are changes of more than one sign. Few examples of SC and SI observed at Huancayo are shown in Fig. 1. The magnetograms contain normal recordings of

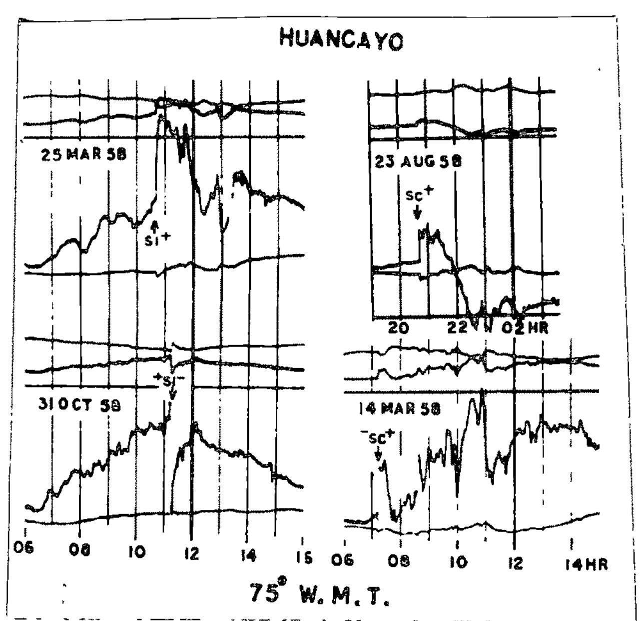

Figure.1.

H, D, Z as well as insensitive recording of H. The Figs. 1(a) and 1(b) show conventional SI+ and SC+ respectively consisting of only positive main deviations of H. Simultaneous deviations in D and Z components are also seen. Fig. 1(c) shows an example of SI consisting of a small positive deviation followed by a major negative deviation in H (SI+ -). Fig. 1(d) shows the example of SC- + consisting of main positive deviation preceded by a small negative deviation.

The distributions of the number of occurrence of SC and SI at Huancayo with the local time are shown in Fig. 2 for the IGY/IGC period and for the period 1951-61

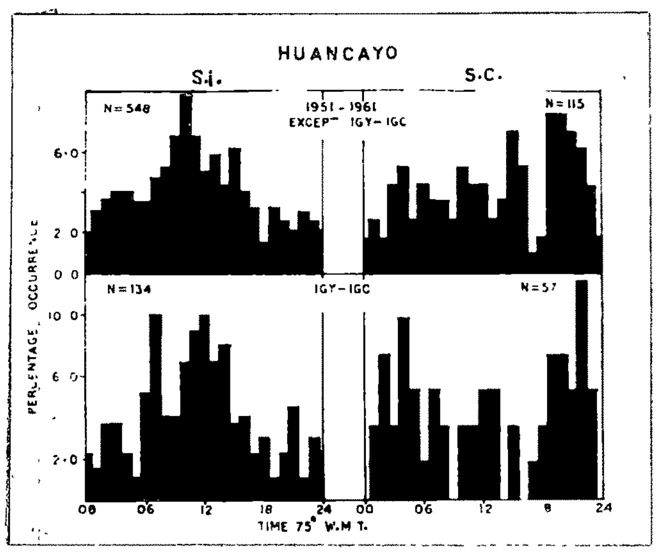

Figure.2.

excluding the IGY/IGC. Referring to SC histograms, during the IGY/IGC the occurrences were more during night than during day. During 1951-61 there is no definite variation except a maximum around 19 hr. Referring to SI histogram, during IGY/IGC the number of occurrences were maximum around midday and minimum near sunrise and sunset periods. During 1951-61, the daytime peak is slightly earlier and the sunrise and sunset minima are not clear. The SI are seen to be most frequent around midday hours. Ferraro et al, (1951), also found that the daily variation in the occurrence of SC in H was very small while that for SI showed marked variation with the time of the day.

Fig. 3 shows the tracings of magnetograms

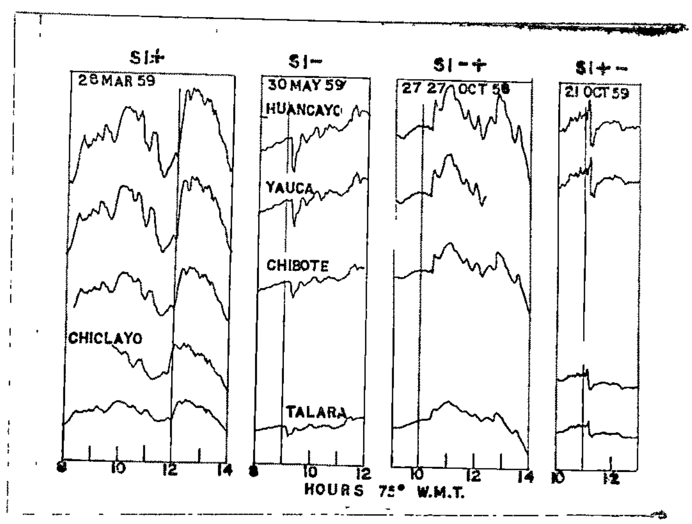

Figure.3.

showing different types of SI recorded at the equatorial stations in Peru, South America. It is seen that the fluctuations in H at all these stations are remarkably similar. While reading the amplitudes of SC and SI at all these stations, care was taken to measure the distance between identical points of a particular event at different stations. It is also clearly seen from Fig. 3 that the amplitude of SI progressively decreases from Huancayo to Talara.

The mass plot of the amplitude and time of occurrence of all SC+, SI+ and SI- at the equatorial station Huancayo and the mid-latitude station San Juan are separately shown in Fig. 4. It is clearly seen that

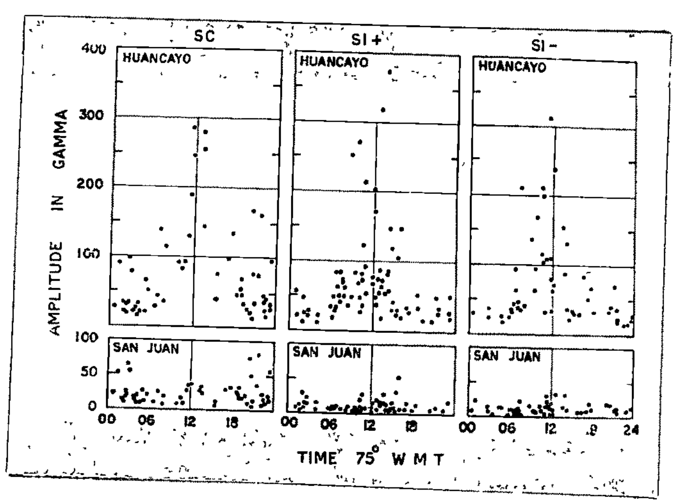

Figure.4.

SC+, SI+ or SI- at Huancayo show an enhancement of the amplitude around noon, while there is no clear diurnal variation of the different types of sudden changes in H at San Juan. The amplitude distributions of SI+ and SI- at each station are similar and therefore both SI+ and SI- are grouped together and designated as SI hereafter.

Fig. 5 shows the mass plot of the amplitude

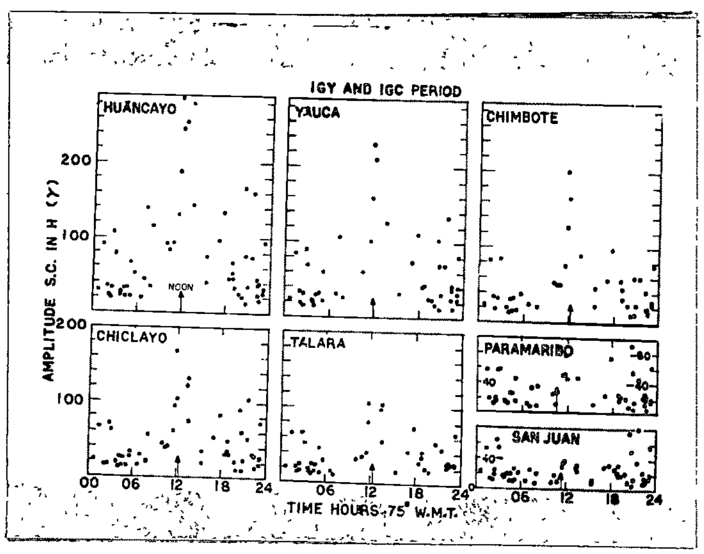

Figure.5.

and time of occurrence of SC in H at all the seven stations studied. The midday enhancement of SC amplitude is greatest at Huancayo and there is systematic decrease of the midday amplitude of SC from Huancayo to Talara. At Paramaribo and San Juan there is no day-time enhancement of the amplitude. Similar features are seen in the case of SI amplitudes shown in Fig. 6.

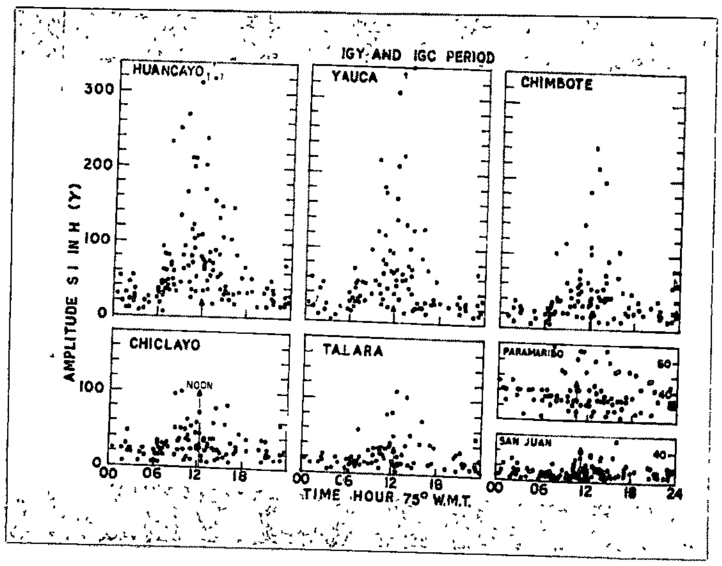

Figure.6.

At any particular hour the range of amplitude of SC or SI is fairly large due to the different intensity of solar disturbances causing these. The average diurnal variation of amplitude of SC or SI is therefore difficult to be drawn. To determine the daily variation of SC or SI amplitude, the ratio of a particular SC or SI at any station to the amplitude of the same SC or SI at Huancayo were calculated. The variation of this ratio with the solar time at different stations are shown in Fig. 7 for SC's and in Fig. 8 for SI's.

Referring to Fig. 7 one sees that the normalized

SC amplitude at any of the stations shows a distinct

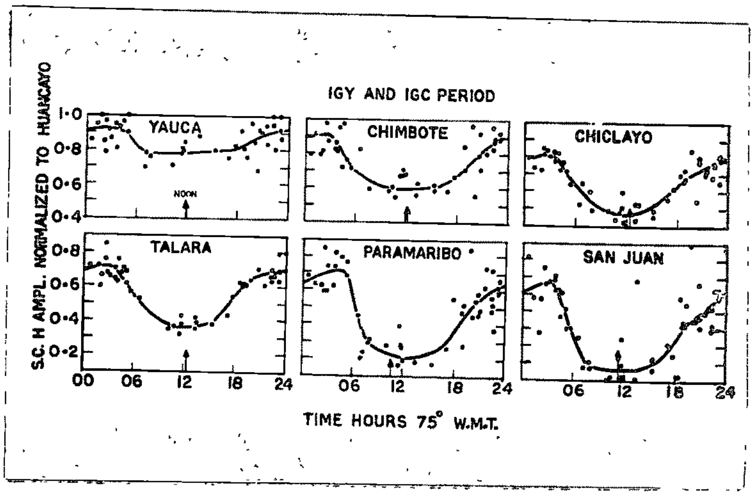

Figure.7.

diurnal variation with a minimum around noon and a constant value during the night. The daily variation curve for normalized SC amplitudes at any of the stations is fairly symmetrical about noon. At San Juan the SC amplitude are reduced to 0.7 times that at Huancayo during the night-time and less than 0.2 times that at Huancayo during the day-time hours. Thus the increase of SC amplitude with decreasing latitude is most pronounced at noon.

Referring to Fig. 8 showing normalized SI amplitude one finds similar daily variation as for SC except that the curve at any station is significantly unsymmetrical about noon, the minimum being around 10 hr.

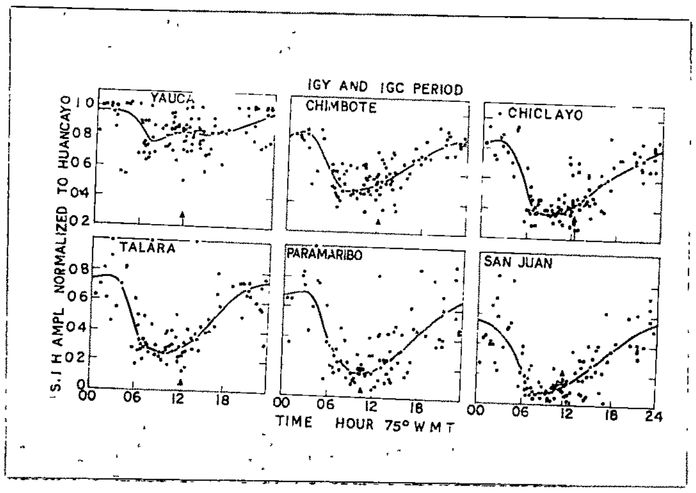

Figure.8.

Further the normalized amplitude increases progressively from San Juan to Yauca the increase being smaller during night than during day.

In Fig. 9 are shown the latitudinal variations of normalized amplitude of SC and SI for the day-time period (1000-1400 hr.) and for the night-time period (2100-0300 hr.). The average value of normalized amplitude of SC and SI amplitudes with its standard deviation are given in Table 2. The decrease of normalized amplitude with latitude is identical for SC and for SI. The latitudinal variation of SI or SC near the equator is very

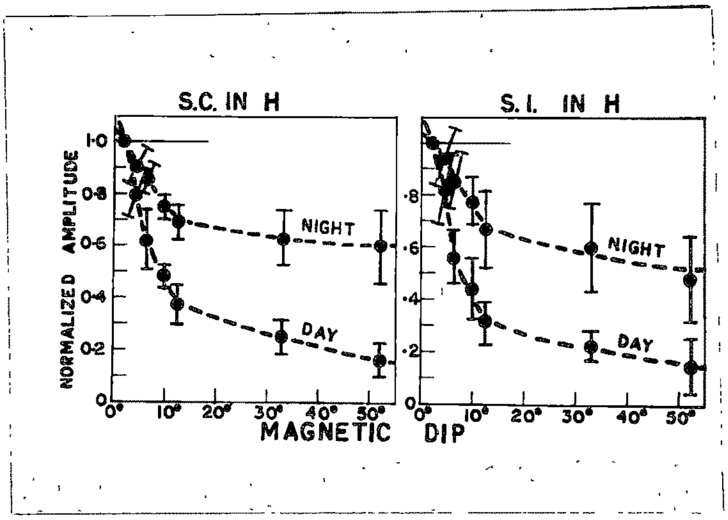

Fig.9.

similar to that of the solar daily range of H. Thus the

Table-2-. Average amplitude of sudden changes normalized to that at Huancayo for day-time (10-14 hr.) and for night-time (21-03 hr.).

Station	S.C.Day	S.I.Day	S.C.Night	S.I.Night
Huancayo	1.00	1.00	1.00	1.00
Yauca	0.80±0.05	0.82±0.14	0.91±0.08	0.95±0.12
Chimbote	0.62±0.06	0.56±0.11	0.86±0.06	0.85±0.11
Chiclayo	0.48±0.05	0.44±0.12	0.75±0.05	0.77±0.09
Talara	0.37±0.04	0.28±0.09	0.69±0.07	0.67±0.15
Paramaribo	0.25±0.07	0.22±0.06	0.63±0.10	0.60±0.17
San Juan	0.16±0.07	0.15±0.11	0.60±0.14	0.48±0.16

enhancement of the amplitude of SC or SI are definitely associated with the equatorial electrojet currents.

It is further seen that during the night-time also both SC and SI show the enhancement near the magnetic equator.

These results indicate the essential similarities in the mechanisms of both SC and SI recorded at ground magnetometer.

Acknowledgement

Authors are thankful to Professors K.R. RAMANATHAN and P.R. PISHAROTY for discussions and suggestions during the course of work.

References

Akasofu S.I. and Chapman S.	1960	The sudden commencements of geomagnetic storms, Variana, No. 250.
Beagley J.W.	1952	Geomagnetic sudden commencement analysis - Amberley, New Zealand, J. Sci. and Technology, 33B, 460-470.

Ferraro V.C.A., Parkinson W.C. and Unthank H.W. 1951 Sudden commencements and sudden impulses in geomagnetism, J. Geophys. Research., 56, 177-195.

Ferraro V.C.A. and Unthank H.W. 1951 Sudden commencements and sudden impulses in geomagnetism, Geofis. pura e appl., 20, 3-6.

Matsushita S. 1960 Studies on sudden commencements of geomagnetic storms using IGY data from U.S. Stations, J. Geophys. Research, 65, 1423-1435.

Maeda H. and Yamamoto M. 1960a A note on daytime enhancement and the amplitude of geomagnetic storm sudden commencements in the equatorial region, J. Geophys. Research, 65, 2538-2539.

Maeda H. and Yamamoto M. 1960b Day-time enhancement of the amplitude of geomagnetic sudden impulses in the equatorial region, Rept. Ionosphere & Space Research, Japan, 14, 443-444.

Nishida A. and Jacobs J.A. 1962 World-wide changes in the geomagnetic field, J. Geophys. Research, 67, 525-540.

Rastogi R.G., Trivedi N.B. and Kaushika N.D. 1964 Some relations between the sudden commencement in H and the equatorial electrojet, J. Atmosph. Terr. Phys., 26, 771-776.

Rastogi R.G., Trivedi N.B. and Kaushika N.D. 1966a Night-time sudden commencements in H within the equatorial electrojet region, J. Atmosph. Terr. Phys., 28, 131-136.

Rastogi R.G., Kaushika N.D. and Trivedi N.B. 1966b Night-time disturbance fluctuations in geomagnetic field at equatorial stations, J. Atmosph. Terr. Phys. 28, 303-310.

Sugiura M. 1953 The solar diurnal variation in the amplitude of sudden commencements and

geomagnetic storms at
geomagnetic equator, J.
Geophys. Research, 58,
558-559.

2.3(f) VI Studies of sudden changes in H and Z at equatorial stations in the Indian zone

Abstract

The storm time commencements (SC) and sudden impluses (SI) in H and Z at equatorial stations in the Indian Zone during IGY/IGC are discussed. The amplitude of both SC and SI in H at the equatorial stations are enhanced during the midday hour. At any particular hour during the day-time the amplitudes are enhanced over a narrow zone over the magnetic equator. There is no distinct latitudinal enhancement of SC or SI during night-time but the amplitudes are significantly higher at Annamalainagar. The latitudinal variation of the amplitude of SC in Z in Indian zone do not conform to the simple thin sheet model of the electrojet and the interpretation should be sought in the abnormal induced currents.

Introduction:- The enhancement of the amplitudes of sudden changes in the horizontal component (SC or SI) in H have been shown at stations close to the magnetic equator by various authors (Sugiura, 1953; Srinivasamurthy, 1960; Maeda and Yamamoto, 1960a, b and Rastogi, 1963). Forbush and Vestine (1955) suggested that the daytime enhancement of the sizes in SC(H) are closely associated with the current system responsible for large diurnal variation in H viz. equatorial electrojet currents.

The enhancement of the midday values of SC, SI and crochet over the magnetic equator was shown first by Forbush and Casaverde (1961) and it has been studied in detail by Rastogi et al (1964, 1965) for both the American and Indian zones. The variations of the amplitudes of day-time SC in H and Z at the American station were found to be similar to that expected from a thin current sheet model of the electrojet (Forbush and Casaverde, 1961, and Rastogi et al, 1966b). The study of SC in H during the night-time hours showed that there is a significant equatorial enhancement in American zone (Rastogi et al, 1966a).

Chapman and Raja Rao (1965) have shown that the ratio of the storm time fluctuations in H under electrojet and non-electrojet stations indicate a daytime enhancement in the Pacific, Atlantic and Indian zones. The enhancement did not continue during the night-time and it was suggested that this was due to depletion of E layer ionisation and the absence of electrojet currents. However Rastogi et al, (1966b) showed that in the American zone the fluctuation ratio between Huancayo and San Juan is 8.0 ± 3.4 for the day-time hours and 1.73 ± 0.66 for the night-time hours. The ratio was significantly greater than unity and was suggested due to remnant electrojet currents flowing in the night-time in the American zone.

In a recent article Rastogi and Trivedi (1968) had studied in detail the sudden changes due to SC or SI in H at different hours of the day at all low latitude stations in the American zone, during the period IGY/IGC. The midday enhancements or the equatorial enhancements were found to be identical for SI and SC. It was suggested that the mechanism for equatorial enhancements of SC and SI is the same. The present paper describes similar studies carried out for Indian stations for the period IGY/IGC. The coordinates of the stations are given in Table 1. It is seen that the three observatories - Trivandrum,

Table-1. Coordinates of the stations

Observatory	Geographic latitude	Geographic longitude	Geomagnetic latitude	Dip
Trivandrum	8.5°N	77.0°E	0.9°S	0.7°S
Kodaikanal	10.2°N	77.5°E	0.7°N	3.6°N
Annamalainagar	11.4°N	79.7°E	1.4°N	5.3°N
Alibag	18.6°N	75.9°E	9.5°N	24.6°N

Kodaikanal and Annamalainagar are within the equatorial electrojet zone while Alibag is outside. The amplitudes of SC or SI were directly read from the microfilm copy of the magnetograms and extreme care was taken that they corresponded to identical points for different stations. The amplitudes were measured from the pre-disturbed value to the first major excursion and reverse minor excursions before the main one were not taken into account.

Fig. 1 shows the mass plot of the amplitude

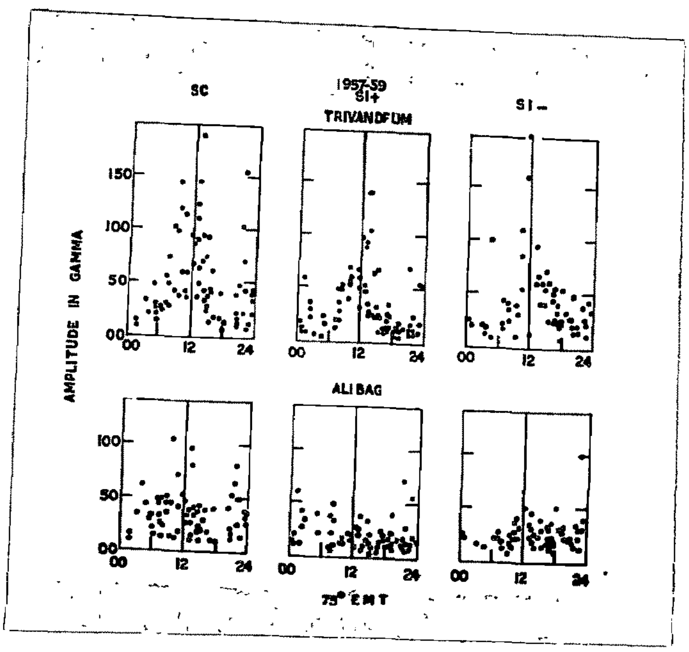

Figure.1.

versus local time for SC, SI+ and SI- at the equatorial station (Trivandrum) and non-equatorial station (Alibag). It is clearly seen that SC+, SI+ or SI- at Trivandrum show an enhancement of the amplitude around noon whereas there is no clear diurnal variation of the amplitude at Alibag. Further it is seen that the daily variation of SI+ or SI- are identical and these are grouped together and designated as SI hereafter, in later descriptions.

Fig. 2 shows the mass plots of amplitude versus

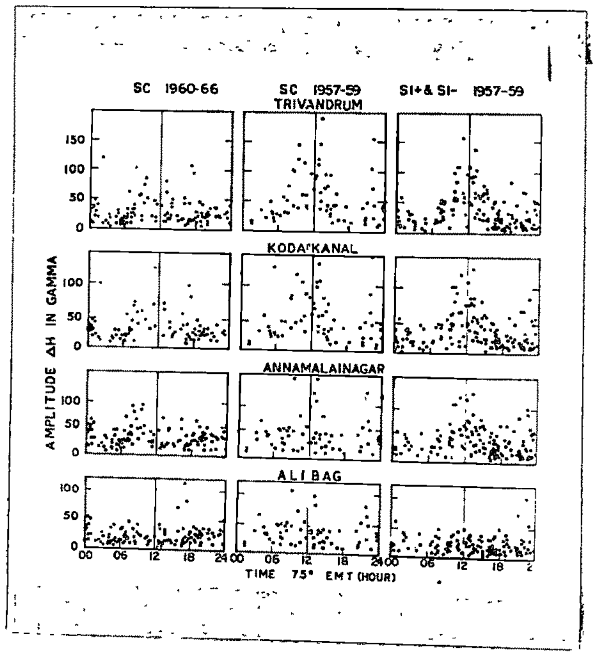

Figure.2.

local time of SC and SI during IGY/IGC at each of the observatories. The mass plots of SC(H) during the period 1960-66 are also shown for comparison. It is seen that during the IGY/IGC there is a distinct midday enhancement of the amplitude of SC as well as SI at equatorial electrojet stations though the enhancements decrease from Trivandrum to Annamalainagar. The enhancement was rather less distinct during the low sunspot period, 1960-66, probably due to fewer severe magnetic disturbances.

The mass plots described in previous paragraphs would not show the true diurnal variation due to the wide variations in the intensity of individual magnetic storm. Therefore to determine the latitudinal variations of the sudden changes in H, it was thought proper to normalize the individual amplitudes at any particular station with the amplitude of the same event at the equatorial station which in the present case has been taken as Trivandrum. The mass plot of this normalized amplitude versus local time for the SCs during 1957-66 and in SI during the period 1957-59 are shown in Fig. 3. It is seen from the

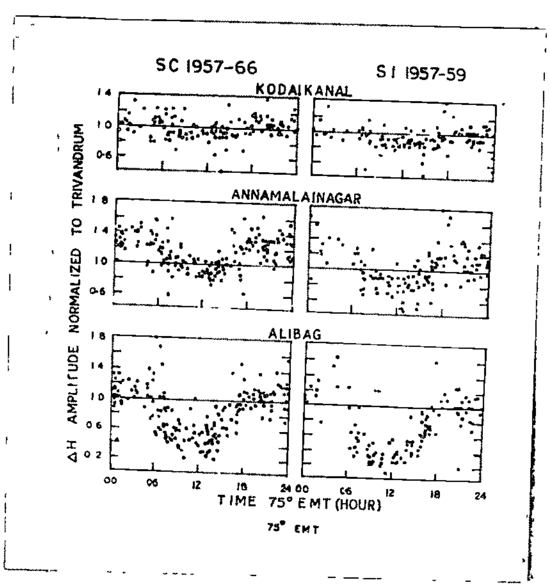

Figure.3.

Figure that this ratio for any station is minimum around midday hours and the midday depression is more at higher latitudes. This indicates the enhancement of the SC and SI amplitude during the midday hours over the magnetic equator. Referring to Kodaikanal diagrams the values are mostly less than 1.0 for the daytime and greater than 1.0 for the night-time indicating that amplitudes during the night-time are slightly greater at Kodaikanal than at Trivandrum. This is much more clear for Annamalainagar where the ratio is 1.2 to 1.4 for night-time. Referring to Alibag diagrams, the diurnal variation of the normalized amplitude seems to be fairly symmetrical about local noon and thus it is slightly different from similar diagrams for the American zone where the SI was found to have a minimum value at few hours before noon. Enhancement seems to start almost with sunrise is maximum around noon and vanishes by sunset, and is clearly associated with the development of the electroject current systems.

To determine the latitudinal variations of the amplitude, the data were grouped into day-time period (10-14 hrs.) and the night-time period (21-03 hrs.), The average value of normalised amplitude of SC and SI with its standard deviation are given in Table 2 whereas these are plotted against dip angle in Fig. 4. It is seen that during the day-time both SC and SI show distinct enhancement at the equator. The diagram indicates that the enhancement of SC is slightly more than that for SI. At the American zone, no such difference is detected between the enhancements of SI and SC. Referring to the SC or SI amplitudes in the night-time it is found that the amplitudes are almost the same at Trivandrum, Kodaikanal and Alibag whereas at Annamalainagar the amplitudes are about 1.2 times that at

Table 2.

Average amplitude of sudden changes normalized to that at Trivandrum for day-time (1000 to 1400 hrs.) and for night-time (2100 to 0300 hrs.) during IGY/IGC.

Station	SC Day	SI Day	SC Night	SI Night
Trivandrum	1.00	1.00	1.00	1.00
Kodaikanal	0.91±0.06	0.88±0.08	1.00±0.06	0.96±0.14
Annamalainagar	0.89±0.07	0.78±0.17	1.21±0.09	1.14±0.18
Alibag	0.41±0.11	0.32±0.11	0.99±0.13	1.02±0.18

other observatories. This could be interpreted as the absence of equatorial enhancement with abnormal value at Annamalainagar, or as the shift of the latitude of enhancement at Annamalainagar during the night. With the

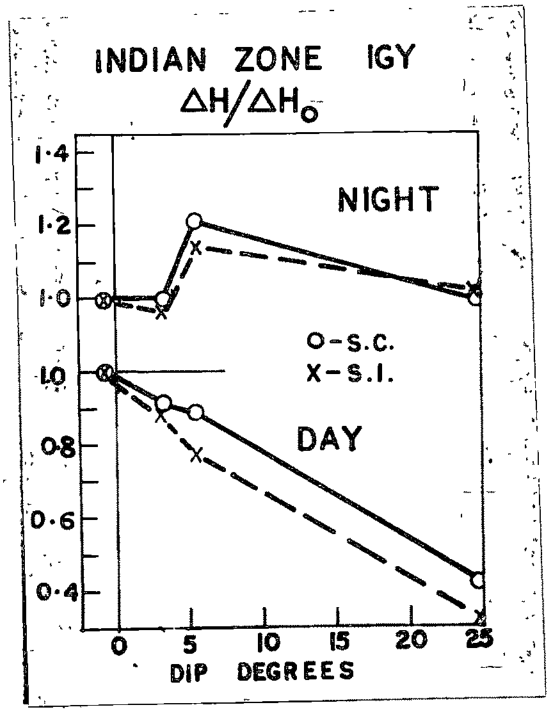

Figure.4.

present amount of data this could not be decided.

In Fig. 5 are shown the latitudinal variations

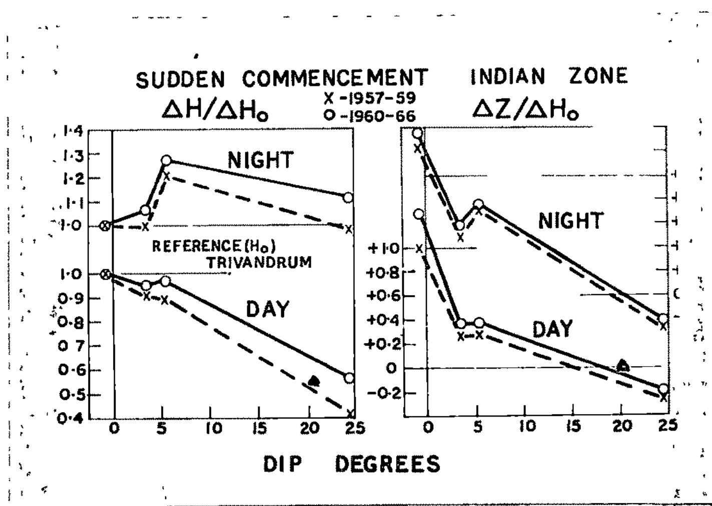

Figure.5.

Figure.5.

of the amplitude of SC in H and Z normalized to the same at Trivandrum for the event occurring during the day-time as well as the night-time. The data for the period 1960-66 also have been added for comparison with the results for IGY/IGC period. During the day-time the SC(H) shows the maximum at the equator and reverse their sign between 15 to 20° dip whereas the theoretical considerations on the basis of thin current sheet model of the electrojet requires the reversal in Z component to occur at latitude very close to the equator. The changes in Z due to SC and SI during the night-time are very similar to that for the day-time.

An additional magnetic observatory was established at Hyderabad (Geographic latitude 17.4°N, longitude 78.6°E and dip 20.5°) around middle of 1964. During 1965-66 very few sudden commencements occurred due to low solar activity. Based on available published data, the mean ratios of SCs in H and Z were computed and indicated as a closed triangle in Fig. 5. It is seen that normalized ratio for SC(H) falls within the curves based on the results of Annamalainagar and Alibag. Regarding the ratio of SC(Z) the amplitudes are found to be very small of the order of 2 or 3 and were some time positive and some time negative confirming our earlier conclusions that a change over in the sign of sudden commencements in H during the day-time in the Indian zone occurs at latitude close

close to the equator. In the American zone it was found (Rastogi and Trivedi, 1968) that during the daytime SC(Z) changes its sign at dip closed to 2° while in the night this change over region changes to about 8° dip. In the Indian zone this change over happens close to Hyderabad latitude i.e. around dip of 20°. Any explanation of these abnormalities in the Indian zone should be sought in abnormal induced currents inside the earth which would greatly affect the variations of Z, both the daily variations as well as the short time variations.

To study the variations in sudden changes with respect to the electrojet it was considered desirable to check the latitudinal variation of the normalized solar daily range of H and Z at the equatorial stations and these are shown in Fig. 6. The range of H is found to decrease

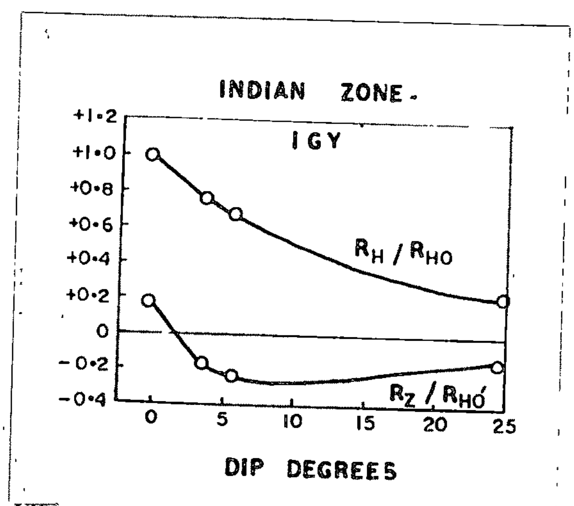

Figure.6.

systematically from the equator with the increase of dip angle. Range in Z changes from positive to negative value at the latitude, very close to the equator. Its maximum negative value is around 5 to 10° dip, and it decreases with further increase of latitude. Chapman (1951) has shown that if the electrojet is assumed to flow along a band of infinely small thickness and width 2C (in the N-S direction) at height h then the Z component would be zero at band axis centre and attains its maximum value at a distance of $\sqrt{h^2 + c^2}$ from the axis. Thus so far as the daily variations of H or Z is concerned, the thin sheet model of the electrojet current is fairly valid for the Indian region. However the latitudinal variation in the sudden changes in Z are different and do not conform to the simple band model of the electrojet.

Acknowledgement

Sincere thanks are due to Colaba and Alibag Observatories, Colaba, Bombay, Astrophysical Observatory, Kodaikanal and to the World Data Center for Geomagnetism, Washington DC, U.S.A. for providing the copies of magnetograms utilised in the present study. The authors are greatly thankful to PROFESSOR K.R. RAMANATHAN for the useful discussions and suggestions during the course of study.

REFERENCES

Chapman S. and K.S. Raja Rao, The H and Z variations along and near the equatorial electrojet in India, Africa and the Pacific, J. Atmosph. Terr. Phys., 27, 559-581, 1965.

Forbush S.E. and E.H. Vestine, Day-time enhancement of size of sudden commencements and initial phase of magnetic storms at Huancayo, J. Geophys. Res., 60, 299, 1965.

Forbush S.E. and M. Casaverde, Equatorial Electrojet in Peru, CIW, 1961, Publ. No. 620, 1961.

Maeda H. and M. Yamamoto, A note on day-time enhancement and the amplitude of geomagnetic storm sudden commencements in the equatorial region, J. Geophys. Res., 65, 25-38, 1960a.

Maeda H. and M. Yamamoto, Day-time enhancement of the amplitude of geomagnetic sudden impulses in the equatorial region, Rept. Ionosphere and Space Research, Japan, 14, 443-444, 1960b.

Rastogi R.G., Longitudinal inequalities in the lunar tide and in sudden commencement in H near the magnetic equator, J. Atmosph. Terr. Phys., 25, 393-397, 1963.

Rastogi R.G., N.D. Kaushika and N.B. Trivedi, Solar flare crochet and sudden commencement in H within the equatorial electrojet region, J. Atmosph. Terr. Phys., 27, 663-668, 1965.

Rastogi R.G., N.B. Trivedi and N.D. Kaushika, Night-time sudden commencements in H within the equatorial electrojet region, J. Atmosph. Terr. Phys., 131-136, 1966a.

Rastogi R.G., N.D. Kaushika and N.B. Trivedi, Night-time disturbance fluctuations in geomagnetic field at equatorial stations, J. Atmosph. Terr. Phys., 28, 303-310, 1966b.

Rastogi R.G., N.B. Trivedi, Studies of sudden changes in H at equatorial stations in American zone, Ann. de. Geophys. (in press).

Srinivasamurthy B., The diurnal variations of sizes of sudden commencements and impulses in the Kodaikanal magnetograms, Ind. Jour. Met. and Geophys., 1960, 11, 64.

Sugiura M., The solar diurnal variation in the amplitude of sudden commencements and geomagnetic storms at geomagnetic equator, J. Geophy. Res., 58, 558-559, 1953.

REFERENCES

Akasofu S.I. and Chapman S., Variana No.250, 1960.

Beagley J.W., J.Sci.and Technology, 33B,460,1952.

Balfour Stewart, Encylopedia Brittanica (9th edit.)1882.

Balsley B.B., J.Geophys.Res. 70,3175,1965.

Baker and Martyn.,Phil.Trans.Roy.Soc.London A,246,281,1953.

Cahill L.J., J.Geophys.Res.64,489,1959.

Chapman.S., Phil.Trans.Roy.Soc.London,A,213,279,1913.

Chapman.S. Phil.Trans.Roy.Soc.London A,218,1,1919.

Chapman S and Bartels.J. Geomagnetism,Oxford University Press (1940)

Chapman S., Terr.Magn.Atmosph.Elec.53,247,1948.

Chapman S., Arch.Meteorol.Geophys. Bio-Climatol A,4,368,1951.

Chapman S., Nuovo Cimento,4,Suppl .1385,1956.

Chapman S. and Raja Rao K.S., J.Atmosph.Terr.Phys.27,559, 1965.

Cowling T.G., Mon.Not.Roy.Astro.Soc., 93,90 (1933).

Cowling T.G. and R. Borger, Nature,162,143 (1948).

Davis T.N., K.Burrows, J.L. Stolarik., J.Geophys.Res. 72, 1845,1967.

Egedal J., Nature,161,4?3,1948.

Ellison M.A., Observatory 75,61,1955.

Ferraro,V.C.A., Parkinson W.C., and Unthank H.W., J.Geophys., Res.,56,177,1951.

Ferraro,V.C.A and Unthank H.W., Geofis.Pura e appl.20,3,1951.

Ferraro,V.C.A., J.Geophys.Res. 59,309,1954.

Forbush,S.E. and Vestine E.H., J.Geophys.Res.60,299,1955

Forbush, S.E. and Casaverde M., Equatorial Electrojet in Peru C.I.W. Publ.No.620,1961.

Giesecke, A.A., Trans.Brussels Meeting 1951.

Godivier, R. and Y.Crenn, Ann.Geophys.21,143,1965.

Gulatee B.L., Survey Ind.Tech-Rept.Pt.3, 1949-50.

Hirono, M.J.Geomagn.Geoelect.4',7,1952.

Hutton.R., J.Atmosph.Terr.Phys.29,1411,1967.

Madwar, M.R., Bull.Inst.Egypt. 36, 5,1953.

Maeda H. and Yamamoto M., J.Geophys.Res.65,2538,1960.

Maeda H. and Yamamoto M., Rept.Ionosphere and Space Res. Japan,14,443,1960.

Martyn, D.F., Nature,163,685,1949.

Matsushita, S., J.Geomagn.Geoelec., 1, 35,1949.

Matsushita, S., J.Geomagn.Geoelec. 2,9,1950.

Matsushita, S., J.Geophys.Res.65,1423,1960.

Maynard, N.C. and L.J. Cahill, T.S.G. Sastry., J.Geophys. Res.70,1241,1965.

Maynard, N.C. J.Geophys.Res.72,1863,1967.

Nagata, T., J.Geophys.Res.57, 1, 1952.

Nishida.A and Jacobs J.A., J.Geophys.Res.67,525,1962.

Ogbuehi, P.O. and C.A. Onwumechilli., J.Geophy.Res.68,2421, 1963.

Onwume-chilli, C.A., J.Atmosph.Terr.Phys.13,222,1959.

Onwumechilli, C.A., Physics of the Geomagnetic Phenomena Ed.S.Matsushita and W.Campbell 1967.

Pekeris, C.L., Proc.Roy.Soc.A,158,650 (1937).

Pisharoty, P.R. and Sreenivasan, P.K., Indian J.Met.Geophys. 13,554,1962.

Pontier, L., Ann.Geophys.6,238,1950.

Pramanik S.K. and Yegnanarayanan, Indian J.Met.Geophys. 3,212,1952.

Pramanik S.K. and Hariharan, P.S., Indian J.Met.Geophys., 4,353,1953.

Price,A.T. and D.J. Stone , IGY 35,62,1964.

Rastogi R.G., J.Atmosph.Terr.Phys.24,1031,1962.

Rastogi R.G., J .Atmosph.Terr.Phys.25,393,1963.

Rao K.N., D.R.K. Rao and M.S. Raja Rao., Tellus XIX,337,1967.

Schuster,A. ,Phil.Trans. Roy.Soc.A,208,163,1908.

Srinivasmurthi,B., Indian J.Met.Geophys. 11,64,1960.

Sugiura, M., J.Geophys.Res.58,558,1953.

Sugiura., M.and J.C.Cain, J.Geophys.Res.71,1869,1966.

Taylor,G.I.,Proc.Roy.,Soc.A,156,318,1936.

Volland H. and Taubenheim J., J.Atmosph.Terr.Phys.12, 258,1958.

Wilkes,M.V., Cambridge Univ.Press,London and New York 1949.

Yacob A, and Khanna, M.B.K., Indian J.Met.Geophys.14, 470,1963.

PART - 3

3.1 Introduction

The occurrence of transient changes in the geomagnetic field was recognized more than two centuries ago. Graham in 1722 reported these regular daily variations in the geomagnetic field based on his observations of the small movements of a compass needle. Later in 1740-41 Celsius and Graham showed that the magnetic disturbance was often simultaneous at two stations. Celsius also correlated aurora with magnetic disturbance. In 1843 Schwabe reported the intensity of magnetic disturbance varying with sunspot cycle. About this time, Kreil of Prague was seeking regular periodic variation in the geomagnetic field depending on the lunar hour angle. Only by 1850 Kreil could establish lunar variations with certainty. Airy, one of pioneers of the study of lunar effects in the geomagnetic field determined S and **L** for each magnetic element at Greenwich for the period 1848-1857. Airy's results were based on measurement of the magnetic elements at each solar hour and each lunar hour and were the earliest reliable determinations of **L**.

Before describing the methods for determining **L** it would be useful to describe some details regarding the motion of the moon around the earth. In such studies it is considered that the moon revolves round the earth with a uniform angular speed, i.e. all the data reduction are made with reference to the mean moon. Mean lunar time (τ) is defined, by analogy with mean solar time (t). At a lower transit of the mean moon $\tau = 0$ lunar hour or 0°, while at the upper transit of the moon $\tau = 12$ lunar hour or 180°. The time interval between two successive lower transits of the moon i.e. the length of one lunar day is $24^{h}50.47^{m}$ in solar time or 24 lunar hours. The moon's sidereal period of rotation around the earth is $27^{d}7^{h}43^{m}$. The time between two successive crossings of the meridian half plane containing the sun is 29.5306 days, a period called a lunation, lunar month or synodic month. The moons phases depend on the angle between the meridian half planes containing (mean) sun and (mean) moon. The angle is measured positive when the moon is east of the sun, and is called lunar age denoted by ν . The lunar age ν can be expressed as 0 to 360 degrees or as 0 to 24 lunar hours. At <u>New Moon</u> the sun and the moon are in the same meridian plane and the lunar age ν is taken as 0° or 0 lunar hour. Similarly at full moon $\nu = 180°$ or 12 lunar hour. In the course of one synodic month ν changes from 0° to 360°.

The solar (t) and lunar times τ are related by the equation

$$t = \tau + \nu$$

where t , τ and ν may be reckoned in degrees or in hours. Some years back, people used straight astronomical data of the position of the moon for such analysis and the relative position of moon with respect to the sun was described by lunar phase μ which is related to the lunar age by the equation

$\mu = 24 - \nu$ (hr.) or $360 - \nu$ (degrees). Bartels and Fanselau (1937,1938) have given the formulae and tables for calculating μ for the Greenwich noon for any day between 1850 to 1970. Recently Sugiura and Fanselau (1966) have published ' ν ' tables for the years 1850 to 2050.

The periodic lunar daily variations were found to change in a definite way, in the course of the change of the angle between sun and moon from 0 to 2π as viewed from the earth - i.e. in a time of whole lunation. In 1874 Broun studied the lunar daily variations of the Declination of the geomagnetic field at Trivandrum for the period 1854 to 1864. He discovered that simple semidiurnal character of L variations is an average picture of the lunar daily variations determined from a number of lunations. At any particular epoch in the lunation, the lunar daily variation does not show a perfect semidiurnal character. Broun determined L from the data of a large number of days having the same lunar phase. He calculated average lunar daily variation for three days centered on new moon and similarly on seven other groups of days centered at one eighth phase, first quarter, three eighth phase, full moon and so on. The lunar daily variation for each epoch showed approximately two waves of unequal amplitude. The part of the curve showing greatest movement occurred earlier and earlier in the lunar day as the lunation progressed. The part with the greatest movement in the curve is also found to take place during day-time. Chambers (1887) got similar results. Moos (1910) while studying lunar variations in geomagnetic field at Bombay, made a significant suggestion that a luni-solar variation may be regarded as a simple lunar variation the amplitude of which is enhanced during day-time hours. Moos expressed this idea mathematically taking the whole lunation mean curve by an equation

$$L = C \cos (2\tau + \alpha) \qquad \ldots\ldots\ldots(1)$$

where τ denotes lunar time. The amplitude factor C was replaced by another constant 'C'' whose amplitude varies with solar time such that it is maximum at midday and minimum at midnight; expressed by the equation

$$C' = C\,(1 - a \cos t) \qquad \ldots\ldots\ldots(2)$$

At midday $t = 12$ hr. $= \pi$, $C' = C(1+a)$

At midnight $t = 0$ hr. $= 0°$, $C' = C(1-a)$

For simplicity Moos took a = 1.
Substituting (2) in (1) one gets

$$L = c\ (1-a\ \cos t)\ \cos\ (2\tau + \alpha\ ) \qquad ....(3)$$

The values of C and α he took from the lunar daily variation curves. The curves obtained from the equation turned out to be similar to the observed lunar variations confirming Moos's idea that the daily variation is produced by the moon but that its amplitudes depend on the sun.

By this time, Balfour Stewart (1882) had already proposed a "dynamo theory" to account for the daily variation in the geomagnetic field. He stated that the magnetic variations at the ground must arise from electric currents flowing in the upper atmosphere. Schuster (1908) developed "dynamo theory" quantitatively. It is now generally accepted that the daily magnetic variations are caused by the movements of the ionised layers of the upper atmosphere and that D and E regions of the ionosphere are the main seat of electric currents producing solar (S) and lunar (L) variations. The current systems of S and L may be the resultant of motions in different levels of the atmosphere. The horizontal conductivity of different layers depends upon the electron density, composition of the ionized gas and the restrictions to ion movements in presence of the geomagnetic field. The net current contribution of the dynamo region depends on its integrated horizontal conductivity and the average velocity of motion of ions and electrons. For the S variations, the motions in the air are generated by pressure gradients due to temperature differences whereas the L variations must be generated by the action of the lunar air tide acting on the upper atmosphere.

The dependence of the conductivity of the dynamo region on the position of the sun could be translated in the lunar daily variation as the lunar variation being more during day light hours compared to night-time. Chapman (1913) showed that lunar daily variation must include harmonics arising from the varying ionization caused by the sun. He extended the expression (3) given by Moos to describe L. Chapman replaced the term of solar time t in equation (3) by $\tau + \nu$.

The expression (3) becomes

$$L = C \left\{ 1 - \bar{a} \cos(\tau + \nu) \cos(2\tau + \nu) \right\} \quad \ldots(4)$$

or

$$L = \tfrac{1}{2}C \left\{ -\bar{a} \cos(\tau + \alpha - \nu) + 2 \cos(2\tau + \alpha) - \bar{a} \cos(3\tau + \alpha + \nu) \right\} \quad \ldots\ldots\ldots(5)$$

This expression showed the presence of three harmonic components in L. The amplitudes of the first and third harmonics are shown to be nearly the same with their phase angles $\pi + \alpha - \nu$ and $\pi + \alpha + \nu$. The semi-diurnal component shows a constant phase angle. It is seen from the above that as ν changes by 2π during a lunation, the phases of the first and third components respectively decrease and increase by 2π per lunation. Chapman analysed the inequalities given by Broun, Chambers and Moos and confirmed the formula for L given by Moos. Moreover Chapman empirically discovered the fourth harmonic component which changed by 4π during the whole lunation. Chapman gave an expression for L in any element (up to fourth harmonic):

$$L = \sum_{n=1}^{4} C_n \sin \left\{ n\tau + (n-2)\nu + \alpha_n \right\} \ldots\ldots(6)$$

The letters C and α in the equation (6) are the amplitude and phase of the lunar variation L.

The lunar tide being a function of two variables solar time t and lunar age ν , two ways are possible for the computation of lunar tides.

(1) Fixed lunar age ν method (Broun's method) studies lunar daily (L) variations on days with fixed lunar ages.

(2) Fixed solar hour method (Van'der Stok's method) studies lunar monthly (M) variations at fixed solar hours.

Chapman and Miller (1940) have presented fixed age method in detail. Ts-chu (1949) has described the practical use of Chapman and Miller method for the determination of lunar and luni-solar daily variation in any geophysical element. Bossolasco (1937), Rooney (1938) and others have used fixed hour method. Usually the mean lunar daily variation is determined despite the fact that the effect of the moon on the geomagnetic field is different during the hours of day light and night hours. In the present study lunar daily (L) variation and lunar monthly (M) variation are determined using both fixed age and fixed solar hour methods respectively.

The lunar tidal oscillations in the horizontal magnetic field 'H' have been shown to be abnormally large at equatorial stations viz. Huancayo (Bartels 1936), Ibadan (Onwumechilli and Alexander 1959) and Kodaikanal (Raja Rao and Sivaraman 1958). It has been also shown that the latitudinal as well as longitudinal variations of the amplitude of lunar tidal oscillations in the solar daily range of H at the equatorial stations is very similar to the corresponding variations of electrojet current itself, suggesting that lunar tides in the magnetic field at equatorial stations were closely associated with the electrojet current (Rastogi 1963, 1964, 1965). Recently lunar diurnal as well as lunar monthly variations in H at Huancayo have been described in detail for the low sunspot period 1951-55 and for the high sunspot period 1957-59 (Rastogi 1968a, b). As the strength of the electrojet currents in the Indian zone is found to be much weaker than that in the American zone (Rastogi 1962, Maynard and Cahill 1965a, b), it was thought desirable to compute the lunar tidal oscillations in the magnetic field at equatorial stations in the Indian zone and compare the results with those at equatorial stations along different longitudes. These results are discussed in the following chapter.

3.2 Method of analyses of lunar daily and monthly oscillations

The periods of S and L are nearly the same and the magnitude of L is much smaller than that of S which makes the determination of L difficult. It is necessary to have a large volume of continuous data for the computation of L. Most of the available results on lunar tides refer to mean lunar daily variation despite the fact that the effect of the moon on the geomagnetic field is different during the hours of daylight and night hours. In the present study, lunar tides in geomagnetic field are calculated both by fixed age method as well as by fixed solar time method. The method of computation of L is illustrated by the following analysis of Kodaikanal H data.

Kodaikanal magnetic data used in this study were obtained from the "Kodaikanal Observatory Bulletins" published by the Indian Meteorological Department of the Government of India. The coordinates of the Kodaikanal Magnetic Observatory are:

Geographic latitude	= 10°.2N
Geographic longitude	= 77°.5E
Geomagnetic latitude	= + 0.6
Geomagnetic longitude	= 147.1
dip	= 3.4°N.

The Kodaikanal Observatory is equipped with Watson variometers recording H, D and Z elements of the geomagnetic field. The absolute observations of H.F. and V.F. are made with a Kew magnetometer. The inclination is measured by an earth inductor. The tables of H, D and Z list 24 entries of 24 hourly values per day. The units used for H.F. and V.F. are gamma ($10^5\gamma$ = 1 gauss) and for D the unit is minutes of arc. Each hourly value is the average for sixty minutes centered at full hours of G.M.T. The data used for the present study are 1951 to 1960. The data are continuous and with almost no failures. Certain missing values, values one or two in a whole day, were interpolated.

The geomagnetic field variation consists of Sq + L + (other disturbances). The magnitude of L being small, it is not easy to separate L variation from Sq. It becomes still more difficult in presence of other disturbances besides normal Sq. Therefore, the magnetically disturbed days are not utilized in the computation of L, and only the days with C_p index less than 1.2 are taken into considerations. The number of days having $C_p \geq$ 1.2 are listed below for each year which have been considered for the analysis of lunar tides in the Kodaikanal geomagnetic field.

Year	No. of days $C_p \geq 1.2$
1956	72
1957	82
1958	84
1959	97
1960	103
Total................	438

It is seen that about 20 per cent of data are discarded from the entire data to remove the irregular disturbance effects.

The computations are made on IBM 1620 electronic computer. The tables presented are the listing

Table – 1.

Magnetic data for January 1959.

KD 01 56

14	01	01	56	474	478	476	482	510	521	541	545	543	529	515	490	479	476	477	478	473	449	451	465	468	465	456	456
15	02	01	56	452	455	464	482	492	501	509	517	540	540	521	495	482	474	467	462	458	472	459	465	474	467	462	471
16	03	01	56	473	467	458	462	490	513	539	548	539	534	505	491	484	480	476	476	471	465	464	466	467	468	476	481
17	04	01	56	484	483	477	483	494	492	516	535	525	515	504	483	473	474	475	477	478	473	470	492	486	481	481	489
17	05	01	56	495	497	487	484	491	507	516	528	539	527	513	499	498	492	488	483	490	484	473	491	482	475	480	481
18	06	01	56	473	474	480	493	515	541	587	598	594	568	543	531	507	478	454	442	433	437	447	448	463	471	467	469
19	07	01	56	469	469	472	484	502	519	544	566	565	535	504	488	490	483	472	453	455	473	453	463	464	471	475	477
20	08	01	56	478	480	492	507	529	548	556	556	541	521	500	491	490	485	478	479	480	479	472	473	477	473	478	477
21	09	01	56	473	471	473	470	480	479	510	526	546	534	504	468	444	428	438	462	471	467	454	458	466	473	478	476
23	12	01	56	462	478	500	516	536	560	564	530	512	493	475	456	444	429	418	417	408	393	386	383	419	427	429	431
00	13	01	56	434	446	467	477	501	511	522	525	515	501	488	477	470	475	477	472	461	460	461	461	460	462	467	466
01	14	01	56	466	465	465	482	498	515	539	550	538	519	506	485	484	479	477	477	471	462	462	469	468	469	477	474
02	15	01	56	471	470	477	486	508	535	562	567	556	528	504	493	484	474	476	482	483	485	482	482	484	490	486	484
02	16	01	56	484	483	493	516	561	587	612	604	583	545	509	493	500	494	493	490	488	486	485	485	492	494	492	486
03	17	01	56	484	483	487	514	543	571	576	569	566	536	510	492	485	474	466	464	466	466	468	472	472	475	473	476
06	20	01	56	447	448	457	471	509	548	564	560	541	511	485	479	474	468	465	465	462	463	460	463	465	468	468	468
06	21	01	56	470	467	465	471	501	527	548	556	554	541	524	508	495	486	479	473	472	473	473	479	473	482	492	499
08	23	01	56	482	483	497	499	510	551	581	594	559	533	506	492	488	483	478	480	482	476	462	463	463	452	442	444
10	25	01	56	437	455	454	485	496	507	516	502	498	488	478	469	461	453	452	453	454	458	453	453	446	445	453	458
11	26	01	56	462	462	461	475	498	518	541	553	555	535	512	502	490	482	477	474	471	470	470	470	471	473	473	477
13	29	01	56	452	456	475	497	522	533	517	520	505	481	475	476	474	465	446	447	432	432	448	445	452	460	460	459
14	30	01	56	459	463	476	492	520	534	537	520	486	463	457	465	469	468	452	438	428	441	453	455	452	460	472	468
15	31	01	56	463	467	481	496	529	546	547	542	506	490	477	465	467	470	462	462	461	473	463	456	458	458	463	461

of the computer output. The form of the basic magnetic data used in the lunar tide computations is shown in Table 1. The data for each day are punched on a card. The first eight places on the card are assigned for the lunar age, date, month and year and the remaining seventy two places are for twenty-four three-digit hourly values.

The first step towards determining the lunar variation should be to remove S variation from the data utilized. By adding all the values in each column and dividing by the total number of values monthly mean twenty-four hourly values are obtained. These twenty-four values represent the average variation over a month. The average S variation in subtracted from the daily variation of each day and 24 hourly deviation values are obtained as shown in Table 2. The deviations are tabulated as in Table 2 for all the months considered in the analysis. These deviations contain the lunar daily variation.

At the completion of tables of hourly deviation, the values for all the months are grouped according to the season, viz.

(a) D-months - November, December, January and February.

(b) E-months - March, April, September and October.

Table - 2.

Deviations from the Average.

KD	0	0	14	1	7	8	1	-6	0	-8	-4	-3	4	9	14	4	1	3	10	13	10	-13	-9	2	2	-3	-14	-15
KD	0	0	15	2	-15	-15	-11	-6	-18	-28	-36	-31	1	20	20	9	2	1	0	-3	-5	10	-1	2	8	-1	-8	0
KD	0	0	16	3	6	-3	-17	-26	-20	-16	-6	0	0	14	4	5	4	7	9	11	8	3	4	3	1	0	6	10
KD	0	0	17	4	17	13	2	-5	-16	-37	-29	-13	-14	-5	3	-3	7	1	8	12	15	11	10	29	20	13	11	18
KD	0	0	17	5	28	27	12	-4	-19	-22	-29	-20	0	7	12	13	18	19	21	18	27	22	13	28	16	7	10	10
KD	0	0	18	6	6	4	5	5	5	12	42	50	55	48	42	45	27	5	-13	-23	-30	-25	-13	-15	-3	3	-3	-2
KD	0	0	19	7	2	-1	-3	-4	-8	-10	-1	18	26	15	3	2	10	10	5	-12	-8	11	-7	0	-2	3	5	6
KD	0	0	20	8	11	10	17	19	19	19	11	8	2	1	-1	5	10	12	11	14	17	17	12	10	11	5	8	6
KD	0	0	21	9	6	1	-2	-18	-30	-50	-35	-22	7	14	3	-18	36	-45	-29	-3	8	5	-6	-5	0	5	8	5
KD	0	0	23	12	-5	8	25	28	26	31	19	-18	-27	-27	-26	-30	36	-44	-49	-48	-55	-69	-74	-80	-47	-41	-41	-40
KD	0	0	0	13	-33	-24	-8	-11	-9	-18	-23	-23	-24	-19	-13	-9	10	2	10	7	-2	-2	1	-2	-6	-6	-3	-5
KD	0	0	1	14	-1	-5	-10	-6	-12	-14	-6	2	-1	-1	5	-1	4	6	10	12	8	0	2	6	2	1	7	3
KD	0	0	2	15	4	0	2	-2	-2	6	17	19	17	8	3	7	4	1	9	17	20	23	22	19	18	22	16	13
KD	0	0	2	16	17	13	18	28	51	58	67	56	44	25	8	7	20	21	26	25	25	24	25	22	26	26	22	15
KD	0	0	3	17	17	13	12	26	33	42	31	21	27	16	9	6	5	1	-1	-1	3	4	8	9	6	7	3	5
KD	0	0	6	20	-20	-22	-18	-17	-1	19	19	12	2	-9	-16	-7	6	-5	-2	0	-1	1	0	0	-1	0	-2	-3
KD	0	0	6	21	3	-3	-10	-17	-9	-2	3	8	15	21	23	22	15	13	12	8	9	11	13	16	7	14	22	28
KD	0	0	8	23	15	13	22	11	0	22	36	46	20	13	5	6	8	10	11	15	19	14	2	0	-3	-16	-28	-27
KD	0	0	10	25	-30	-15	-21	-3	-14	-22	-29	-46	-41	-32	-23	-17	19	-20	-15	-12	-9	-4	-7	-10	-20	-23	-17	-13
KD	0	0	11	26	-5	-8	-14	-13	-12	-11	-4	5	16	15	11	16	10	9	10	9	8	8	10	7	5	5	3	6
KD	0	0	13	29	-15	-14	0	9	12	-4	-28	-28	-34	-39	-26	-10	6	-8	-21	-18	-31	-30	-12	-18	-14	-8	-10	-12
KD	0	0	14	30	-8	-7	1	4	10	5	-8	-28	-53	-57	-44	-21	11	-5	-15	-27	-35	-21	-7	-8	-14	-8	2	-3
KD	0	0	15	31	-4	-3	6	8	19	17	2	-6	-33	-30	-24	-21	13	-3	-5	-3	-2	11	3	-7	-8	-10	-7	-10

Table-3.

Mean Lunar Daily Variations in Terms of Solar Hour.

12	0	-1.0	.2	.1	-1.6	.1	2.0	-2.0	-3.3	.9	3.5	5.6	.7	1	004
12	0	-6.5	-3.3	.8	2.2	1.1	3.6	4.4	-1.4	-.9	-.5	3.4	-6.7	2	005
12	1	2.7	-.9	-.6	-1.9	-.5	-2.5	-3.9	-5.3	1.2	9.3	6.6	4.0	1	006
12	1	-3.0	-1.5	1.8	1.7	-2.0	1.5	3.2	-3.3	-7.1	-.6	5.0	-3.2	2	007
12	2	8.5	.0	2.7	.3	-1.7	-5.2	-9.7	-8.3	.4	6.1	9.3	8.4	1	008
12	2	.5	3.0	3.5	2.6	-4.9	.1	-1.0	-6.9	-10.1	-2.5	4.3	.0	2	009
12	3	12.0	3.8	9.5	4.0	-3.5	-3.6	-10.8	-10.7	-.4	4.7	10.6	6.7	1	010
12	3	1.1	7.5	4.9	8.5	.1	-.6	-7.5	-12.6	-16.4	-8.1	5.7	-4.0	2	011
12	4	13.4	6.4	14.0	7.5	-.2	-4.2	-10.1	-11.4	-3.2	3.4	8.8	1.9	1	012
12	4	.3	10.5	11.2	14.0	-6.7	3.1	-6.3	-12.2	-22.8	-15.1	4.7	-5.1	2	013
12	5	11.3	7.5	18.5	9.9	5.6	-4.2	-6.5	-9.1	-2.0	.0	1.1	-5.2	1	014
12	5	-6.5	2.9	15.8	20.8	5.4	2.4	-13.7	-13.8	-24.5	-16.4	4.7	-4.4	2	015
12	6	7.0	7.9	16.5	14.2	4.5	-4.5	-9.2	-13.0	-.0	-1.7	7.0	-7.8	1	016
12	6	-9.1	5.7	14.4	20.6	6.5	4.0	-6.8	-9.7	-18.2	-19.1	3.5	-14.3	2	017
12	7	2.4	5.1	10.7	7.4	5.8	-.2	-13.1	-14.1	3.8	-3.6	6.5	-7.8	1	018
12	7	-7.6	3.8	11.3	19.2	6.0	9.3	-4.2	-4.3	-14.5	-7.4	4.2	-16.3	2	019
12	8	-5.5	-3.6	4.1	6.4	8.2	1.4	-12.6	-9.6	6.3	-7.8	1.8	-6.1	1	020
12	8	-11.9	.7	2.8	9.3	5.8	16.2	7.8	1.9	-6.2	4.4	3.5	-14.2	2	021
12	9	-7.8	-4.3	-.6	.3	7.1	-1.5	-8.7	-3.2	6.6	-1.9	-.2	-1.7	1	022
12	9	-16.1	-4.2	-6.2	-3.8	5.8	17.5	12.3	7.5	4.0	9.3	5.2	-11.5	2	023
12	10	-8.7	-8.1	-3.0	-2.0	4.8	-1.8	-4.6	1.2	7.6	3.0	4.8	.5	1	024
12	10	-12.6	-.7	-8.9	-8.3	.5	12.0	10.6	5.4	4.8	9.7	6.3	-12.0	2	025
12	11	-3.5	-5.5	.6	-2.3	1.9	-4.2	-1.8	1.4	5.5	6.0	3.5	6.1	1	026
12	11	-3.6	-2.1	-5.4	-5.0	-1.6	5.4	7.8	2.0	.5	3.0	6.6	-10.3	2	027
12	12	-1.7	-2.1	3.8	.6	.8	-5.7	-4.7	-2.4	3.2	7.1	6.0	7.3	1	028
12	12	-6.2	-5.4	-4.2	-.6	.4	1.7	2.2	-.1	-1.5	-2.7	5.7	-5.7	2	029
12	13	2.7	3.2	7.7	.8	-1.9	-6.0	-4.1	-3.2	-2.0	5.8	8.0	5.3	1	030

Table-3. contd.

Mean Lunar Daily Variations in Terms of Solar Hour.

12	13	-6.5	-4.1	-2.7	2.5	1.0	2.7	-.4	-1.8	-5.9	-4.3	5.2	-2.9	2	031
12	14	3.0	2.2	8.8	1.7	-1.6	-3.7	-1.3	-3.7	-3.0	4.6	7.3	6.2	1	032
12	14	-6.7	-2.4	-6.6	3.1	-4.8	4.1	-1.2	-3.0	-3.0	-1.1	2.5	-2.2	2	033
12	15	4.1	4.0	6.1	3.1	-5.3	-2.9	-1.2	-1.3	.7	6.1	8.4	5.5	1	034
12	15	-8.3	.8	-15.1	2.5	-5.0	3.4	-.8	-1.5	-5.5	.3	1.0	-.8	2	035
12	16	2.0	7.5	5.7	2.0	-1.7	-3.4	-2.0	-3.4	1.5	5.1	14.1	7.2	1	036
12	16	-8.3	.1	-13.3	.3	-5.6	1.2	-.7	-1.2	-5.0	1.2	.9	-2.5	2	037
12	17	2.0	8.4	4.1	2.1	-5.5	-1.2	-1.5	-4.6	2.6	5.4	14.4	3.0	1	038
12	17	-7.8	1.1	-12.7	2.7	-6.5	-.1	-2.2	.3	-2.8	3.9	2.4	-5.0	2	039
12	18	2.1	7.1	2.4	2.5	-4.7	-1.8	-2.9	-4.1	3.6	4.6	7.2	2.0	1	040
12	18	-6.4	.8	-13.3	3.0	-4.1	-.5	3.0	.8	1.8	2.8	.4	-7.9	2	041
12	19	3.0	6.9	2.2	1.3	-2.6	-2.4	-1.7	-3.7	4.7	4.5	8.5	1.6	1	042
12	19	-4.7	-.5	-12.8	3.3	-1.5	-.4	2.9	2.8	-3.8	1.8	-1.0	-7.1	2	043
12	20	4.7	7.8	1.1	1.4	-.9	.6	-.8	-4.4	5.5	5.1	2.4	-3.3	1	044
12	20	-6.8	-1.5	-12.4	2.5	-1.9	.2	5.1	1.5	-3.2	2.4	-1.8	-5.7	2	045
12	21	3.0	6.1	1.1	2.5	.4	1.5	-.3	.0	3.9	4.3	6.2	-3.2	1	046
12	21	-8.0	-3.7	-9.6	-.4	-1.2	1.5	4.6	.7	-2.8	2.5	-4.2	-5.9	2	047
12	22	3.2	6.3	-.6	2.2	1.1	2.3	.5	-1.2	2.6	3.9	5.9	-6.5	1	048
12	22	-9.6	-2.8	-6.8	.0	.9	3.0	2.9	1.9	-2.5	2.5	-2.7	-5.7	2	049
12	23	2.3	4.9	-1.1	.9	1.4	2.8	1.5	-.7	1.7	2.6	5.2	-4.5	1	050
12	23	-9.2	-4.0	-6.6	-.3	1.0	3.6	.6	1.6	-1.7	1.0	-.1	-5.9	2	051

(c) J-months - May, June, July and August.

For each season of 4 months, twenty tables similar to Table 2 for the months of 5 years are collected. Till this stage, the data are tabulated with respect to solar date. For using the fixed lunar age method to obtain luni-solar daily variations, it would be necessary to connect the deviations with lunar hours. Although the twenty-four hourly values are at solar hour intervals, they also essentially represent lunar daily variation.

Hourly deviation values for all the days in a particular season are fed to the computer for further processing. Now the machine is programmed to do the following operation: It read s the complete data, sorts out the days with the same ν values and gives the average hourly deviation values for the days having the same values. Thus the average lunar daily variation for a complete season on different lunar ages is obtained. The matrix in Table 3 represents the mean lunar daily variations in terms of twenty-four solar hourly deviation values derived separately for the days with different lunar ages i.e. ν = 00 to 23.

For further analysis, three consecutive days are grouped to get the average lunar daily variation values for days with lunar age 00, 03, 06, 09, 12, 15, 18 and

Table - 4.

Grouped Lunar daily variations

12	0	-6.	.	10.	13.	16.	13.	-.	-11.	-22.	-24.	-24.	-14.	1	003
12	0	-3.	4.	6.	8.	7.	4.	3.	7.	5.	5.	3.	-5.	2	004
12	3	-9.	-11.	-6.	3.	15.	26.	25.	15.	8.	-3.	-8.	-6.	1	007
12	3	-2.	-.	-1.	-3.	-5.	-7.	-7.	-6.	-5.	-5.	-6.	-9.	2	008
12	6	8.	-1.	-12.	-14.	-13.	-9.	-15.	-14.	-7.	1.	7.	4.	1	011
12	6	-1.	.	5.	4.	4.	3.	3.	6.	11.	13.	15.	10.	2	012
12	9	-2.	5.	4.	2.	-5.	-12.	-7.	-7.	-11.	-4.	3.	3.	1	015
12	9	2.	-2.	-.	6.	10.	6.	5.	2.	2.	1.	-2.	-2.	2	016
12	12	-3.	6.	18.	21.	16.	-3.	-5.	-7.	-13.	-13.	-2.	5.	1	019
12	12	1.	2.	3.	4.	3.	2.	2.	-3.	-8.	-12.	-12.	-5.	2	020
12	15	3.	1.	1.	13.	21.	41.	40.	31.	11.	-9.	-16.	-10.	1	023
12	15	-3.	-4.	-14.	-19.	-18.	-16.	-13.	-12.	-12.	-8.	-7.	1.	2	024
12	18	4.	-2.	-12.	-23.	-20.	-26.	-13.	4.	26.	31.	21.	8.	1	027
12	18	-1.	-3.	-3.	-3.	-4.	-2.	2.	3.	4.	5.	3.	3.	2	028
12	21	7.	2.	-4.	-16.	-29.	-31.	-26.	-8.	11.	24.	22.	12.	1	031
12	21	4.	1.	2.	1.	5.	9.	5.	2.	1.	2.	4.	6.	2	032

21. The mean lunar daily variation at lunar ages 23, 00, 01 is taken as the lunar daily variation on lunar age 00. The mean of the lunar daily variation on lunar age 02, 03, 04 is represented as the lunar daily variation on lunar age 03 and likewise for lunar ages 06, 09, 12, 15, 18 and 21. Table 4 is obtained from Table 3 after the operation of grouping.

It is necessary to represent the lunar daily variation for different lunar ages in terms of lunar hours rather than solar hours. A mean lunar day equals 1.03505 solar days or $24^h 50.47^m$. The amplitudes given in Table 4 against each lunar daily age are plotted according to solar hours and a lunar daily variation curve is drawn. Now from this curve amplitudes are read at an interval of one lunar hour. The lunar hour being a little larger than a solar hour, only the first twenty three values could be read from the above mentioned curve. The above mentioned curve is extended by one solar hour by plotting the value at the zeroth hour as the 25th hour. Then the reading of the 24th lunar hour amplitude becomes possible. This empirical method does not lead to any serious error. Thus a new Table 5 can be prepared representing mean lunar daily variation in terms of plotting the lunar daily variation in terms of lunar hours.

The cumbersome procedure of plotting the

Table - 5.

Lunar daily variations in terms of L.Hrs.

12	0	-6.	-.	9.	12.	15.	15.	1.	-7.	-22.	-22.	-27.	-18.	3	001
12	0	-8.	4.	4.	8.	8.	6.	2.	3.	7.	4.	4.	2.	4	002
12	3	-9.	-10.	-6.	2.	13.	26.	27.	16.	10.	-1.	-8.	-7.	3	005
12	3	-2.	-1.	1.	-3.	-1.	-7.	-7.	-6.	-6.	-3.	-5.	-5.	4	006
12	6	8.	-.	-11.	-13.	-14.	-8.	-15.	-15.	-9.	-1.	6.	6.	3	009
12	6	-1.	-1.	2.	6.	2.	4.	2.	3.	6.	12.	13.	15.	4	010
12	9	-2.	4.	3.	2.	-3.	-13.	-6.	-5.	-11.	-7.	3.	2.	3	013
12	9	4.	-.	-3.	3.	8.	10.	3.	5.	.	2.	.	-2.	4	014
12	12	-3.	5.	17.	21.	18.	-2.	-5.	-5.	-11.	-16.	-6.	6.	3	017
12	12	1.	.	3.	3.	4.	2.	2.	2.	-5.	-8.	-12.	-11.	4	018
12	15	3.	.	.	12.	17.	41.	40.	35.	17.	-4.	-17.	-12.	3	021
12	15	-5.	.	-9.	-18.	-19.	-17.	-15.	-11.	-12.	-11.	-6.	-6.	4	022
12	18	3.	-1.	-10.	-23.	-18.	-28.	-15.	-2.	22.	34.	24.	12.	3	025
12	18	.	-2.	-3.	-1.	-3.	-5.	.	2.	3.	3.	4.	2.	4	026
12	21	6.	2.	-3.	-14.	-28.	-31.	-29.	-12.	6.	23.	25.	14.	3	029
12	21	6.	-.	3.	.	1.	8.	9.	1.	2.	.	2.	3.	4	030

lunar daily variation curve and reading its amplitudes at the interval of 1 hr is dispensed with by using an arithmetical formula and processing it by the computer to get Table 5. The relation between the amplitudes in terms of solar hours and lunar hours is given by Egedal (1956)-

$$L(h) = S(h) + (h-1) \times 0.035 \left\{ S\,(h+1) - S\,(h) \right\}$$

where

h is the hour

L(h) is lunar hour

S(h) is solar hour.

Table 5 gives the mean lunar daily variation or a luni-solar variation for lunar ages ν = 00, 03, 06, 09, 12, 15, 18 and 21. As mentioned earlier, luni-solar variation is expressed by an equation called the phase law.

$$L = \sum_{n=1}^{4} C_n \sin \left\{ n\tau + (n-2)\nu + \alpha_n \right\}$$

One can easily verify Chapman's phase law by finding harmonic coefficients (four) using 24 values of the periodic lunar daily variation. The harmonic analysis results giving amplitudes and phases of first four harmonics and a built up curve of mean lunar daily variation are shown in Table 6. The lunar daily variation in Table 5 is in G.M.T. So proper longitude correction is incorporated in the programme of the harmonic analysis otherwise phase angles obtained would be incorrect.

Luni-solar variation is determined using the fixed lunar age method. The lunar monthly variation at different solar hours is determined by fixed lunar method i.e. Van'der Stok method. In Table 3, the columns give the amplitudes of lunar tide on days of different lunar ages at a fixed solar hour. The plot of lunar age (ν) versus amplitude at fixed hour will represent lunar monthly variation. This enables to study lunar monthly variation at different times of the solar day. The harmonic coefficients are calculated for lunar monthly curve at each solar hour. Table 7 is the computer output giving first and second harmonic coefficient and a built up curve of lunar monthly variation. One gets r_1 and r_2 the lunar monthly and semi-monthly components and θ_1 and θ_2 their corresponding phases in terms of lunar age. In computing the phases of lunar monthly (M_1) and lunar semi-monthly (M_2) oscillations, proper corrections are necessary, as the values of lunar age (ν_0) are assigned with respect to Greenwich noon. The corrections needed are

(1) local time correction, and

(2) longitude correction.

Table - 6.

Harmonic coefficients and Built up curve for
Lunar Daily variations.

-.20	6.47	-4.92	-3.47	10.72	-6.54	-3.31	-.79	-.07					12	0	001
12	0	8.13	127.2	11.27	-17.9	7.34	243.1	.79	264.7						002
12	0	49.7	-172.9	10.6	-45.2										3
12	0	8.13	49.7	11.27	-172.9	7.34	10.6	.79	-45.2						004
12	0	5.	6.	5.	1.	-2.	-4.	-1.	6.	13.	17.	13.	3.	1	005
12	0	-9.	-20.	-24.	-22.	-15.	-5.	2.	7.	8.	6.	4.	4.	2	006
-.29	-1.14	9.40	-7.73	2.26	-2.93	-6.43	1.66	-.43					12	3	007
12	3	9.47	-6.9	8.05	-73.7	7.06	204.5	1.72	104.5						008
12	3	-39.4	-138.7	107.0	-25.4										9
12	3	9.47	5.5	8.05	-138.7	7.06	62.0	1.72	-115.4						010
12	3	-5.	-7.	-9.	-10.	-6.	2.	13.	23.	25.	19.	8.	-1.	1	011
12	3	-6.	-6.	-2.	.	-.	-2.	-4.	-6.	-6.	-5.	-5.	-4.	2	012
.33	.36	-9.56	4.36	-5.57	.84	-.87	-1.20	-2.38					12	6	013
12	6	9.56	177.8	7.07	141.9	1.21	136.1	2.67	206.9						014
12	6	190.3	166.9	173.6	256.9										015
12	6	9.56	280.3	7.07	166.9	1.21	83.6	2.67	76.9						016
12	6	-2.	-8.	-11.	-13.	-14.	-14.	-12.	-7.	-1.	3.	4.	2.	1	017
12	6	.	.	3.	4.	4.	3.	4.	7.	13.	15.	13.	5.	2	018
-.12	-.46	-5.09	1.62	2.18	.42	3.51	-.91	-.57					12	9	019
12	9	5.11	185.1	2.72	36.6	3.54	6.8	1.08	237.7						020
12	9	242.6	151.6	179.3	107.7										021
12	9	5.11	17.6	2.72	151.6	3.54	44.3	1.08	197.7						022
12	9	-2.	-7.	-10.	-10.	-7.	-2.	.	1.	.	.	1.	4.	1	023
12	9	6.	7.	6.	3.	1.	-.	-1.	-1.	.	2.	3.	1.	2	024

Table - 6.

Harmonic coefficients and Built up curve for Lunar Daily variations.

-.12		1.33	1.55	1.82	10.28	-3.18	4.96	-.75	-.43					12	12	025
12	12	2.04	40.5	10.44	10.0	5.90	-32.7	.86	240.0							026
12	12	143.0	215.0	274.7	290.0											27
12	12	2.04	323.0	10.44	215.0	5.90	94.7	.86	290.0							028
12	12	-11.	-12.	-9.	-3.	.	2.	3.	2.	3.	3.	3.	1.		1	029
12	12	-2.	-6.	-10.	-11.	-9.	-2.	7.	15.	18.	15.	5.	-4.		2	030
.08		6.43	18.88	-7.87	2.42	-2.65	-8.33	6.91	.43					12	15	031
12	15	19.95	18.8	8.24	-72.8	8.74	197.6	6.93	86.4							032
12	15	166.3	222.1	280.1	316.4											033
12	15	19.95	31.3	8.24	222.1	8.74	55.1	6.93	226.4							034
12	15	-14.	-11.	-5.	-4.	-10.	-17.	-20.	-17.	-12.	-11.	-11.	-10.		1	035
12	15	-6.	-.	2.	1.	1.	7.	21.	36.	42.	32.	12.	-6.		2	036
.08		-6.68	-1.81	3.24	-14.00	7.53	4.06	-2.75	2.45					12	18	037
12	18	6.92	254.8	14.37	166.9	8.55	61.6	3.68	-48.2							038
12	18	87.3	191.9	279.1	1.7											039
12	18	6.92	357.3	14.37	191.9	8.55	9.1	3.68	181.7							040
12	18	-4.	-4.	-3.	-2.	-1.	-.	2.	4.	5.	4.	2.	1.		1	041
12	18	-1.	-8.	-18.	-26.	-26.	-14.	.4.	21.	28.	23.	11.	.		2	042
.25		-6.66	-7.39	7.70	-9.32	7.68	7.23	-2.54	.64					12	21	043
12	21	9.95	222.0	12.09	140.4	10.55	46.7	2.62	-75.6							044
12	21	99.[illegible]	255.4	39.2	154.3											045
12	21	9.95	54.5	12.09	255.4	10.55	84.2	2.62	244.3							046
12	21	5.	6.	4.	2.	1.	1.	3.	4.	6.	4.	-2.	-14.		1	047
12	21	-27.	-32.	-26.	-11.	7.	20.	22.	15.	5.	-.	-.	2.		2	048

Lunar monthly and semi-monthly coefficients with built up curve

```
0    0 58.3333E-03   -.63   -.44    .77 215.  -1.18   -.14   1.19 187.     001
   0 -1.8 -1.8 -1.4  -.9  -.2   .3   .7   .8   .6   .2  -.1  -.4           002
   0  -.5  -.3   .0   .6  1.1  1.5  1.6  1.3   .7   .0  -.7 -1.4           003
0    1 29.1666E-03  -1.46    .13   1.47 174.   1.49  -1.06   1.83 324.     004
   1   .0  -.6 -1.3 -2.0 -2.2 -2.0 -1.3  -.2  1.0  2.1  3.0  3.2           005
   1  2.9  2.1  1.0  -.1 -1.0 -1.5 -1.6 -1.2  -.6  -.0   .3   .3           006
0    2-25.0000E-03  -1.70    .38   1.74 167.   5.43   -.17   5.43 358.     007
   2  3.7  3.0  1.2 -1.1 -3.3 -4.8 -5.0 -3.8 -1.3  1.6  4.5  6.5           008
   2  7.1  6.1  3.8   .7 -2.3 -4.7 -5.8 -5.4 -3.7 -1.3  1.2  3.0           009
0    3 37.5000E-03  -2.21   1.56   2.71 144.   7.73   3.30   8.41  23.     010
   3  5.5  6.6  5.5  2.8  -.7 -4.1 -6.1 -6.2 -4.2  -.6  3.7  7.5           011
   3  9.9 10.0  7.8  3.7 -1.2 -5.9 -9.2-10.4 -9.1 -5.9 -1.7  2.4           012
0    4 79.1666E-03  -2.08   2.10   2.96 134.   8.26   6.76  10.67  39.     013
   4  6.1  9.0  9.2  6.7  2.5 -2.2 -6.1 -7.9 -7.1 -3.8  1.1  6.3           014
   4 10.3 12.0 10.7  6.7   .9 -5.2-10.3-13.1-12.8 -9.7 -4.5  1.2           015
0    5-16.6666E-03   -.40   2.45   2.48  99.   6.24  10.40  12.12  59.     016
   5  5.8 10.8 12.9 11.8  7.8  2.0 -3.7 -8.1 -9.7 -8.3 -4.3  1.2           017
   5  6.6 10.3 11.2  8.9  3.9 -2.4 -8.6-13.0-14.4-12.4 -7.4  -.8           018
0    6-66.6666E-03  -1.46   1.08   1.82 143.   4.24  10.62  11.44  68.     019
   6  2.7  7.8 10.6 10.3  7.2  2.3 -3.1 -7.5 -9.6 -8.8 -5.2   .0           020
   6  5.7 10.1 12.0 10.8  6.8   .9 -5.3-10.4-12.9-12.4 -8.8 -3.3           021
0    7 10.0000E-02  -1.63  -1.17   2.01 215.   1.89   8.09   8.31  76.     022
   7   .2  5.8  5.9  6.1  4.2   .8 -3.0 -6.4 -8.1 -7.7 -5.2 -1.1           023
   7  3.5  7.5  9.9 10.0  7.8  3.9  -.7 -4.9 -7.7 -6.4 -6.8 -3.6           024
```

Lunar monthly and semi-monthly coefficients with built up curve

0	8 12C9166E-02	-.19	-3.56	3.57	266.	-3.51	4.48	5.70	128.				025
8	-3.7	-1.9	.1	1.8	2.4	1.7	-.0	-2.5	-5.1	-6.8	-7.2	-6.0	026
8	-3.3	.3	4.0	7.1	8.8	8.7	7.0	4.1	.8	-2.1	-4.0	-4.5	027
0	9 16.2500E-02	1.35	-4.06	4.28	288.	-6.37	-.91	6.44	188.				028
9	-5.0	-5.7	-4.8	-2.8	-.4	1.4	2.3	1.7	-.2	-2.9	-5.6	-7.4	029
9	-7.7	-6.2	-3.1	1.0	5.2	8.6	10.4	10.2	8.1	4.7	.8	-2.7	030
0	10 20.8333E-03	-.12	-1.93	1.93	266.	-5.72	-3.82	6.88	213.				031
10	-5.8	-7.4	-7.2	-5.2	-2.1	1.1	3.7	5.0	4.5	2.5	-.4	-3.4	032
10	-5.6	-6.2	-5.1	-2.3	1.2	4.9	7.6	8.7	7.7	5.1	1.3	-2.6	033
0	11 20.8333E-02	-1.20	-.27	1.23	192.	-2.31	-3.07	3.85	233.				034
11	-3.5	-4.7	-5.0	-4.1	-2.3	-.1	2.0	3.5	4.1	3.7	2.4	.6	035
11	-1.1	-2.3	-2.6	-2.0	-.6	1.0	2.5	3.4	3.4	2.4	.6	-1.5	036
0	12-17.5000E-02	-.64	.35	.73	151.	-.05	-1.71	1.71	268.				037
12	-.7	-1.4	-1.8	-1.9	-1.4	-.6	.4	1.4	2.1	2.4	2.1	1.5	038
12	.5	-.3	-1.1	-1.5	-1.4	-.9	-.3	.3	.8	1.0	.7	.0	039
0	13-37.5000E-03	.10	.33	.34	72.	1.89	-.00	1.89	359.				040
13	1.9	1.8	1.1	.3	-.6	-1.2	-1.5	-1.3	-.7	.1	1.0	1.6	041
13	1.7	1.4	.6	-.3	-1.2	-1.9	-2.2	-1.9	-1.1	-.1	.8	1.6	042
0	14-33.3333E-03	.82	.91	1.23	47.	1.64	-.34	1.68	348.				043
14	2.4	2.2	1.6	.8	.0	-.5	-.7	-.5	-.1	.4	.8	1.0	044
14	.8	.2	-.6	-1.5	-2.3	-2.6	-2.5	-1.9	-.8	.2	1.3	2.1	045
0	15-70.8333E-03	1.06	1.67	1.98	57.	1.31	-1.64	2.10	308.				046
15	2.3	1.7	.9	.2	-.1	-.0	.3	1.0	1.6	2.0	2.0	1.3	047
15	.2	-1.1	-2.5	-3.5	-4.0	-3.8	-2.9	-1.6	-.1	1.2	2.1	2.5	048

Lunar monthly and semi-monthly coefficients with built up curve

```
0   16 70.8333E-03    .80   2.13   2.28  69.   1.83 -2.01   2.72 312.   049
 16  2.6  1.9   .9   .0  -.4  -.3   .2  1.2  2.2  2.9  3.0  2.3         050
 16  1.0  -.7 -2.5 -4.0 -4.9 -4.8 -3.9 -2.4  -.6  1.0  2.2  2.8         051
0   17 10.4166E-02    .88   1.62   1.84  61.   1.62 -2.45   2.94 303.   052
 17  2.5  1.4   .2  -.6 -1.0  -.8   .0  1.1  2.2  2.9  2.9  2.1         053
 17   .7 -1.0 -2.8 -4.2 -4.7 -4.4 -3.2 -1.5   .3  1.9  2.8  3.0         054
0   18-66.6666E-03    .90    .45   1.01  26.    .18 -1.90   1.91 275.   055
 18  1.0   .2  -.5  -.9  -.8  -.4   .2   .9  1.5  1.5  1.1   .3         056
 18  -.7 -1.7 -2.5 -2.8 -2.5 -1.7  -.6   .5  1.6  2.2  2.2  1.8         057
0   19 54.1666E-03    .35    .87    .94  67.    .09 -1.39   1.39 273.   058
 19   .4  -.0  -.4  -.5  -.3   .1   .7  1.3  1.7  1.7  1.3   .6         059
 19  -.2 -1.1 -1.9 -2.2 -2.1 -1.7  -.9  -.1   .5  1.0  1.1   .8         060
0   20-10.0000E-02   1.77    .84   1.96  25.  -1.00  -.73   1.24 216.   061
 20   .7   .7   .8  1.1  1.4  1.7  1.8  1.5   .9   .0  -.9 -1.9         062
 20 -2.7 -3.1 -3.1 -2.5 -1.7  -.7   .1   .8  1.2  1.3  1.2   .9         063
0   21-41.6666E-03   1.37   1.56   2.08  48.  -1.80  -.71   1.94 201.   064
 21  -.4  -.1   .4  1.3  2.3  3.0  3.3  3.0  2.1   .8  -.7 -2.1         065
 21 -3.1 -3.6 -3.4 -2.7 -1.7  -.6   .2   .7   .8   .5   .1  -.2         066
0   22 33.3333E-03   1.58    .88   1.81  29.  -2.14  -.13   2.14 183.   067
 22  -.5  -.1   .6  1.6  2.5  3.0  3.0  2.3  1.1  -.3 -1.8 -3.0         068
 22 -3.7 -3.6 -2.9 -1.8  -.6   .5  1.2  1.4  1.2   .6  -.0  -.4         069
0   23-12.5000E-02   1.46    .93   1.73  32.  -2.17  -.30   2.19 187.   070
 23  -.7  -.3   .3  1.3  2.3  3.0  3.1  2.5  1.4  -.0 -1.6 -2.8         071
 23 -3.6 -3.6 -3.0 -1.9  -.7   .4  1.2  1.5  1.2   .6  -.0  -.5         072
```

$$\nu = \nu_0 - 0.0339 \times 75.3 + 0.0339\,(t - 180)$$

In the above equation, the second term is for latitude correction and third term is for local time correction. The above equation can be written as

$$\nu_0 = \nu - 0.0339\,(t - 180 + 75.3)$$
$$= \nu - 0.0339\,(t - 104.7).$$

where t is L.M.T. in degrees.

The phase angle could as well be presented in terms of lunar time τ. The relation between ν and τ is known to be $t = \nu + \tau$. Table 7 can be changed to Table 8.

Table 8.

S.hr.	lunar monthly amplitude	phase in lunar age	phase in lunar time	lunar semi-monthly amplitude	phase in lunar age	phase in lunar time
	h_1	ν_1	τ_1	h_2	ν_2	τ_2
0						
1						
2						
3						
4						
'						
'						
'						
'						
'						
'						
'						
23						

Harmonic analysis and the harmonic dial

Periodic variations like S and L can be represented by their sinusoidal components as determined by harmonic analysis. The periodic variations (say of interval T) such as are discussed in the last few pages can be represented by the series

$$\sum_n C_n \sin(nt + \theta_n) = \sum(a_n \cos nt + b_n \sin nt)$$

where n = 1, 2,...... and t denotes time reckoned in angle at the rate 360° per interval T. The integer n is the order of the harmonic, C_n and θ_n are its amplitude and phase. The harmonic has maximum amplitude at the time $t = (90° - \theta_n)/n$.

The geomagnetic variations could be described with sufficient accuracy by using only the first-four harmonics n = 1, 2, 3, 4. The harmonic coefficients could be conveniently calculated from the standard trigonometrical formulae,

$$a_0 = \frac{1}{r} \sum_{n=0}^{23} \Delta H_r \quad \text{..........(1)}$$

$$a_n = \left(\frac{2}{r}\right) \sum_{n=0}^{23} \Delta H_r \cos nt_r \quad \text{........(2)}$$

$$b_n = \left(\frac{2}{r}\right) \sum_{n=0}^{23} \Delta H_r \sin nt_r \quad \text{........(3)}$$

r is the number of hourly values.

The actual details of the method of computing the harmonic coefficients depend on the type of the computing machine available.

The most convenient graphical representation of harmonics is by the harmonic dial. The harmonic dial is essentially a vector diagram of a particular harmonic component, the length and direction of the vector representing the magnitude and hour of maximum of the particular harmonic component of the daily variation. In this representation the harmonic for any hour is plotted in cartesian coordinates with a_n as the ordinate and b_n as the abscissa. The amplitude $C_n = \sqrt{a^2 + b^2}$ is the distance from the origin.

The phase $\theta_n = \tan^{-1} a_n/b_n$ is the angle from the b_n axis in the counter-clockwise direction to the line connecting the line and the point. The time scale is represented by a dial starting with +ve axis and moves forward in a clockwise direction each hour being 15° for n = 1, 30° for n = 2, 45° for n = 3 and so on.

The lunar monthly and lunar semi-monthly tide can be studied better by the use of harmonic dials. The harmonic dials can be prepared for $r_1 \nu_1$, $r_1 \tau_1$ and $r_2 \nu_2$, $r_2 \tau_2$ obtained from the Table 7. An illustrative example of harmonic dial is presented for semi-monthly lunar tide in H at Kodaikanal. In Fig.

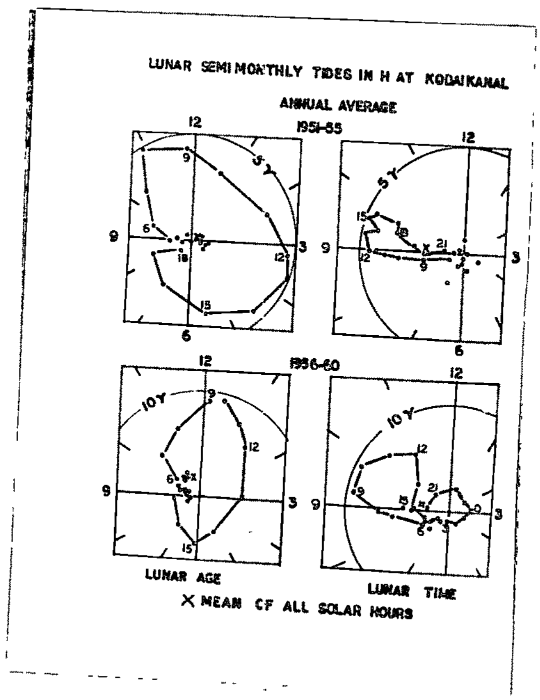

on the left side semi-monthly tide amplitude r_2 are plotted on a harmonic dial in terms of lunar age ν_2. The plot encircles the origin. The sign cross in the diagram shows the vectorial mean point of all the r_2 ν_2

points. The vectorial mean of r_2 amplitude in terms of lunar age ν_2 is quite small. On the right side of the diagram same r_2 amplitudes are plotted in terms of lunar time τ_2. The picture emerging out from this plotting is not the same as the previous plot. The cross on the diagram shows the vectorial average of $r_2\ \tau_2$ points and it is seen that vectorial mean of $r_2\ \tau_2$ points is quite large as all the $r_2\ \tau_2$ points have concentrated in a narrow sector. These diagrams help us to study how the factors lunar age and lunar time control the lunar semi-monthly oscillations.

<u>Probable errors</u>

Probable errors in the determination of the amplitudes are calculated according to the method described by Rastogi (1962). The determination of a particular coefficient may be considered significant only if its value exceeds three times its probable error, after Chapman (1951). The probable error estimation in the present study is done at an earlier stage of the analysis rather than calculating it from the harmonics of L variation. Here the probable error calculations are made along with the average ΔH daily variation calculation for each ν value (ν = 0 to 23) are made on IBM 1620. The procedure is as follows: As already discussed, the first step to determine the L variations from the data is to remove the average monthly S variation from the data of the month. After the removal of the average S variation from each day of the respective month, one is left with 24 hourly H values containing lunar daily variation. Refer Table 3 for its format. The second step described in this analysis was to compute the average ΔH in daily variation for each ν value. What was obtained in Table 4 is

ν	0........................23 solar hours.
0	$\overline{\Delta H}_0$, $\overline{\Delta H}_1$, $\overline{\Delta H}_2$ .... $\overline{\Delta H}_{23}$
1	
2	
3	
4	
'	
'	
'	
'	
23	

After getting H values for all the 24 hours for all values, the following are computed:

(1) $(\overline{\Delta H})^2$

(2) ΔH^2 $\left\{\begin{array}{l}\text{where N is total number}\\ \text{of H values used to get } \overline{\Delta H} \text{ on}\end{array}\right.$

(3) N

a particular ν value.

From this, the probable error calculation are simple.

(Standard Deviation) $\sigma = \Sigma \Delta H^2/N - \Sigma \overline{\Delta H}^2/N$

Probable error $= 0.275 \times \sigma.$

The symbols used are listed below:

t	local solar mean time
τ	local lunar mean time
ν_0	lunar age at Greenwich noon
ν	local lunar age
l.hr.	lunar hour = 1/24th mean lunar day.
s.hr.	solar hour = 1/24th mean solar day.
$L_1(H)_\nu$	lunar diurnal oscillation in H at fixed lunar age ν.
$L_2(H)_\nu$	lunar semi-diurnal oscillation in H at fixed lunar age ν.
C_n, ϕ_n, α_n	amplitude, phase angle and phase constant of the n^{th} harmonic of lunar daily variation according to $L = C_n \sin \{ n\tau + \phi_n \}$ $= C_n \sin \{ n\tau + (n-2)\nu + \alpha_n \}$
$M_1(H)_t$	lunar monthly oscillation in H at fixed solar time t.

$M_2(H)_t$	lunar semi-monthly oscillation in H at fixed solar time t.
A_n, β_n	amplitude and phase angle of the harmonic of lunar daily oscillation averaged over the whole lunation.
$(r_1\ \theta_1)$ $(r_2\ \theta_2)$	amplitude and time of maximum positive deviation of M_1 and M_2 oscillations respectively.

3.3 (1) Lunar tide in H at Kodaikanal during periods of low and high sunspots

The lunar daily and lunar monthly oscillations in H at Kodaikanal for the periods 1951-55 and 1956-60 are determined according to the method described in 3.2.

Annual average daily variation at fixed lunar ages

The mean lunar daily variations of ΔH values are derived separately for days with lunar ages $\nu_0 = 00$, 03, 06, 09, 12, 15, 18 and 21 lunar hours. The whole-year average lunar variations in H at Kodaikanal for each of the eight lunar ages for the periods 1951-55 and 1956-60 are shown in Fig. 1. The positions of the solar midday

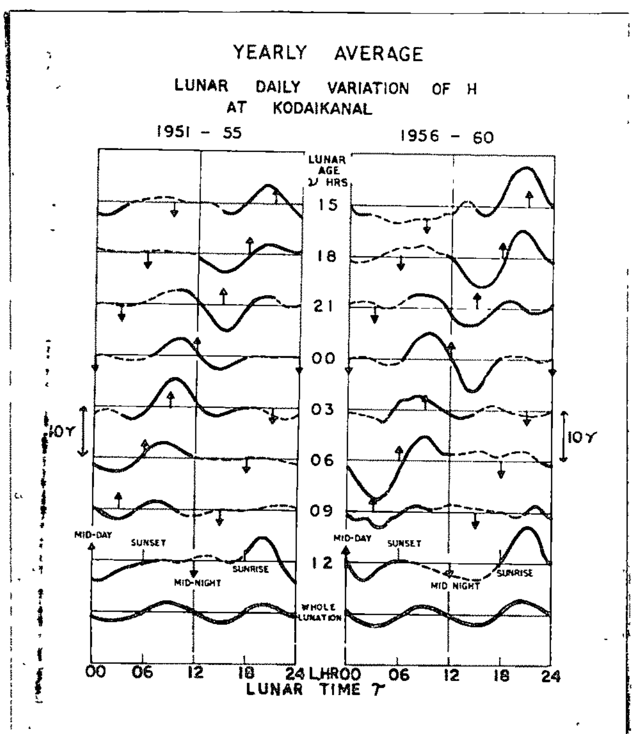

Fig.1.

and midnight are indicated by the upward and downward arrows respectively. The presence of lunar diurnal L_1 and lunar semi-diurnal L_2 variation is noticeable from any lunar daily variation curve by its distinct two peaks. Both set of curves have great similarities viz. (a) The part of the curve having greatest movement fall during daylight hours and is found to occur earlier and earlier in lunar day with the progress of the lunation. (b) The whole lunation curve i.e. average of all lunar daily variation curve for different lunar ages (ν_0 = 00, 03 ....21) is almost a sinusoidal curve with two peaks within one lunar day.

The tide is slightly more during 1956-60 than in the period 1951-55, The yearly average amplitude of tides is found to be 1.55 γ in 1951-55 and 2.01 γ in 1956-60.

The harmonic coefficients (C_n) and phase constants (α_n) of the average lunar daily variations in H field at Kodaikanal for different seasons and the whole year on different lunar ages according to the equation

$$L = \sum_{n=1}^{4} C_n \sin \left\{ n\tau + \Phi_n \right\}$$

where $\Phi_n = \left\{ \alpha_n + (n-2)\nu \right\})$
are given in tables 1a, 1b, 1c, 1d.

Table - 1a.

Coefficients of Annual Average lunar daily variations in H at Kodaikanal at different lunar ages according to the equation, $L = \sum_{n=1}^{4} C_n \sin\{n\tau + (n-2)\nu + \alpha_n\}$

Annual (1951- 55)

Lunar age	C1 Gamma	α_1 Degree	C2 Gamma	α_2 Degree.	C3 Gamma	α_3 Degree	C4 Gamma	α_4 Degree.
00	0.99	331	1.58	164	1.0	360	0,25	151
03	2.24	341	1.79	173	1.71	335	0.35	186
06	1.56	358	1.58	200	0.56	21	0.32	183
09	0.23	285	1.22	205	0.90	355	0.28	120
12	2.05	382	1.78	216	1.59	292	0.77	315
15	(.33	293	1.98	206	1.17	333	0;47	224
18	1.48	334	1.44	188	0.74	324	0.53	230
21	1.04	322	2.49	179	1.10	357	0.47	135
Mean	1.28 ±0.69	325 ±23	1.73 ±0.25	196 ±14	1.09 ±0.36	337 ±21	0.40 ±.14	193 ±59

Annual (1956 - 60)

Lunar age	C1 Gamma	α_1 Degree	C2 Gamma	α_2 Degree.	C3 Gamma	α_3 Degree	C4 Gamma	α_4 Degree.
00	1.66	362	2.8	176	2.00	352	0.36	112
03	0.89	348	1.07	214	1.08	388	0.14	309
06	3.30	324	2.90	175	1.42	367	0.59	142
09	1,32	344	0.78	150	0.66	357	0.08	170
12	2.29	300	2.92	193	1.55	391	0.37	215
15	3.93	344	1:96	175	1,63	369	0:93	223
18	1.87	317	3.20	185	1.69	348	0.58	152
21	1.24	333	1.42	202	1.33	413	0.29	135
Mean	2.07	334	2.12	184	1.42	329	0.42	182
Standard Deviation.	0.99	18	0.89	18	0.12	49	0.25	60

Table – 1 b

Coefficients of lunar daily variations in H at Kodaikanal at different lunar ages according to the equation $L = \sum_{n=1}^{4} C_n \sin \{n\tau + (n-2)\nu + \alpha_n\}$

D-Months(1951-55)

Lunar age	C1 Gamma.	α1 Degree	C2 Gamma	α2 Degree	C3 Gamma	α3 Degree	C4 Gamma	α4 Degree
00	2.31	354	1.73	160	1.13	354	0.36	160
03	3.0	25	1.56	195	1.76	362	0.80	209
06	1.75	319	1.95	183	0.78	47	.5	182
09	1.1	195	1.59	255	1.16	53	.33	151
12	2.21	66	2.76	266	3.14	104	2.03	313
15	1.21	174	2.31	253	2.1	73	.91	257
18	3.31	5.0	1.31	235	0.89	61	.75	283
21	0.29	73	1.30	207	0.43	78	0.2	80

D-Months (1956-60)

Lunar age	C1 Gamma.	α1 Degree	C2 Gamma	α2 Degree	C3 Gamma	α3 Degree	C4 Gamma	α4 Degree
00	2.7	50	3.8	187	3.4	11	0.30	315
03	3.2	6	2.7	221	2.4	62	0.6	245
06	3.2	280	2.3	167	0.4	84	0.9	77
09	1.7	18	0.90	152	1.2	44	0.4	198
12	0.7	323	3.5	215	2.0	95	0.3	290
15	6.6	31	2.7	222	2.9	55	2.3	226
18	2.3	357	4.8	192	2.9	9	1.2	182
21	3.3	555	4.0	255	3.5	84	0.9	244

Table - 1 C

Coefficients of lunar daily variations in H at Kodaikanal at different lunar ages according to the equation $L = \sum_{n=1}^{4} C_n \sin\{n\tau + (n-2)\nu + \alpha_n\}$

E-Months (1951-55)

Lunar age.	C1 Gamma.	α_1 Degree	C2 Gamma	α_2 Degree	C3 Gamma	α_3 Degree	C4 Gamma	α_4 Degree
00	0.23	46	2.42	182	1.8	2.3	0.40	172
03	0.67	304	1.49	158	1.6	325	0.49	150
06	2.21	366	2.3	211	0.6	338	0.55	169
09	0.42	232	1.8	201	1.3	346	0.68	262
12	2.33	353	1.8	185	0.9	39	0.43	250
15	1.14	30	2.3	191	1.26	350	.33	157
18	1.63	336	2.26	182	1.49	22	0.53	200
21	1.63	290	2.9	170	1.53	334	0.56	120

E-Months (1956-60)

Lunar age.	C1 Gamma.	α_1 Degree	C2 Gamma	α_2 Degree	C3 Gamma	α_3 Degree	C4 Gamma	α_4 Degree
00	4.0	314	4.8	148	3.6	339	1.5	137
03	1.9	310	1.2	175	1.6	339	0.4	181
06	4.3	338	2.9	170	2.7	6	1.0	181
09	1.4	25	1.6	154	1.0	310	0.3	7
12	4.3	306	3.0	173	2.7	358	1.0	209
15	1.6	12	1.9	126	1.7	357	0.1	80
18	5.3	290	4.2	165	3.0	321	1.5	133
21	2.9	251	2.3	132	1.5	346	0.5	105

Table 1 d.

Coefficients of lunar daily variations in H at Kodaikanal at different lunar ages according to the equation $L = \sum_{n=1}^{4} C_n \sin\{n\tau + (n-2)\nu + \alpha_n\}$

J- Months (1951- 55)

Lunar age.	C1 Gamma	α_1 Degree	C2 Gamma	α_2 Degree	C3 Gamma	α_3 Degree	C4 Gamma	α_4 Degree
00	1.5	274	0.8	134	0.15	332	0.15	071
03	4.32	316	2.5	165	2.17	321	.13	181
06	1.45	32	0.8	201	0.70	20	.05	260
09	1.46	20	1.6	153	1.13	307	.28	120
12	2.64	170	3.5	184	2.04	28	0.6	34
15	0.70	20.0	2.3	177	1.46	349	.41	210
18	1.82	248	1.46	159	.10	178	.33	127
21	3.04	332	3.46	178	2.02	4.0	.81	153

J-Months (1956-60)

Lunar age.	C1 Gamma	α_1 Degree	C2 Gamma	α_2 Degree	C3 Gamma	α_3 Degree	C4 Gamma	α_4 Degree
00	0.9	58	1.7	245	0.2	332	0.7	13
03	1.8	166	0.5	353	0.2	93	0.9	16
06	3.8	343	3.5	186	1.6	354	0.6	155
09	1.0	1.0	0.1	0	0.6	343	0.3	175
12	2.4	283	2.7	187	1.6	19	0.2	117
15	3.8	349	3.0	163	1.9	333	0.7	206
18	1.2	89	1.3	231	0.3	112	0.8	333
21	2.9	325	1.7	160	0.5	358	0.8	84

The relations between ϕ and ν for any particular harmonic are shown in Fig. 2.

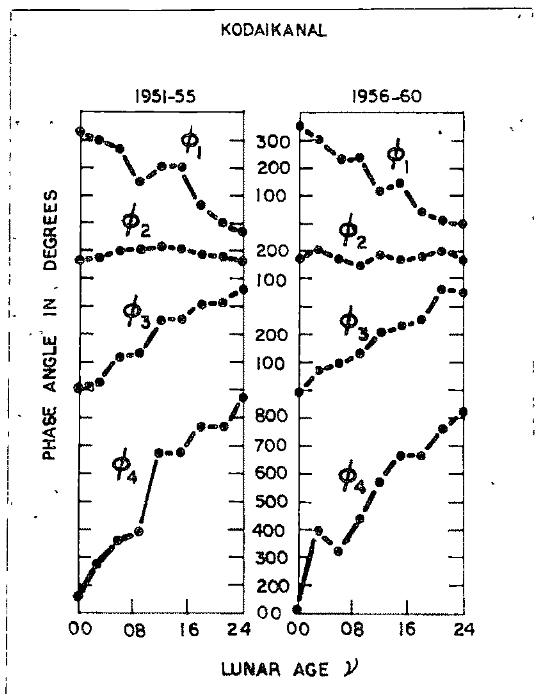

Fig. 2.

It is seen from Fig. 2 that the phase angle ϕ_2 for both the periods 1951-55 and 1956-60 remain about the same during a whole lunation. Further the annual average values of C_n are nearly same for the two periods. The phase angle ϕ_1 progressively decreases by about 360° and phase angle ϕ_3 progressively increases by 360° in one complete lunation. Similarly ϕ_4 is to follow through 720° during one lunation. Referring to table 1, it is seen that the magnitudes of harmonic coefficients of lunar daily variation do not show any relationship with the lunar age and are nearly same for all values of ν. During the period of low sunspots (1951-55) the annual average C_1 amplitude is 1.28 ± 0.26 γ , the annual average C_2 amplitude is 1.73 ± 0.13 γ . During the period of high sunspots (1956-60) the average C_1 amplitude is 2.07 ± 0.99 γ and the average C_2 amplitude is 2.12 ± 0.89 γ. The higher harmonics are progressively smaller in magnitude.

The phase constant α_1 is 325° ± 23° during 1951-55 and 334° ± 18° during 1956-60. The phase constant α_2 is 196° ± 14° during 1951-55 and 184° ± 18° during 1956-60. The phase constant has nearly same values for the two solar epochs. Unlike the phase angles ϕ_n the phase constants remain nearly the same during a whole lunation.

The lunar daily variation averaged over a complete lunation is shown in Fig. 1. The harmonic coefficients of the whole lunation average oscillations for Kodaikanal during 1951-55 and 1956-60 are given in table 3. It is seen that most significant component is the lunar semi-diurnal one (A_2) and other harmonics including the A_1 are very small as they cancel out in averaging. The lunar semi-diurnal component A_2 is 1.6 γ and lunar diurnal component A_1 is 0.4 γ for the whole year during the period 1951-55. Similarly during 1956-60 A_2 is 2.01 γ and A_1 is 0.33 γ . Thus the amplitudes of all components except A_2 are statistically insignificant.

The phase angle β_2 for the A_2 oscillation is found to be 189° during 1951-55 and 182° during 1955-60. The phase of the lunar tide does not seem to change with the solar activity. The mean tide for the entire period 1951-60 is 1.8 γ with a phase angle of 185° i.e. the maximum positive deviation would occur at 8.8 hours local lunar time.

Annual average lunar monthly variations at fixed solar times

Lunar tides can also be estimated by studying lunar monthly M_1 and lunar semi-monthly M_2 variation of ΔH at each fixed solar hour. Fig. 3 shows the

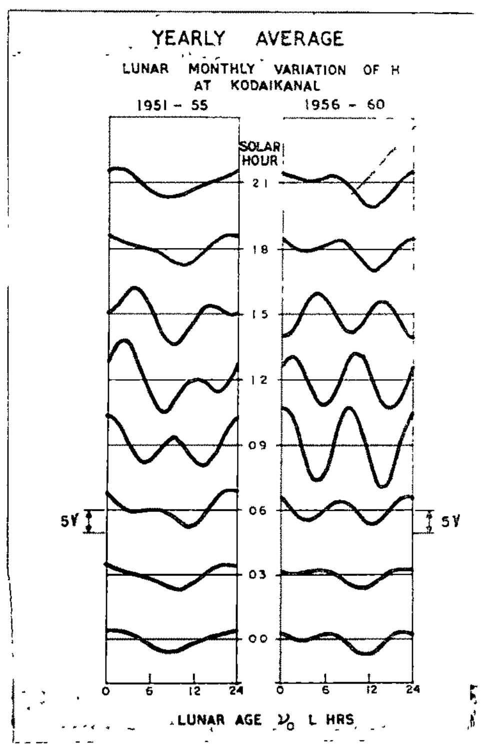

Fig. 3.

Table - 2.

Coefficients of ANNUAL AVERAGE lunar monthly M_1 and lunar semi-monthly M_2 oscillations in H at Kodaikanal for the period 1951-55 and 1956-60.

	1951-55					1956-60				
Time L.M.T.	39000+ ΔH Gamma	r_1 Gamma	θ_1 in lunar age degree	r_2 Gamma	θ_2 in lunar time degree	39000+ ΔH Gamma.	r_1 Gamma.	θ_1 in lunar age. degree	r_2 Gamma	θ_2 in lunar time degree
00	427	2.3	8	0.5	243	497	1.6	43	2.0	80
01	431	2.2	5	0.4	288	497	2.0	36	1.5	114
02	429	2.1	6	0.0	213	500	2.1	45	1.3	150
03	431	2.6	9	0.6	210	500	1.8	37	1.1	190
04	431	2.7	6	0.3	186	500	2.1	33	1.3	240
05	429	3.1	356	0.8	246	495	0.9	340	1.2	219
06	430	3.0	360	2.0	261	499	0.7	13	2.8	242
07	439	2.8	360	3.2	264	514	0.5	31	5.4	262
08	457	1.9	9	4.8	279	543	0.7	70	6.8	267
09	477	2.5	5	4.3	282	578	0.8	103	9.3	279
10	493	3.1	12	3.4	285	605	0.8	154	9.4	294
11	494	3.9	15	3.8	267	615	0.9	123	7.8	310
12	487	5.3	18	4.6	270	606	0.6	156	6.3	326
13	472	4.0	23	4.9	288	588	0.6	163	4.0	309
14	454	4.1	26	4.6	291	563	0.4	209	3.6	370
15	440	4.1	23	3.5	291	542	0.9	122	4.5	272
16	430	3.6	17	2.5	276	528	1.1	84	3.4	271
17	431	3.2	12	2.0	267	519	1.3	82	2.5	252
18	430	3.2	8	1.1	279	510	2.0	71	2.5	227
19	427	3.2	11	0.6	354	502	2.4	63	2.6	247
20	426	3.3	8	0.7	123	499	2.6	62	2.2	279
21	425	3.2	3	0.8	177	497	2.9	64	2.1	320
22	425	3.1	5	0.5	198	496	2.5	54	2.3	13
23	426	2.6	15	0.5	267	497	2.0	53	1.7	54

Table - 3.

The coefficients of lunar daily oscillations in H averaged over the whole lunation during different seasons for Kodaikanal (1951-55 and 1956-60) according to the equation $L = A_n \sin(n\tau + \beta_n)$

Station.	Period	Season	A_1 Gamma.	β_1 Degree	A_2 Gamma	β_2 Degree	A_3 Gamma	β_3 Degree	A_4 Gamma	β_4 Degree
Kodaikanal	1951-55	D-Months	0.5	345	1.4	225	0.7	327	0.4	334
		E-Months	0.2	220	2.0	195	0.3	303	0.2	321
		J-Months	0.9	280	1.8	171	0.1	303	0.2	22
		Annual	0.4	285	1.6	189	0.4	315	0.2	342
Kodaikanal	1956-60	D-Months	1.1	143	2.7	208	0.7	325	0.5	318
		E-Months	0.8	297	2.6	157	0.2	258	0.2	270
		J-Months	0.6	125	1.4	189	0.3	165	0.2	22
		Annual	0.3	146	2.0	182	0.1	297	0.2	339

annual average curves of ΔH at fixed solar hours 00, 03.....................21 as a function of lunar age ν_0 (at Greenwich moon) for both the periods 1951-55 and 1956-60. The coefficients of lunar monthly and semi-monthly oscillations derived from these curves are given in Table 2. In the tables the phase of M_1 oscillations are presented in terms of local lunar age ν whereas the phase of M_2 oscillations are presented in terms of local lunar time τ .

Referring to Fig. 3 one sees similarity between the two sets of curves for the two periods of different solar activity. The tide for both the periods is significantly large during daytime hours and its amplitude reaches maximum value near midday. During night-time, oscillations are small and insignificant. The phases of the oscillations are roughly the same for the two epochs. The oscillations during the day-time have a predominant periodicity of twelve lunar hours while the night-time oscillations have predominant twenty four lunar hours component. However the yearly average lunar monthly variation curves for the period 1956-60 indicate the presence of twelve lunar hour period even during night-time. The amplitudes of M_1 oscillations (r_1) do not show any dependence on the solar time. Its value being between 2 to 5 γ for both the stations, the amplitude of M_2 oscillations (r_2) is very small for the night-time hours, starts rising with the sunrise has a large value around midday and reduces to a low value by the sunset. It is however to be noted that the maximum amplitude of r_2 during 1951-55 is about 5 γ and during 1956-60 the maximum r_2 amplitude is 9.4 γ at Kodaikanal.

The (r_1 θ_1) points for different solar hours are plotted on a harmonic dial of lunar age and lunar time in Fig. 4. On the harmonic dials of lunar time

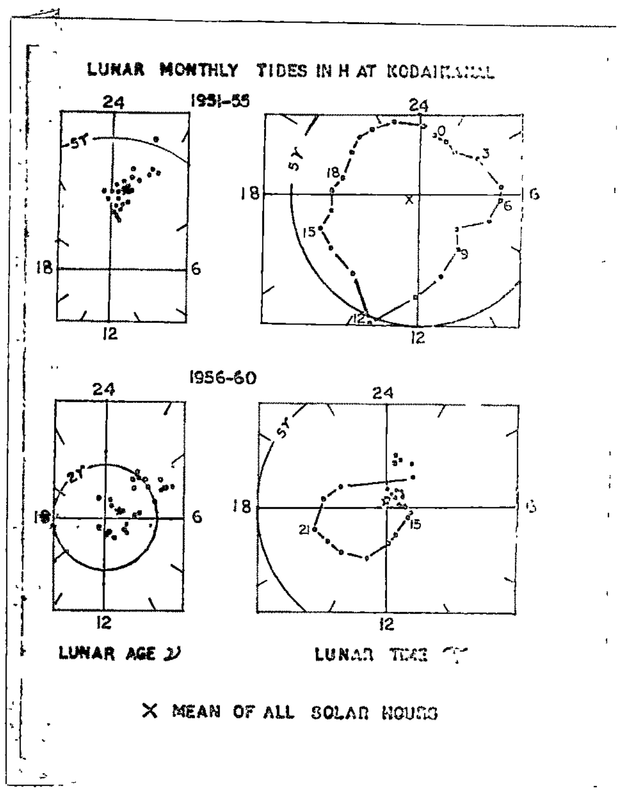

Fig.4.

various (r_1 θ_1) points for both high and low solar activity periods move progressively around the origin with increasing solar time and form a loop during the course of one complete solar day. The vectorial average of the amplitudes over the whole solar day is reduced to a small value of 0.57 γ whereas solar mean value is 1.42γ for the period 1956-60 and corresponding figures for 1951-55 period are 0.46 γ and 3.13 γ respectively. On the lunar age dial the points (r_1 ν_1) corresponding to different solar hours group themselves in a rather narrow sector and thus vector average value of the amplitude is not different from the individual value of the amplitude. Its vectorial mean for Kodaikanal 1956-60 is 1.17 γ and arithmetic mean is 1.42 γ and similar figures for the period 1951-55 are 3.11 γ and 3.13 γ .

The amplitude and phase of lunar semi-monthly oscillations (r_2 θ_2) for different solar hours are plotted on the harmonic dials of lunar age and lunar time in Fig.5. On the lunar age dial the points for different hours of the day move around the origin giving rise to a very small value of the vector average from all the hours. On the lunar time dial the points for various hours of the day-time do not move around the origin giving rise to a very small value of the vector average from all the hours, but lie within a narrow sector and solar hour average of the M_2 amplitudes are comparable to arithmetical (scalar) average. At Kodaikanal (1956-60) arithmetical average of M_2 amplitude (r_2) is 3.63 γ and the vectorial average is 2.67 γ . Corresponding figures for (1951-55) period are 2.09 γ and 1.9 γ respectively. The phase of maximum deviation of M_2 on

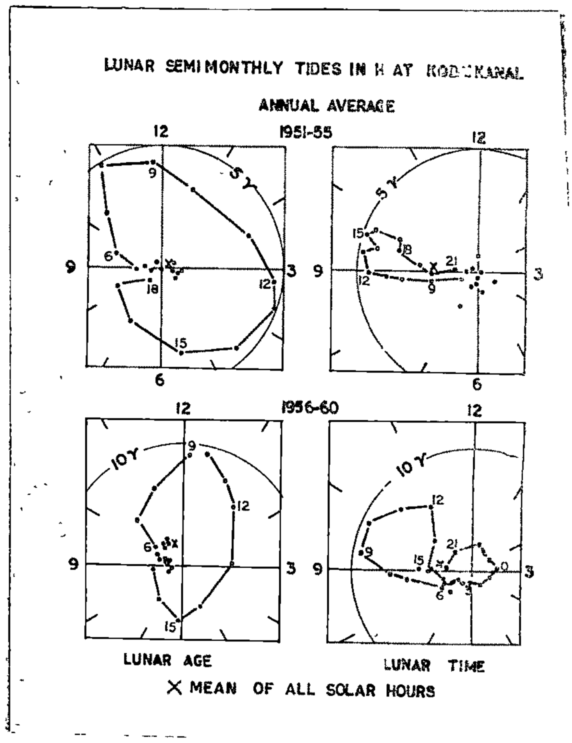

Fig.5.

the lunar time dial is 9.4 l.hr. for the period 1951-55 and for the period 1956-60 9.20 l.hr.

Lunar daily variation of H during different seasons of the year

Lunar daily variation at the eight lunar age groups were computed separately for each season and resulting curves were similar to curves obtained for the annual lunar daily variation showed in Fig. 1. For any particular season, the whole lunation average curves were also derived by averaging eight individual curves. As described earlier for the annual average curves, it is found that during any particular season also, the oscillations are predominant during the day-time hours and the peak occurs earlier in lunar time with increasing age of the moon. Individual curves were harmonically analysed for finding the coefficients C_n and α_n for each season. During any of the seasons the variation of the phase of a particular harmonic with the lunar age was found as expected of Chapman's phase law. The whole lunation average curves were harmonically analysed and the amplitude and phases in individual seasons are given in Table 3.

It is seen from the table that most significant component is the second harmonic component with periodicity of 12 lunar hours. Amplitude A_2 (1956-60) ranges between 1.4 γ to 2.7 γ in contrast to A_2 amplitudes (1951-55) ranging from 1.4 γ to 2.0 γ. The phase of A_2 amplitudes i.e. β_2 (1956-60) is 208° during D-months, 157° during E-months and 189° during J-months. Thus the maximum deviation due to A_2 oscillation occurs about 2 hours later during equinoxial months, than D-months. In the low solar activity period the picture was little different, the maximum deviation due to A_2 oscillation occurs about 2 hours later during J-months than during D-months. Regarding amplitudes, one finds that for Kodaikanal (1956-60) the maximum amplitude of A_2 occurs during D-months (2.7 γ) little less during E-months (2.60 γ) and least in J-months (1.43 γ). During (1951-55) the maximun amplitude of A_2 occur during E-months (2.0 γ) than follows J-months (1.8 γ) and lastly by D-months (1.4 γ).

<u>Lunar monthly oscillations in H at fixed solar time during different seasons of the year</u>

In Fig. 6 comparison is made between diurnal

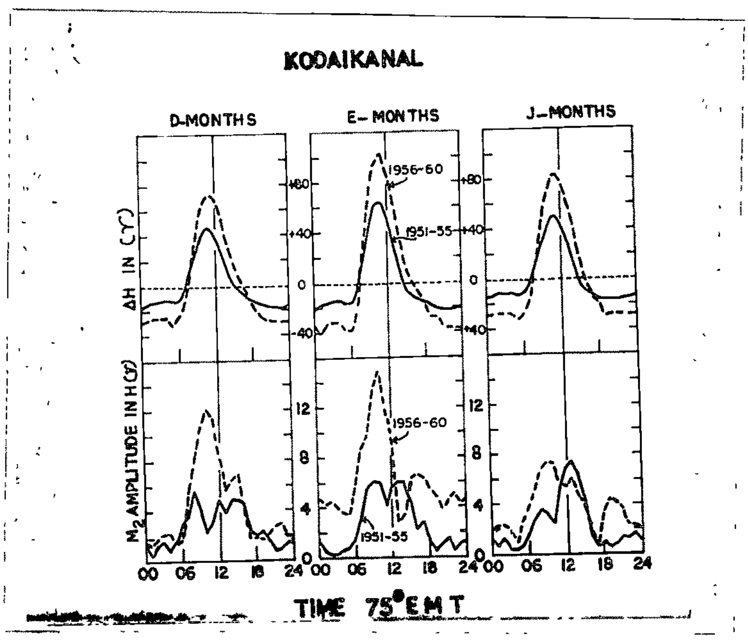

Figure.6.

variation of M_2(H) amplitude and normal diurnal variation in H. The diagram presents the picture of each season during the periods 1951-55 and 1956-60. The curves drawn with dotted lines are for the period 1956-60. The following things stand out:-

a) $M_2(H)$ and H itself vary in a similar way during the course of a day.

b) The range of daily variation in both $M_2(H)$ and H itself is greater in the period of higher solar activity 1956-60 than during the period of low solar activity 1951-55 with an exception of $M_2(H)$ range in J-months being about the same for both periods.

c) The range in H itself is greatest during equinoxial months and are comparable in D-months and J-months.

d) The range in $M_2(H)$ during 1956-60 is greatest in E-months less in D-months and least in J-months.

e) The range of $M_2(H)$ during 1951-55 seem to be more during J-months and comparable in D-months and E-months.

The lunar monthly (M_1) and lunar semi-monthly (M_2) oscillations in H in each of the solar hours were computed separately for different seasons of the year.

(r_2 τ_2) points in different solar hours for each season are plotted in the harmonic dial of lunar time in Fig. 7'. Similar curves for Huancayo (IGY/IGC) are drawn in the same figure for comparison. It is seen that the most of the points for the day-time fall in a narrow sector forming a loop. In tables 4a and 4b' r_2, $\theta_2(\tau)$,

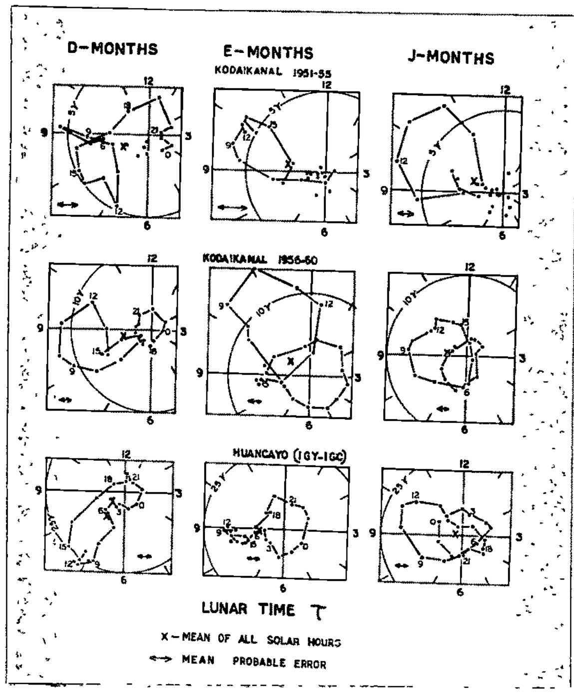

Figure.7.

$2(\quad)$, ΔH and probable error values for each solar hour are given.

Table 4 (a)

Coefficients of lunar semi-monthly M_2 oscillations in H at Kodaikanal (1951-55) averaged over different seasons.

L.M.T.	D-Months.				E-Months				J-Months			
	39000 + ΔH Gamma.	r_2 Gamma	Probable error.	Phase τ_2 lunar time °	39000 + ΔH Gamma.	r_2 Gamma	Probable error.	Phase τ_2 lunar time °	39000 + ΔH Gamma	r_2 Gamma	Probable error.	Phase τ_2 lunar time °
00	413	1.20	1.6	131	428	1.20	2.0	255	439	1.2	1.2	291
01	415	0.4	1.7	196	431	0.54	2.1	300	440	0.6	1.2	312
02	416	1.2	1.8	183	432	0.36	2.0	261	442	1.2	1.3	346
03	417	1.4	1.9	206	434	0.31	1.9	207	441	0.3	1.2	245
04	418	0.8	1.7	199	434	0.52	1.8	81	442	0.4	1.1	256
05	416	1.5	1.6	246	432	0.70	1.7	183	439	0.7	1.1	294
06	417	2.8	1.3	263	432	1.56	1.6	252	442	1.6	1.0	266
07	426	3.6	1.1	262	442	3.28	2.6	261	449	2.8	0.9	276
08	443	5.6	1.0	274	465	5.53	1.5	276	464	3.5	0.8	293
09	459	3.9	1.0	267	492	6.14	1.6	285	483	3.2	0.8	287
10	472	2.4	1.0	256	511	6.00	1.6	300	497	2.5	0.7	272
11	474	3.0	1.0	219	513	4.96	1.6	297	502	5.3	0.7	266
12	467	4.9	0.9	203	501	5.70	1.6	294	496	7.0	0.8	286
13	455	3.9	0.9	226	479	6.09	1.6	297	483	7.4	1.0	306
14	440	5.0	0.9	231	457	6.03	1.7	300	466	6.6	0.6	325
15	429	4.9	0.9	242	443	4.46	1.5	306	450	4.2	0.6	331
16	424	4.6	0.8	259	437	2.24	1.5	282	444	1.5	1.0	324
17	421	2.4	0.8	273	435	2.84	1.5	255	441	0.8	0.6	272
18	417	2.1	0.9	317	433	1.23	1.5	246	437	1.0	0.6	225
19	414	2.4	0.8	13	430	0.48	1.5	255	437	0.5	0.6	114
20	412	1.5	0.9	69	428	1.07	1.5	171	436	0.8	0.7	153
21	411	0.8	0.9	80	426	1.47	1.5	204	436	1.3	0.8	172
22	411	0.8	1.3	103	427	0.52	1.7	243	437	1.3	0.9	220
23	411	1.5	1.2	114	428	1.13	1.9	261	437	1.7	1.0	293

Table 4 (b)

Coefficients of lunar semi-monthly M_2 oscillations in H at Kodaikanal (1956-60) averaged over different seasons.

	D-months.				E-months.				J-months.			
L.M.T.	39000 + ΔH Gammas.	$\hbar_2$ Gammas	Probable error.	Phase τ_2 lunar time.	39000 + ΔH Gammas	$\hbar_2$ Gammas	Probable error.	Phase τ_2 lunar time	39000 + H Gammas	$\hbar_2$ Gammas	Probable error.	Phase τ_2 lunar time
00	500	1.4	1.1	86	490	4.8	1.2	102	502	2.0	1.0	289
01	501	1.2	1.1	172	487	4.4	1.1	129	502	2.2	0.9	11
02	503	1.9	1.1	216	494	4.6	1.1	150	503	2.3	0.9	19
03	503	2.1	1.0	263	495	4.0	1.0	181	503	2.0	0.8	55
04	503	2.2	1.0	288	495	3.6	1.0	216	502	0.9	0.9	70
05	497	1.2	1.2	341	489	3.5	1.3	246	499	2.8	1.0	151
06	504	1.8	1.2	233	489	5.8	1.3	280	503	3.9	1.1	185
07	519	5.4	1.3	228	508	8.7	1.4	299	515	5.4	1.2	233
08	543	8.4	1.6	233	544	9.9	1.6	307	542	7.0	1.4	249
09	571	10.7	1.8	245	589	13.4	2.0	308	575	7.4	1.6	275
10	593	12.1	2.0	254	622	14.9	2.1	331	601	7.2	1.7	284
11	601	11.4	2.1	274	631	11.3	2.2	350	614	5.6	1.7	303
12	596	8.3	2.0	295	611	8.9	2.1	7	610	5.4	1.7	309
13	581	5.7	1.9	272	588	2.8	2.0	7	594	6.0	1.7	318
14	561	6.4	1.7	241	558	3.5	1.8	252	571	4.6	1.5	335
15	544	6.9	1.5	245	537	6.3	1.6	263	546	4.0	1.4	345
16	532	3.9	1.4	254	525	6.6	1.3	263	526	1.8	1.2	361
17	523	1.7	1.3	248	518	6.4	1.3	258	515	0.8	1.2	127
18	512	1.9	1.3	186	508	5.5	1.4	271	511	3.4	1.2	177
19	505	1.7	1.3	226	499	4.9	1.4	296	501	4.4	1.1	198
20	501	2.1	1.3	295	495	3.8	1.4	350	503	4.0	1.1	222
21	499	2.7	1.3	320	491	4.5	1.3	11	502	3.6	1.0	244
22	498	2.9	1.3	358	490	5.1	1.3	46	501	2.3	1.1	279
23	499	1.9	1.2	55	490	4.3	1.3	79	501	2.0	1.0	303

3·3 (2) Lunar tide in 'D' at Kodaikanal during periods of low and high sunspots

The lunar daily and lunar monthly oscillations in D at Kodaikanal for low sunspot period (1951-55) and high sunspot period (1956-60) are determined.

Annual average lunar daily variations at fixed lunar ages

The mean lunar daily variations of ΔD values are derived separately for the days with lunar ages, ν_0 = 00, 06, 09, 12, 15, 18 and 21 lunar hours. The whole year average lunar variations in D at Kodaikanal for each of the eight lunar ages for the periods 1951-55 and 1956-60 are shown in Fig. 1. The positions of the

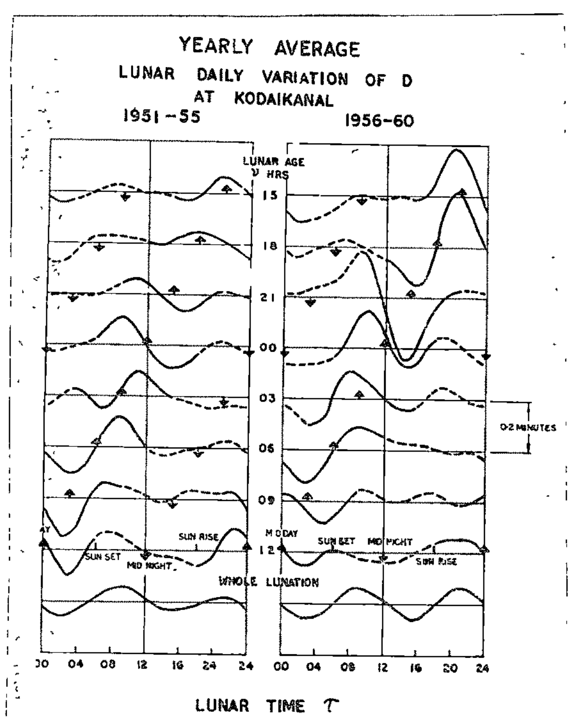

Figure.1.

solar midday and midnight are indicated by the upward and downward arrows respectively. The presence of lunar diurnal L_1 and lunar semi-diurnal L_2 variation is noticeable from the distinct two peaks in lunar daily variation curves. The lunar daily variation curves for the low sunspot period (1951-55) and high sunspot period (1956-60) are similar in character. The amplitudes of the lunar daily variation are greater during high sunspot period (1956-60) than low sunspot period (1951-55). The part of the curve having greatest movement fall during daylight hours and is found to occur earlier and earlier in lunar day with the progress of the lunation.

The harmonic coefficients C_n and α_n of the average lunar daily variations in D at Kodaikanal are computed according to the Chapman's phase law expression. In Table 1 coefficients of annual average lunar daily variations in D for the periods 1951-55 and 1956-60 are presented. It is seen from the Tables that amplitudes C_n are independent of lunar age. The relations between ϕ and ν for any particular harmonic are shown in Fig. 2. The Fig. 2 verifies Chapman's phase law. The phase constants α_n unlike phase angles ϕ_n remain nearly same during the whole lunation.

Table – 1.

The coefficients of annual average lunar daily variation in 'D' at Kodaikanal for different lunar ages according to the equation $L = \sum_{n=1}^{4} C_n \sin\{n\tau + (n-2)\nu + \alpha_n\}$

Annual (1951–55)

Lunar age	C1 1/30 mnt.	α_1 degree	C2 1/30 mnt.	α_2 degree	C3 1/30 mnt.	α_3 degree	C4 1/30 mnt.	α_4 degree
00	1.40	352	1.82	187	0.46	351	0.24	260
03	1.24	341	0.91	80	0.91	266	0.54	118
06	1.11	4	2.05	182	0.74	351	0.16	80
09	1.34	21	1.85	206	0.85	12	0.54	222
12	0.49	180	1.67	167	1.38	323	0.38	151
15	0.14	24	1.15	190	0.54	346	0.30	216
18	0.99	162	1.14	245	0.11	308	0.28	350
21	0.84	293	1.06	149	0.52	343	0.08	50

Annual (1956–60)

Lunar age	C1 1/30 mnt.	α_1 degree	C2 1/30 mnt.	α_2 degree	C3 1/30 mnt.	α_3 degree	C4 1/30 mnt.	α_4 degree
00	1.46	294	2.03	180	1.25	342	0.22	181
03	1.00	318	2.06	199	0.69	19	0.52	306
06	2.09	351	1.40	179	0.72	19	0.14	290
09	0.86	345	0.72	125	1.05	267	0.08	110
12	1.05	324	0.90	215	0.35	335	0.30	126
15	2.26	41	2.31	195	0.94	13	0.58	208
18	2.05	9	2.92	193	1.62	337	0.58	140
21	3.20	335	3.16	187	1.54	39	0.58	268

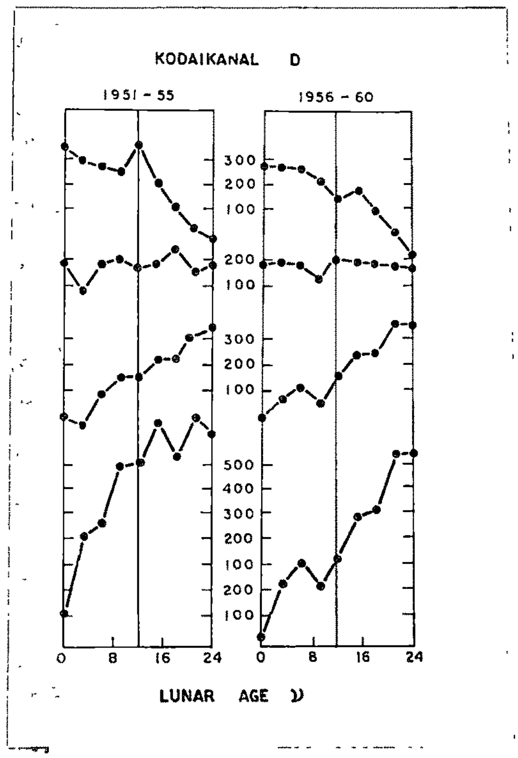

Figure.2.

The lunar daily variation averaged over a complete lunation is shown in Fig. 1. The harmonic coefficients of the average lunar daily variation for the whole lunation for the periods 1951-55 and 1956-60 are given in Table 2. The lunar semi-diurnal component L_2 is the most prominent component, others are very small. The amplitude of L_2 is 0.046 minute and L_1 is 0.02 minute for the whole year during the period 1951-55. Similarly during 1956-60 L_2 is 0.067 minute and L_1 is 0.012 minutes. The phase angle β_2 for the L_2 oscillation is found to be 183° during 1951-55 and 193° during 1956-60.

Table - 2.

The coefficients of lunar daily oscillations in D averaged over the whole lunation during different seasons for Kodaikanal according to the equation $L = A_n \sin(n\tau + \beta_n)$

Annual (1951-55)

Station.	Period	Season	A_1 1/30 mts.	β_1 degrees	A_2 1/30 mts.	β_2 degrees.	A_3 1/30 mts.	β_3 degrees.	A_4 1/30 mts.	β_4 degrees
Kodaikanal	1951-55	D-months	0.28	161	2.58	232	0.06	247	0.25	270
		E-months	0.55	298	0.88	162	0.69	170	0.22	191
		J-months	1.58	303	2.10	133	0.23	195	0.22	169
		Annual	0.66	297	1.39	183	0.14	145	0.16	210

Annual(1956 - 60)

Station.	Period	Season	A_1 1/30 mts.	β_1 degrees	A_2 1/30 mts.	β_2 degrees.	A_3 1/30 mts.	β_3 degrees.	A_4 1/30 mts.	β_4 degrees
Kodaikanal	1956-60	D-months	1.77	167	4.68	239	0.56	315	0.14	180
		E-months	0.89	343	1.86	148	0.30	22	0.16	270
		J-months	0.46	273	2.55	131	0.34	280	0.08	30
		Annual	0.37	228	2.02	193	0.34	350	0.08	30

Annual average lunar monthly variations at fixed solar times

Lunar tides are estimated by studying lunar monthly M_1 and lunar semi-monthly M_2 variation of ΔD at each fixed solar hour. Fig. 3 shows annual average curves

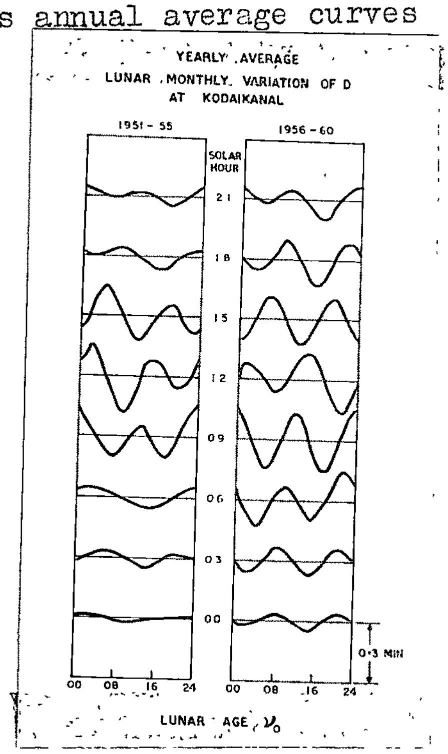

Figure.3.

of ΔD at fixed solar hours 00, 03.................21 as a function of lunar age ν_0 (at Greenwich noon) for the periods 1951-55 and 1956-60. The coefficients of lunar monthly and semi-monthly oscillations derived from these curves are given in table 3. In the tables the phase of M_1 oscillations are presented in terms of local lunar age ν and the phase of M_2 oscillations are presented in terms of local lunar time τ.

Table - 3.

The coefficients of annual average lunar monthly M_1 and lunar semi-monthly M_2 oscillations in D at Kodaikanal.

L.M.T.	1951-55 $2^{\circ}+\Delta D$ 1/10mts.	r_1 1/10mts.	θ_1 in lunar age degree	r_2 1/10mts.	θ_2 in lunar time degree.	1956-60 $2^{\circ}+\Delta D$ 1/10mts.	r_1 1/10mts.	θ_1 in lunar age degree.	r_2 1/10 mts.	θ_2 in lunar time degree.
00	356	0.23	7	0.06	281	359	0.13	34	0.38	100
01	356	0.22	358	0.17	105	358	0.08	46	0.45	149
02	355	0.24	18	0.19	215	358	0.04	76	0.59	171
03	356	0.30	42	0.32	244	359	0.04	102	0.71	183
04	357	0.33	29	0.31	251	359	0.03	46	0.92	215
05	356	0.59	34	0.18	229	358	0.26	272	0.97	237
06	354	0.62	20	0.09	276	355	0.44	299	1.17	270
07	353	0.77	7	0.47	278	353	0.74	291	1.48	283
08	353	0.74	4	0.86	277	356	0.37	258	1.56	293
09	357	0.70	357	1.00	288	363	0.15	11	1.53	296
10	363	0.61	301	0.76	284	372	0.56	125	1.56	285
11	368	0.74	313	0.86	264	380	0.81	136	1.28	298
12	370	0.71	341	1.22	295	384	0.70	157	1.11	308
13	368	0.58	5	1.15	286	381	0.41	163	0.96	287
14	363	0.68	46	1.09	293	374	0.11	244	1.19	261
15	358	0.52	51	1.05	303	366	0.15	20	1.17	270
16	355	0.75	57	0.55	349	361	0.26	45	1.04	272
17	355	0.64	46	0.39	306	359	0.34	58	1.00	271
18	356	0.48	57	0.32	266	358	0.36	57	1.00	268
19	356	0.46	75	0.46	233	358	0.42	59	0.96	276
20	357	0.43	57	0.46	245	359	0.51	48	0.74	304
21	359	0.28	50	0.37	273	360	0.39	57	0.61	320
22	357	0.25	23	0.24	312	360	0.35	54	0.37	388
23	357	0.17	7	0.23	291	359	0.29	36	0.39	71

Referring to Fig. 3, one sees similarity in character between the two sets of curves for the two periods of different solar activity. The tide for both the periods is significantly large during day-time hours and its amplitude reaches maximum value near midday. During night-time oscillations are quite small. The phases of the oscillations are roughly same for the two epochs. The oscillations during the day-time have a predominant periodicity of twelve lunar hours while the night-time oscillations have predominance of twenty four lunar hour components. However the yearly average lunar monthly variation curves for the period 1956-60 indicate the presence of twelve lunar hour period even during night-time.

The amplitudes r_1 of lunar monthly oscillations are so small that the representation of (r_1 Θ_1) points on a harmonic dial will not serve any quantitative purpose. The probable errors will mask the picture. Hence (r_1 Θ_1) points for different solar hours are not represented on a harmonic dial.

The amplitude and phase of lunar semi-monthly oscillations (r_2 Θ_2) for different solar hours are plotted on the harmonic dials of lunar age and lunar time in Fig. 4. On the lunar age dial the points for different hours of the day move around the origin giving rise to a very small value of the vector average from all the hours. On the lunar time dial the points for various

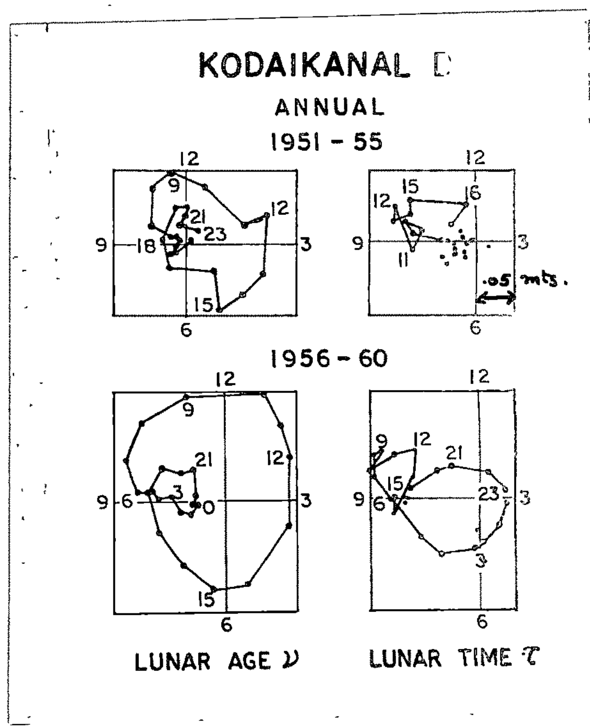

Figure.4.

hours of the day-time trace a loop with an elongation in a preferred direction. During 1951-55 the scalar average of r_2 is 0.053 minutes and the vectorial mean of r_2 in lunar age dial is 0.013 minutes and the vectorial mean of r_2 in lunar time dial is 0.045 minutes. During 1956-60 the scalar average of r_2 is 0.096 minutes and the vectorial mean of lunar time dial is 0.07 minutes. The phase of maximum deviation of M_2 on the lunar time dial is 9.5 l.hr. or 284° during 1951-55 and 9.2 l.hr. or 275° during 1956-60.

Lunar daily variation of D during different seasons

Lunar daily variations at the eight lunar age groups are computed separately for each season and the resulting curves are shown in Fig. 5 and Fig. 6. The

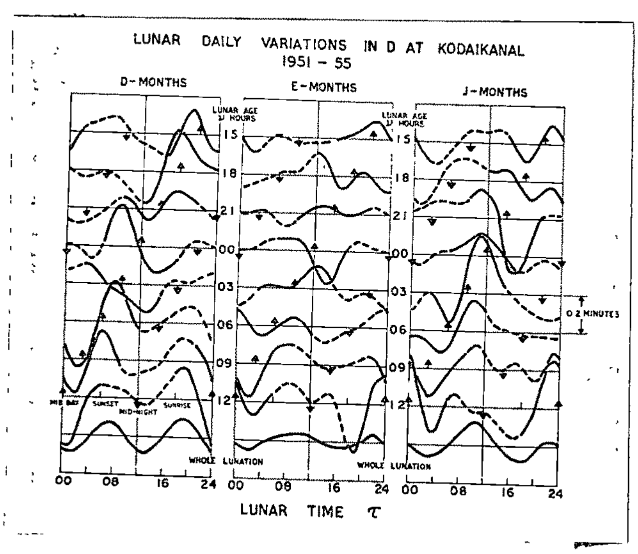

Figure.5.

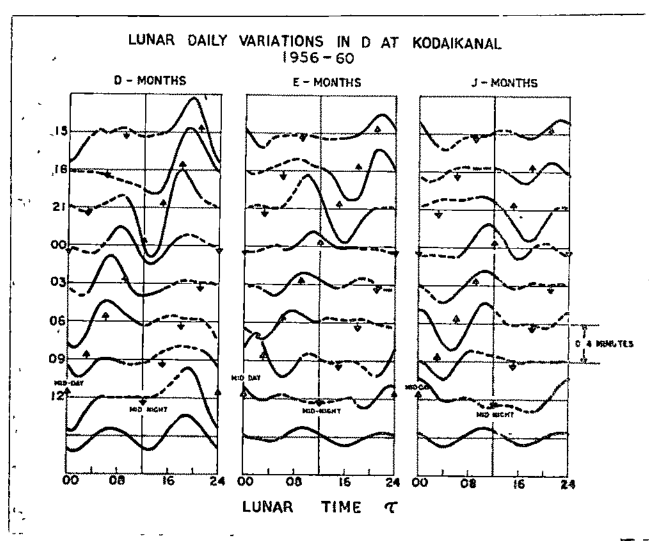

Figure.6.

whole lunation average curves for each season are also drawn. In character these curves are identical to the curves in Fig. 1. Here also Chapman's phase law is obeyed. The harmonic coefficients for the whole lunation lunar daily variation curves are presented in Table 2.

It is seen that semi-diurnal component A_2 is the most prominent. The amplitudes of A_2 range between .029 minutes and 0.86 minutes during 1951-55, in the order

D-months	0.86 minutes
E-months	0.029 minutes
J-months	0.70 minutes

The phase β_2 is

232° during D-months

162° during E-months, and

133° during J-months.

The amplitudes of A_2 range between 0.062 minutes and 0.156 minutes during 1956-60 in the order

D-months	0.156 minutes
E-months	0.062 minutes
J-months	0.085 minutes.

The phase β_2 is

239° during D-months

148° during E-months

131° during J-months .

Lunar monthly oscillations in D at fixed solar time during different seasons

In Fig. 7 and Fig. 8 comparison is made

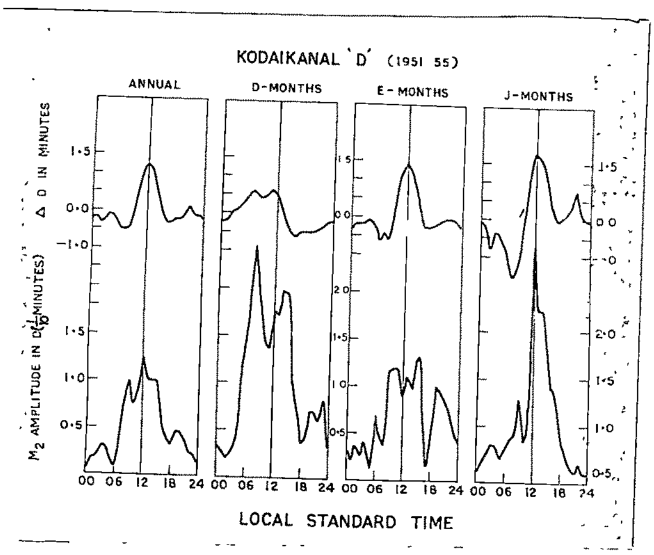

Figure.7.

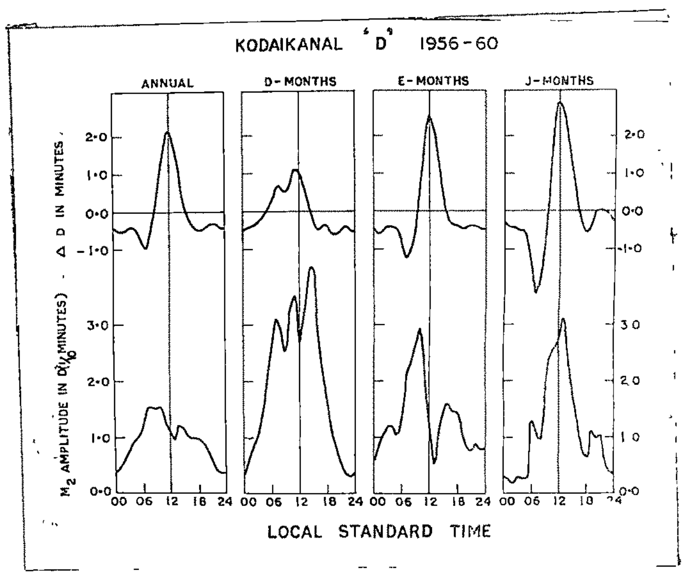

Figure.8.

between diurnal variation of $M_2(D)$ amplitude and the normal diurnal variation in D. $M_2(D)$ and D itself vary in a similar way during the course of a day. The range of daily variation in D is least in D-months and greatest in J-months for both the periods of low and high sunspot number. During 1951-55 range in $M_2(D)$ is comparable in D and J-months and least in E-months. During 1956-60 the $M_2(D)$ range is greatest in D-months and least in

E-months.

In Tables 4a and 4b' r_2, $\theta_2(\tau)$, ~~$_2(\;)$~~, ΔD and probable error values for each solar hour are given. In Fig. 9 the (r_2 τ_2) points in different solar

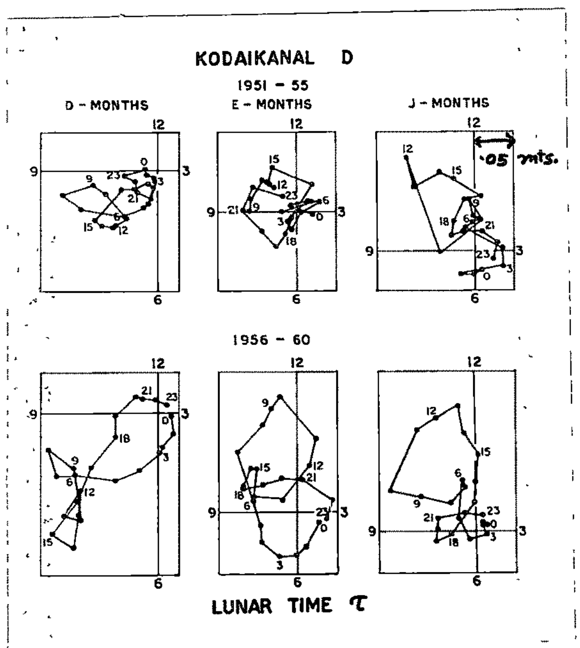

Figure.9

hours for each season during the period 1951-55 and 1956-60 are separately plotted in the harmonic dial of lunar time. The (r_2 τ_2) points trace a loop with a marked elongation in a preferred direction in D-months and during E- and J-months elongation of loop traced is not so marked. In general both the set of harmonic dials for different solar activity period are similar in character.

Table 4 (a)

The coefficients of lunar semi-monthly M_2 oscillations in D at Kodaikanal (1951-55) averaged over different seasons.

L.M.T.	D-Months. 2°+ ΔD 1/10 mts.	h_2 1/10 mts.	Probable error	Phase τ_2 lunar time degree.	E-Months. 2°+ ΔD 1/10 mts.	h_2 1/10 mts.	Probable error	Phase τ_2 lunar time degree.	J-Months 2°+ ΔD 1/10 mts.	h_2 1/10 mts.	Probable error	Phase τ_2 lunar time degree.
00	355	0.33	0.25	280	345	0.42	0.28	92	359	0.50	0.29	160
01	355	0.27	0.26	254	355	0.22	0.28	44	358	0.60	0.30	184
02	357	0.20	0.28	198	355	0.36	0.28	49	352	0.68	0.30	213
03	358	0.27	0.27	197	355	0.27	0.27	142	356	0.79	0.30	113
04	359	0.40	0.28	193	356	0.39	0.28	156	356	0.77	0.31	83
05	360	0.97	0.28	198	355	0.12	0.31	87	353	0.63	0.33	336
06	362	1.39	0.32	218	351	0.66	0.37	62	348	0.73	0.35	357
07	363	2.13	0.38	244	352	0.45	0.49	55	344	0.83	0.38	9
08	362	2.44	0.37	256	351	0.36	0.35	272	347	0.89	0.39	0
09	361	1.62	0.41	258	356	1.17	0.39	271	355	1.27	0.42	354
10	362	1.40	0.43	246	363	1.19	0.46	286	365	0.82	0.53	10
11	363	1.37	0.44	217	369	1.20	0.50	314	373	0.91	0.45	269
12	362	1.76	0.43	219	371	0.85	0.53	319	378	2.92	0.84	324
13	358	1.73	0.42	218	369	1.09	0.49	316	376	2.21	0.44	316
14	354	1.97	0.40	226	363	1.00	0.45	316	372	2.19	0.43	335
15	352	1.97	0.38	232	357	1.28	0.41	332	366	1.88	0.42	343
16	351	1.01	0.35	244	354	0.82	0.48	389	361	1.39	0.39	367
17	352	0.73	0.31	234	354	0.16	0.36	224	359	1.29	0.36	348
18	352	0.37	0.28	213	355	0.57	0.32	209	360	0.91	0.33	324
19	352	0.41	0.28	190	355	1.00	0.33	212	362	0.70	0.31	304
20	353	0.71	0.27	192	356	0.96	0.30	242	363	0.55	0.30	332
21	353	0.71	0.26	227	356	0.87	0.30	299	367	0.50	0.30	380
22	354	0.62	0.25	247	356	0.77	0.28	320	361	0.58	0.29	70
23	355	0.81	0.33	261	355	0.56	0.28		360	0.49	0.29	114

Table - 4(b)

The coefficients of lunar semi-monthly M_2 oscillations in D at Kodaikanal (1956-60) averaged over different seasons.

	D-Months.				E-Months				J-Months.			
L.M.T.	2°+ ΔD 1/10 mts.	r_2 1/10 mts.	Probable error.	Phase τ_2 lunar time degree.	2°+ ΔD 1/10 mts.	r_2 1/10 mts.	Probable error.	Phase τ_2 lunar time degree.	2°+ ΔD 1/10 mts.	r_2 1/10 mts.	Probable error.	Phase τ_2 lunar time degree.
00	358	0.34	0.29	101	356	0.58	0.33	118	362	0.29	0.28	68
01	359	0.64	0.31	145	355	0.90	0.31	167	361	0.25	0.27	36
02	359	0.89	0.32	172	356	1.07	0.32	183	361	0.21	0.29	55
03	360	1.00	0.33	177	357	1.19	0.34	203	360	0.28	0.31	114
04	362	1.49	0.33	199	357	1.19	0.34	233	360	0.28	0.30	215
05	363	1.98	0.35	213	356	1.02	0.37	252	356	0.26	0.35	302
06	365	2.61	0.39	234	351	1.15	0.44	285	348	1.29	0.42	344
07	369	3.06	0.43	239	348	2.13	0.49	315	342	1.12	0.45	345
08	369	2.93	0.50	252	351	2.33	0.49	338	348	0.93	0.51	315
09	368	2.54	0.58	238	360	2.65	0.55	346	360	1.64	0.52	301
10	370	3.31	0.61	216	371	2.92	0.62	351	375	2.39	0.55	295
11	374	3.47	0.62	223	381	1.88	0.69	14	386	2.91	0.57	329
12	374	2.68	0.60	226	386	1.21	0.71	14	393	2.96	0.58	340
13	369	3.27	0.58	218	382	0.53	0.69	309	391	3.11	0.59	352
14	364	3.97	0.54	213	374	1.16	0.63	288	384	2.42	0.58	353
15	360	3.99	0.48	222	365	1.50	0.53	316	375	1.87	0.55	361
16	358	2.98	0.44	223	358	1.62	0.45	313	366	1.21	0.49	359
17	359	2.16	0.38	232	357	1.46	0.40	295	361	0.73	0.44	355
18	359	1.26	0.33	241	357	1.43	0.38	294	359	0.65	0.39	260
19	357	1.07	0.30	266	356	1.14	0.37	307	362	1.06	0.36	255
20	357	0.68	0.28	305	357	0.94	0.36	335	365	0.99	0.34	271
21	358	0.51	0.28	310	357	0.80	0.35	368	365	1.02	0.31	288
22	359	0.33	0.28	350	357	0.90	0.34	70	365	0.45	0.30	325
23	358	0.29	0.29	51	356	0.77	0.32	104	364	0.41	0.28	388

(3) Lunar tide in 'Z' at Kodaikanal during periods of low and high sunspots.

The mean lunar daily and lunar monthly oscillations in Z at Kodaikanal for the periods 1951-55 and 1956-60 were determined.

Annual average lunar daily variations at fixed lunar ages

The mean lunar daily variations of ΔZ are derived separately for the days with lunar ages ν_0 = 00, 06, 09, 12, 15, 18and 21 lunar hours. The whole-year average lunar variations in Z at Kodaikanal for the periods 1951-55 and 1956-60 are shown in Figure 1. The presence of lunar

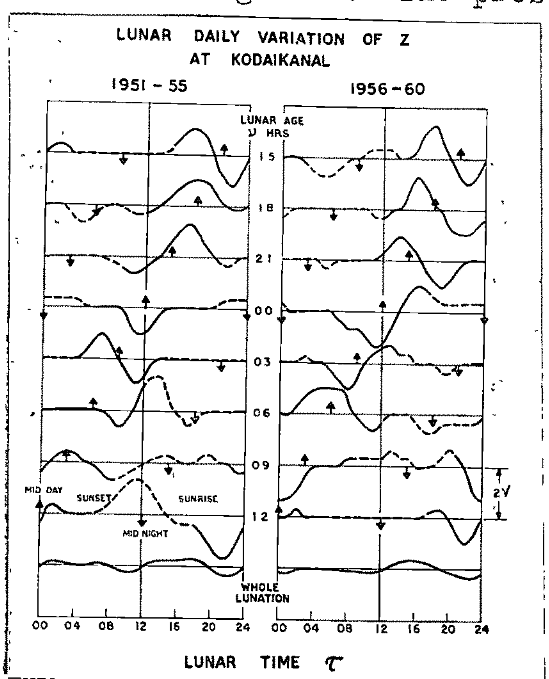

Figure 1.

diurnal L_1 and lunar semi-diurnal L_2 variation in the lunar daily variation is indicated by two distinct peaks in the lunar daily variation curves. The two sets of curves for the two periods have general similarities.

The maximum amplitudes fall during daylight hours and are found to occur earlier and earlier in lunar days with the progress of the lunation. The average lunar daily variation for a whole lunation does not seem to contain a significant diurnal component.

The harmonic coefficients (c_n) and (α_n) of the average lunar daily variations in Z at Kodaikanal for different seasons and for the whole year are computed according to Chapman's phase law equation and listed in table 1. The results presented in this table confirm Chapman's phase law.

The relations between ϕ and ν for the first four harmonics are shown in Fig.2. It is seen from Fig.2 that

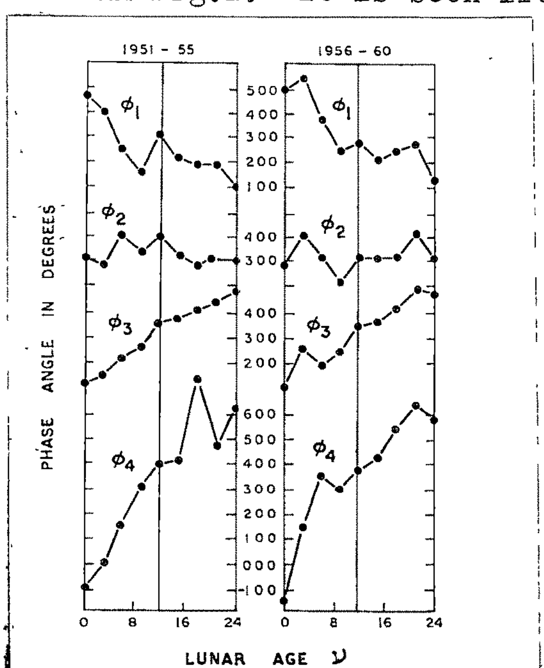

the phase angle ϕ_2 for both the periods 1951-55 and

Table - 1.

The coefficients of Annual Average lunar daily variations in Z at Kodaikanal for different lunar ages according to the equation, L= $\sum_{n=1}^{4} C_n \sin\{n\tau + (n-2)\nu + \alpha_n\}$

Annual (1951-55)

Lunar age	C_1 Gamma	α_1 Degree	C_2 Gamma	α_2 Degree	C_3 Gamma	α_3 Degree	C_4 Gamma	α_4 Degree
00	1.76	101	0.66	305	0.61	117	0.66	260
03	0.82	88	1.1	287	1.20	108	0.76	269
06	1.07	342	1.4	412	1.48	132	0.99	200
09	0.91	295	1.1	345	0.88	130	0.52	34
12	3.49	127	1.6	407	1.32	178	0.88	39
15	1.07	81	1.8	328	1.53	152	0.72	313
18	2.24	98	1.1	276	0.69	137	0.54	192
21	1.56	142	1.6	314	1.00	132	0.57	200

Annual (1956-60)

Lunar age	C_1 Gamma	α_1 Degree	C_2 Gamma	α_2 Degree	C_3 Gamma	α_3 Degree	C_4 Gamma	α_4 Degree
00	0.86	135	0.52	311	0.32	99	0.19	232
03	0.16	230	0.57	315	0.23	210	0.15	70
06	0.71	105	0.42	315	0.31	100	0.15	181
09	0.74	32	0.40	222	0.38	113	0.22	31
12	0.21	103	0.31	324	0.23	173	0.29	25
15	0.71	87	0.13	313	0.53	138	0.29	345
18	0.30	167	0.72	324	0.41	154	0.13	9
21	0.27	234	0.54	59	0.31	185	0.12	13

1956-60 remain about the same during the whole lunation.

The phase angle ϕ_1 progressively decreases by 360°, and phase angle ϕ_3 progressively increases by 360° in one complete lunation. Similarly ϕ_4 changes by nearly 720° during one lunation. The phase constants α_n unlike the phase angles ϕ_n remain nearly same during the whole lunation.

The lunar daily variation averaged over a complete lunation is shown in Fig.1. The harmonic coefficients of the whole-lunation average lunar daily variations in Z for Kodaikanal during 1951-55 and 1956-60 are given in table 2. The amplitude of the harmonic coefficients are very small. In (1951-55), the annual average of A_1 is 0.10 γ and of A_2 is 0.22 γ. In (1956-60) the annual average of A_1 is 0.41 γ and of A_2, it is 0.12 γ. During the low sunspot period $A_2 > A_1$ and during high sunspot period $A_1 > A_2$. Higher harmonics are very small. The phase anlge β 2 for the A_2 oscillation is found to be 332° during 1951-55 and 290° during 1956-60.

Annual average lunar monthly variations at fixed solar times.

In Fig.3 are shown the annual average lunar monthly variations at fixed solar times for the period 1951-55 and 1956-60. The coefficients of lunar monthly and semi-monthly oscillations derived from these curves

Table - 2.

The coefficients of lunar daily oscillations in Z averaged over the whole lunation during different seasons for Kodaikanal according to the equation $L = A_n \sin(n\tau + \beta_n)$

1951-55.

Station	Period	Season	A_1 Gamma	β_1 degree	A_2 Gamma	β_2 degree	A_3 Gamma	β_3 degree	A_4 Gamma	β_4 degree
Kodaikanal	1951-55	D-months	0.42	174	0.23	52	0.36	17	0.33	88
		E-months	0.37	224	0.57	301	0.11	1	0.22	10
		J-months	0.10	229	0.54	304	0.03	9	0.20	41
		Annual	0.10	223	0.22	332	0.06	47	0.13	28

1956-60

Station	Period	Season	A_1 Gamma	β_1 degree	A_2 Gamma	β_2 degree	A_3 Gamma	β_3 degree	A_4 Gamma	β_4 degree
Kodaikanal	1956-60	D-months	0.09	30	0.68	91	0.24	150	0.17	20
		E-months	0.37	193	0.79	296	0.12	291	0.12	82
		J-months	0.38	277	0.43	316	0.26	9	0.15	228
		Annual	0.41	202	0.12	290	0.08	174	0.05	197

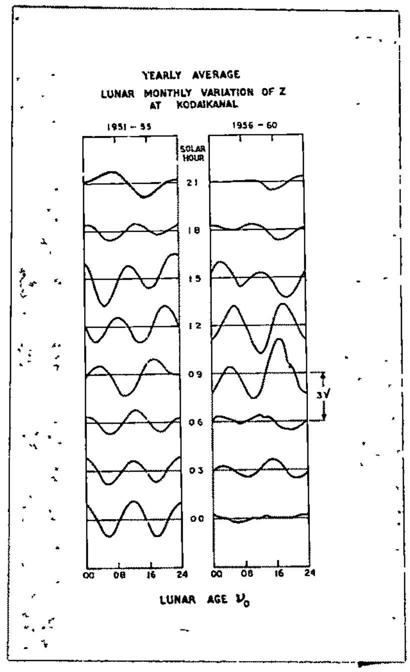

Figure.3.

are given in Table 3. In the tables the phases of M_1 oscillations are presented in terms of local lunar age ν whereas the phase - of M_2 oscillations are presented in terms of local lunar time τ.

It is seen from Fig.3 that two sets of curves for low and high sunspot years have some differences. During the period (1956-60) of high sunspots, the lunar monthly oscillations are greater during daylight hours than during nighttime hours. Near midday the oscillations are greatest, and in nighttime the oscillations are very small. The oscillations during daytime show a semi-diurnal character . In the low sunspot period (1951-55) the picture is different. The semi-diurnal character of the lunar oscillation is seen in almost all the hours,

Table 3

The coefficients of Annual Average lunar monthly M_1 and lunar semi-monthly M_2 oscillations in Z at Kodaikanal. Phases θ_1 and θ_2 indicate lunar age or time of maximum positive displacement.

	1951-55					1956-60				
L.M.T.	2000 + ΔZ Gamma	r_1 Gamma	θ_1 in lunar age degree.	r_2 Gamma	θ_2 in lunar time degree.	2000 + ΔZ Gamma	r_1 Gamma	θ_1 in lunar age degree	r_2 Gamma	θ_2 in lunar Time degree
00	421	0.51	327	0.51	184	339	0.16	311	0.26	351
01	420	0.35	339	0.54	196	339	0.09	314	1.83	303
02	418	0.36	305	1.01	51	339	0.05	159	2.70	336
03	419	0.91	280	1.72	210	339	0.19	241	2.86	360
04	419	0.50	283	1.50	197	339	0.03	261	3.3	16
05	421	0.62	288	1.19	199	341	0.25	113	2.56	92
06	423	0.49	270	0.97	198	343	0.37	116	1.26	159
07	421	0.31	266	0.73	205	342	0.05	279	3.26	128
08	418	0.21	278	0.48	222	340	0.44	279	3.80	141
09	414	0.12	50	0.22	282	334	0.89	262	4.93	136
10	409	0.77	78	0.27	41	323	1.06	286	5.56	146
11	.405	0.80	163	0.68	39	316	0.87	318	6.03	161
12	404	0.13	277	0.96	27	312	0.57	352	6.6	173
13	406	0.06	277	1.09	49	312	0.36	42	6.3	210
14	409	0.17	173	1.15	83	313	0.76	47	7.2	213
15	412	1.12	162	1.0	126	319	0.65	79	1.63	49
16	414	0.20	309	0.84	139	322	0.73	40	1.86	71
17	415	0.10	318	0.82	176	326	0.47	62	1.13	122
18	416	0.20	248	0.78	201	363	0.37	100	11.70	194
19	416	0.15	230	0.78	241	331	0.35	40	0.46	200
20	418	0.23	203	0.63	240	332	0.25	35	7.80	9
21	418	0.23	222	0.57	210	334	0.32	37	9.83	337
22	419	0.46	290	0.71	231	332	0.12	357	8.30	52
23	418	0.70	313	0.74	218	338	0.17	347	9.16	55

and the amplitudes of the oscillation during nighttime are comparable to those during daytime.

The amplitudes r_1 of lunar monthly oscillations are so small and the probable errors so large that $(r_1\,\theta_1)$ representation in a harmonic dial for different solar hours is not considered worth while.

The amplitude and phase of lunar semi-monthly oscillations $(r_2\theta_2)$ for different solar hours are plotted on harmonic dials of lunar age and lunar time in Fig.4.

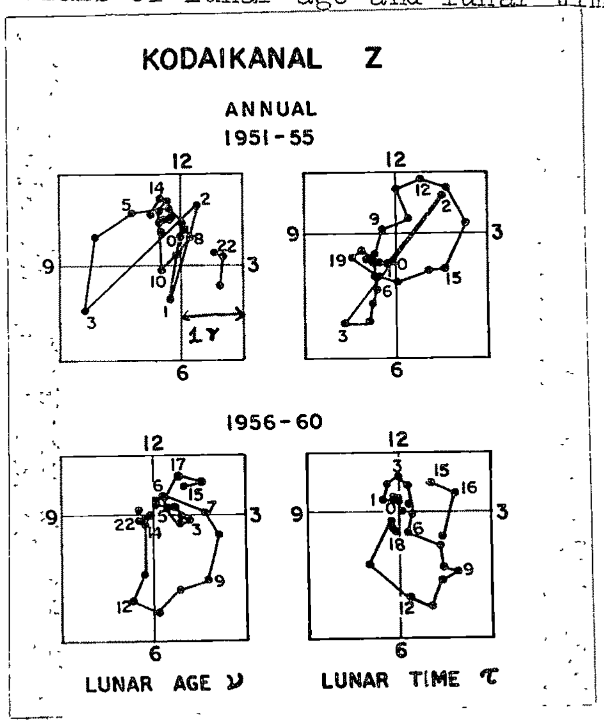

Figure.4.

This diagram presents a confused picture as compared to the similar diagram for Kodaikanal 'H' field. The amplitudes of r_2 are very small and the probable errors are comparable to r_2. This can be seen from tables 4a and 4b:.

Table 4 (b)

The coefficients of lunar semi-monthly M_2 oscillations in Z at Kodaikanal (1956-60) averaged over different seasons:

L.M.T.	D-months 2000 + ΔZ Gamma	r_2 Gamma	Probable error.	Phase τ_2 lunar time degree	E-months 2000 + ΔZ Gamma	r_2 Gamma	Probable error.	Phase τ_2 lunar time degree.	J-months 2000 + ΔZ Gamma.	r_2 Gamma	Probable error.	Phase τ_2 lunar time degree.
00	336	0.53	0.29	300	339	0.18	0.27	9	341	0.38	0.23	65
01	336	0.78	0.29	315	339	0.25	0.26	343	341	0.23	0.24	43
02	336	1.14	0.31	314	340	0.38	0.24	43	342	0.22	0.24	353
03	336	1.29	0.28	352	340	0.51	0.23	14	341	0.06	0.23	124
04	336	1.17	0.27	19	340	0.43	0.24	13	342	0.12	0.23	244
05	338	1.05	0.26	86	341	0.33	0.29	47	345	0.65	0.25	239
06	337	0.92	0.27	115	345	0.30	0.28	235	349	0.44	0.27	204
07	336	0.58	0.33	113	343	1.25	0.37	146	347	0.95	0.39	113
08	339	0.25	0.45	314	338	2.23	0.51	149	342	1.62	0.53	131
09	332	1.16	0.61	345	329	2.83	0.64	155	342	2.50	0.65	129
10	325	1.90	0.71	3	318	3.50	0.73	162	325	2.09	0.70	151
11	320	1.76	0.81	28	308	4.04	0.81	174	320	2.11	0.77	171
12	317	1.40	0.84	19	305	3.65	0.80	190	315	1.95	0.80	194
13	315	1.66	0.82	8	306	3.07	0.78	206	316	1.51	0.92	194
14	314	2.05	0.75	13	311	1,96	0.67	211	314	0.82	0.78	162
15	317	2.32	0.61	17	317	0.93	0.57	196	323	1.20	0.75	87
16	319	2.12	0.47	34	321	0.54	0.45	138	327	1.29	0.57	105
17	323	0.56	0.40	46	325	1.36	0.35	134	331	1.00	0.41	135
18	327	0.32	0.36	173	329	0.46	0.41	251	332	0.52	0.27	160
19	330	0.62	0.41	240	330	0.68	0.45	161	333	0.24	0.23	10
20	331	0.30	0.31	332	332	0.14	0.39	95	334	0.23	0.22	27
21	332	0.54	0.29	318	334	0.20	0.26	9	337	0.12	0.23	360
22	333	0.35	0.32	359	336	0.40	0.29	56	338	0.28	0.24	130
23	335	0.33	0.29	320	338	0.02	0.26	321	340	0.37	0.28	112

Table 4 (a)

The coefficients of lunar semi-monthly M_2 oscillations in Z at Kodaikanal (1951-55) averaged over different seasons.

	D-months.					E-months				J-months			
L.M.T.	2000 + ΔZ Gamma	r_2 Gamma	Probable error	Phase τ_2 lunar time degree.	2000 + ΔZ Gamma	r_2 Gamma	Probable error.	Phase τ_2 lunar time degree	2000 + ΔZ Gamma	r_2 Gamma	Probable error.	Phase τ_2 lunar time degree.
00	413	0.86	0.33	342	420	2.07	1.14	32	429	0.88	0.35	353
01	414	1.08	0.32	1	419	1.47	1.09	61	428	0.10	0.35	64
02	413	0.91	0.33	18	414	1.58	1.09	90	428	0.50	0.34	57
03	412	0.86	0.32	50	419	1.67	1.08	131	428	0.59	0.35	277
04	412	1.09	0.31	61	418	1.72	1.08	157	428	0.48	0.35	121
05	413	0.60	0.44	60	419	2.09	1.09	204	430	0.54	0.33	168
06	412	0.88	0.34	89	425	1.63	1.10	221	432	0.69	0.34	172
07	412	0.87	0.36	73	419	1.18	1.10	219	431	1.22	0.39	142
08	411	0.78	0.40	93	415	0.56	1.10	237	428	1.81	0.46	174
09	410	0.63	0.50	20	410	0.80	1.14	161	423	1.92	0.53	167
10	406	1.13	0.62	280	403	1.20	1.17	154	417	1.59	0.59	190
11	404	1.60	0.70	309	398	1.69	1.18	153	413	1.29	0.62	159
12	404	1.70	0.69	6	397	1.85	1.19	154	412	2.29	0.67	137
13	404	1.66	0.66	25	401	3.44	1.96	158	413	2.78	0.67	160
14	405	2.10	0.64	27	405	3.32	1.20	[illegible]	416	2.30	0.66	168
15	407	2.08	0.59	41	409	2.49	1.17	155	420	1.84	0.62	173
16	408	1.57	0.48	55	411	1.67	1.15	169	424	1.40	0.53	154
17	408	0.92	0.41	78	413	1.01	1.12	123	425	1.07	0.43	144
18	410	0.62	0.37	98	413	0.87	1.09	152	424	0.69	0.38	149
19	410	0.60	0.36	121	414	0.75	1.13	292	424	0.52	0.37	214
20	411	0.63	0.35	189	417	1.55	1.73	6	425	0.43	0.35	243
21	411	0.43	0.34	257	417	1.79	1.08	317	426	0.60	0.35	273
22	412	0.67	0.33	301	418	1.59	1.09	340	427	0.88	0.35	301
23	413	0.83	0.33	224	414	1.74	1.09	357	428	0.92	0.36	327

Table 4 (b)

The coefficients of lunar semi-monthly M_2 oscillations in Z at Kodaikanal (1956-60) averaged over different seasons:

	D-months				E-months				J-months			
L.M.T.	2000 + ΔZ Gamma	r_2 Gamma	Probable error.	Phase τ_2 lunar time degree	2000 + ΔZ Gamma	r_2 Gamma	Probable error.	Phase τ_2 lunar time degree.	2000 + ΔZ Gamma.	r_2 Gamma	Probable error.	Phase τ_2 lunar time degree.
00	336	0.53	0.29	300	339	0.18	0.27	9	341	0.38	0.23	65
01	336	0.78	0.29	315	339	0.25	0.26	343	341	0.23	0.24	43
02	336	1.14	0.31	314	340	0.38	0.24	43	342	0.22	0.24	353
03	336	1.29	0.28	352	340	0.51	0.23	14	341	0.06	0.23	124
04	336	1.17	0.27	19	340	0.43	0.24	13	342	0.12	0.23	244
05	338	1.05	0.26	86	341	0.33	0.29	47	345	0.65	0.25	239
06	337	0.92	0.27	115	345	0.30	0.28	235	349	0.44	0.27	204
07	336	0.58	0.33	113	343	1.25	0.37	146	347	0.95	0.39	113
08	339	0.25	0.45	314	338	2.23	0.51	149	342	1.62	0.53	131
09	332	1.16	0.61	345	329	2.83	0.64	155	342	2.50	0.65	129
10	325	1.90	0.71	3	318	3.50	0.73	162	325	2.09	0.70	151
11	320	1.76	0.81	28	308	4.04	0.81	174	320	2.11	0.77	171
12	317	1.40	0.84	19	305	3.65	0.80	190	315	1.95	0.80	194
13	315	1.66	0.82	8	306	3.07	0.78	206	316	1.51	0.92	194
14	314	2.05	0.75	13	311	1.96	0.67	211	314	0.82	0.78	162
15	317	2.32	0.61	17	317	0.93	0.57	196	323	1.20	0.75	87
16	319	2.12	0.47	34	321	0.54	0.45	138	327	1.29	0.57	105
17	323	0.56	0.40	46	325	1.36	0.35	134	331	1.00	0.41	135
18	327	0.32	0.36	173	329	0.46	0.41	251	332	0.52	0.27	160
19	330	0.62	0.41	240	330	0.68	0.45	161	333	0.24	0.23	10
20	331	0.30	0.31	332	332	0.14	0.39	95	334	0.23	0.22	27
21	332	0.54	0.29	318	334	0.20	0.26	9	337	0.12	0.23	360
22	333	0.35	0.32	359	336	0.40	0.29	56	338	0.28	0.24	130
23	335	0.33	0.29	320	338	0.02	0.26	321	340	0.37	0.28	112

The annual average $r_2\tau_2$ is 0.36 γ in 1951-55 and 0.34 γ in 1956-60. The vector average of annual average $r_2\nu_2$ is 0.86 γ in 1951-55 and 0.32 γ in 1956-60, whereas the scalar mean of r_2 is 0.79γ(1951-55) and 4.59 γ (1956-60).

Lunar daily variation of Z during different seasons

Lunar daily variations at the eight lunar age groups were computed separately for each season and the resulting curves are shown in Fig.5. (1951-55) and Fig.6 (1956-60). For all the seasons the whole lunation average

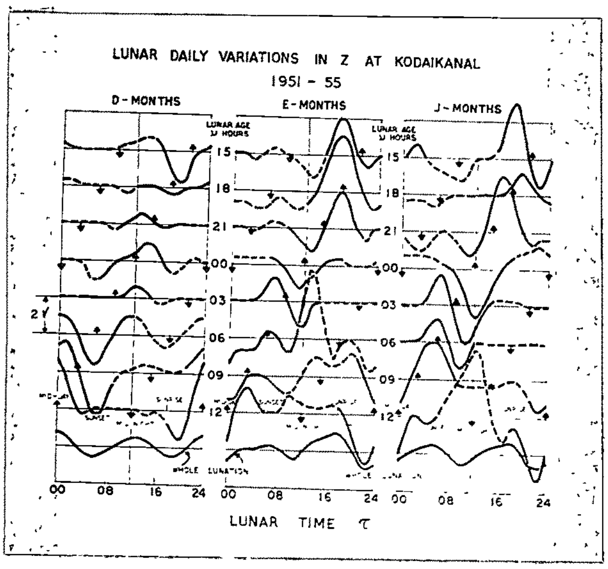

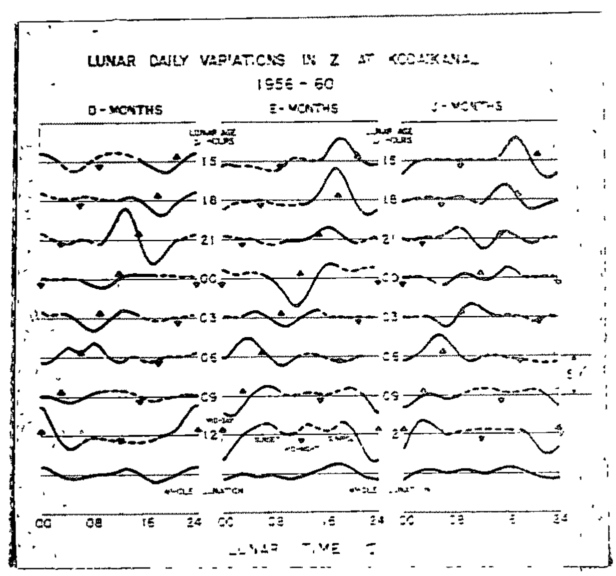

Figure.5.

Figure.6.

curves were also drawn. As described earlier for the annual average curves, one finds that during any season the oscillations are predominant during the daytime hours and peak tends to occur earlier in lunar time with increasing age of the moon. The individual curves are harmonically analysed, and Chapman's phase law is found to hold good for lunar daily variation in every season. The whole lunation average curves for each season were harmonically analysed, the coefficients are given in table 2. It is seen that the semi-diurnal component A_2 is comparable and in some cases less than A_1. The phase of A_2 oscillations i.e. β_2 (1951-55) is 412° in D-months, 301° in E-months and 304° in J-months, and β_2 (1956-60) is 451° in D-months, 296° in E-months and 316° in J-months. The phase angle β for D-months is different from E and J months. This is seen from Fig.5 and Fig.6. The whole lunation lunar daily variation curve for D-months has a different phase from similar curves for E and J-months.

Lunar monthly oscillation Z at fixed solar time during different seasons.

The lunar monthly M_1 and lunar semi-monthly M_2 oscillations in H for each of the solar hours were computed separately for different seasons of the year. The coefficients of M_2 oscillations are listed in Tables 4a and 4b. The probable errors are also included in Tables 4a and 4b.

In Figure 7 a comparison is made between diurnal

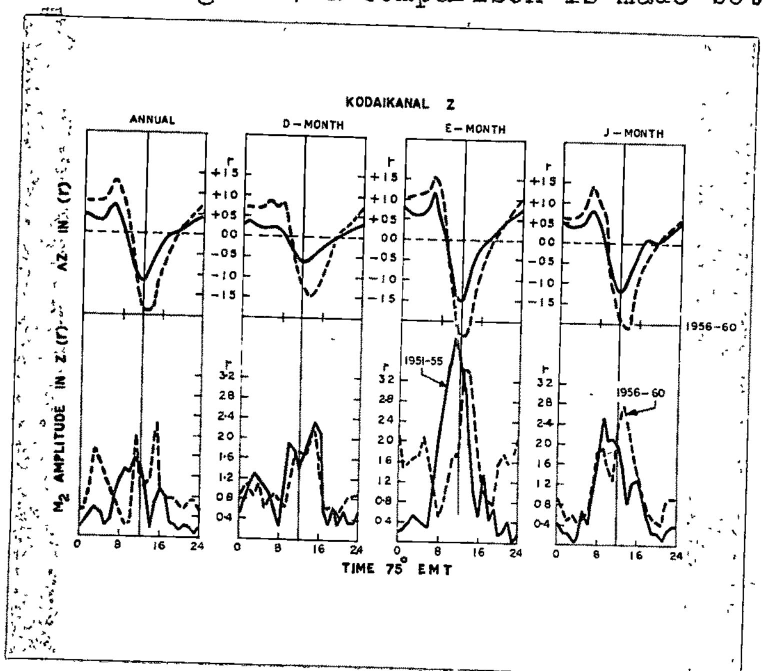

Figure [redacted] 7

variation of M_2 (Z) amplitude and normal diurnal variation in Z. The diurnal variation in Z is derived from the data utilised in this analysis. The diagram shows that M_2(Z) varies inversely as Z during the course of the day in both the periods. At about midday, the value of Z reaches a minimum and the value of M_2 (Z) reaches a maximum. The diurnal variation in Z was greater in 1956-60 than in 1951-55. A similar proportion in the diurnal variation of M_2 (Z) is not observed in the periods 1956-60 and 1951-55. M_2 (Z) seems to be of comparable amplitude in both the periods. Only in E-months M_2 (Z) is a little larger in 1951-55 than in 1956-60.

$r_2\tau_2$ points for different solar hours for each season are plotted in a harmonic dial of lunar time in Fig.8. The picture is not very clear. However, some

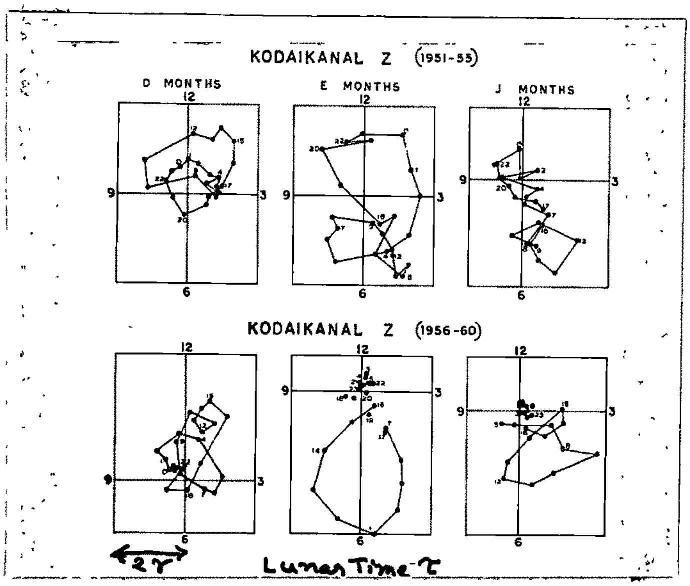

Figure.8.

similarity is seen in the plots of both the periods viz. 1951-55 and 1956-60.

(4) Summary

In earlier portions of this chapter are described the lunar tidal oscillations separately in the components H, D and Z at Kodaikanal. Here, the results are summarized so as to compare the oscillations in the three components.

Fig. 1 shows the lunar tidal variations of

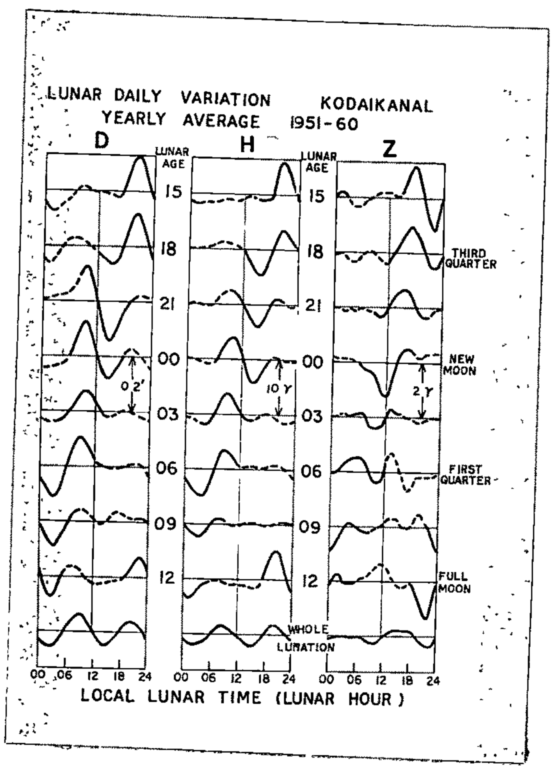

Figure.1.

these parameters for individual lunar ages averaged for the whole year. It is seen that the curves for D and H for any of the individual lunar ages are almost identical indicating that any increase in H is associated with a similar increase in the westward declination. Variations in Z seem to be approximately in quadrature with the variations in D or H.

In Fig. 2 are drawn the lunar monthly variations of the three parameters at different fixed solar

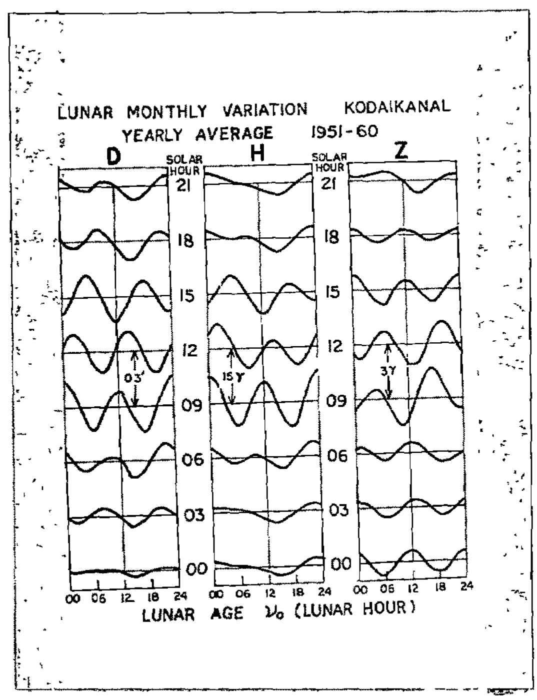

Figure.2.

hours. It is seen that the largest lunar tidal effects in any of the seasons happen in the hours around midday (9-15 hrs.), although the tides in Z do not entirely vanish during night-time. The general indication is that the lunar tides in all the three parameters at Kodaikanal are closely associated with the electrojet currents.

In Fig. 3 are shown harmonic dials of lunar semi-monthly oscillations in D, H and Z averaged for the

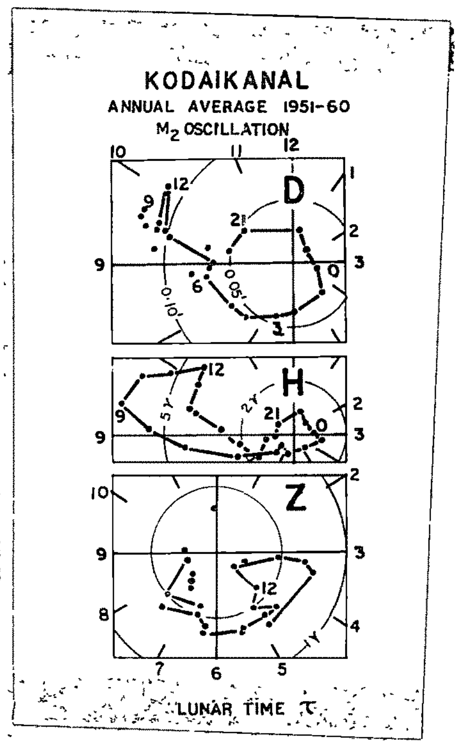

Figure.3.

entire period. It is seen that both D and ~~Z~~ H have a long loop centered between 9 and 10 hours, whereas the night-time displacements are small and the loop is centered round the origin, indicating direct relationship between D and ~~Z~~ H variations. The end points of the vectors for Z do not show any clear loop but lie between 3 to 9 lunar hours. The average coefficients would differ roughly by 90° from the corresponding coefficients for D or H. To get the seasonal variation in the lunar tides the M_2 oscillations averaged over 11 to 13 hours are subjected to harmonic analysis and the coefficients are plotted in Fig. 4. It is seen that the seasonal variation

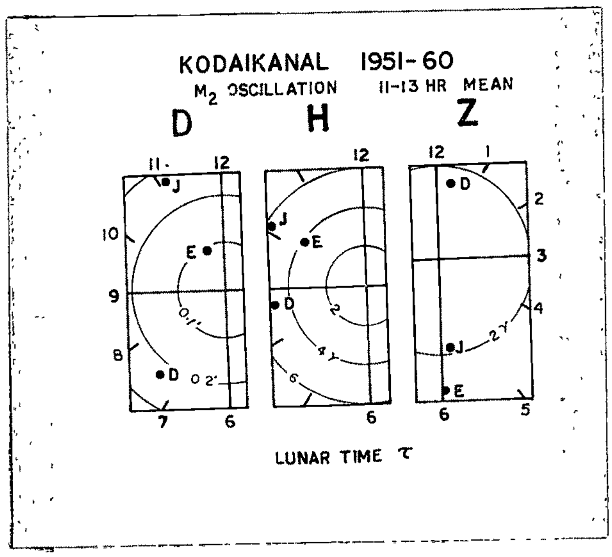

Figure.4.

in the amplitudes and phases of M_2 oscillations in D and H are almost identical further confirming that the tides at D and H are related to each other.

3.4 Lunar tidal oscillations in H during IGY/IGC at equatorial stations

The lunar tide oscillations in H field at various stations on the magnetic equator are determined for the IGY/IGC period. The stations considered are

(1) Trivandrum

(2) Addis Ababa

(3) Koror

(4) Jarvis

(5) Huancayo

The results of lunar tide at Huancayo previously determined by Rastogi (1968) have been included in the discussion for comparative study. The results for each station are described separately, and at the end, the results for all the stations are summarized.

(1) Trivandrum

Trivandrum is situated on the Western Coast in the Southern part of the Indian Peninsula. Its position can be described as

Geographic latitude	8°29'N
Geographic longitude	76°57'E
Geomagnetic latitude	1°05'S
Geomagnetic longitude	146°21'E
Dip angle =	0.6°S

Trivandrum magnetic data used in this study (IGY/IGC) are published by the India Meteorological Department of the Government of India. The data tabulated are hourly values. Each hourly value is the average for sixty minutes centered at each full hour of G.M.T. The data are continuous. By the suitable choice of the tabular base value, the printed entries in the Tables are three-digit positive quantities. The data for days on which C_p index was 1.2 or more are not included in the analysis. About 20% of the total data were discarded to remove irregular disturbance effects.

At Trivandrum the mean value of the H field is about 40050 gamma and the mean vertical field is -450 gamma.

The lunar daily variation at fixed lunar ages

The annual average lunar daily variation in H at Trivandrum (1957-60) for lunar ages centered on 00, 03, 06, 09, 12, 15, 18 and 21 hr. are shown in the Fig.1. The presence of lunar diurnal L_1 and lunar semidiurnal L_2 variation is shown in each lunar daily variation curve by two distinct peaks of unequal amplitudes. The part of the curve having greatest movement falls in daylight hours and occurs earlier and earlier in lunar hours with the progress of the lunation. The whole lunation curve is nearly sinusoidal with two peaks of nearly the same magnitude within one lunar day. The lunar diurnal component seems to be largely cancelled out by averaging the curve over a whole lunation.

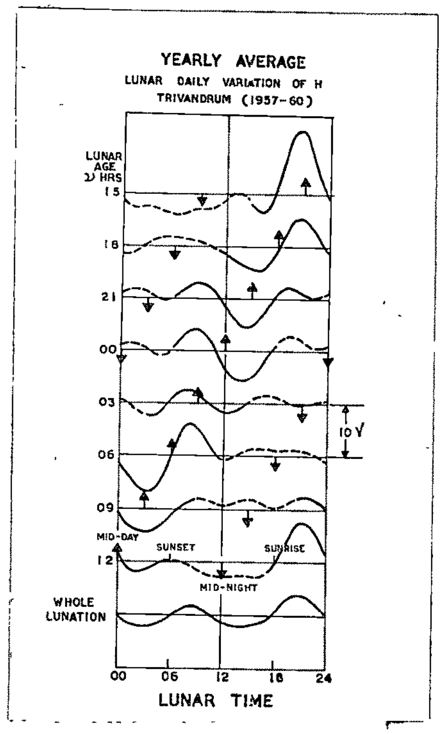

Fig.1

The harmonic coefficients (C_n) and phases α_n of the average lunar daily variations in H at Trivandrum for different seasons and for the whole year at different lunar ages calculated according to the equation

$$L = \sum_{n=1}^{4} C_n \ \mathrm{Sin} \left\{ n\tau + \phi_n \right\}$$

where $\phi_n = \left\{ (n-2)\nu + \alpha_n \right\}$

are given in Tables 1a, 1b, 1c, 1d. It can be seen that the amplitudes of the harmonic coefficients do not show any definite relationship with the lunar age.

Themean value of C1 → is 2.3 γ and of C_2 is 2.5 γ . The higher harmonics are progressively smaller in magnitude. Only the semidiurnal component is prominent. In Fig.2 are shown the variation of phase angles with lunar

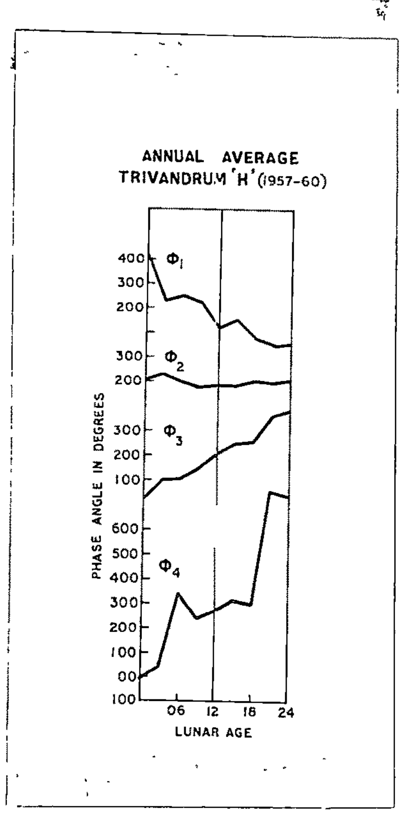

Fig.2

The coefficients of Annual Average lunar daily variations in H at Trivandrum for different lunar ages according to the equation

$$L = C_n \sin \left\{ n\tau + (n-2)\nu + \alpha_n \right\}$$

Annual - Trivandrum (1957 - 60)

Lunar age	C_1 Gamma	α_1 Degree	C_2 Gamma	α_2 Degree	C_3 Gamma	α_3 Degree	C_4 Gamma	α_4 Degree
00	1.8	56	3.0	201	1.7	19	0.4	344
03	0.3	269	1.2	230	1.4	48	0.2	308
06	2.5	338	3.1	196	2.0	11	0.6	153
09	2.2	356	1.8	171	1.0	8	0.4	330
12	3.1	295	2.7	187	1.7	25	0.3	266
15	4.8	15	3.4	181	3.1	20	1.6	223
18	1.9	340	2.8	201	1.6	346	0.6	119
21	1.8	360	2.1	192	1.6	44	0.2	123

Table 1a

The coefficient of lunar daily variations in 'H' at Trivandrum for different lunar ages averaged for the whole year according to the equation

$$L = C_n \operatorname{Sin} \left\{ n\tau + (n-2)\nu + \alpha_n \right\}$$

D-months – Trivandrum (1957-60)

Lunar age	C_1 Gamma	α_1 Degree	C_2 Gamma	α_2 Degree	C_3 Gamma	α_3 Degree	C_4 Gamma	α_4 Degree
00	5.1	61	6.2	209	3.4	37	0.9	277
03	2.1	33	4.6	249	3.8	82	1.2	281
06	3.3	285	3.4	195	0.9	37	0.7	88
09	2.7	9	2.4	187	1.2	29	0.3	31
12	1.7	267	3.2	226	1.6	138	0.5	37
15	8.6	27	4.9	218	5.0	48	2.8	218
18	3.1	62	4.8	217	2.2	19	0.8	162
21	6.1	58	5.0	255	4.6	72	1.8	245

Table 1b.

The coefficients of lunar daily variations in 'H' at Trivandrum for different lunar ages averaged for the whole year according to the equation

$$L = C_n \sin \left\{ n\tau + (n-2)\nu + \alpha_n \right\}$$

E-months - Trivandrum (1957-60)

Lunar age	C_1 Gamma	α_1 Degree	C_2 Gamma	α_2 Degree	C_3 Gamma	α_3 Degree	C_4 Gamma	α_4 Degree
00	1.6	320	5.3	160	4	3	0.7	184
03	2.4	335	1.5	165	2.0	344	0.4	166
06	3.9	8	3.0	198	2.6	17	1.2	182
09	2.0	329	2.1	145	0.7	306	0.8	328
12	4.4	310	2.9	154	3.5	352	1.0	223
15	0.6	53	2.7	124	2.5	338	0.7	226
18	5.7	299	4.6	175	3.5	332	1.4	124
21	2.3	251	3.1	150	1.8	1.0	0.8	84

Table 1c

The coefficients of lunar daily variations in 'H' at Trivandrum for different lunar ages averaged for the whole year according to the equation

$$L = C_n \operatorname{Sin} \left\{ n\tau + (n-2)\nu + \alpha_n \right\}$$

J- months - Trivandrum (1957-60)

Lunar age	C_1 Gamma	α_1 Degree	C_2 Gamma	α_2 Degree	C_3 Gamma	α_3 Degree	C_4 Gamma	α_4 Degree
00	1.4	107	2.9	317	2.0	193	1.6	19
03	4.0	198	1.1	56	0.3	335	1.0	56
06	2.3	353	3.0	191	2.6	357	0.5	156
09	2.4	4	1.0	188	1.6	12	0.3	284
12	3.6	293	3.2	179	2.8	33	0.8	279
15	6.0	355	5.2	176	3.2	10	1.3	228
18	1.2	10	0.7	333	0.5	216	0.9	19
21	4.3	315	2.4	135	1.0	273	1.4	82

Table 1d.

age. Chapman's phase law is seen to be obeyed. The phase angles of the first harmonic and third harmonic are seen to decrease and increase by 2π over a whole lunation. The phase angle of the second harmonic does not change appreciably over a lunation. The phase of the fourth harmonic increases by 4π in a whole lunation.

The annual average lunar daily variation averaged over a complete lunation is shown in Fig.1. The harmonic coefficients of the average lunar daily oscillations (over a whole lunation) for Trivandrum (1957-60) are shown in Table 2. The amplitude of lunar semidiurnal oscillation A_2 is 2.4 γ and the amplitude of lunar diurnal oscillation A_1 is 1.0 γ. The amplitudes of all components except the second are statistically insignificant. The phase angle β_2 for the A_2 oscillation isfound to be 193°.

Annual average lunar monthly variations at fixed solar time

The annual average curves of ΔH at fixed solar hours (00, 03, 06, 09 ....21) as a function of lunar age ν_o are shown in the Fig.3 It is seen that the tide is significantly large for the daytime hours and that the maximum tide occurs near midday. The oscillations are small during nighttime. The oscillations during daytime

The coefficients of lunar daily oscillations in H averaged over the whole lunation during different seasons for Trivandrum (1957-60) according to the equation

$$L = A_n \sin \left\{ n\tau + \beta_n \right\}$$

Station	Period	Season	A_1 Gamma	β_1 Degree	A_2 Gamma	β_2 Degree	A_3 Gamma	β_3 Degree	A_4 Gamma	β_4 Degree
Trivan-drum	1957-60	D-months	2.2	137	4.0	222	0.7	4	0.5	317
		E-months	0.6	313	3.0	161	0.08	245	0.5	387
		J-months	1.3	130	1.30	180	1.0	243	0.33	330
		Annual	1.0	132	2.4	193	0.17	259	0.5	307

Table-2

have a periodicity of twelve lunar hours, while the nighttime oscillations indicate a twenty-four lunar-hour component.

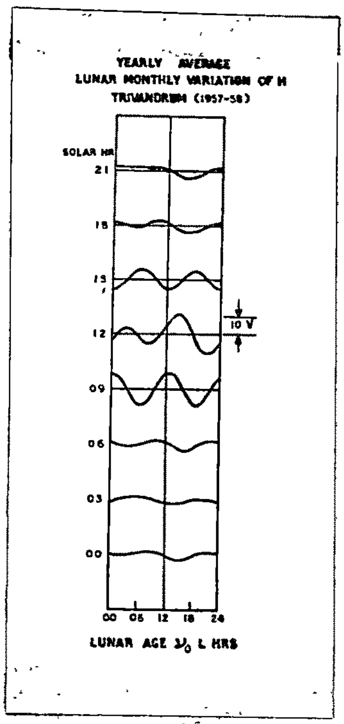

Fig.3

The coefficients of annual average lunar monthly M_1 and lunar semimonthly M_2 oscillations are given in Table 3. The amplitudes r_1 of lunar monthly component are seen to lie between 0.45 γ and 4.41 γ . The amplitudes r_1 do not seem to vary systematically with the solar time whereas amplitudes r_2 vary systematically with the solar time. The values of r_2 are very small at night and start increasing at sunrise, reaches a maximum value round about midday and

Coefficientsof Annual average lunar monthly M_1 and lunar semi-monthly M_2 oscillations in H at Trivandrum.

IGY-IGC

L.M.T.	39000 + ΔH Gamma	r_1 Gamma	θ_1 (Lunar age) ν_1 (Degree)	r_2 Gamma	θ_2 (Lunar Time) τ_2 (Degree)
0	531	1.67	49	1.48	110
1	532	1.72	55	1.13	168
2	533	1.77	70	0.96	203
3	533	1.51	65	0.97	250
4	534	1.51	64	1.13	284
5	528	0.45	73	1.02	252
6	530	0.89	69	2.46	255
7	546	1.34	88	5.37	266
8	578	1.23	96	6.54	270
9	618	1.36	178	8.69	266
10	648	2.78	193	9.16	277
11	660	3.54	190	8.22	280
12	652	4.41	188	7.81	292
13	630	3.58	184	7.05	297
14	604	1.44	185	5.37	273
15	581	0.47	83	5.60	273
16	565	1.17	84	3.71	279
17	554	1.42	81	2.70	257
18	544	1.74	83	2.25	231
19	536	2.65	75	1.71	237
20	532	2.43	62	1.75	277
21	531	2.61	63	1.26	323
22	530	2.25	58	1.35	49
23	530	1.97	54	1.53	94

Table -3

start falling thereafter to the small nighttime value. The amplitude r_2 of the semimonthly lunar oscillation in H at midday is 7.8 γ at Trivandrum (1957-60).

The amplitudes r_1 of lunar monthly oscillations are so small that the representation of (r_1 θ_1) points on a harmonic dial do not show anything significant. The probable errors mask the picture. Hence (r_1 θ_1) points for different solar hours are not represented on a harmonic dial.

The amplitude and phase of lunar semi-monthly oscillations (r_2 θ_2) for different solar hours are plotted on the harmonic dials of lunar age and lunar time in Fig.4.

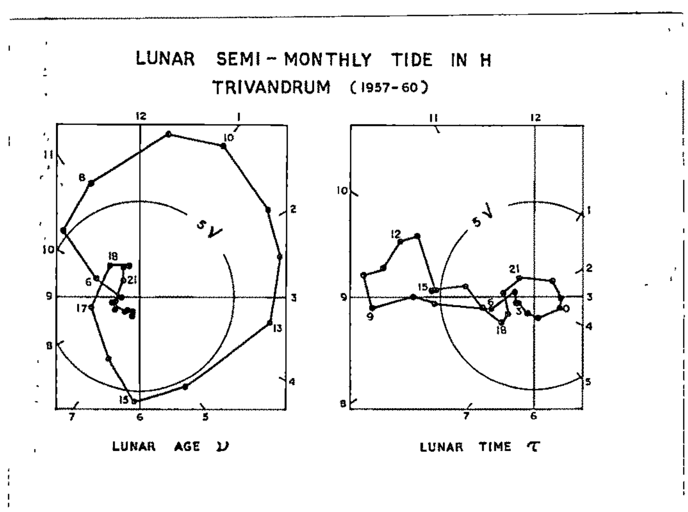

Fig.4

On the lunar age dial the points for the different hours of the solar day move around the origin with a very small value of the vector average from all the hours. On the lunar time dial the points for various solar hours do not move around the origin but lie within a narrow sector. At Trivandrum the mean amplitude for all hours gives an annual average value of 3.7 γ while the vector mean is 3.2 γ on a lunar time dial, and 0.79 γ on the lunar age dial. The phase of maximum deviation of M_2 on the lunar time dial is 277° i.e. 9.2 l.hr.

Lunar daily variation of H during different seasons

Lunar daily variations at the eight lunar age groups were computed separately for each season and the resulting curves are shown in Fig.5. For any particular season,

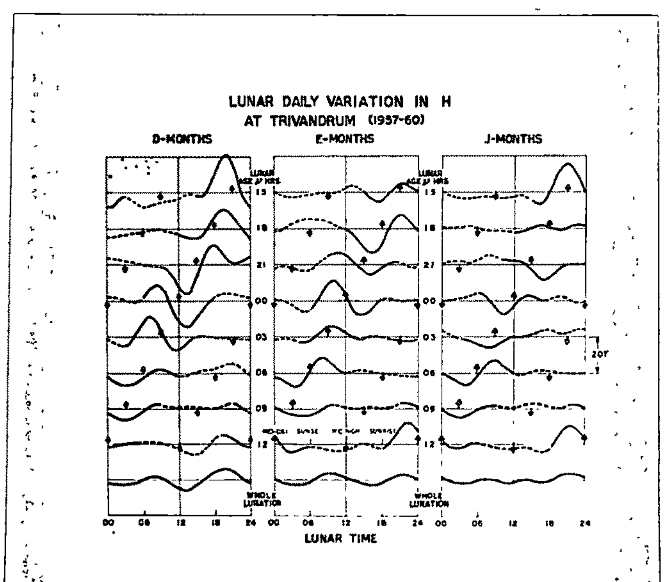

Fig,5

the whole lunation average curve were also derived by averaging eight individual curves and the resultant curves are also shown in the diagram. As described earlier for the annual average curves, one finds that during any season the oscillations are predominant during the daytime hours and the peak occurs earlier in lunar time with increasing age of the moon. Individual curves are harmonically analysed to find the coefficients C_n and α_n for each season. Chapman's phase law is found to hold good for lunar daily variation in every season. The whole lunation average curves for each season were harmonically analysed, the coefficients are given in Table 2. It is seen from the Table 2 that the second harmonic component is significantly larger than the other harmonics. The amplitude of the second harmonic component lies between 1.3 γ and 4.0 γ whereas the first harmonic amplitudes range from 0.6 γ to 2.2 γ . The higher harmonics are still smaller. The phase of A_2 oscillations i.e. β_2 is 222° during D-months, 161° during E. months and 180° during J months. Thus the maximum positive deviation due to A_2 oscillation occurs earliest in D-months, nearly one and quarter hour later in J-months and about two hours later in E-months. The maximum semi-diurnal component A_2 of 4 γ is in D-months, during E-months A_2 is 3 γ and during J-months A_2 is 1.3 γ .

Lunar monthly oscillations in H at fixed solar time during different seasons:

The lunar monthly M_1 and lunar semimonthly M_2 oscillations in H for each of the solar hours were computed separately for different seasons of the year. The coefficients of M_2 (H) oscillations are listed in Table 4. The probable errors are also included in the Table 4.

In Fig.6 comparison is made between diurnal variation of M_2 (H) amplitude and normal diurnal variation in H. The

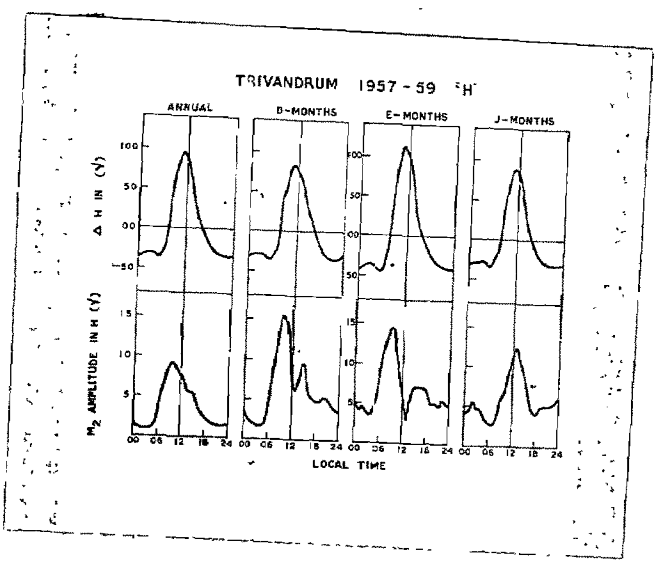

Fig.6

TVM - H 1957-60

L.M.T.	D-months: 39000 + ΔH Gamma	P.E.	r_2 Gamma	τ_2 degree	E-months: ΔH Gamma	P.E.	r_2 Gamma	τ_2 Degree	J-months: ΔH Gamma	P.E.	r_2 Gamma	τ_2 Degree
0	529	1.4	3.36	57	525	1.5	4.84	102	538	1.2	4.23	234
1	530	1.4	2.43	113	527	1.4	4.18	137	539	1.2	4.51	278
2	531	1.3	2.24	170	529	1.3	4.64	147	539	1.2	5.32	310
3	531	1.3	1.66	223	531	1.2	3.89	172	539	1.1	4.60	332
4	531	1.2	1.59	243	530	1.2	3.52	217	541	1.1	4.46	3
5	526	1.6	1.88	224	523	1.5	4.70	255	534	1.4	3.29	61
6	529	1.7	4.04	233	522	1.5	6.95	287	539	1.5	3.05	117
7	546	1.8	7.44	232	541	1.7	11.01	302	550	1.7	2.54	203
8	574	2.1	9.79	231	582	2.0	12.36	312	578	1.9	3.59	229
9	607	2.5	14.01	235	630	2.4	14.47	314	616	2.0	5.74	227
10	633	2.8	15.32	249	667	2.7	14.35	328	644	2.2	6.39	238
11	643	2.9	14.22	262	680	2.9	9.44	349	658	2.3	9.00	250
12	637	2.7	11.17	284	664	2.8	6.03	356	656	2.3	10.60	270
13	619	2.5	6.27	283	633	2.6	2.85	317	638	2.3	12.48	300
14	598	2.2	7.48	219	601	2.4	5.40	251	612	2.2	10.64	323
15	579	2.0	9.71	224	578	2.0	7.19	264	586	2.0	9.06	341
16	565	1.8	6.05	225	565	1.7	7.05	263	564	1.7	6.88	2
17	553	1.7	4.96	215	557	1.5	7.08	255	552	1.5	4.42	23
18	541	1.7	4.88	207	545	1.6	6.90	263	547	1.4	3.92	78
19	532	1.6	4.74	238	535	1.6	4.96	290	542	1.5	4.81	114
20	528	1.7	5.19	265	531	1.6	5.11	324	538	1.4	4.87	143
21	527	1.6	5.33	306	527	1.6	4.78	7	538	1.4	5.09	164
22	526	1.6	4.39	343	525	1.6	5.40	48	538	1.3	5.12	176
23	527	1.5	3.83	23	525	1.6	5.06	78	537	1.3	5.26	201

Coefficients of lunar semimonthly M_2 oscillations in H at Trivandrum.

Table-4

diurnal variation in H is derived from the data utilised in the analysis. The diagram shows that M_2 (H) and H itself vary in a similar way during the course of a day. The range in H variation is greatest in E-months and are comparable in D and J months: whereas the range in M_2 (H) variation is more during D-months than E and J months. The range in M_2 (H) variation in J-months is the least.

$(r_2 \; \tau \; 2)$ points for different solar hours for each season are plotted in harmonic dial of lunar time in Fig.7.

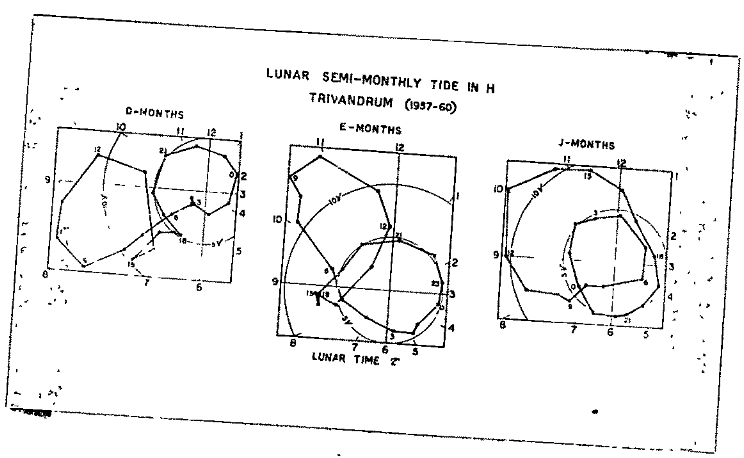

Fig.7

It is seen that most of the points for the daytime form a loop elongated in a preferred direction. But it is noteworthy that nighttime points also tend to form a separate loop of oourse with no preferred elongation. But nighttime tide amplitudes are fairly large.

3·3 (2) ADDIS ABABA.

Addis Ababa is situated in the northern geographic hemisphere and south of magnetic equator. Its coordinates are:

Geographic latitude	9°01'N
Geographic longitude	38°45'E
Geomagnetic latitude	5°3'N
Geomagnetic longitude	109°2'
dip angle	1.8 S.

The hourly values of the H field at Addis Ababa are taken from the Bulletin of the Geophysical Observatory, published by The University College of Addis Ababa. In the present analysis the data for the period 1958, 1959 and first six months of 1960 are used. The data are good and continuous. The days on which C_p index is 1.2 or more are dropped from the analysis.

At Addis Ababa the mean value of the H field is about 36100 gamma and the mean value of the vertical field is about -600 gamma.

The lunar daily variation ~~at~~ fixed lunar ages:

The annual average lunar daily variation in H at Addis Ababa (1957-60) for lunar ages centered on 00, 03, 06, 09, 12, 15, 18 and 21 are shown in Figure 1.

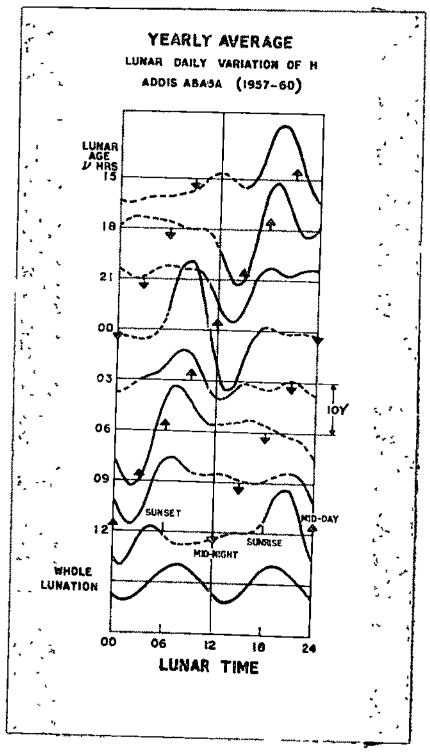

Fig.1

The presence of lunar diurnal L_1 and lunar semi-diurnal L_2 component is indicated in any lunar daily variation curve by peaks of unequal amplitude. The part of the curve having greatest movement falls during daylight hours and is found to occur earlier and earlier in lunar day as the lunation progresses. The average lunar daily variation curve for the whole lunation is a sinusoid with two peaks of nearly equal amplitude.

The harmonic coefficients(C_n) and (α_n) of average lunar daily variation in H at Addis Ababa for different seasons and a whole year on different ages of the moon are computed according to the Chapman's phase law expression and are tabulated in tables 1a, 1b, 1c, 1d.

It can be seen that amplitudes of harmonic coefficients do now show any definite relationship with the lunar age. The mean value of C_1 is 3.6 γ . and the mean value of C_2 is 3.7 γ . The higher harmonics are progressively smaller in magnitude.

In Fig.2 are shown the variation of phase angles

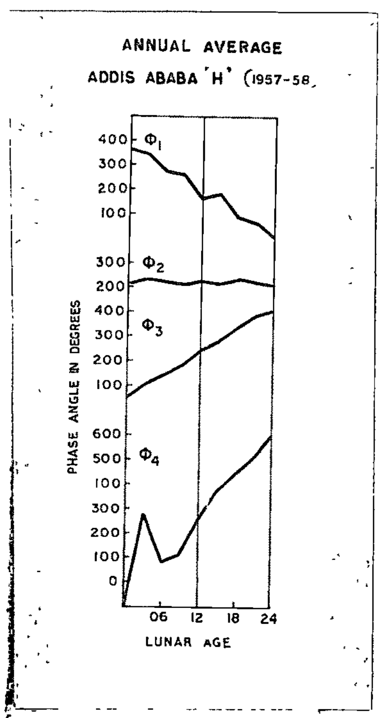

Fig.2

Coefficients of lunar daily variations in H at Addis Ababa for different lunar ages according to the equation

$$L = C_n \sin \left\{ n\tau + (n-2)\nu + \alpha_n \right\}$$

Annual - Addis Ababa (1957-60)

Lunar age	C_1 Gamma	α_1 Degree	C_2 Gamma	α_2 Degree	C_3 Gamma	α_3 Degree	C_4 Gamma	α_4 Degree
00	4.2	2	6.4	210	4.2	52	1.2	241
03	2.3	30	2.4	230	3.0	55	1.3	185
06	5.1	2	4.5	223	2.7	54	0.7	266
09	2.7	38	3.1	213	2.3	47	0.7	204
12	3.1	346	2.8	229	3.0	62	1.3	251
15	5.0	47	3.3	216	2.9	60	0.8	281
18	3.6	357	4.1	233	3.8	67	1.5	261
21	2.9	17	2.9	222	1.5	73	1.2	241

Table 1a.

Coefficients of lunar daily variations in H at Addis Ababa for different lunar ages according to the equation

$$L = C_n \sin \left\{ n\tau + (n-2)\nu + \alpha_n \right\}$$

D – months (1957-60)

Lunar age	C_1 Gamma	α_1 Degree	C_2 Gamma	α_2 Degree	C_3 Gamma	α_3 Degree	C_4 Gamma	α_4 Degree
00	5.0	11	9.4	208	5.9	43	1.6	225
03	7.0	35	6.4	242	3.6	97	1.6	220
06	4.0	325	5.0	225	3.3	35	1.3	249
09	6.9	39	7.3	213	4.1	51	1.8	221
12	6.7	343	5.1	248	3.3	35	2.4	264
15	6.0	75	4.6	264	4.2	116	2.6	319
18	5.4	31	8.3	246	6.2	82	2.8	281
21	9.2	71	7.3	275	5.9	118	2.7	306

Table 1b.

Coefficients of lunar daily variations in H at Addis Ababa for different lunar ages according to the equation

$$L = C_n \sin \left\{ n\tau + (n-2)\nu + \alpha_n \right\}$$

E-months (1957-60)

Lunar age	C_1 Gamma	α_1 Degree	C_2 Gamma	α_2 Degree	C_3 Gamma	α_3 Degree	C_4 Gamma	α_4 Degree
00	3.9	322	6.8	199	4.9	50	2.8	252
03	2.0	314	1.7	177	1.1	17	1.4	165
06	5.1	40	2.5	244	2.0	89	1.1	280
09	1.9	295	2.4	222	1.8	31	0.6	213
12	2.3	54	2.0	217	4.0	68	1.4	222
15	4.6	70	3.1	179	3.5	31	1.5	204
18	6.2	333	4.7	220	5.5	52	2.6	252
21	3.5	298	5.1	158	3.6	356	2.7	197

Table 1c.

Coefficients of lunar daily variations in H at Addis Ababa for different lunar ages according to the equation

$$L = C_n \sin \left\{ n\tau + (n-2)\nu + \alpha_n \right\}$$

J-months (1957-60)

Lunar age	C_1 Gamma	α_1 Degree	C_2 Gamma	α_2 Degree	C_3 Gamma	α_3 Degree	C_4 Gamma	α_4 Degree
00	4.7	25	3.6	240	2.0	83	0.6	90
03	1.5	146	0.26	0	1.6	303	1.2	167
06	8.2	357	6.1	213	3.0	57	0.3	28
09	2.5	83	0.13	56	1.1	58	0.5	89
12	2.4	296	2.2	191	2.3	89	0.4	266
15	7.0	6	5.0	193	3.7	30	0.3	214
18	0.8	319	0.9	119	0.1	38	0.5	150
21	4.8	323	2.4	190	0.9	306	1.0	192

Table 1d.

with lunar age, verifying Chapman's phase law. The phase angles of first and third harmonic are seen to decrease and increase by 2π over a whole lunation. The phase angle of second harmonic does not change appreciably over a lunation. The phase of the fourth harmonic increases by 4π in a whole lunation. The phase constant do not vary appreciably with lunar age. The phase constant of 2nd harmonic α_2 and the phase angle of the second harmonic are found to be same and do not vary over a lunation. This is in accordance to Chapman's phase law.

The annual average lunar daily variation averaged over a complete lunation is shown in Fig.1. The harmonic coefficients of the whole lunation average lunar daily oscillations for Addis Ababa (1957-60) are given in Table-2. The amplitude of lunar semidiurnal oscillation A_2 is 3.6 γ. and the amplitude of lunar diurnal oscillation A_1 is 0.2 γ. The amplitudes of all components except A_2 are statistically insignificant. The phase angle β_2 for the A_2 oscillation is found to be 221°.

<u>Annual average lunar monthly variations at fixed solar times:</u>

The annual average curves of ΔH at fixed solar hours (00, 03, 06, 09 ....21) as a function of lunar age ν_0 degree are shown in Fig.3. It is seen

The coefficients of lunar daily oscillations in H averaged over the whole lunation during different seasons for Addis Ababa (1957-60) according to the equation

$$L = A_n \sin (n\tau + \beta_n)$$

Station	Period	Season	A_1 Gamma	β_1 Degree	A_2 Gamma	β_2 Degree	A_3 Gamma	β_3 Degree	A_4 Gamma	β_4 Degree
Addis Ababa	1957-60	D-months	1.2	172	6.2	238	1.4	67	0.3	172
		E-months	1.1	304	3.2	250	1.2	298	0.2	170
		J-months	0.5	17	2.3	255	0.6	232	0.1	284
		Annual	0.2	262	3.6	221	0.3	338	0.2	172

Table-2

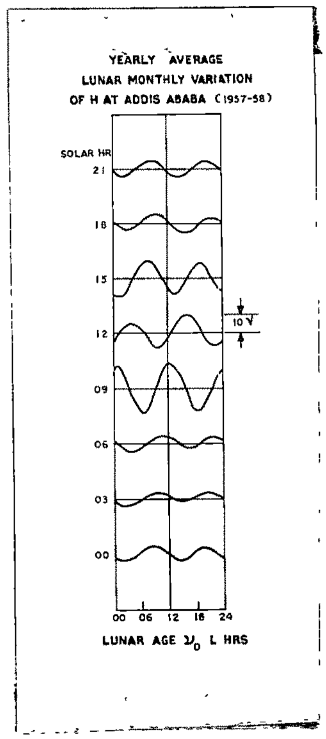

Fig.3

from the Fig.3 that the tides are significantly large for the daytime hours and the maximum tide occurs near midday. The oscillations are small during nighttime. The oscillations during daytime have a predominant periodicity of twelve lunar hours while the nighttime oscillations have predominant - twenty four lunar hours component.

The coefficients of annual average lunar monthly M_1 and lunar semi-monthly M_2 oscillations are given in Table 3.

Coefficients of lunar monthly M_1 and lunar semi-monthly M_2 oscillations in H at Addis Ababa (1957-60) averaged over the whole year.

38.5 E.M. T.	36000 + ΔH Gamma	r_1 Gamma	θ_1 in Lunar age degree	r_2 Gamma	θ_2 in Lunar time degree
00	64	0.8	126	3.9	100
01	66	1.4	142	3.0	127
02	65	0.4	128	3.1	153
03	61	1.7	218	2.9	187
04	60	1.6	214	2.8	210
05	58	1.2	216	2.9	240
06	57	1.1	223	3.8	237
07	69	0.2	227	7.6	227
08	100	0.3	319	10.9	243
09	144	1.2	196	12.7	255
10	178	2.0	201	12.3	266
11	192	2.6	204	9.1	266
12	187	2.4	251	7.6	239
13	168	1.2	226	10.2	235
14	143	2.3	162	10.6	233
15	120	2.3	159	9.3	225
16	104	3.3	156	8.4	214
17	92	2.6	136	5.9	222
18	80	1.5	116	4.1	239
19	71	1.4	119	3.8	290
20	67	0.6	113	4.1	337
21	65	0.4	104	4.5	362
22	64	0.4	217	4.0	393
23	64	0.6	117	4.0	70

Table-3

The amplitudes (r1) of lunar monthly component are seen to lie between 0.2 γ and 3.3 γ . The amplitudes r_1 do not seem to vary systematically with the solar time but amplitudes r2 vary systematically with solar time. The values of r2 are very small at night and early morning, start increasing at sunrise reach a maximum value at about midday and start falling thereafter to the nighttime small value. The amplitude of r2 at midday is 7.6γ.

The amplitudes r1 of lunar monthly oscillations are so small that the representation of (r1 θ1) points on a harmonic dial will not serve any quantitative purpose. The probable errors will mask the picture. Hence (r1 θ1) points for different solar hours are not represented on a harmonic dial.

The amplitude and phase of lunar semi-monthly oscillations (r2 θ2) for different solar hours are plotted on the harmonic dials of lunar age and lunar time in Fig.4. On the lunar age dial the points for the different hours of the solar day move around the origin giving rise to a very small value of the vector average from all the hours. On the lunar time dial the points for various solar hours do not move around the origin but lie within a narrow sector and here the Scalar average and vector average of M_2 amplitudes are comparable. At Addis Ababa the amplitudes for all hours

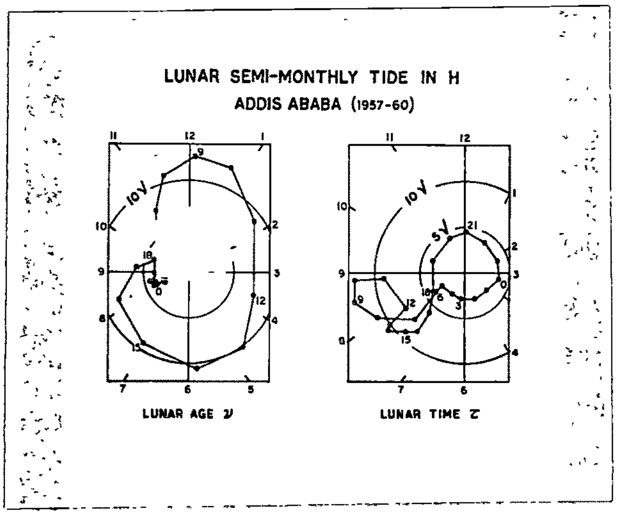

Fig.4

give an annual solar hour mean of 6.3 γ while the vector mean is 4.3 γ on a lunar time dial and 2.06 γ on a lunar age dial. The phase of maximum deviation of M_2 on the lunar age dial is 255° or 8.5 l.hr.

Lunar daily variation of H during different seasons:

Lunar daily variations at the eight lunar age groups were computed separately for each season and resulting curves are shown in Fig.5. For each season the whole lunation

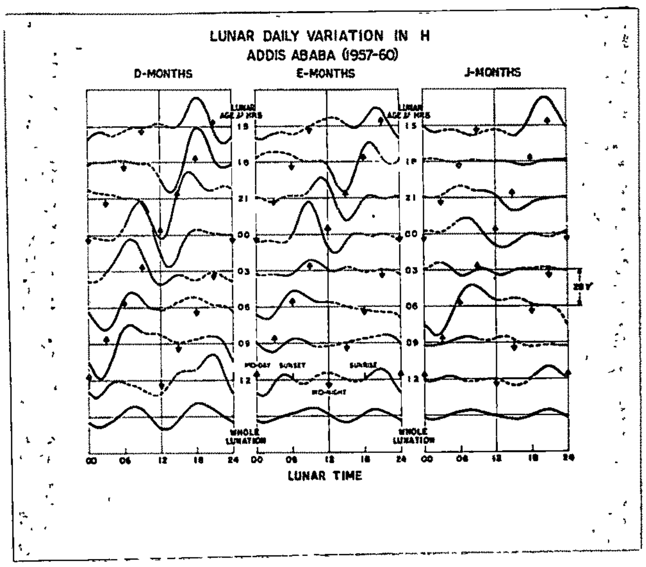

Fig.5

average curves were also derived by averaging eight individual curves and the resultant curves are also shown, in the diagram. As described earlier for the annual average curves, one finds that during any season the oscillations are predominant during the daytime hours and the peak occurs earlier in lunar time with increasing age of the moon. Individual curves are harmonically analysed to find the coefficients C_n and α_n for each season. Chapman's phase law is found to hold good for lunar daily variation in every season.

The whole lunation average curves for each season were harmonically analysed. The coefficients are given in Table 2. It is seen from the Table 2 that the second harmonic component is significantly larger than the other harmonics. The amplitude of the second harmonic (A_2) component lies between 2.3 γ to 6.2 γ and the first harmonic amplitudes lie between 0.5 γ to 1.2 γ . The higher harmonics are quite small. The phase of A_2 i.e. β_2 is 238° during D-months 250° during E-months and 255° during J-months. The maximum positive deviation due to A_2 oscillation occurs earliest in J months, almost at the same time in E months and about half an hour later in D-months.

The maximum amplitude of A_2 (6.2 γ) occurs in D-months, during E-months A_2 is 3.2 γ , and during J-months A_2 is 2.3 γ .

<u>Lunar monthly oscillations in H at fixed solar time during different seasons:</u>

The M_1 (H) and M_2 (H) for each of the solar hours were computed separately for different seasons of the year. The coefficients of M_2 (H) oscillations are listed in Table 4. The probable errors are also included in the Table 4.

Coefficients of lunar semi-monthly M_2 oscillations in H at Addis Ababa (1957-60)

38.5 E.M.T.	D-months: 36000 + ΔH Gamma	D-months: r_2 Gamma	D-months: Proba-ble error	D-months: θ_2 Phase in lunar time. degree	E-months: 36000 + ΔH in Gamma	E-months: r_2 Gamma	E-months: Proba-ble error	E-months: θ_2 Phase in lunar time degree	J-months: 36000 + ΔH in Gamma	J-months: r_2 Gamma	J-months: Proba-ble error	J-months: θ_2 Phase in lunar time degree
00	65	5.6	1.6	58	61	6.9	1.7	78	67	3.8	1.3	194
01	66	4.6	1.6	117	64	5.7	1.6	98	67	3.6	1.2	222
02	65	4.8	1.5	146	64	4.5	1.5	143	67	2.9	1.1	133
03	61	4.7	1.7	149	60	6.3	1.8	186	63	3.3	1.4	303
04	59	5.1	1.6	182	58	6.3	1.7	213	62	3.3	1.5	350
05	56	4.9	1.5	213	55	7.0	1.7	242	62	3.3	1.4	24
06	55	7.4	1.5	223	52	7.5	1.6	267	64	2.9	1.6	99
07	68	12.4	1.8	216	66	9.3	1.8	269	72	5.4	1.8	183
08	98	16.2	2.3	227	106	13.7	2.2	280	95	7.5	2.3	212
09	141	22.1	2.8	233	157	16.0	2.5	297	134	6.2	2.6	232
10	174	22.5	3.2	247	193	15.4	3.0	315	166	6.8	2.5	230
11	187	18.5	3.2	256	205	6.3	3.3	332	184	7.2	2.5	244
12	181	10.9	3.2	244	193	3.1	3.3	225	186	8.9	2.5	244
13	161	11.4	2.8	217	170	9.2	3.1	230	172	11.5	2.6	257
14	134	15.4	2.6	199	145	11.3	2.5	233	147	11.7	2.6	280
15	116	16.4	2.5	200	124	9.7	2.0	223	121	8.0	2.2	289
16	102	13.5	2.3	205	109	10.7	1.8	208	100	5.5	1.8	290
17	90	9.5	2.0	206	98	9.6	1.9	214	87	4.0	1.7	325
18	78	8.7	2.0	213	82	6.7	2.0	252	79	2.9	1.6	12
19	70	8.8	2.0	255	69	6.6	1.9	299	73	4.6	1.5	49
20	67	7.2	2.0	292	64	7.6	1.9	333	69	5.6	1.5	70
21	65	7.8	1.9	324	61	7.2	2.0	359	68	5.1	1.5	91
22	65	7.3	1.7	357	61	6.6	1.8	34	67	4.0	1.5	126
23	65	6.3	1.7	51	61	6.8	1.7	56	67	3.7	1.4	169

Table 4

In Fig.6, comparison is made between the diurnal variation of theamplitude of M_2 (H) and the normal diurnal

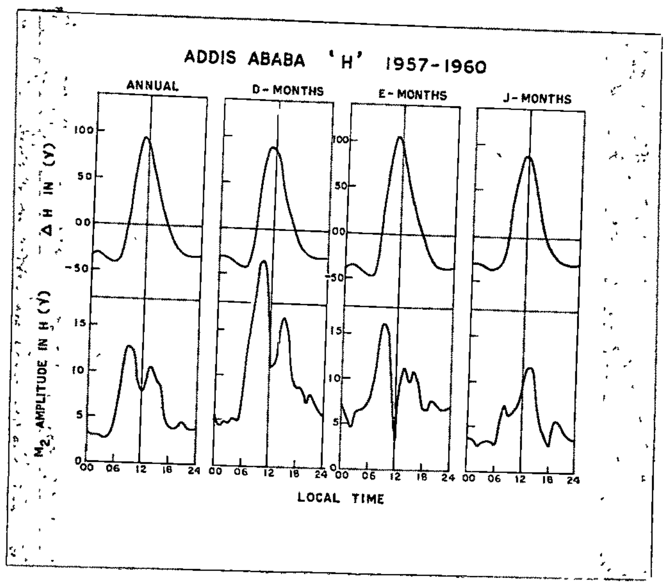

Fig.6

variation in H. The diurnal variation in 'H' is derived from data utilized in this analysis. The diagram shows that M_2 (H) and H itself vary in a similar way during the course of a day. The range in H variation is greatest in E-months and comparable in D and J months; whereas the range in M_2 (H) variation is largest in D-months, the range M_2 (H) in E months is slightly less than that of D-months and least in J-months.

(r_2 τ_2) points for different solar hours for each season are plotted in harmonic dial of lunar time in Fig.7. It is seen that most of thepoints for the daytime

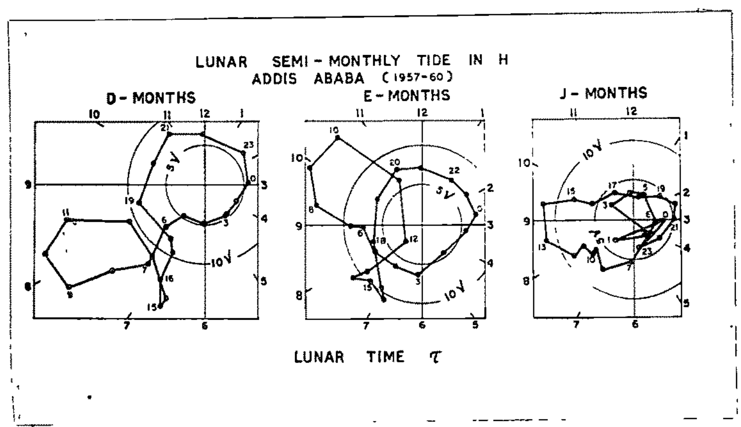

Fig.7

form a loop elongated in a preferred direction. But it is noteworthy that nighttime points also tend to form a separate loop rather roundish with no preferred elongation. But nighttime amplitudes are fairly large.

(3) Koror:

A magnetic observatory at Koror, an island in the Palau group of islands was established at the beginning of the IGY programme. The coordinates of the observatory are:

Geographic latitude	7°20'N
Geographic longitude	134°30'E
Geomagnetic latitude	-3°.2°
Geomagnetic longitude	213°.4°
dip angle	= 0.1°S

The hourly values of H at Koror are taken from the data book issued by the Coast and Geodetic Survey, Washington. In the present analysis, data for the years 1957-58 are used. For lunar tide analysis, 15 months data are too short a period to give a definite picture of the phenomenon. However Koror being an important station on the magnetic equator, an attempt has been made to study the lunar effects on the geomagnetic field. Only days with C_p index less than 1.2 are considered in the computation of lunar tides.

At Koror the mean value of the H field is about 37850 gamma and the mean value of the vertical field is about -10 gamma.

The lunar daily variation at fixed lunar ages

The annual average lunar daily variation in

H at Koror (1957-58) for lunar ages centered on 00,03, 06, 09, 12, 15, 18 and 21 are shown in Fig.1.

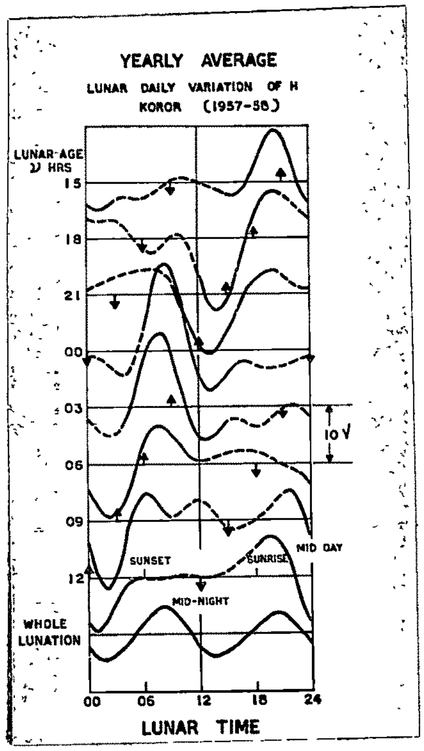

Figure.1.

The presence of $L_1(H)$ and L_2 (H) is indicated by the two unequal peaks in the lunar daily variation curves. The part of the curve having greatest movement fall during daylight hours and is found to occur earlier and earlier in lunar day with the progress of the lunation. The whole lunation average lunar daily variation curve is nearly a sinusoid with two equal peaks.

The harmonic coefficients C_n and α_n of the average lunar daily variations in H at Koror for different seasons and the whole year are computed according to

Chapman's phase law expression and listed in tables 1a, 1b, 1c and 1d.

It is seen from the Table 1 that the amplitudes C_n are independent of lunar age. The relations between ϕ and ν for any particular harmonic are shown in fig.2.

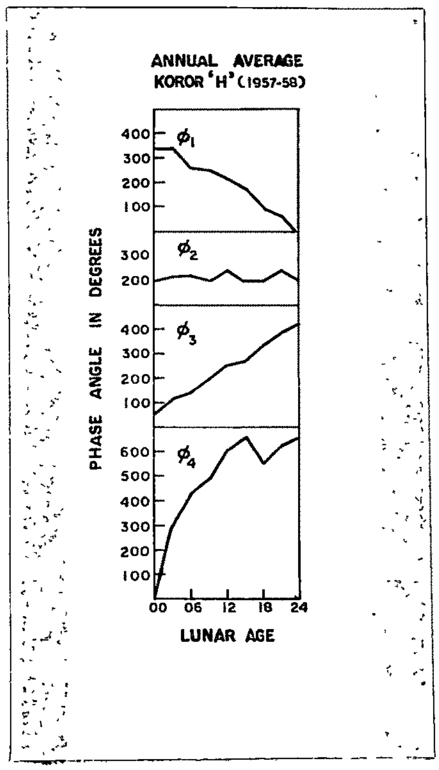

Figure.2.

The fig.2 verifies Chapman's phase law. The phase constants αn unlike the phase angles ϕn remain nearly same during the whole lunation.

The lunar daily variation averaged over a complete lunation is shown in Fig.1. The harmonic coefficients

Table - 1 (a)

Coefficients of lunar daily variations in H at KOROR for different lunar ages according to the equation L = $\sum_{n=1}^{4} C_n \sin\{n\tau + (n-2)\nu + \alpha_n\}$

Annual - KOROR (1957-58)

Lunar age	C_1 Gamma	α_1 °	C_2 Gamma	α_2 °	C_3 Gamma	α_3 °	C_4 Gamma	α_4 °
00	5.2	335	5.3	198	4.2	67	1.2	290
03	4.4	27	5.2	214	3.4	69	1.0	206
06	4.1	350	3.7	218	2.1	41	0.5	243
09	2.8	22	4.4	197	3.6	63	1.9	226
12	3.8	31	3.9	238	2.0	74	0.9	244
15	3.0	42	3.7	194	2.3	42	3.1	206
18	6.3	2	4.3	197	3.1	63	0.7	12
21	5.0	19	4.4	238	1.2	68	0.4	0

Table - 1 (b)

Coefficients of lunar daily variations in H at Koror for different lunar ages according to the equation $L = \sum_{n=1}^{4} C_n \sin\{n\tau + (n-2)\nu + \alpha_n\}$

D - months - Koror(1957-58)

Lunar age	C_1 Gamma	α_1°	C_2 Gamma	α_2°	C3 Gamma	α_3°	Gamma	α_4°
00	4.8	326	5.5	175	3.00	.61	1.1	262
03	5.2	20.0	7.3	248	5.6	62	1.9	252
06	3.5	296	1.5	226	1.0	63	0.6	337
09	2.4	29	6.1	242	6.0	65	3.4	259
12	4.3	94	6.2	291	4.1	128	0.8	293
15	4.3	46	4.1	230	2.9	85	0.5	308
18	4.4	5	4.0	233	3.3	113	1.7	347
21	2.3	63	1.7	232	2.2	169	1.0	356

Table - 1 (c)

Coefficients of lunar daily variations in H at Koror for different lunar ages according to the equation $L = \sum_{n=1}^{4} c_n \sin\{n\tau + (n-2)\nu + \alpha_n\}$

E-months - Koror (1957-58)

Lunar age	C1 Gamma	α_1 °	C2 Gamma	α_2 °	C3 Gamma	α_3 °	C4 Gamma	α_4 °
00	10.6	342	9.6	196	8.2	55	3.0	274
03	6.0	46	5.2	215	2.6	72	1.4	172
06	8.2	17	7.7	214	4.2	45	0.5	213
09	5.1	27	7.2	179	4.3	51	2.3	212
12	6.8	39	2.3	230	4.4	49	0.6	286
15	4.4	79	3.3	226	2.7	63	2.6	207
18	9.5	4	5.2	170	4.4	42	0.6	90
21	7.7	27	6.3	247	1.9	46	0.7	19

Table 1 -(d).

Coefficients of lunar daily variations in H at Koror for different lunar ages according to the equation $L = \sum_{n=1}^{4} C_n \sin\{n\tau + (n-2)\nu + \alpha_n\}$

J-months - Koror (1957-58)

Lunar age	C_1 Gamma	α_1 °	C_2 Gamma	α_2 °	C_3 Gamma	α_3 °	C_4 Gamma	α_4 °
00	0.5	296	2.7	256	2.7	117	1.3	24
03	2.9	357	6.0	170	3.0	81	0.8	159
06	3.2	335	2.3	227	1.3	10	1.4	224
09	1.1	341	2.9	150	0.9	107	1.1	161
12	5.6	334	7.5	201	3.8	24	1.7	213
15	3.1	331	6.5	154	3.6	348	0.5	154
18	5.1	357	5.3	197	3.1	43	0.3	52
21	6.5	354	5.3	229	2.6	37	3.8	191

of the average lunar daily variation for the whole lunation are given in table 2. The lunar semidiurnal component A_2 is the most prominent component; others are very small. The amplitude of A_2 is 4.2 γ while A_1 is only 0.4 γ. The phase angle β_2 is found to be 212°.

Annual average lunar monthly variations at fixed solar times:

In Fig.3 are shown annual average lunar monthly

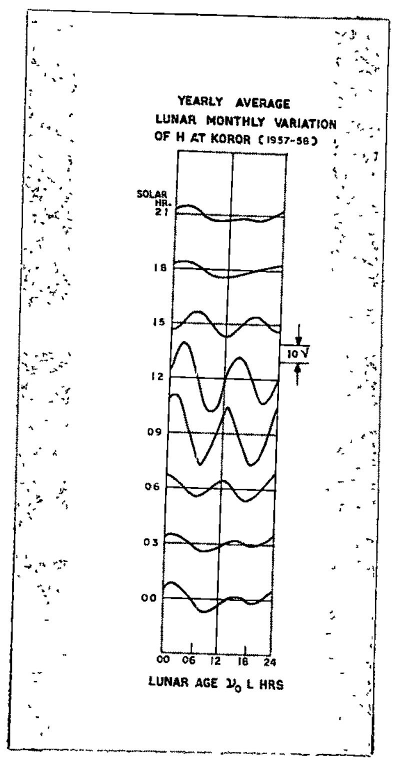

Figure.3.

variations at fixed solar times. The coefficients of lunar monthly and semimonthly oscillations derived from

Table - 2.

The coefficients of lunar daily oscillations in H averaged over the whole lunation during different seasons for Koror (1957-58) according to equation L = $A_n \sin\{n\tau + \beta_n\}$

Station	Period	Season	A_1 Gamma	β_1 °	A_2 Gamma	β_2 °	A_3 Gamma	β_3 °	A_4 Gamma	β_4 °
Koror	1957-58	D-months	0.8	270	3.8	239	0.5	101	0.5	207
		E-months	1.3	329	5.6	207	0.5	68	0.8	287
		J-months	1.0	94	4.1	193	0.7	201	0.1	113
		Annual	0.4	337	4.2	212	0.3	119	0.4	247

these curves are given in Table 3. In the table the phase of M_1 oscillations are presented in terms of local lunar age whereas the phase of M_2 oscillations are presented in terms of local lunar time .

It is seen from Fig.3 that the lunar monthly oscillations are greater only during daylight hours and it reaches maximum near midday. During nighttime the oscillations are very small. The oscillations during daytime show semidiurnal character while nighttime oscillations show predominant diurnal character.

The amplitudes λ_1 do not show any dependence on solar time and ranges between 2.0 γ to 6.8 γ, whereas λ_2 show solar diurnal variation with maximum value near midday and minimum at night. The λ_2 values range from 0.2 γ to 18.0 γ. The (λ_1, θ_1) points for different solar hours are plotted on a harmonic dial of lunar age and lunar time in Fig.4. It is seen that (λ_1, θ_1) points in

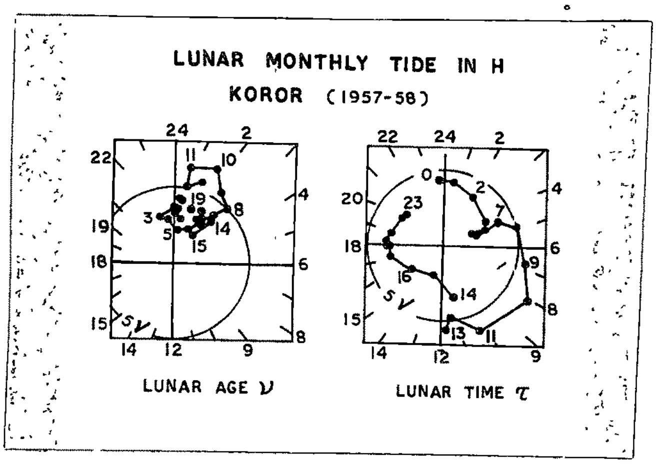

Figure.4.

Table - 3.

Coefficients of lunar monthly M_1 and lunar semi-monthly M_2 oscillation in H at KOROR (1957-58) averaged over the whole year.

L.S.T.	37500+ ΔH Gamma.	r_1 Gamma.	θ_1 in lunar age degree. ν_1	r_2 Gamma	θ_2 in lunar time degree. τ_2
00	304	4.3	3	4.7	284
01	306	4.2	6	3.9	316
02	307	3.7	359	3.6	352
03	307	3.2	342	3.0	22
04	307	3.0	352	2.8	54
05	306	2.0	7	2.7	109
06	312	2.3	21	5.8	176
07	336	4.0	39	11.1	204
08	368	5.0	44	15.2	222
09	430	5.7	33	17.1	234
10	468	6.8	24	18.3	247
11	479	6.3	9	18.0	254
12	465	4.9	7	15.9	271
13	437	5.6	18	13.7	276
14	404	3.6	41	8.5	285
15	376	2.1	32	5.3	278
16	356	2.8	8	2.5	290
17	339	3.5	358	0.2	301
18	326	3.7	4	1.2	87
19	319	3.7	16	2.4	117
20	316	3.8	27	2.2	160
21	313	3.5	31	2.0	204
22	312	3.2	28	1.6	235
23	312	3.2	36	1.4	276

lunar time dial move around the origin and form a loop during the course of a solar day. The vectorial averageof over a day comes to be 0.52 γ and just scalar mean of r_1 is 3.9 γ. When plotted on lunar age dial ($r_1 \theta_1$), the points group themselves in a narrow sector and here the vector average and scalar average of r_1 come out to be nearly the same, the vectorial mean being 3.74 γ and solar mean 3.9 γ. Similarly ($r_2 \theta_2$) points are plotted on a harmonic dial in Fig.5 on the lunar age dial and lunar time dial.

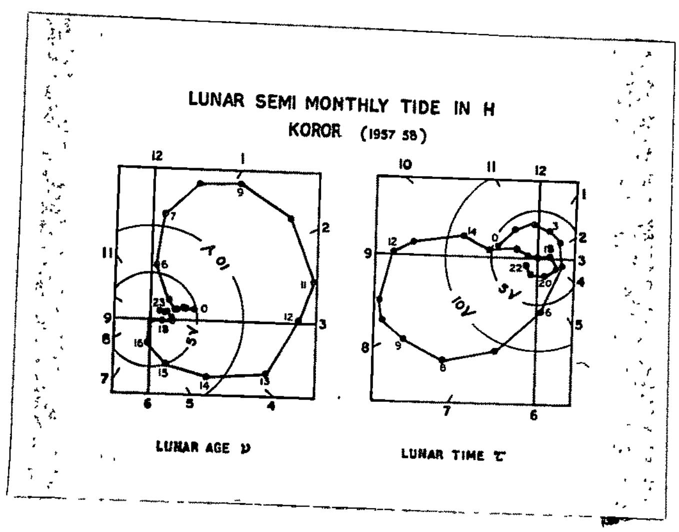

Figure.5.

The ($r_2 \theta_2$) points trace a near circular loop., but the whole of it is on the right side of the origin. So the vectorial average of r_2 of 6.06 γ is comparable to the scalar average of 6.7 γ . On the lunar time dial ($h_2\theta_2$) points trace a loop with an elongation in a preferred direction. In lunar time, vectorial average of h_2 is 4.76 γ and the phase of the maximum deviation of h_2 in lunar time is 252° or 8.4 l.hr.

Lunar daily variation of H during different seasons

Lunar daily variation at the eight lunar age groups are computed separately for each season and the resulting curves are shown in Fig.6. The whole lunation average

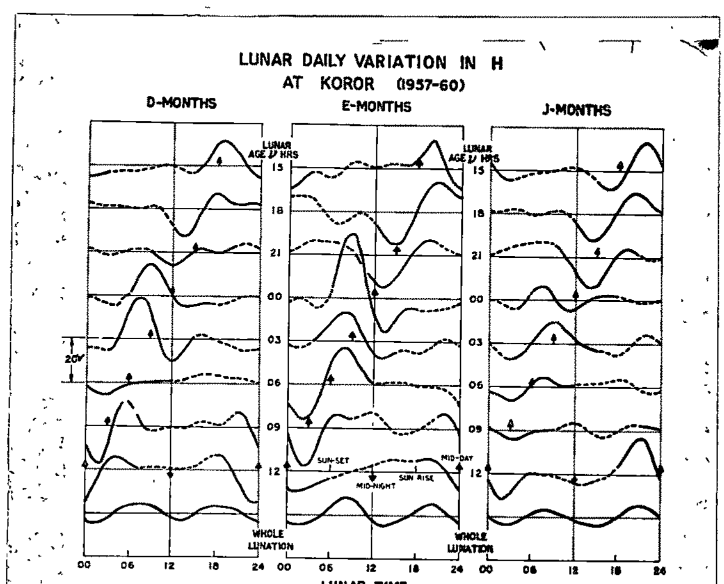

Figure.6.

curves for each season are also drawn. In character these curves are identical to the annual daily variation curves described previously. Here also Chapman's phase law is obeyed. The harmonic coefficients for the whole lunation lunar daily variation curves are presented in Table 2. It is seen that the semidiurnal component A_2 is the most prominent harmonic. The amplitudes of A_2 range between 3.8 γ and 5.6 γ in the order of

E-months	5.6 γ
J-Months	4.1 γ
D-months	3.8 γ

The phase β_2 is 239° during D months, 207° during E-months and 193° during J-months. Thus the maximum deviation of A_2 oscillation occurs about one and quarter hour later during D-months than in J-months.

<u>Lunar monthly oscillations in H at fixed solar time during different seasons.</u>

In Fig.7 comparison is made between diurnal variation of M_2 (H) amplitude and normal diurnal variation in H.M2(H) and H itself vary in a similar way during the course of a day. The range of daily variation in H and M_2 (H) is least in J-months and nearly same in D and E months.

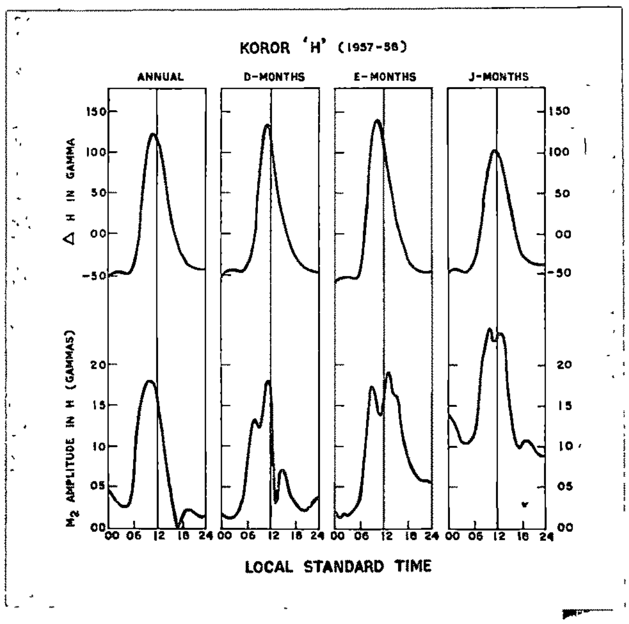

Figure.7.

In Table 4, -------- r_2, $\theta_2(\tau)$, ΔH and the probable errors for each solar hour are presented. The ($r_2\tau_2$) points for different solar hours for each season are plotted in the harmonic dial of lunar time. (Fig.8.)

The ($r_2\tau_2$) points for D and E-months when plotted in a harmonic dial trace a loop with a marked elongation in a preferred direction and the ($r_2\tau_2$) points for J-months trace - two circles, the inner smaller one representing nighttime, and the outer bigger one

Table - 4.

Coefficients of lunar semi-monthly M_2 oscillations in H at Koror (1957-58) averaged for different seasons.

L.M.T.	D-months. 37500+ ΔH Gamma.	r_2 Gamma	P.E.	θ_2 in lunar time degree.	E-months. 37500+ ΔH Gamma.	r_2 Gamma	P.E.	θ_2 in lunar time degree.	J-months. 37500+ ΔH Gamma	r_2 Gamma	P.E.	θ_2 in lunar time degree.
00	310	1.7	2.3	1	297	1.8	3.4	191	306	14.0	2.6	285
01	312	1.6	2.2	61	299	1.4	3.0	175	307	13.2	2.3	313
02	313	1.4	2.1	87	301	1.8	2.9	194	307	12.6	2.2	349
03	313	1.5	2.0	127	302	1.6	2.7	227	306	10.9	2.2	18
04	313	2.3	1.9	160	302	2.0	2.6	280	306	10.5	2.1	50
05	311	3.4	1.9	185	300	2.6	2.4	283	306	10.6	2.0	89
06	316	7.0	1.9	207	307	3.5	2.6	233	315	11.5	2.3	141
07	338	11.9	2.2	217	338	8.2	2.9	215	333	14.5	2.6	187
08	348	13.3	2.5	227	391	13.8	3.7	229	364	18.9	3.1	214
09	435	12.1	3.2	228	451	17.5	4.3	247	406	22.2	3.7	236
10	476	14.7	3.6	240	490	16.2	4.5	247	439	24.3	3.9	252
11	490	18.2	3.9	245	493	13.8	4.7	246	454	22.8	3.7	265
12	469	9.4	3.9	251	471	16.8	4.1	260	456	23.2	4.0	287
13	436	3.0	3.6	245	435	19.2	4.0	249	440	23.0	3.4	302
14	402	6.8	3.3	151	397	16.7	3.3	251	414	21.7	3.3	326
15	375	7.3	2.6	159	370	16.3	2.8	249	384	15.1	2.9	347
16	355	5.6	2.1	175	352	13.6	2.5	264	360	11.2	2.5	31
17	349	3.9	1.9	188	338	10.3	2.5	288	340	9.9	2.1	84
18	328	3.0	1.9	214	322	8.3	2.4	230	328	10.4	2.0	116
19	321	2.6	1.9	210	315	7.4	2.3	8	321	10.6	1.9	141
20	318	2.2	2.0	230	311	6.3	2.2	22	318	10.7	1.9	172
21	316	2.6	1.9	264	309	5.9	2.2	47	316	10.0	1.8	204
22	314	2.6	1.9	302	308	5.9	2.1	82	316	9.3	1.7	237
23	313	3.5	1.9	349	308	5.7	2.1	112	315	8.8	1.6	264

representing daytime variation. The bigger and outer loop is elongated to the left side of the origin. So that the vector average of ($h_2\tau_2$) during J-months is not small.

The average of

($h_2\tau_2$) D-months is 4.4 γ , 221°
($h_2\tau_2$) E-months is 6.2 γ , 256°
($h_2\tau_2$) J-months is 4.8 γ , 274°.

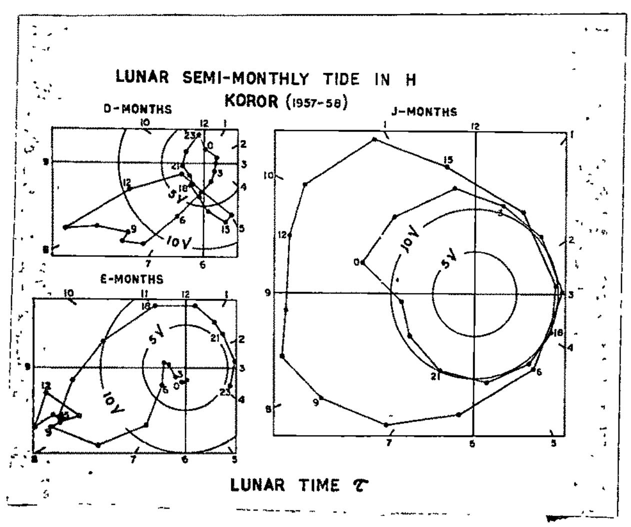

Fig - 8

(4) Jarvis

Jarvis island is near to a junction of the geographic and magnetic equators and hence of a special value for study of the equatorial electrojet. The position of the magnetic observatory at Jarvis can be described as

Geographic latitude	0°23' South
Geographic longitude	160°02' West
Geomagnetic latitude	-0.6°
Geomagnetic longitude	269.1°
dip angle	= 2.2°North.

The hourly values of H field at Jarvis are taken from the data book issued by Coast and Geodetic Survey, Washington. In the present analysis data for the years 1957-58 are used.

The mean value of H field at Jarvis is about 34458 Gamma and the mean value of **V** field is about 1335 Gamma.

The lunar daily variation at fixed lunar ages

The annual average lunar daily variation in H at Jarvis (1957-58) for lunar ages centered on 00,03,06, 09,12,15,18 and 21 are shown in Fig.1. The presence of L_1 (H) and L_2 (H) is indicated by the two unequal peaks in the lunar daily variation curves. The part of the curve

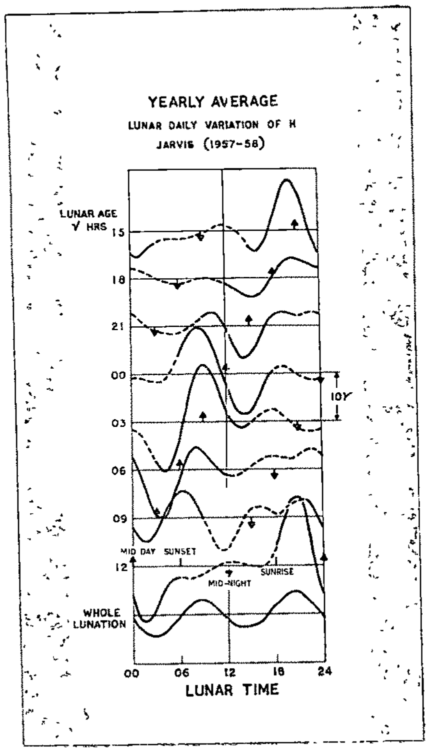

Figure.1.

having greatest movement fall during daylight hours and is found to occur earlier and earlier in lunar day with the progress of the lunation. The whole lunation lunar daily variation curve is a sinusoid with two nearly equal peaks.

The harmonic coefficients C_n and α_n for each of the average lunar daily variation curves are presented in Table 1a. It is seen from the Table 1a that amplitudes C_n are independent of lunar age. The relations between ϕ and ν for any particular harmonic are shown in Fig.2. The phase constants α_n unlike phase angles ϕ_n remain nearly same during the whole lunation.

Table 1 (a)

Coefficents of lunar daily variations in H at Jarvis for different lunar ages according to the equation $L = \sum_{n=1}^{4} C_n \sin\{n\tau + (n-2)\nu + \alpha_n\}$

Jarvis (1957-58) Annual average.

Lunar age	C_1 Gamma.	α_1 °	C_2 Gamma	α_2 °	C_3 Gamma	α_3 °	C_4 Gamma	α_4 °
00	3.6	358	5.3	206	2.3	32	0.4	36
03	4.8	308	4.9	174	3.9	2	0.6	231
06	2.8	290	4.0	181	3.1	9	0.7	242
09	1.2	240	4.0	253	3.1	25	0.8	335
12	6.1	4.0	5.6	198	4.1	49	1.1	241
15	2.7	39	3.9	195	3.2	37	1.1	231
18	2.4	8	2.0	166	0.7	26	0.5	169
21	1.8	43	3.0	171	1.9	42	1.0	216

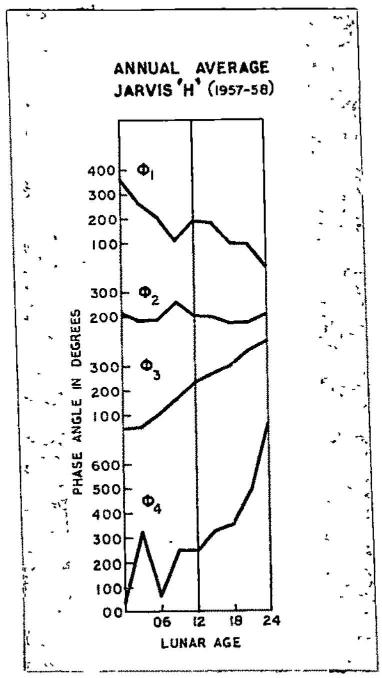

Figure.2.

The lunar daily variation averaged over a complete lunation is shown in Fig.1. The harmonic coefficients of the average lunar daily variation for the whole lunation are given in Table 2. The lunar semidiurnal component A_2 is the most prominent component, others are small. The amplitude of A_2 is 3.6 γ while A_1 is 1.0 γ. The phase angle β_2 is 194°.

<u>Average lunar monthly variations at fixed solar times.</u>

In Fig.3 are shown annual average lunar

Table – 2.

The coefficients of lunar daily oscillations in H averaged over the whole lunation during different seasons for Jarvis (1957-58) according to the equation $L = A_n \sin(n\tau + \beta_n)$

Station	Period	Season	A1 Gamma	β_1 °	A2 Gamma	β_2 °	A3 Gamma	β_3 °	A4 Gamma	β_4 °
Jarvis	1957-58	D-months	3.68	226	6.06	189	0.68	318	0.53	66
		E-months	1.66	304	3.23	199	0.76	186	0.58	300
		J-months	4.0	116	1.86	203	0.98	70	0.31	248
		Annual	1.02	185	3.6	194	0.11	94	0.17	314

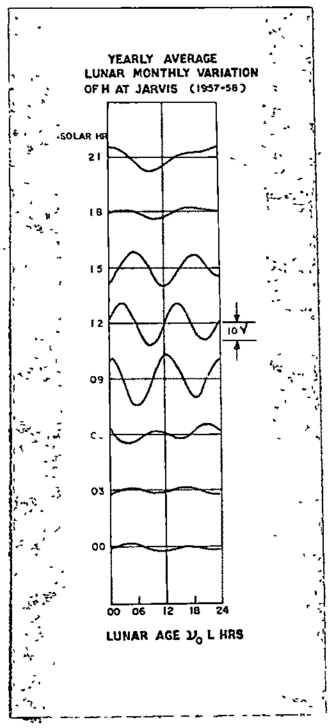

Figure.3.

monthly variations at fixed solar times. The coefficients of lunar monthly and semimonthly oscillations derived from these curves are given in Table 3. In Table 3, the phase of M_1 oscillations are presented in terms of local lunar age ν whereas the phase of M_2 oscillations are presented in terms of local lunar time τ.

It is seen from Fig.3 that the lunar monthly oscillations are greater only during daylight hours and it reaches maximum near midday. During nighttime the oscillations are very small. The oscillations during

Table 3

Coefficients of lunar monthly M1 and lunar semi-monthly M_2 oscillations in H at Jarvis (1957-58) averaged over the whole year.

150 W.M.T.	34000 + ΔH Gamma	λ_1 Gamma	θ_1 in lunar age degree.	λ_2 Gamma	θ_2 in lunar time degree.
00	410	0.48	60	1.83	140
01	411	0.58	48	1.36	123
02	413	0.32	105	1.84	124
03	414	0.58	187	1.69	127
04	414	0.48	187	1.88	133
05	414	0.67	177	2.35	149
06	419	0.63	31	1.04	176
07	445	2.18	295	3.79	289
08	482	1.17	238	8.38	329
09	522	3.05	244	10.22	338
10	553	3.66	245	11.88	11.0
11	566	4.95	261	10.76	43.0
12	557	1.30	280	10.60	72.0
13	538	1.54	339	10.90	84.0
14	516	2.82	35	10.96	122.0
15	492	3.87	51	10.87	150.0
16	472	3.60	20	7.47	179.0
17	455	2.01	340	3.61	220.0
18	437	1.31	314	+1.19	184.0
19	421	2.36	325	1.34	144.0
20	414	3.92	320	1.58	117.0
21	411	4.51	323	2.42	91.0
22	408	5.77	331.0	2.34	74.0
23	408	5.48	338.0	2.51	68

daytime show semidiurnal character while nighttime oscillations show predominant diurnal character. Unlike h_2 amplitudes h_1 does not show any dependence on solar time. The $(h_1\theta_1)$ points are plotted on a harmonic dial of lunar age and lunar time. Fig.4. The picture emerging from $(h_1\theta_1)$ plots is confusing.

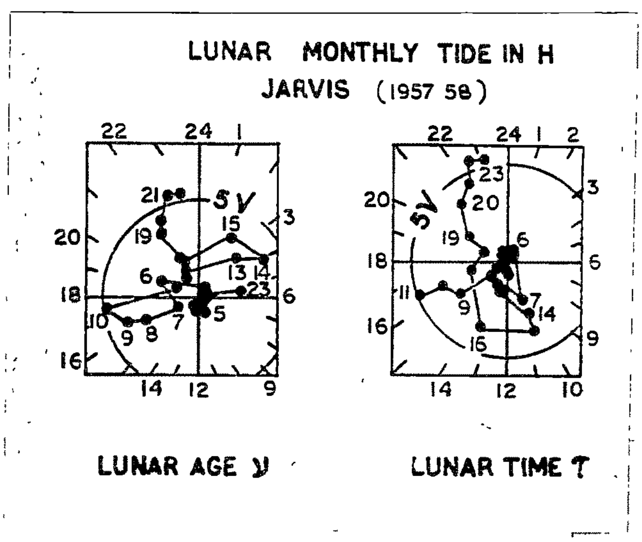

Figure.4.

The vector average of $(h_1\theta_1)_\nu$ is 1.26 γ, 20° and the vector average of $(h_1\theta_1)_\tau$ is 0.8 γ, 270°. The scalar average of h_1 is 2.3 γ. Similarly $(h_2\theta_2)$ points are plotted on a harmonic dial in fig.5 on the lunar

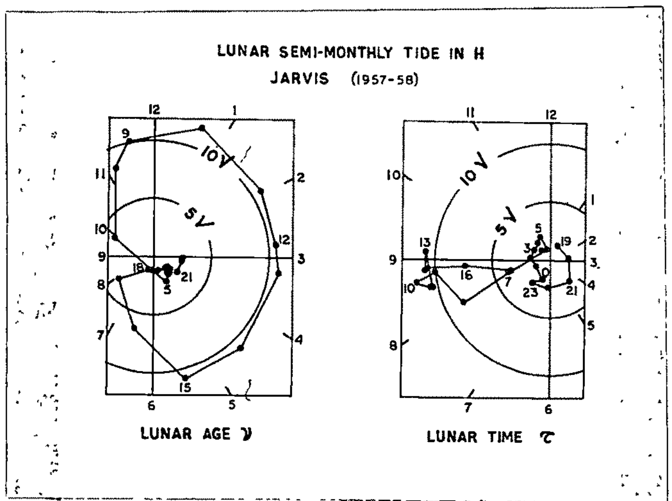

Figure.5

age dial ($r_2\theta_2$) points trace a near circular loop, with most of the part on the right side of the origin. The vectorial mean of r_2 is 2.0 γ and scalar average is 5.1 γ. on the lunar time dial ($r_2\theta_2$) trace a loop with a marked elongation in the third quadrant. In lunar time r_2 vectorial average is 4.4 γ and the phase of the maximum deviation of r_2 in lunar time is 8.8 l.hr.

<u>Lunar daily variation of H during different season.</u>

Lunar daily variations at the eight lunar age groups are computed separately for each season and the resulting curves are shown in Fig.6. The whole lunation average curves for each are also drawn. In Character

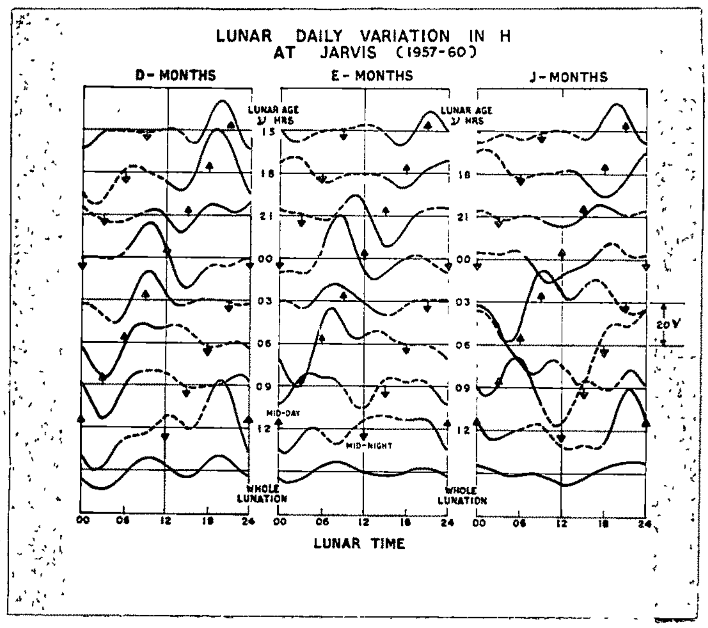

Figure.6.

these curves are identical to the curves in Fig.1. Here also Chapman's phase law is obeyed. The harmonic coefficients of lunar daily variations in each of the seasons are tabulated in Tables 1b, 1c, 1d. The harmonic coefficients for the whole lunation lunar daily variation curves are presented in Table 2. It is seen that semidiurnal component L_2 is the most prominent harmonic. The amplitudes of the L_2 range between 1.9 γ to 6.1 γ in the following order

Table – 1 (b)

Coefficients of lunar daily variations in H at Jarvis for different lunar ages according to equation $L = \sum_{n=1}^{4} c_n \sin\{n\tau + (n-2)\nu + \alpha_n\}$

D-months Jarvis (1957-58)

Lunar age	C_1 Gamma	α_1 °	C_2 Gamma	α_2 °	C_3 Gamma	α_3 °	C_4 Gamma	α_4 °
00	7.9	346	7.1	170	3.9	8	1.2	144
03	4.9	314	6.0	160	4.2	349	0.9	185
06	8.6	345	5.2	158	4.0	37	1.0	200
09	5.2	18	7.1	163	2.9	351	1.6	185
12	12.7	19	9.1	204	5.7	65	1.1	9
15	3.0	42	4.9	218	5.2	49	2.1	251
18	7.2	93	4.9	2.8	2.7	12	1.2	257
21	2.3	81	3.3	185	2.7	55	1.4	217

Table - 1 (c)

Coefficients of lunar daily variations in H at Jarvis for different lunar ages according to equation $L = \sum_{n=1}^{4} C_n \sin\{n\tau + (n-2)\nu + \alpha_n\}$

E-months (Jarvis -1957-58)

Lunar Age	C_1 Gamma	α_1 °	C_2 Gamma	α_2 °	C_3 Gamma	α_3 °	C_4 Gamma	α_4 °
00	6.3	319	9.5	208	4.5	58	1.9	300
03	3.3	39	4.4	194	0.8	44	1.0	301
06	9.5	1	7.2	211	6.0	55	2.3	225
09	1.1	213	6.4	287	1.1	66	2.9	14
12	6.3	35	2.1	290	4.2	60	1.5	203
15	0.8	48	4.7	151	3.8	342	0.8	167
18	4.3	338	3.8	79	0.7	22	1.4	106
21	4.0	338	6.7	147	3.7	358	1.0	219

Table-1 -d.

Coefficients of lunar daily variations in H at Jarvis for different lunar ages according to the equation $L = \sum_{n=1}^{4} C_n \sin\{n\tau + (n-2)\nu + \alpha_n\}$

J-months- Jarvis (1957-58)

Lunar age	C_1 Gamma.	α_1 °	C_2 Gamma	α_2 °	C_3 Gamma	α_3 °	C_4 Gamma	α_4 °
00	6.0	106	4.1	286	0.8	236	1.9	57
03	10.6	286	4.6	174	7.1	6	0.9	219
06	16.2	202	1.8	122	6.2	292	1.7	356
09	7.0	217	7.3	280	6.3	33	1.8	301
12	6.5	280	8.3	175	3.6	4	2.6	248
15	4.2	36	4.1	215	3.9	67	1.1	243
18	5.7	307	6.5	75	1.2	180	0.9	170
21	3.0	90	1.8	276	1.9	115	0.7	197

D-months	6.1 γ
E-months	3.2 γ
J-months	1.9 γ

The phase β_2 is 189° during D-months, 199° during E-months, 203° during J-months.

Lunar monthly oscillations in H at fixed solar time during different seasons.

In Fig.7 comparison is made between diurnal

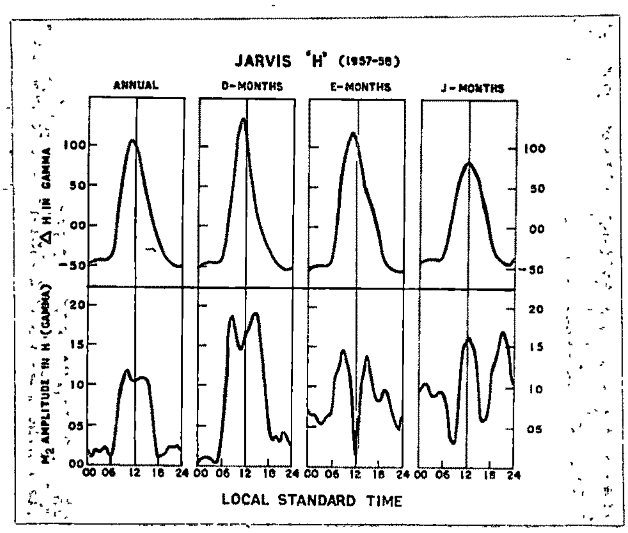

Figure.7.

variation of M_2(H) amplitude and normal diurnal variation in H . M_2 (H) and H itself vary in a similar way during the course of a day. The range of daily variation in H is least in J-months and greatest in D-months. The range of daily variation in M_2 (H) is greater in D-months and about the same in E and J months.

In Table 4, (λ_2), $\theta_2(\tau)$, Δ H and the probable errors for each solar hours are given. The $(\lambda_2\tau_2)$ points for different solar hours for each season are plotted in the harmonic dial of lunar time.(Refer Fig.8)

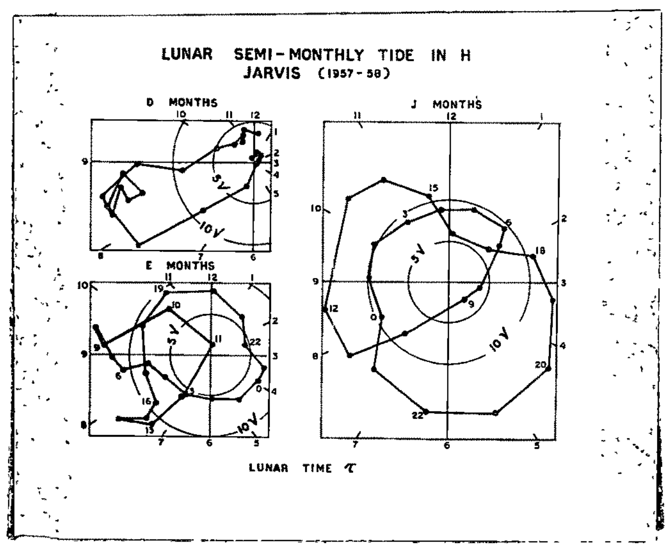

Fig-8

The $(\lambda_2\tau_2)$points for D-months when plotted on a harmonic dial trace a loop with a marked elongation in a preferred direction, whereas $(\lambda_2\tau_2)$ points for E and J months trace two near circles cutting each other. One loop is formed

Table - 4

Coefficients of lunar semi-monthly M_2 oscillations in H at Jarvis (1957-58)

L.M.T.	D-months. 34000+ ΔH	r_2	θ_2 in lunar time		E-months 34000+ ΔH	r_2	θ_2 in lunar time		J-months 34000+ ΔH	r_2	θ_2 in lunar time	
	Gamma	Gamma	P.E.	degree	Gamma	Gamma	P.E.	degree.	Gamma	Gamma	P.E.	degree.
00	417	0.61	1.80	340	411	6.96	2.18	101	402	9.58	2.07	243
01	418	0.93	1.78	21	413	6.72	1.90	117	403	10.12	2.01	273
02	420	1.30	1.71	19	415	6.46	1.79	146	404	10.56	1.96	296
03	421	1.20	1.66	46	416	5.54	1.72	178	405	9.15	1.89	324
04	421	0.75	1.59	75	417	5.57	1.68	212	404	9.14	1.82	353
05	421	0.27	1.54	116	417	6.27	1.68	245	405	9.54	1.81	18
06	424	3.13	1.72	196	423	6.82	1.74	262	411	9.45	1.92	44
07	447	8.56	2.00	226	453	11.09	2.64	260	435	7.85	2.20	52
08	491	17.67	2.99	234	497	12.15	2.81	259	458	3.81	2.73	97
09	544	18.85	3.03	253	542	14.66	3.53	283	480	2.76	2.92	135
10	589	16.43	3.49	265	572	13.22	3.71	275	499	8.45	3.37	221
11	600	14.37	3.81	254	583	7.69	4.04	316	517	15.43	3.68	233
12	580	16.46	4.33	254	566	1.39	4.04	009	525	16.00	3.21	257
13	547	17.09	4.25	259	544	5.93	3.85	214	523	16.35	3.31	309
14	512	18.72	3.61	248	521	11.09	3.27	221	515	15.08	3.34	326
15	480	19.28	3.31	257	499	13.88	2.88	285	497	10.46	2.97	347
16	463	14.65	3.16	269	483	11.26	2.57	225	470	5.93	3.11	3
17	452	8.90	2.39	263	466	8.84	2.68	229	448	6.30	3.57	52
18	441	4.93	2.24	291	443	8.30	2.62	255	426	10.72	3.23	73
19	428	3.32	2.82	314	424	9.16	2.67	293	412	12.96	3.16	99
20	419	3.75	3.38	348	417	9.47	2.85	323	406	16.15	3.11	130
21	416	3.06	3.52	331	414	7.86	2.86	002	403	17.13	2.97	160
22	413	4.32	4.26	342	411	6.14	3.16	038	399	16.20	3.42	190
23	413	3.61	3.95	08	411	4.47	3.00	071	399	14.43	3.35	221

by solar daytime points and other by solar nighttime points.

The vector average of

$(h_2\tau_2)$ D-months is	$7.1\ \gamma$,	263°
$(h_2\tau_2)$ E-months is	$4.5\ \gamma$,	260°
$(h_2\tau_2)$ J-months is	$0.6\ \gamma$,	40°

3.3 (5) Huancayo:

Huancayo is situated on the magnetic equator. Its coordinates are:

Geographic latitude	12.3° South
Geomagnetic latitude	0.6°South
Geographic longitude	75°19'West
Geomagnetic longitude	353.8°East
dip angle =	1.9°North.

Lunar daily variation:

The annual average lunar daily variation in H at Huancayo (IGY-IGC) for lunar ages centered on 00, 03, 06, 09, 12, 15, 18 and 21 are shown in fig.1. The lunar

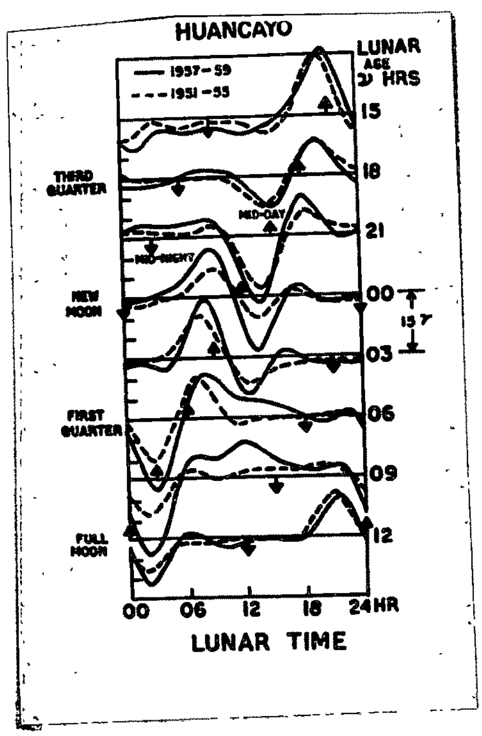

Figure-1.

daily variation at Huancayo is similar in character to the lunar daily variation at other equatorial stations. Compared to other stations on the equator Huancayo shows larger amplitude of lunar daily variation.

The harmonic coefficients (Cn) and (αn) of average lunar daily variation in H at Huancayo are given in table-1. In fig.2 are shown the changes of phase angle

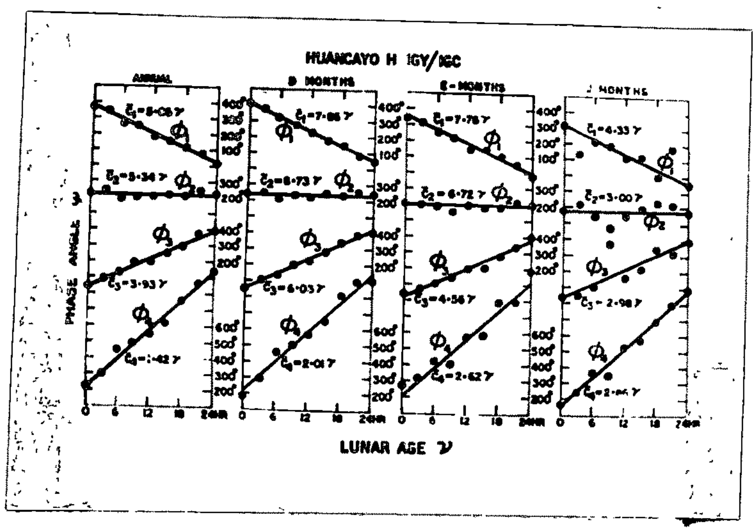

Figure-2.

with lunar age in accordance with Chapman's phase law equation.

The annual average lunar daily variation averaged over a whole lunation is shown in fig-1.

Table - 1.

Coefficients of lunar daily variations in H at Huancayo for different lunar ages according to the equation $L = \sum_{n=1}^{4} C_n \sin\{n\tau + (n-2)\nu + \alpha_n\}$

Annual - Huancayo(IGY/IGC)

Lunar age	C_1 Gamma	α_1 °	C_2 Gamma	α_2 °	C_3 Gamma	α_3 °	C_4 Gamma	α_4 °
00	4.33	9	5.69	220	4.33	35	1.67	208
03	3.46	346	5.69	237	4.86	78	1.97	291
06	7.36	261	5.86	183	4.36	126	1.33	79
09	8.92	251	5.10	196	3.86	185	1.50	128
12	3.20	180	4.50	199	3.76	192	1.00	178
15	6.69	159	5.70	211	3.03	245	1.53	256
18	1.53	115	4.50	203	2.60	294	1.03	29
21	4.96	74	6.30	240	4.63	12	1.30	137

The harmonic coefficients of the whole lunation average lunar daily oscillations during different season are given in table-2.

Lunar monthly variations at fixed solar times:

The lunar monthly variations are computed at fixed solar hours. In table 3 are given the coefficients of lunar monthly (M_1) and lunar semi-monthly (M_2) oscillations obtained from the curves representing annual average lunar monthly variations. In table-3 the phase of M_1, oscillations are presented in terms of local lunar age whereas the phase of M_2 oscillations are presented in terms of local lunar time τ. In table-4 the coefficients of M_2 oscillations are presented for different seasons of a year along with probable error in M_2(H) amplitudes.

Lunar semi-monthly (M_2) tide in H at fixed solar times varies with the solar time in the same way as the electrojet current i.e. the amplitude starts increasing with sunrise, reaches a maximum near noon and decreases to low value by sunset. This is seen from Fig.3.

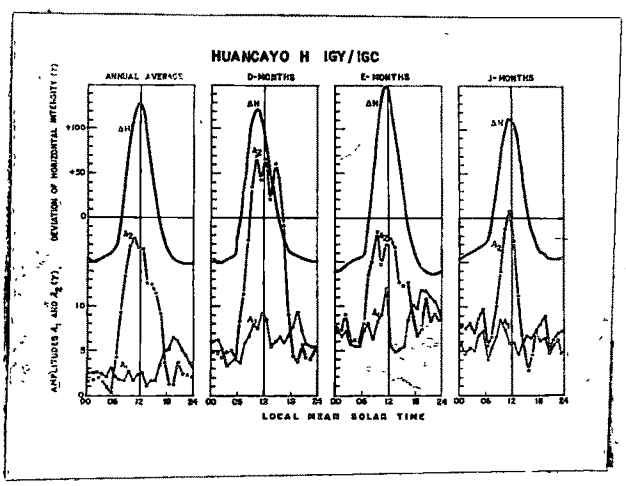

Figure.3

Table - 2.

The coefficients of lunar daily oscillations in H averaged over the whole lunation during different seasons for Huancayo IGY/IGC according to the equation $L = A_n \sin(n\tau + \beta_n)$

Season	A_1 Gamma	β_1 0	A_2 Gamma	β_2 0	A_3 Gamma	β_3 0	A_4 Gamma	β_4 0
D-months	0.47	235	8.73	238	0.43	340	0.87	167
E-months	1.00	261	6.50	187	0.97	125	0.33	325
J-months	1.90	137	1.80	158	0.93	68	0.02	237
Annual	1.33	235	5.07	211	0.73	103	0.37	181

Table - 3.

Coefficients of lunar monthly M_1 and lunar semi-monthly M_2 oscillations in H at Huancayo (IGY/IGC)

Time 75° W.M.T.	Mean ΔH Gamma	Ampl. r1 Gamma	Phase θ_1 in lunar age degree.	Ampl. r2 Gamma.	Phase θ_2 in lunar time degree.
0.5	-50.4	2.6	107	1.5	144
1.5	-49.7	2.6	104	1.7	183
2.5	-47.7	2.7	81	1.9	213
3.5	-44.9	2.6	74	1.4	237
4.5	-42.3	2.2	77	0.8	234
5.5	-39.2	3.2	87	0.2	276
6.5	-31.4	2.2	111	4.1	234
7.5	-7.1	1.9	107	9.2	216
8.5	35.5	1.7	200	13.3	225
9.5	86.0	2.7	213	16.7	231
10.5	116.5	1.70	170	17.6	246
11.5	128.8	2.4	149	16.5	249
12.5	117.6	2.5	203	16.4	255
13.5	87.5	1.1	186	12.5	252
14.5	53.0	1.7	152	12.4	237
15.5	19.2	1.7	95	11.4	234
1[illegible].5	-6.6	3.40	96	9.1	246
17.5	-27.6	5.0	92	3.6	255
18.5	-40.8	5.2	107	1.1	315
19.5	-46.8	6.6	113	1.1	15
20.5	-51.0	6.2	105	3.6	351
21.5	-52.3	5.1	110	2.3	33
22.5	-53.3	4.5	105	2.2	51
23.5	-52.6	3.8	110	2.0	72

Table - 4.

Coefficients of lunar semi-monthly (M_2) oscillations in H at Huancayo (IGY/IGC)

	D-months.			E-months.			J-months.		
Time 75°W.M.T.	Ampl. r_2 Gamma.	Probable error Gamma.	Phase θ_2 in lunar time degree.	Ampl. r_2 Gamma	Probable error Gamma.	Phase θ_2 in lunar time degree.	Ampl. r_2 Gamma	Probable error Gamma.	Phase θ_2 in lunar time degree.
0.5	4.9	3.6	132	7.1	3.5	129	7.8	3.9	300
1.5	4.7	3.6	168	7.5	3.4	159	7.6	3.7	318
2.5	4.2	3.4	204	9.1	3.4	189	8.0	3.7	0
3.5	4.8	3.4	207	6.0	3.3	222	7.0	3.8	21
4.5	4.9	3.4	243	6.3	3.2	237	8.6	3.8	60
5.5	4.3	3.5	246	6.0	3.3	264	9.6	3.8	75
6.5	8.2	3.9	228	9.1	3.4	264	5.6	3.9	114
7.5	11.4	4.4	198	13.5	3.8	249	6.7	4.1	183
8.5	17.5	5.0	207	14.9	4.0	252	10.0	4.4	213
9.5	23.5	5.5	204	18.5	4.5	267	14.1	4.6	237
10.5	27.1	5.6	213	14.8	5.0	267	18.9	4.8	276
11.5	24.3	6.3	207	16.9	5.4	255	20.6	4.7	294
12.5	26.9	5.8	216	17.6	5.4	270	17.3	4.8	306
13.5	22.0	2.5	213	16.6	5.3	261	11.2	4.3	321
14.5	26.1	4.9	213	12.7	5.2	258	6.2	4.5	315
15.5	24.6	4.4	225	12.2	4.8	249	2.7	4.3	330
16.5	19.1	4.2	240	12.8	4.4	249	4.5	4.0	51
17.5	9.0	3.3	258	8.8	4.2	273	7.4	3.9	99
18.5	4.7	4.0	309	6.7	4.0	315	8.0	3.9	123
19.5	3.7	3.9	15	7.4	4.0	312	8.9	3.9	129
20.5	5.6	3.8	3	10.8	3.9	339	5.1	3.9	156
21.5	4.2	3.7	15	8.3	3.8	15	6.4	4.0	174
22.5	4.1	3.7	36	9.2	3.8	39	7.2	3.9	204
23.5	5.0	3.7	81	8.5	3.5	66	7.4	3.8	252

The phase of lunar monthly (M_1) tide in H for a particular season is controlled by lunar age and not by lunar time. The lunar semi-monthly (M_2) tide in H for any hour of the day time hours is maximum at the same lunar time for months September to April and at the same lunar age for months May to August. The lunar semidiurnal (A_2) as well as the lunar semi-monthly (M_2) tide is larger during D-months than E-months. It is suggested that the phase of lunar tides in H at the equatorial stations is caused by two independent sources controlled respectively by the lunar age and by the lunar time at the station, the amplitude being controlled by the local solar time, being maximum near local noon. These observations can be seen in the figures 4,5,6,7 presented below.

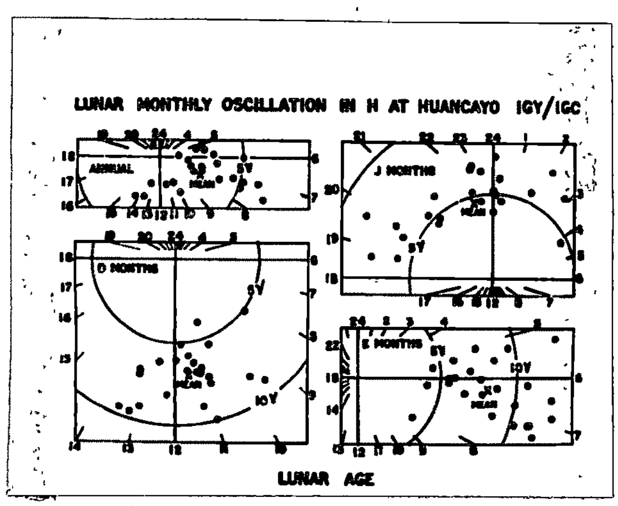

Figure.4.

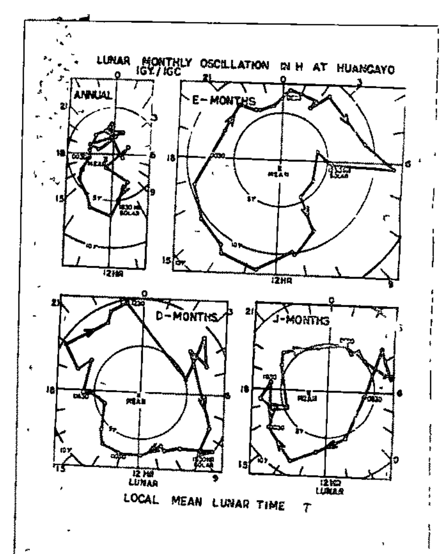

Figure.5.

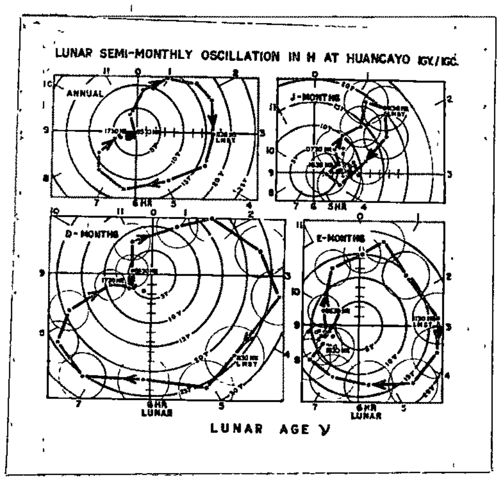
LUNAR SEMI-MONTHLY OSCILLATION IN H AT HUANCAYO IGY/IGC.
ANNUAL
J-MONTHS
D-MONTHS
E-MONTHS
LUNAR AGE ν

Fig-6

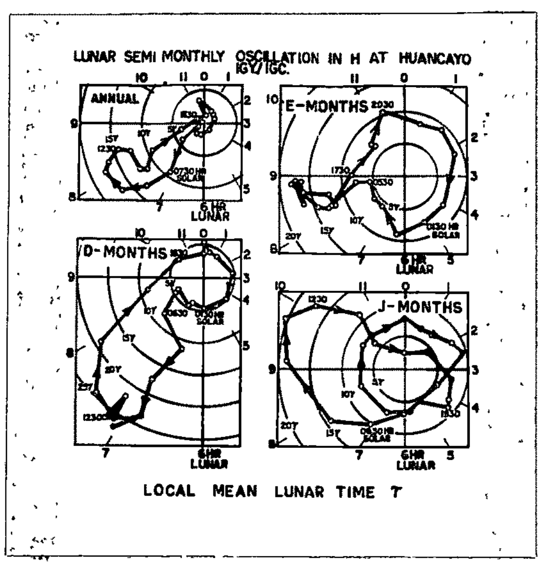
LUNAR SEMI MONTHLY OSCILLATION IN H AT HUANCAYO IGY/IGC.
ANNUAL
E-MONTHS
D-MONTHS
J-MONTHS
LOCAL MEAN LUNAR TIME τ

Fig-7

3.4(b) Summary

The lunar tidal oscillations (L_2) in H field at various stations near the magnetic equator are found to have large amplitudes. It would be natural to connect these large (L_2) oscillations with another well-known abnormality of large daily range in the H field variation near the magnetic equator. In Fig.1 are depicted linear

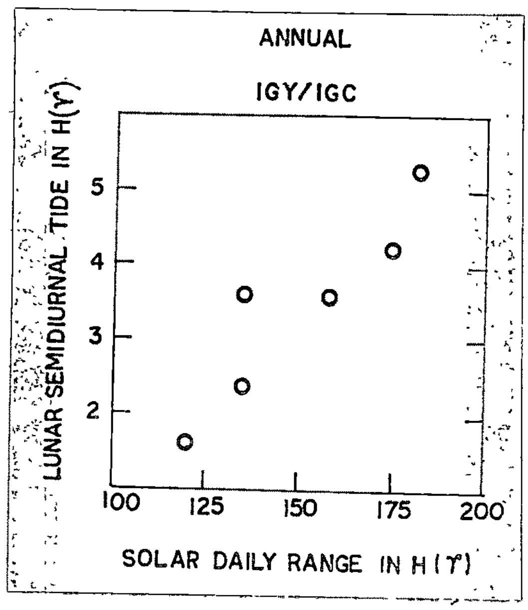

Fig.1

relationship between L_2(H) amplitude and daily range in H observed at various stations. It suggests equatorial electrojet must be included in the lunar current system.

In Fig.2 are shown lunar semi-diurnal (L_2) amplitude in H with the angle at which L_2 is maximum for the station, Trivandrum (TV), Kodaikanal(KD),Addis Ababa(AD), Koror (KO), Jarvis (JA) and Huancayo (Hu). It is seen that the time L_2 maximum remain quite close and fall into the

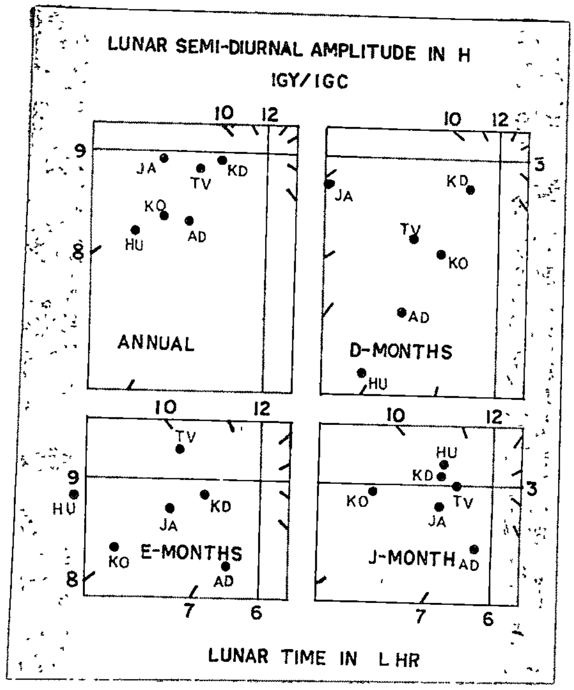

Figure-2.

.. same quadrant. For annual average L_2 max. occur between 0800 and 0900 hrs. in lunar time for all the stations.

During D-months L_2(H) amplitudes are more but angle of maximum L_2 (H) show greater scatter but fall in a same quadrant. While during E-months and J-months L_2 (H) amplitudes are lesser than D-months. Although angle of L_2 (H) maximum show greater scatter, remain not very different for all the stations. Moreover angle of L_2 (H) maximum seems to increase from D-months towards J-months.

From the study of semi-monthly (M_2) oscillations in H field at various station, daily variation of ($r_2 \tau_2$) points in J-months have shown striking character. In the figures of $r_2\tau_2$ harmonic dials for each of the station it is seen that r_2 amplitudes during J-months at nighttime are quite large. Moreover r_2 τ_2 graph create two loops centered at the origin. The larger loop is formed during daytime and smaller during nighttime. This character has been consistently noticed at all the equatorial station considered here. Same semi-monthly oscillations (M_2) are plotted on a harmonic dial in terms of lunar age i.e. r_2 ν_2 plotting, the striking character for J-months vanish. In Fig.3 are shown r_2 ν_2 variations at stations Trivandrum, Addis Ababa, Jarvis, Koror and Huancayo.

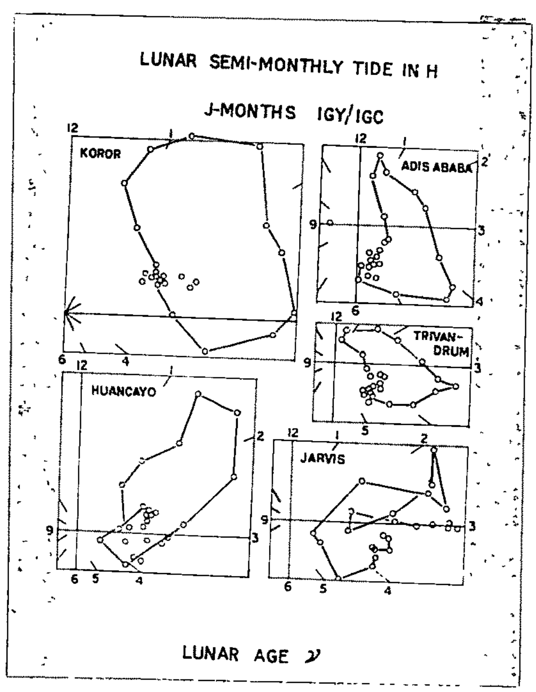

Figure-3.